Aalborg Universitet

Predictability and Variability of Wave and Wind

wave and wind forecasting and diversified energy systems in the Danish North Sea

Chozas, Julia Fernandez; Kofoed, Jens Peter; Sørensen, Hans Christian

Predictability and Variability of Wave and Wind

Wave and Wind Forecasting and Diversified Energy Systems in the Danish North Sea

Julia Fernández-Chozas
Hans Christian Sørensen
Jens Peter Kofoed

DEPARTMENT OF CIVIL ENGINEERING
AALBORG UNIVERSITY

Aalborg University
Department of Civil Engineering
Wave Energy Research Group

DCE Technical Report No. 156

Predictability and Variability of Wave and Wind
- Wave and Wind Forecasting and Diversified Energy Systems in the Danish North Sea-

by

Julia Fernández-Chozas
March 2013

Scientific Publications at the Department of Civil Engineering

Technical Reports are published for timely dissemination of research results and scientific work carried out at the Department of Civil Engineering (DCE) at Aalborg University. This medium allows publication of more detailed explanations and results than typically allowed in scientific journals.

Technical Memoranda are produced to enable the preliminary dissemination of scientific work by the personnel of the DCE where such release is deemed to be appropriate. Documents of this kind may be incomplete or temporary versions of papers—or part of continuing work. This should be kept in mind when references are given to publications of this kind.

Contract Reports are produced to report scientific work carried out under contract. Publications of this kind contain confidential matter and are reserved for the sponsors and the DCE. Therefore, Contract Reports are generally not available for public circulation.

Lecture Notes contain material produced by the lecturers at the DCE for educational purposes. This may be scientific notes, lecture books, example problems or manuals for laboratory work, or computer programs developed at the DCE.

Theses are monograms or collections of papers published to report the scientific work carried out at the DCE to obtain a degree as either PhD or Doctor of Technology. The thesis is publicly available after the defence of the degree.

Latest News is published to enable rapid communication of information about scientific work carried out at the DCE. This includes the status of research projects, developments in the laboratories, information about collaborative work and recent research results.
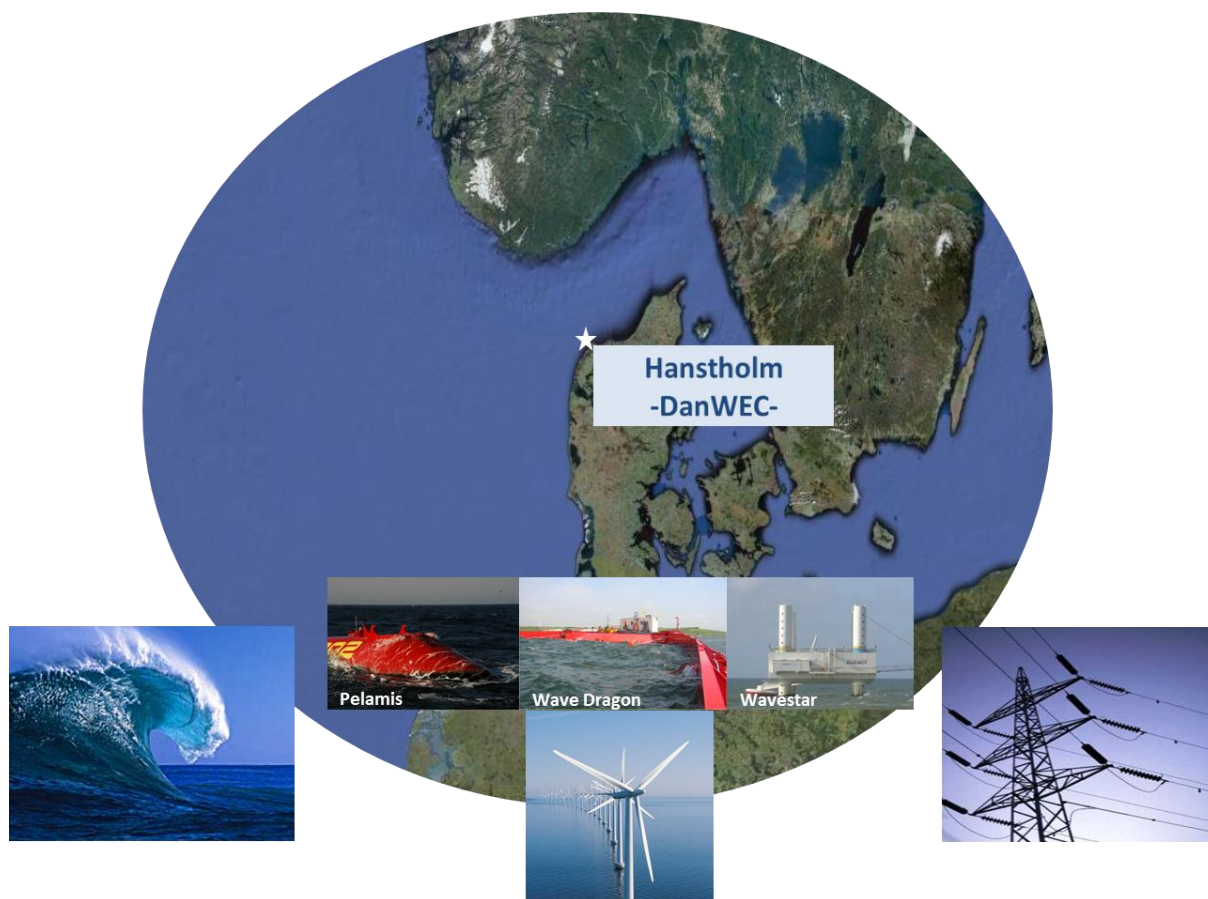
WAVE AND WIND FORECASTING AND DIVERSIFIED ENERGY SYSTEMS IN THE DANISH NORTH SEA

FINAL REPORT

Julia Fernández Chozas[1,2], Hans Christian Soerensen[2] and Jens Peter Kofoed[1]

[1] Spok Aps, (Copenhagen, Denmark)
julia@spok.dk; consult@spok.dk

[2] Aalborg University, Civil Engineering Dpt., (Aalborg, Denmark)
jfch@civil.aau.dk; jpk@civil.aau.dk

This project covers two fields of study:
   a) Wave energy predictability and electricity markets.
   b) Variability of the power output of WECs in diversified systems: diversified renewable systems with wave and offshore wind production.

Wave energy predictability and electricity markets

One of the most commonly mentioned advantages of wave energy is related to the predictability of waves. Sentences like 'waves are predictable' or 'waves are more predictable than winds' can largely be found on literature. However, a quantifiable number evaluating wave predictability is not easily found on literature and research on wave forecasting is limited to few studies. As a result, the aim of this research project has been to quantify the value of waves predictability.

Because of the fact that waves are created by winds, waves can be forecasted at a particular site by knowing the corresponding winds that affect wave generation and propagation, and the site´s characteristics.

Accurate wave forecasts are of benefit to a number of fields. Merchant and fishing fleet aside, waves forecasting provides significant advantages for the offshore wind and the wave energy sector. For example, to schedule installation and maintenance activities, to define control strategies according to the predominant wave conditions, or to plan for storm events. Moreover, accurate wave forecasting can also be of interest to electricity markets. In the day-ahead electricity market, all the electricity that will be generated and consumed on the next day is traded, and hence, electricity producers bid in the market the electricity they expect to produce on the next day. In the case of Denmark, which participates in the Nord Pool Spot, gate closure of day-ahead markets is at noon. Thus, bids have to be made at least 12 to 36 hours ahead the actual generation hour. This applies to all electricity producers, both for conventional power plants and for renewable generation. For hydropower plants, coal or gas fire plants, day-ahead bids are significantly accurate. However, for wind power producers or eventually for wave power producers – when technologies reach the commercial stage –, bids might have a considerable error related to the partial unpredictability of the resources. The error in the power production estimates has an associated cost. In electricity markets this is known as balancing costs.

Energinet.dk is the Danish national body responsible of managing the grid, including the imbalances of the electric system. The introduction of large quantities of wind generation into the Danish system has increased system imbalances, and Energinet.dk invests on balancing premium tariffs that wind producers receive to manage their power imbalances. Accordingly, Energinet.dk has raised its interest on the imbalances wave generation would add or reduce to the system, compared to the current imbalances of wind production. It aims to have an

estimate of the balancing costs of wave energy compared to the current balancing costs of wind energy. This issue is the scope of the first part of this research project.

In line with this, the purpose of this study has been:
i. Quantify how accurately waves can be predicted and compare that value to winds predictability.
ii. Estimate WECs and wind turbines power productions predictability.
iii. Estimate the errors incurred in the bids to the day-ahead market, both for wave and for wind energy, if the productions had been traded in day-ahead electricity markets.
iv. Evaluate economically the errors of day-ahead bids and assess the economic benefits, in terms of reduction in balancing costs, of including wave energy in a system based on wind energy solely.

On the whole, the research focus has been the economic value of waves' predictability. To the authors knowledge, it is the most comprehensive study on wave power forecasting in the North Sea waters, both for waves and for WECs power productions.

Results suggest that for day-ahead forecasts, waves are 23% more predictable than winds, the power output of WECs is 35% more predictable than for wind turbines, and the inclusion of wave energy in a wind-only system reduces balancing costs up to 35%. This would imply annual savings to the Danish system of 13 MEUR (i.e. 95 MDKK/y) and a balancing premium tariff for wave energy of 1.8 EUR/MWh (compared to the current premium tariff of wind turbines of 3 EUR/MWh).

In a nutshell, results have shown the benefits of waves' predictability.

Variability of the power output of WECs in diversified systems
The second research study has focused on the opportunities of combining the power production of different technologies in the same site to provide a continuous power output. Particularly, it has investigated the combined power production of WECs and of wind turbines.

The term diversified renewable systems refers to an energy system composed of various renewable resources, located in a range of areas within the same or in a different energy system. The two key benefits of diversification are that the variability of the produced power can be decreased, and power availability can be increased. These benefits can be achieved by combining different resources, the more un-correlated the better. Otherwise, when only one resource is available – wind energy for example – these benefits can only be realised by aggregating the power of geographically disperse sites.

The study has focused on the benefits of a combined wave and wind power output compared to the individual productions. This is investigated through theoretical and real case studies

that analyse the individual power productions of WECs and of wind turbines and compares them to the combined power production. To the authors best knowledge the study comprises the first research investigating and comparing real power productions of WECs and of wind turbines.

The most indicative finding is that the combined power output is smoother and provides higher availability than the individual productions: both the peaks and the fast changes found in the individual productions reduce when these are combined, and the percentage of time with null production reduces to a minimum. Variability reduces up to 31% and the percentage of time with zero production decreases to 6%.

Overall, the project has carried out an optimisation analysis which has sought to find the mix of WECs and of wind turbines and WECs, that resulted in an optimal electricity supply from the WEC system. The most predictable and most constant energy output has been chosen as the optimisation parameter.

TABLE OF CONTENTS

SYMBOLS

C_g	Wave group velocity	[m/s]
d	Water depth	[m]
$delay$	Time delay	
E_{anual}	Annual energy production	
f	Capacity factor	
g	Gravity acceleration	[m/s^2]
H_{m0}	Significant wave height spectral estimate	[m]
H_s	Significant wave height	[m]
H_{max}	Maximum individual wave height	[m]
k	Wave number	[m^{-1}]
L	Wave length	[m]
l	Length	[m]
λ	Scale ratio	
μ	Mean	
MWD_{wave}	Mean wave direction	[°][1]
MWD_{wind}	Mean wind direction	[°]
N	Number of samples	
$P_{forecast}$	Power productions forecasts	[W]
P_{MOD}	Forecast power production	[W]
P_{OBS}	Observed power production	[W]
P_{prod}	Power production	[W]
P_{rated}	Rated power	[W]
$P_{real-time}$	Power productions measured at real-time	[W]
P_{wave}	Wave power per unit of crest width	[kW/m]
P_{wind}	Wind power per unit of area	[W/m^2]
$\emptyset$	Diameter	[m]
R^2	Determination coefficient	
$\rho_{salt\,water}$	Salt water density	[kg/m^3]
ρ_{air}	Air density	[kg/m^3]
$SI_{unbiased}$	Unbiased scatter index	
σ	Standard deviation	
t	Forecast horizon, time lag or time delay (indicates future from present time)	[h]
T_e	Energy period	[s]
T_p	Peak period	[s]
T_z	Zero-crossing period	[s]

---

[1] 1°= (π/180) rad

T_{02}	Zero-crossing period spectral estimate	[s]
u_{wind}	Wind speed	[m/s]
w	Width	[m]

ABBREVIATIONS

AAU	Aalborg University
CAPEX	Capital Expenditures
CC	Cross-Correlation Coefficient
CCGT	Combined Cycle Gas Turbines
COE	Cost of Energy
DanWEC	Danish Wave Energy Centre
DHI	Danish Hydraulic Institute
DKK	Danish krone
EC	European Commission
ECMWF	European Centre for Medium Range Weather Forecasts
EMEC	European Marine Energy Centre
ENTSO-E	European Network of Transmission System Operators for Electricity
EU	European Union
EUR	Euro
GFS	Global Forecast System
MAE	Mean Absolute Difference
MOD	Modelled, Calculated or Forecast Data
N	at the beginning of a word indicates a "normalised" value
NBias	Normalised Bias in percentage of installed power
NMAE	Normalised Mean of Absolute Difference in percentage of installed power
NRMSE	Normalised Root Mean Square of Difference in percentage of installed power
O&M	Operation and Maintenance
OBS	Observed or measured data
OPEX	Operational Expenditures
P	Pelamis
PTO	Power Take-Off
RMSE	Root Mean Square of the Difference
TSO	Transmission System Operator
UTC	Coordinated Universal Time [dd/mm/yyyy]
UTM	Universal Transverse Mercator [N, E]
WD	Wave Dragon
WEC	Wave Energy Converter
WRF	Weather Research and Forecasting
WS	Wavestar

ACKNOWLEDGMENTS

CHAPTER I – INTRODUCTION

I.1. PROBLEM STATEMENT

The potential of waves around the globe is very large (Mørk et al., 2010). High wave and offshore wind energy potentials are available along the West and North coasts of Europe. If both resources are harnessed they can become a large-scale contributor to our future renewable electricity mix. In fact, it has been assessed that 15% of Danish electricity consumption can be provided by wave energy converters (WECs) deployed in Danish waters (Kofoed, 2009).

There are some challenges ahead before it is possible to implement wave energy converters into our energy systems. Firstly, WECs need to prove their long-term survivability into the harsh sea environment as well as long-term operation; and secondly, they need to be cost competitive. There are also some issues related to the integration of wave energy into the electric grid. This project focuses on two challenges:

a) Wave energy predictability and electricity markets: as non-fully predictable renewables make their bids into electricity markets there is an associated increment of the electricity price.

b) Variability of the power output of WECs: electricity power supply has to secure continuous supply and the variability inherent to some renewables, like wave and wind energy, has been claimed to work against that request.

Electricity markets were first designed to accommodate conventional power generation. Besides hydropower, the contribution from renewable energy sources was scarce. Nowadays, as the percentage of renewable generation within the electricity mix increases (EREC, 2011), the uncertainty on the planned generation has also risen. The reason is that some of the most promising renewable energy sources such as wave power or wind power are not entirely predictable. This partial unpredictability is causing Transmission System Operators (TSOs), producers and/or electricity users large expenditures to cope with the costs of balancing the system (IEA, 2008).

The Danish electricity market is part of the Nord Pool, also integrated by Norway, Sweden and Finland. In the Nord Pool Spot Market, also known as the day-ahead market or Elspot, power producers and power consumers give their bids to the market (Nor1). Since the bidding closes at noon, deliveries 12 to 36 hours in advance need to be made (Figure 1). At gate closure, there is a set price for each hour in the following 12 to 36 hour period.
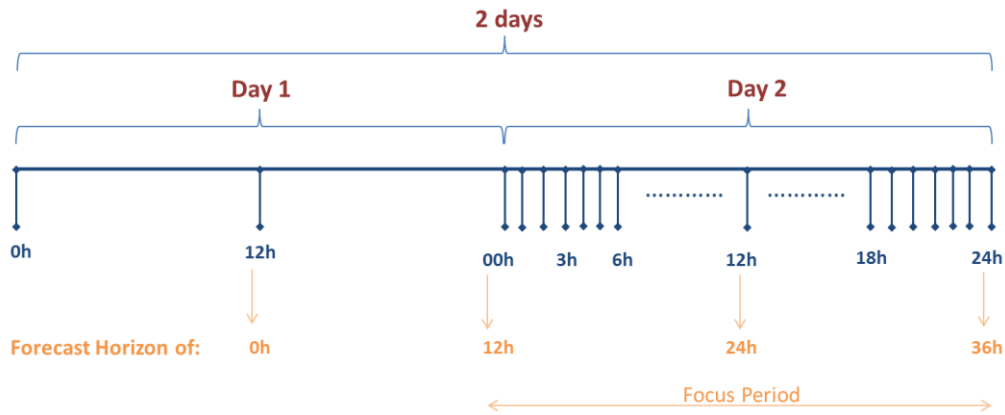
Figure 1. Focus period and forecast horizons of the Danish day-ahead electricity market.

In the intraday market, i.e. the Elbas market, energy is traded to minimize the deviations from production and consumption determined in the day-ahead market. The Elbas market closes one hour before the operational hour.

The last corrections of any imbalances between supply and demand take place within the regulating and the balancing market, which starts one hour before the actual generation time. This market is particularly important for non-fully predictable resources such as wave energy or wind energy. Here, the actors contributing to the imbalances (i.e. over-producing or under-producing the estimated power) have to cover the costs for balancing the system. In general terms, these costs, also known as balancing costs, cover the difference between the bid to the day-ahead market and the actual power produced.

In Denmark balancing costs are ultimately passed on to the Danish power consumers. As a result, provided wave energy can become part of the Danish electricity system, it is of great importance to estimate balancing costs of wave energy. It is also of interest to propose new strategies towards electricity markets that can accommodate higher percentage of fully predictable power outputs without increasing balancing costs. Since the study also looks into combinations of wind and wave energy, the economic benefit of integrating wind along with wave to reduce balancing costs of the former is also examined.

At present time and according to the Danish electricity rules, wind power producers who are able to balance the power receive 3 EUR/MWh (in case of onshore wind turbines) on top of the feed-in tariff. The balancing costs correspond to about 7% of the overall costs of wind generated electricity (Morthorst, 2007).

The difference between the spot market price of conventional electricity generation and the wind turbine generation market price (feed-in tariff plus balancing costs premium) is ultimately passed onto Danish electricity consumers.

This project carries out an economic analysis. The objective is to estimate the balancing costs for wave energy electricity generation. This figure is compared with the current balancing costs of wind energy. It is expected that the combination of wave and wind electricity generation reduces the balancing costs of wind turbines.

Moreover, predictability of wave parameters is not only useful for the integration of technologies into day-ahead markets but also for WEC operation. Long-term weather forecasts allows estimating and evaluating future power production of a WEC, scheduling installation, tests and maintenance activities, and planning for storm events. Short-term forecasts are useful to define and improve control strategies and WEC performances.

In the second stage, also the opportunities of combining wind and wave power productions, are analysed.

Accordingly, this project addresses:
a) Wave energy predictability and electricity markets
   - Predictability of wave parameters.
   - Predictability of wind parameters.
   - Predictability of the power output of three WECs working in normal operating conditions.
   - Predictability of the power output of two wind turbines working in normal operating conditions.
   - Predictability of the power productions from a combination of WECs, in normal and in storm operating conditions.
   - Predictability of the power productions from combinations of WECs and wind turbines, in normal and storm operating conditions.
   - The economic benefit of wave energy predictability: estimation of the accuracy of wave power bids in the day-ahead electricity market and the corresponding costs for wave energy integration into the electric grid.

b) Variability of the power output of WECs.
   - Variability of wave and wind energy.
   - Variability of WECs.
   - Variability of wind turbines.
   - Variability of the power output of combinations of WECs and wind turbines.
   - Results verification with sea-measured and modelled power productions.

As result, this study presents the first approach of the Danish TSO towards the study of predictability of WECs' power output and its economic costs. It also looks into wave power output variability.

I.2. RELEVANCE OF THE PROJECT

Very few investigations have been carried out covering power output predictability of wave energy converters.

On the other hand, the idea of combining wave and wind is widely mentioned at this point of development of the wave energy sector, although there are only a few desk-studies on this subject and barely any related to real-sea data. Three previous international works assess the correlation between the wind and the wave resource and the advantages of combining both, in terms of reliability and variability of the electrical power production. One of the studies is based on Ireland (Fusco, et al., 2010), a second one in California (Stoutenburg, et al., 2010), and the third one in Danish waters (Soerensen, et al., 2005).

The latter investigation was carried out by Ramboll and Spok ApS and analyses the wave climate at Horns Reef, off the west cost of Jutland, Denmark. Horns Reef presents environmental conditions very similar as the proposed study location.

Furthermore, there is an ongoing European funded project, i.e. Marina Platform (MarinaPlatform, 2013) looking also to the advantages of combining wind and wave. The project examines three locations: the Biscay Bay (Spain), off Bretagne (France) and Belmullet (Ireland). The Denmark-based utility Dong Energy is participating within this project.

Nevertheless, none of these studies considers the predictability fact, which is the main focus of this study.

I.3. NOVELTIES OF THE PROJECT

The idea behind the described investigation is very unique. Originally proposed by Energinet.dk, this project is the first national as well as international approach towards a study of this kind.

The novelties of this project are:
- To compare theoretical day-ahead forecast power productions with theoretical buoy-measured power productions.
- To consider different combinations of the power outputs from the three different WECs.
- To look into combinations of wave energy and wind energy.
- To compare desk-results with real sea-measured power productions from a WEC and a wind turbine.
- To locate the study in Danish North Sea waters, an area with increasing interest on wave energy testing and development (Soerensen, et al., 2010), (DanWEC).

Moreover, this research project addresses a forthcoming in-house problem of the Danish Transmission System Operator (TSO) Energinet Denmark as well as of wave energy developers. This project represents the first approach towards the study of predictability of wave energy converters' power output carried-out within Energinet.dk funded R&D programmes.

Furthermore, due to the meshed layout and interconnectivity of the European electric grid the main outcomes of this investigation are relevant not only for the Danish TSO but also for all European TSOs as well as the ENTSO-E (European Network of Transmission System Operators for Electricity).

The results achieved are not only of relevance to Energinet Denmark but to all transmission system operators in Europe. Moreover, utilities, which ultimately have to generate electricity in compliance with the rules of the electric grid, might also be interested in this research. This is proved by Dong Energy (Danish utility), Iberdrola (Spanish utility) and ESB (Irish utility), which have shown interest on the study. The wave energy sector and the wind energy industry might also be interested in the project idea.

KEYWORDS

CHAPTER II – PROJECT BIBLIOGRAPHY

This section focuses on bibliography to the project with regard to the two main topics of this report:
   a) Wave energy predictability and electricity markets.
   b) Variability of the power output of WECs in diversified systems.

II.1. WAVE ENERGY PREDICTABILITY AND ELECTRICITY MARKETS

Research on wave forecasting is limited to few studies. Among them Rugbjerg et al. (2006) investigate wave forecasting for offshore wind farms, and Pinson et al. (2012) analyse wave power forecasting.

Bedard (2008) assesses the accuracy of day-ahead forecasts for wave energy projects off Oregon coasts, in United States, and the accuracy of a forecast model, the Wavewatch III model.

The most comprehensive review on balancing costs of wave and wind scenarios has been done by ECI (2006). It assesses the impact on balancing costs when adding 52% of wave energy in a 100% wind scenario, and concludes a diversified system with wave and wind energy decreases the additional balancing costs by 36% compared to the wind-only scenario. This study is based on three WECs (Archimedes Wave Swing, Pelamis and Wave Dragon) located on various sites along the British coast. However, it does not optimise the WECs for the predominant wave conditions of the study site.

Conversely, extensive work has been carried out for wind forecasting and balancing costs of wind (Costa et al., 2008), (Holttinen, 2005).

Kariniotakis et al. (2004a) review the state of the art in short-term prediction of wind power. They reviewed different forecasting models and the results over geographically dispersed sites. They write:
   "Typical forecast accuracies for single wind farms can vary quite dramatically. In the EU ANEMOS project, a comparison of 11 state-of-the-art tools was made for 6 sites in Europe (Martí, 2006), and the comparison shows that the differences between the wind farms, but also between the forecasting models, are quite large. Figure 2 shows the NMAE variation for each site. The forecast errors are generally higher for more complex terrain, and the difference between the tools is also most significant for most complex terrain."
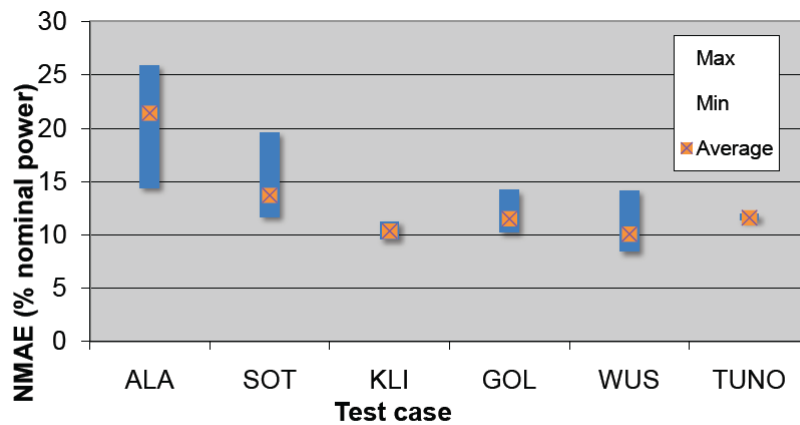
Figure 2. NMAE variation for each test case. 12 hours forecast horizon. Qualitative comparison. The ALA test site is characterized as highly complex, SOT and GOL as complex, KLI and WUS as flat, and TUNO as offshore (Kariniotakis, 2004b).

The next three European projects relate to the development of forecasting tools for wind energy. Anemos compared a number of statistical prediction models and developed forecasting software, which utilises neural network (Anemos, 2013). The Anemos project has been continued by Anemos Plus, which aims to identify instruments to implement Anemos forecasts in the best possible grid management and effective power trading (AnemosPlus, 2013). The Safewind project looks into improvement of the forecasts for extreme wind situations (Safewind, 2013).

Lastly, the next three references address in depth the topic of electricity markets, the integration of non-predictable renewables and balancing costs: IEA (2005), IEA (2011) and Morthorst (2007).

II.2. VARIABILITY OF THE POWER OUTPUT OF WECS IN DIVERSIFIED SYSTEMS

The understanding of the properties and characteristics of diversified system has been the focus of recent research in several countries. Only the studies covering marine resources are described.

ECI (2005) examines the variability of waves and tidal currents at different locations in the United Kingdom, individually and combined, and relates them to the demand. Among the conclusions it indicates that a combined wave and tidal scenario harnessing the resources at different sites has smoother variability when compared to the tidal-only scenario, and highlights the least variability in the production in a diversified scenario composed by offshore and onshore wind, wave and tidal current productions.

This study is continued by ECI (2006), and it looks into a hypothetical scenario with offshore wind, wave and tidal power covering 20% of United Kingdom´s demand. It compares the

21

benefits of an offshore wind, wave and tidal scenario with a wind-only scenario, and concludes the diversified system increases the capacity credit, and reduces the variability and the additional balancing costs of the system.

A comparable theoretical research is done in Denmark for the offshore wind farm Horns Rev I, located off West Jutland (Soerensen et al., 2005). The analysis of co-production of wave and wind proves that the delay in winds and waves reflect in the response of the technologies. Wind turbines reach full production 1 to 6 hours before WECs do, and afterwards WECs continue at full power 6 to 8 hours after the power of offshore wind turbines starts decreasing. The study also discusses the variability of the power output and suggests that the half-hour variability of wind production is 3 times higher than for wave production; and this would strengthen during storm events.

Denniss (2005) compares the variability of wind speeds and wave heights and concludes their relative variability is generally comparable. However, it adds that their respective power distributions exhibit a greater variability for wind power than for wave power (i.e. since wind power is a function of the cube of wind speed, while wave power is primarily a function of the square of wave height). The study defines relative variability as the ratio of the standard deviation of the distribution to its mean.

The opportunities of providing all the electricity supply of a French island with offshore wind and wave energy is the study subject of Babarit et al. (2006). The analysis concludes the power output of the two resources is too similar to allow for a self-sufficient renewable power system, unless a storage system is included. With that configuration high independency would be achieved, and the island could then become a net electricity exporter to the mainland.

The cross-correlation between the wave and wind resources is also the study subject of Fusco et al. (2010), with focus on a number of sites around Ireland. In the locations where the correlation is low, the combination of wave and wind energy allows for a more reliable, less variable and more predictable electrical power production than with the individual productions.

Stoutenburg et al. (2010) also look into the aggregate production of offshore wind and wave energy farms in California by studying the cross-correlation between the two resources. Their findings on variability and capacity credits reduction and increase of system reliability go in line with the findings of the previous studies.

Lastly, Cradden et al. (2011) investigate the same properties of diversified offshore wind and wave systems in three sites around Europe, at EMEC in Scotland, at SEM-REV in France and at the Biscay Marine Energy Platform (BIMEP) in Spain. The study investigates the correlation and the delay between waves and winds, and compares the percentage of time of no production, with full production, and the power variability for different wave and wind

scenarios. It also analyses the correlation of the power output of different scenarios to United Kingdom's power demand. All results coincide with those from previous studies and indicate again that the best match to fulfil United Kingdom's power demand is by utilising both wind and wave energy sources.

Moreover, the following five European funded projects evaluate further the synergies and benefits with combined wave and wind developments. The authors of this report have held discussions with several of the following projects´ partners, and all the results presented in the thesis have been made available and shared with the projects. Orecca (Offshore Renewable Energy Conversion Platforms) has worked towards a roadmap and a framework for knowledge sharing on offshore renewable energies (Orecca, 2013). The Marina Platform has been set as the continuation of Orecca project to establish a set of criteria for the evaluation of multi-purpose platforms for marine renewable energy (MarinaPlatform, 2013). Tropos (Modular Multi-use Deep Water Offshore Platform for Harnessing and Servicing Mediterranean, Subtropical and Tropical Marine and Maritime Resources) aims to develop a floating modular multi-use platform system for use in deep waters (Tropos, 2013). H2Ocean (Development of a Wind-Wave Power Open-Sea Platform Equipped for Hydrogen Generation with Support for Multiple Users of Energy) focuses on a design of a multi-use open-sea platform, where wind and wave energy will be harvested (H2Ocean, 2013). Part of the energy will be used for on-site applications like hydrogen production or aquaculture. Mermaid (Innovative Multi-purpose Offshore Platforms: Planning, Design and Operation) works towards the optimisation of the use of space for offshore wind farms and aquaculture (Mermaid, 2013). The project investigates marine structures with shared resources such as staff allocation, transportation of staff and material from and to the platforms, use of forecasting systems, ships, etc.

Then, the following studies assess further advantages of wave deployments.

Beels et al. (2011) conclude that, if installing a line of Wave Dragons, there would be a 9 to 14% increase in the time to access the wind farm. This is due to the reduction of the wave height behind the overtopping converter.

Margheritini and Nørdgaard (2012) address different uses of WECs apart from electricity production, i.e. coastal protection, breakwater element, water recirculation, fish farming and offshore platform for combination of different technologies. It also overviews the benefits of Wavestar WEC combining wave generation with photovoltaics and wind turbines.

Nørdgaard et al. (2011), Ruol et al. (2010) and Zanuttigh et al. (2010) also evaluate the benefits of including WECs for coastal protection schemes.

III.1. INTRODUCTION

This section describes the methodology of the study. It includes:
   A. Characteristics of the study location – Hanstholm.
   B. Time period of the study.
   C. Data sources: observed and forecast wave and wind data.
   D. Assessment of wave and wind conditions at Hanstholm.
   E. Description of wave converters and wind turbines.
   F. Description of modelled data.
   G. Description of read data.
   H. Description of electric system data.
   I. Description of forecast systems.
   J. Main project assumptions.

III.2. STUDY LOCATION – HANSTHOLM

The selected research site is Hanstholm, at the west coast of Jutland, Denmark, in the Danish part of the North Sea (Figure 3). Despite the North Sea has been mostly considered for wind generation, there are interesting opportunities for wave energy development. Soerensen and Fernández-Chozas (2010) estimate wave energy from the North Sea could provide about 6% (i.e. a yearly production of 77 TWh) of the electricity demand of adjacent countries, and Kofoed (2009) assesses wave energy from the Danish part of the North Sea could provide 15% of Danish electricity demand.

The study refers to a point approximately 1.3 km offshore (the point is about 1.3 km from the coastline and about 1 km from the harbour entrance) and at 17 m water depth (Lat. 57.1315°N, Lon. 8.5821°E; the position in UTM32 Euref89 reference system is 6332100 North, 474700 East).
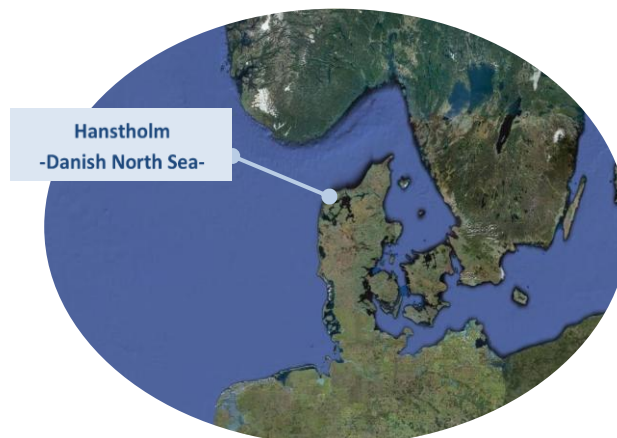
Figure 3. Hanstholm location, Denmark.

The selected location provided good opportunities to carry-out this study: there are comprehensive data sets of co-located forecasts and actual measurements of waves and winds; there is an operating prototype of Wavestar producing electricity and there exist co-located production of a wind turbine and a WEC; and, above all, there is an increasing interest on the wave climate characteristics at this location due to the establishment of the wave energy test site DanWEC, the Danish Wave Energy Centre (DanWEC). DanWEC is a test centre for wave energy converters (Figure 4). All the findings of this project will ultimately beneficiate the WECs to be deployed there, since it will provide further knowledge on the wave conditions at the deployment location, i.e. on wave parameters and on their predictability.
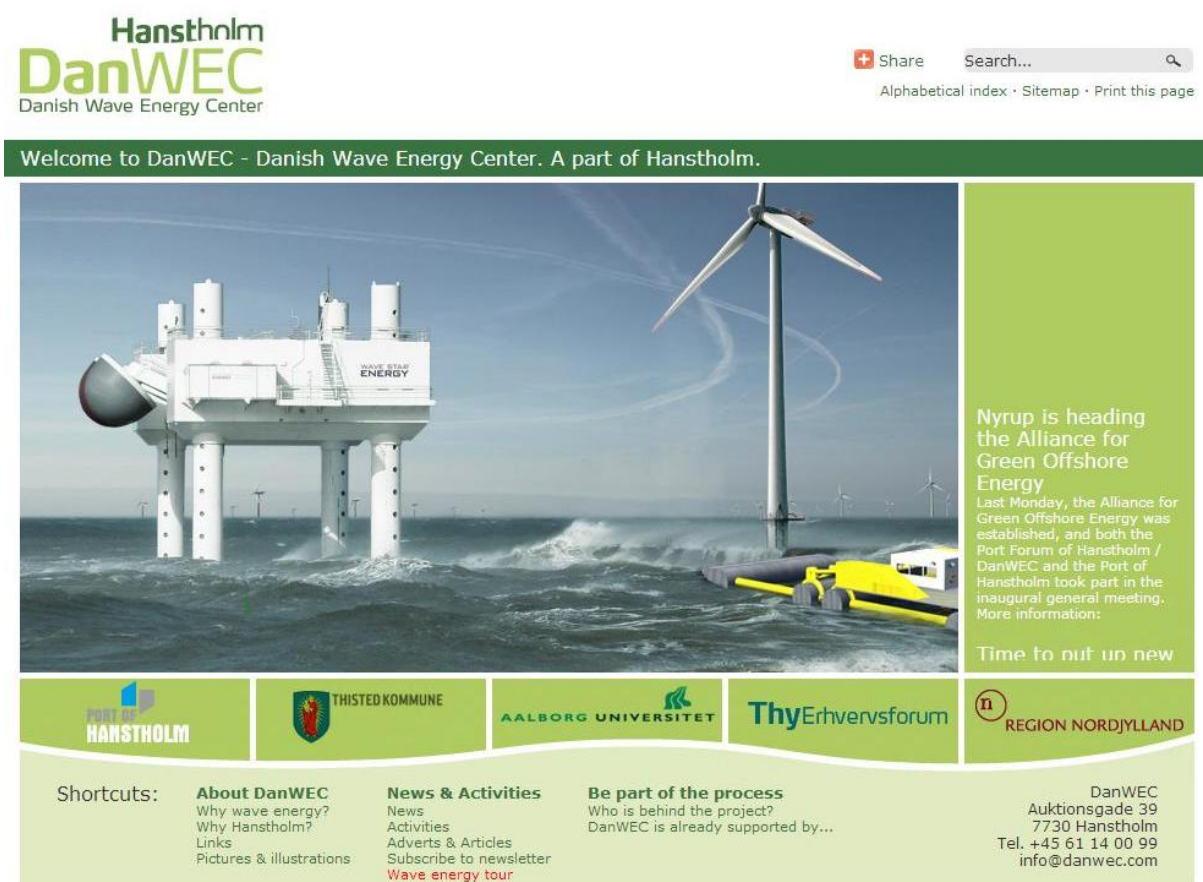
Figure 4 DanWEC, the Danish Wave Energy Centre (DanWEC).

Currently, DanWEC is in the process of building up its infrastructure to become a green lab and the site for future testing of WECs in Denmark at a scale somewhat smaller than required e.g. at the European Maritime Energy Centre (EMEC).

Several WECs have been tested at Hanstholm. In fact, it is expected that phase 4 of *demonstration in large scale*, in the 5-stage development phases, happens at Hanstholm (Figure 5).
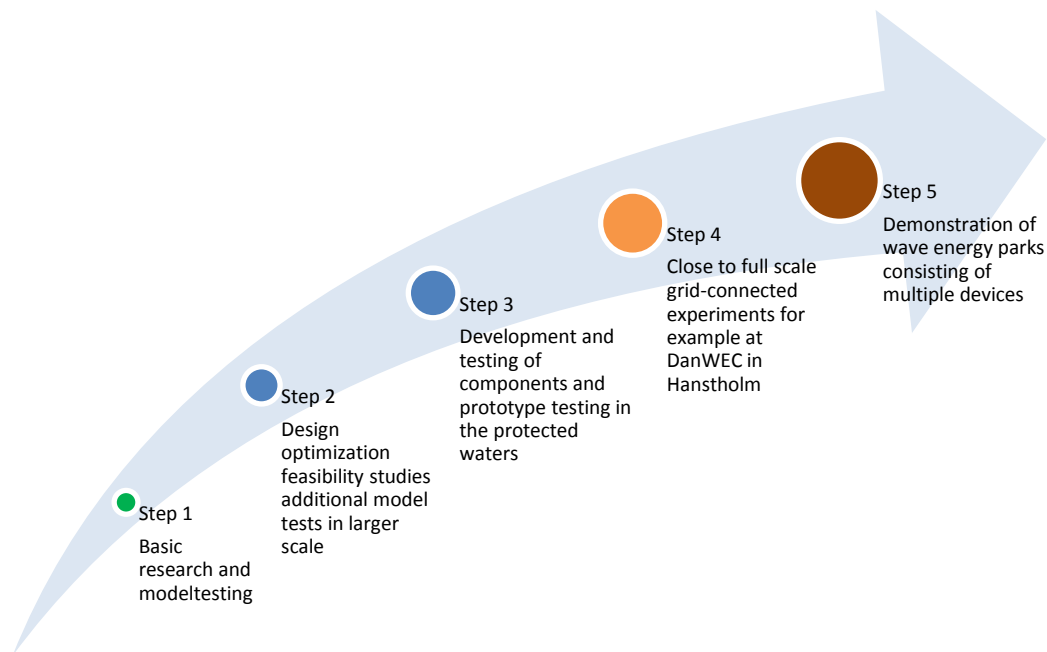
Figure 5. The typical steps of wave energy development (Nielsen, 2012).

The following WECs had or have plans, have been or are being tested at Hanstholm (Nielsen, 2012):

- The **Danish Wave Power point absorber** was tested in scale 1:4 off Hanstholm over a period of 6 months during 1995-96 (Ramboll, 1996).
- The **SSG**, the Seawave Slot-cone Generator, had plans to install various tests plants in the new harbour (Vicinanza, et al., 2012). This project, as well as the company operation, was stopped due to an internal decision of the Board members of the company.
- **WavePlane** (Waveplam, 2013) had permit since October 2008 to August 2009 to be tested at Hanstholm. The plant had a problem with the mooring system and it is currently not deployed.
- **Wavestar** (WaveStar) installed a section of a 1:2 scale machine in Hanstholm in 2009. It holds deployment and power generation permit up to November 2013.
- **Dexawave** (DexaWave) installed a prototype in 2011 on 25 meter deep water. The prototype was a 6 meter wide and 13 meter long test-unit. It had permits for the period July 2009 to August 2012. The plant had a problem with the mooring system and it is currently not deployed.
- In 2011, **Wave Dragon** received support from the Danish funding agency EUDP to prepare a certified design of a full-scale 1.5 MW demonstration unit to the wave conditions at DanWEC (WaveDragon).
- **Resen Energy** has plans to install its "Lever Operated Pivoting Float" (LOPF) in Hanstholm in late summer 2013, with partial support of PSO project (Resen Energy, 2013).
- **Crestwing**, developed by Waveenergyfyn, aims also to deploy and test its WEC at Hanstholm (Crestwing, 2013).

-   **WEPTOS** has plans to install its WEC in a short future, with partial support of PSO project (Pecher et al., 2012).

Figure 6 shows a map of Hanstholm area. The dots show four relevant locations for the study. Wave buoy-data are recorded 1.3 km North-west off the harbour (i.e. Waverider buoy in the figure), at the same location as the forecasts are modelled (i.e. DHI forecasts in the figure); weather data are obtained at the harbour (i.e. weather station in the figure), and the wave and wind technologies are located on the North-East. Wavestar prototype is installed near-shore and the wind turbine ashore. The distance between the Waverider buoy and the weather station is of 1.1 km (i.e. as measured with krak.dk).
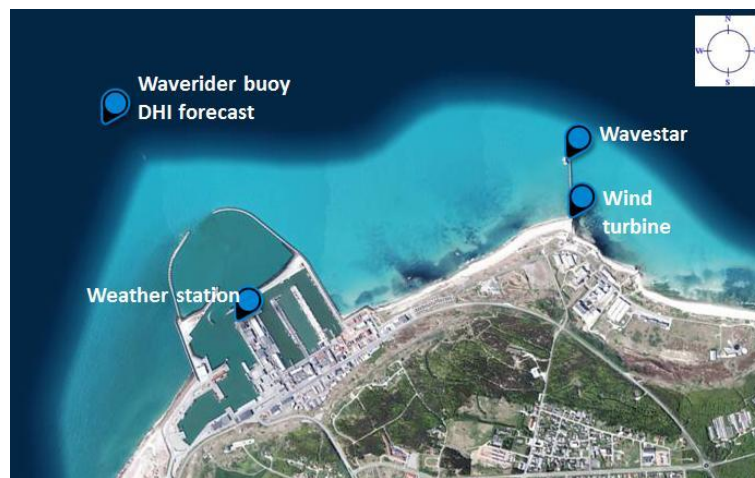
Figure 6 Location of the Waverider buoy, wind and wave forecasts (i.e. DHI forecasts), the weather station, Wavestar prototype and the wind turbine, at Hanstholm, Denmark (©COWI) (kra).

In the comparison between wind forecasts and wind real measurements it is assumed the locations are the same and that the wind resource remains undisturbed from offshore although captured near-shore. In the comparison between winds and waves the former assumption is also accepted, thus, that waves and winds are recorded at the same location. This is further discussed and explained in the "Assumptions" section.

III.3. TIME PERIOD

Typically, a 10-year period of data would be used to characterise the wave climate of a particular site. However, this project focuses on the predictability characteristics of waves rather than on a resource assessment of the site. In fact, whilst there are wave measurements from a number of years, forecast data are limited and comprise the time-limiting factor.

The study covers two periods. One in the autumn and winter seasons of 2010 – 2011 (Period I) and another one in the winter and spring season of 2011 (Period II). This is explained later in detail.

The different time periods within the analysis depend on data validity, the correlation between forecast and measured data, and power production data from the wave and wind technologies.

- Simultaneous and co-located buoy-measurements and wave parameters forecasts, and weather-station measurements and wind parameters forecasts, are available from end of October 2010 to middle of February 2011. Due to validity good data only covers three complete and non-consecutive months.

- There is Wavestar power production data from September 2009 up to present time. However, due to data validity only data from January to May 2011 are used.

- Available wind turbine power production data dates from end of May 2010 up to present time. In order to match it to Wavestar production data, only data from January to May 2011 are used.

The selected time period presents both typical wave conditions as well as three stormy events, on 11th December 2010, 1st January 2011 and 8th February 2011. These allow the analysis of predictability of wave parameters in both situations, in typical and in storm conditions.

Generally at Hanstholm January is the month with the most energetic wave climate, about 6 times more in terms of monthly mean wave power than the less energetic months, April, May, June and July (Waveplam, 2013). Therefore, the time period considered in this study represents the most energetic season.

All times and dates in the study are expressed in the Coordinated Universal Time (UTC) system. To change from Danish local time to UTC time, the following is true:

- DATO (in Danish time: UTC + 1h in winter time; UTC + 2h in Summer time)
- 2010
  - Summer time: changes 28/03/2010 at 2:00 (becomes 3:00): from UTC +1h → UTC+2h
  - *Winter time: files changed on 31.10.2010 at 3:00 (becomes 2:00): from UTC + 2 → UTC +1h*
- 2011
  - *Summer time: changes 27/03/2011 at 2:00 (becomes 3:00): from UTC +1h → UTC+2h*

III.4. DATA SOURCES: OBSERVED AND FORECAST WAVE AND WIND DATA[2]

III.4.1. WAVE DATA

WAVE PARAMETERS

For this study it is suitable to define the wave resource by the significant wave height H_s and the zero crossing period T_z. These parameters can be approximated by $H_{m0}=4\sqrt{m_0}$ and $T_{02}=\sqrt{(m_0/m_2)}$, respectively (Ramboll, 1999a). Thus, this study is based on records of H_{m0} and T_{02}. The maximum wave height H_{max} has also been included, since its evaluation can lead to useful results on buoy measurement errors and WECs' operation and survivability conditions.

OBSERVED WAVE DATA

There are three data sets of wave measurements available: from Kystdirektoratet, from Aalborg Univeristy (AAU) – DanWEC and from Wavestar. Only the two former have been used in the study.

BUOY-MEASURED WAVE DATA FROM KYSTDIREKTORATET

Environmental measurements have been provided by a Datawell non-directional Waverider buoy (Figure 7) (i.e. model 0.9 AISI 316: 0.9 m diameter) operated by The Danish Coastal Authority (i.e. Kystdirektoratet in Danish). Hanstholm Waverider buoy identifier is 1022.

Figure 7. Waverider buoys installed at Galway Bay, Ireland (left) and at the Danish Coasts (Kys) (right).

The buoy is positioned at 6332100 North and 474700 East in the UTM32 Euref89 reference system, at a water depth of about 17 m and about 1.3 km offshore (Figure 8).

Kystdirektoratet wave measured data, i.e. data returned by the Waverider buoy, are half-hourly records with two decimals resolution. Only statistical data are available. Data files received include the following fields:

- Recording time (year, month, day, hour): DATO (in Danish time: UTC + 1h in winter time; UTC + 2h in Summer time).

---

[2] Since the authors do not own most of tha data, no CD has been created with the data. If interested in knowing more about the data please refer to julia.fernandez.chozas@gmail.com.

- For winter time: files changed on 30/10/2010 at 03:00 (becomes 02:00) → UTC +1h.
- For summer time: files changed on 27/03/2011 at 02:00 (becomes 03:00) → UTC+2h.
- Significant wave height: H_M0 (m).
- Average wave period: T_AVG (s).
- Maximum wave height: H_MAX (m).

→ Observed wave data indicate the average of the following 30 minutes.
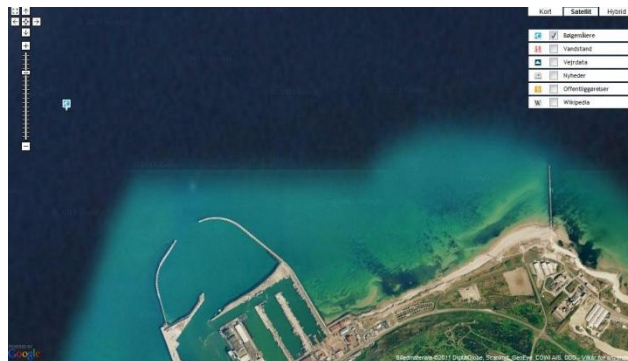
Figure 8. Buoy location at Hanstholm (Kys).

The accuracies in heave measurements indicated by the buoy manufacturer are:
- < 0.5% of measured value after calibration.
- < 1.0% of measured value after 3 year.

Wave data used date from 29/09/2010 at 00:00 to 31/05/2011 at 23:30 (in received time). Data for 2010 have been retrieved from Kystdirektoratet (personal contact) and data for 2011 from a service of Aalborg University (where time domain parameters have been used).

Invalid data in this period are:
- From 25/03/2011 at 22:30 to 11/04/2011 at 08:00 (UTC).
- From 13/01/2011 at 00:00 to 16/01/2011 at 09:30 (UTC).
- From 21/11/2010 at 00:00 to 11/12/2010 at 09:30 (UTC).
- From 13/01/2011 at 11:30 to 16/01/2011 at 09:30 (UTC).

Wave data from Hanstholm are available from 1998. Known files are:
- From 01/01/2011 to 31/12/2011 (in received time), ½-hour detail.
- From 29/09/2010 at 00:00 to 09/02/2011 at 22:30 (in received time), ½-hour detail.
- From 01/01/2006 to 23/08/2010 (in received time), ½-hour detail.
- From 01/01/2005 to 25/02/2009 (in received time), ½-hour detail.

There are also available data for close locations to Hanstholm, from:

- Fjaltring: identifier 2031, located at 6259466 North an 441976 East. Water depth about 17.5 m:
    - From 26/01/2005 to 25/02/2009 (in received time), ½-hour detail.
    - From 11/12/1999 to 26/01/2005 (in received time), 3-hour detail.

- Hirtshals: identifier 1041; located at 6381744 North, 524559 East. Water depth about 17 m:
    - From 28/03/2006 to 25/02/2009 (in received time), ½-hour detail.
    - From 11/08/1999 to 28/03/2006 (in received time), 3-hour detail.

Data can be found at Kystdirektoratet webpage (Kys). Relevant comments on wave measurements are available at: *borgere.kyst.dk/opmaaling-af-boelger.html.*

Data can also be downloaded from the server (http://176.34.96.135/) as a service of Aalborg University (AAU) (Figure 9). Both frequency domain and time domain parameters are available:

- Frequency domain parameters, as half-hour time series, are calculated by AAU.
- Time domain parameters are those calculated by the buoy (same as Kystdirektoratet data) (format *.hiw). Time domain parameters files are all labelled by the start time of the data collection they are based on, therefore, the files have timestamps referring to the beginning of the displacement collection.
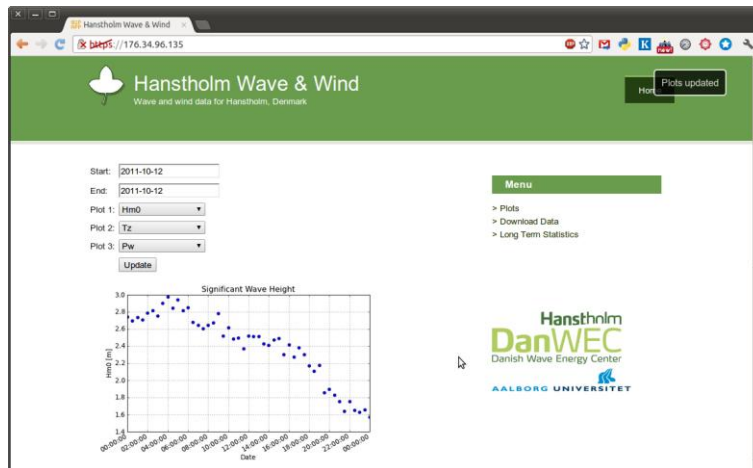
Figure 9. Server of Aalborg University where wave and wind data from Hanstholm and DanWEC can be found.

Comments on matching of data from Kystdirektoratet and from AAU:

- H_s (determined from time-domain analysis) is slightly smaller than H_{mo} (determined from spectrum). Figueras Alvarez (2010) shows a liner relation of $H_s=0.93H_{mo}$. The analysis accepts a linear relation of 1 to 1.
- H_{max} coincides.
- T_{ave} is very similar to T_{02}, although not exactly the same.

- The number of decimals of the data differs: T_{ave} from Kystdirektoratet is rounded-down to one decimal, data from AAU has 2 decimals.

WAVESTAR-MEASURED WAVE DATA

The Wavestar model at Hanstholm has been recording wave data since its installation on September 2009. Wavestar has two wave sensors, an ultrasonic and a pressure sensor, in order to double check that measurements are correct. The ultrasonic sensor (Figure 10) is not working in the presence of rain, water, spray or snow. The pressure sensor is mounted on the sea surface at about 6 m water depth. Data is recovered from the latter sensor by applying linear theory (2D analysis) and hence no wave reflection considered, leading into eventual errors.

Wave data are available at Wavestar´s webpage (WaveStar), precisely in the monthly reports delivered to Energinet.dk.
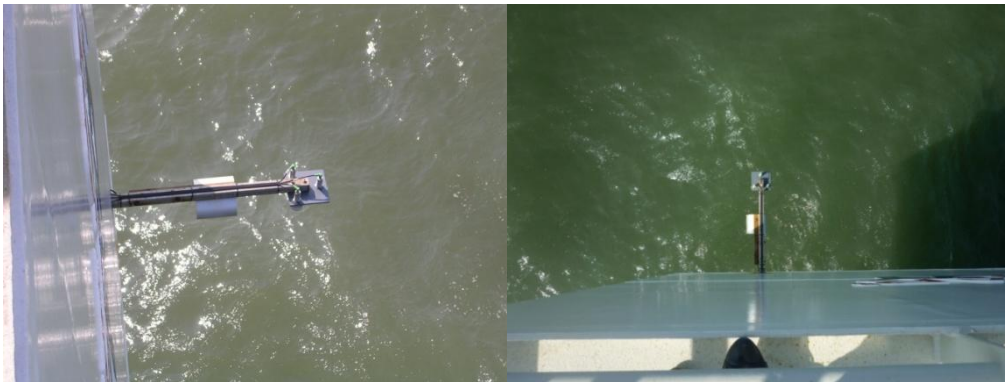
Figure 10 Ultrasonic sensor at Wavestar (Picture from May 2011) (WaveStar).

FORECAST WAVE DATA

Two forecasts are available: DHI and StormGeo. All forecasts used in the study are from DHI, although DHI calculates its forecast based on StormGeo model outputs.

DANISH HYDRAULIC INSTITUTE – DHI FORECAST WAVE DATA

Weather forecasts have been calculated by the spectral wave module of MIKE 21 from the Danish Hydraulic Institute (DHI), a model based on the wave action conservation equation (where the directional-frequency wave action spectrum is the dependent variable). The service is part of The Water Forecast program (Kirkegaard, et al., 2010), (Figure 11). Forecasts are calculated at Lat. 57.132°N, Lon. 8.5816°E.
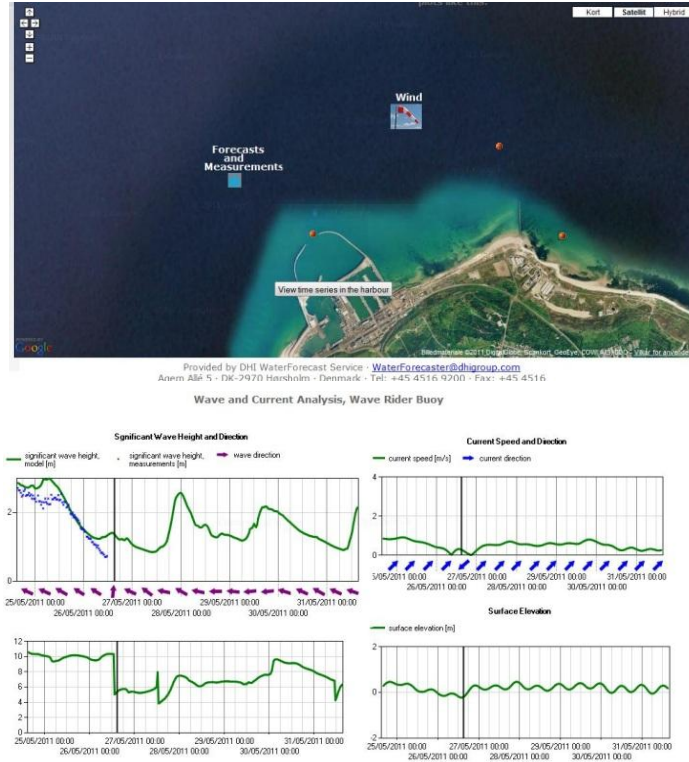
Figure 11. The WaterForecast - a DHI Service (Kirkegaard, et al., 2010).

The forecast wave model is a flexible mesh model with varying element size. In and just around Hanstholm the resolution is 50 m-100 m, while the resolution increases gradually to about 1000 m at a distance of 12 km from Hanstholm (Figure 12). The resolution precisely at the study location is about 150 m. It is a point located in the transition area.
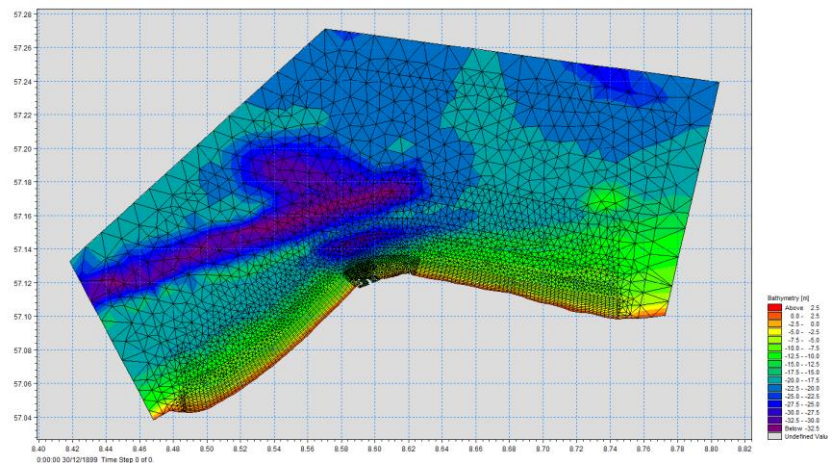
Figure 12. Resolution of The Water Forecast around Hanstholm (DHI).

Forecasts are calculated every 12 hours and provide half-hourly records, with two decimals resolution, of the following wave and wind parameters:
 - Time (UTC)

33

- Sign. Wave Height Hm0 (m)
- Max. Wave Height Hmax (m)
- Peak Wave Period Tp (s)
- Wave Period T01 (s)
- Wave Period T02 (s)
- Wave Period Tm10 (s)
- *Sign. Wave Height Swell (m)
- *Peak Wave Period Swell (s)
- *Wave Period T01 Swell (s)
- *Wave Period T02 Swell (s)
- *Wave Period Tm10 Swell (s)
- *Mean Wave Direction MWD Swell (deg)
- Peak Wave Direction PWD (deg)
- Mean Wave Direction MWD (deg)
- Wind Speed (m/s)
- Wind Direction (deg)

The parameters marked with (*) are only included in the data files from 18/12/2010 at 19:00 and onwards.

Forecast files contain 24 hour hindcast and 5, 5½ or 6 days forecast:
- Files received at 07:00 contain 5½-day forecast (i.e. 265 data rows, 5.5*24*2=264).
- Files received at 19:00 (from 26/10/2010 to 02/11/2010) contain 6 days forecast (i.e. 289 data rows, 6*24*2=288).
- Files received at 19:00 (from 03/11/2010 to 09/02/2011) contain 5 days forecast (i.e. 241 data rows, 5*24*2=240).

➔ Hindcasts have not been considered in the study, and forecasts have been limited to 5 days.

Available forecast data are:
- From 26/10/2010 at 19:00 to 09/03/2011 at 7:00 (in received time).

Used forecast data are:
- From 26/10/2010 at 19:00 to 09/02/2011 22:30 (in received time).

Invalid data are:
- File received 14/01/2011 at 12:00 (UTC).
- From 14/01/2011 at 00:00 to 14/01/2011 at 11:30, corresponding to 23 data rows, forecasts are negative.

➔ Forecasts indicate central estimates, the central half-hour values, i.e. the middle of the half-hour period.

STORMGEO FORECAST WAVE DATA

There is available forecast data from StormGeo, a Norwegian meteorological company (Storm Geo, 2012). The weather forecasts reach 3 days into the future and provide hourly data. Forecasts are calculated every 12 hours or every 24 hours.

Forecasts arrive either with 0-hour delay or with 10, 11 or 12-hour delay, which is the reason why the forecast horizon is negative sometimes.
- Files received at 00:00 contain 3 days forecast (i.e. 72 data rows, equals 3*24).
  - Data have no delay[3].
- Files received at 12:00 contain 3 days forecast (i.e. 72 data rows, equals 3*24).
  - Data have 12-hour delay.
  - The forecast horizon becomes negative sometimes.

Data files available to the authors are from 29/09/2010 at 10:39 to 15/11/2010 00:00 (in received time). Data files include the following fields:
- TimeReceived[4]
- Localtime [5]
- Temperature
- WindDirection
- WindSpd_10m
- WindSpd_10m_gust
- WindSpd_50m
- WindSpd_50m_gust
- WaveHeight_max
- WavePeriod_peak
- WaveHeight_wind
- WaveDirection_wind
- WavePeriod_wind
- WaveHeight_swell
- WaveDirection_swell
- WavePeriod_swell
- WaveHeight_total
- WaveDirection_total
- WavePeriod_total

---

[3] The source does not specified wether there is no delay in the data because the program runs very fast or because it is hindcast data.
[4, 5] The source does not confirm whether these times are Danish or UTC time.

The exact location of StormGeo forecasts need to be investigated. Probably forecasts are calculated at Wavestar's location, aside Roshage pier and at 6 m water depths. Thus, forecasts should take into account near-shore wave patterns and the effects of the pier to the waves and of the mainland to the winds.

III.4.2. WIND DATA

The study is based on half-hour time series of the wind speed (u_{wind}), mean wind direction (MWD_{wind}) and wind power (P_{wind}).

MEASURED WIND DATA

WEATHER STATION MEASURED WIND DATA FROM KYSTDIREKTORATET

Wind measurements are provided by a weather station (Figure 13) from The Danish Coastal Authority (i.e. identifier 3110).
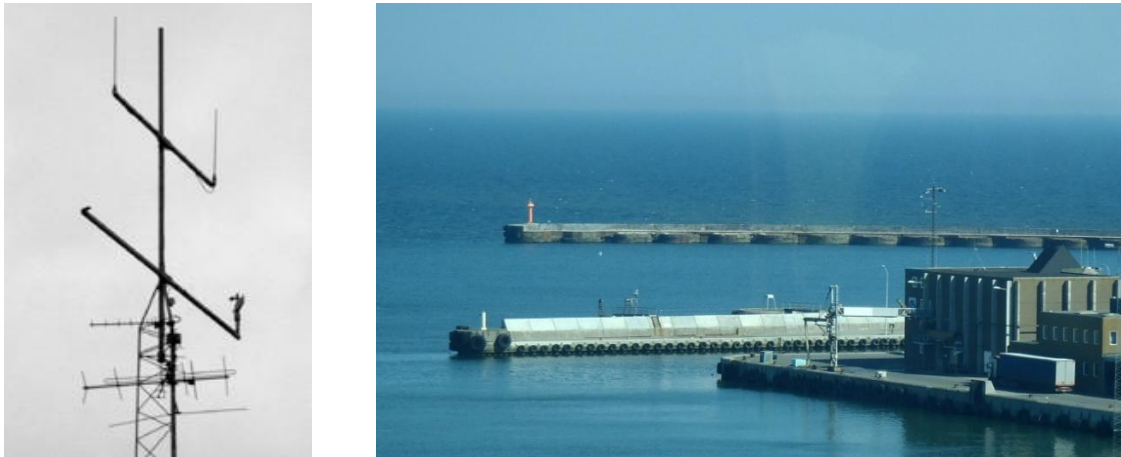
Figure 13. Weather station at Hanstholm harbour (Kys).

The station is located 20 m above ground and is positioned at 6331036 North, 475467 East according to the UTM32 Euref89 reference system (Figure 14).

Figure 14. Weather station location at Hanstholm (Kys).

Kystdirektoratet wind measured data, i.e. data returned by the weather station, are ten-minute records with two decimals resolution. Data files received include the following fields:

- Recording time (year, month, day, hour): DATO (in Danish time: UTC + 1h in winter time; UTC + 2h in Summer time.
  - For winter time: files changed on 30/10/2010 at 03:00 (becomes 02:00) → UTC +1h.
  - For summer time: files changed on 27/03/2011 at 02:00 (becomes 03:00) → UTC+2h.
- Wind speed: HASTIGHED (m/s):
  - Provides the average value of the last 10 minutes.
- Wind direction: RETNING (degrees):
  - Wind direction is with respect to North, i.e. 0° and 360° wind blows from North, 90° wind blows from East, 180° wind blows from South, 270° wind blows from West.

Wind data from AAU – DanWEC server (for 2011) include:

- Actual Windspeed: 1 minute resolution.
- Mean Windspeed: 1 minute resolution.
- Actual wind direction: 1 minute resolution.
- MWD: 1 minute resolution.
- Vindstød – (gusts): 1 minute resolution.

→ Measured wind data (from Kystdirektoratet and from AAU) indicate the average of the past 10-minute values.

The inaccuracies in the weather station acquisition system are unknown.

Wind data used date from 29/09/2010 at 00:00 to 31/05/2011 at 23:30 (in received time). Data for 2010 have been retrieved from Kystdirektoratet (personal contact) and data for 2011 from the AAU – DanWEC server.

To the authors knowledge there are no periods of invalid data.

Wind data from Hanstholm are available since 2005. Known data files are:

- From 01/01/2006 to 23/08/2010 (in received time) - 10 minutes detail.
- From 01/01/2005 to 25/02/2009 (in received time) - 1 hour detail.

There are available wind data for close locations to Hanstholm, from:

- Thyborøn: identifier 4200:
  - From 10/12/1991 to 23/02/2009 (in received time) - 1 hour detail.
- Hirtshals: identifier 1410:
  - From 10/08/1999 to 25/02/2009 (in received time) - 1 hour detail.

Data can be found at Kystdirektoratet webpage (Kys). Data can also be downloaded from the server (http://176.34.96.135/) as a service of Aalborg University, which provides additional environmental data such as:

- Barometer (hPa) → 1 minute resolution.
- Temperature (gC)→ 1 minute resolution.
- Data validity (100%) → 30 minutes resolution.
- Sea level (m) → 1 minute resolution.

WAVESTAR-MEASURED WIND DATA

The Wavestar model at Hanstholm has been recording wind data since its installation on September 2009, however, data validity have not been checked. A new weather-station was installed on May 2011, at 23 m height, which provides 10-minute wind measurements.

FORECAST WIND DATA

Forecast wind data are available from DHI and from Storm Geo.

III.4.3. MATCH OF FORECAST AND OBSERVED WAVE DATA

The study is based on half-hour time series (every '00 and '30 hour) of wave and wind parameters. These indicate the central half-hour value, i.e. the average value of the previous and the next 15 minutes. Hence, a data given on '00 indicates the average value for the period covering from '45 to '15.

The Section above has shown that:

- Measured wave data from Kystdirektoratet and from AAU indicate the average of the following half-hour.
- Measured wind data from Kystdirektoratet and from AAU indicate the average of the previous 10 minutes.
- DHI wave and wind forecast indicate the central half-hour value.

As a result, observed data is re-calculated in order to match forecast data.

For the wave records, to calculate half-hour average values from the 30-minute records the following is used:

- Measurements made at:
  - t'00
  - t'30
  - t1'00
- To calculate the mean value at t'30: = [(value at t'00) + (value at t'30)]/2
- To calculate the mean value at t1'00: = [(value at 't30) + (value at t1'00)]/2

For the wind records, to calculate half-hour average values from the 10-minute records the following is used:

- Measurements made at:
    - t0'40
    - t0'50
    - t'00
    - t'10
    - t'20
    - t'30
    - t'40
    - t'50
- To calculate the mean value at t'00:
    - t'00= [(value at t'00) + (value at t'10) + (value at t0'50)/2 + value at t'20/2)] /3
- To calculate the mean value at t'30:
    - t'30= [(value at t'30) + (value at t'40) + (value at t'20)/2 + value at t'50/2)] /3

III.5. WAVE AND WIND CONDITIONS AT HANSTHOLM

III.5.1. WAVE CONDITIONS AT HANSTHOLM

LONG-TERM WAVE CLIMATE

The long term mean energy flux is estimated at 7 kW/m, at water depths of 17 meters, with mean significant wave heights of 1.5 m and crossing period of 5 s. Mean wave direction is primarily West-North-West and West, i.e. waves arriving from the northern part of the Atlantic Ocean (Margheritini, 2012). The 100 year wave is 8.3 m. In winter storms significant wave heights can be of more than 5 meters (Kirkegaard, et al., 2010). TABLE I presents the long term main characteristics of the site.

TABLE I
Wave Characteristics at Hanstholm (Margheritini, 2012), (Nielsen, et al., 2010).

Water depth	12 -30 m
Design H_s, 10 year	6.6 m
Design T_z , 10 year	10 s
Max. wind speed	30 m/s
Max. current speed	2 m/s
Max. high water level	1.6 m
Min. low water level	-1.5 m
Max. ice thickness	-
Wave power annual average	7.1 kW/m

In front of the port, there can be East-going currents running up to 2 m/s (Juhl, 1994). Kirkegaard (1987) estimates a 100-year current speed of 0.72 m/s in the Danish Northe Sea.

The wave climate is characterized by a wind sea on top of a non-constant swell.

WAVE CONDITIONS IN THE STUDY PERIOD

Throughout the study, the whole study period is divided into two periods: from October 2010 to February 2011 (Period I), and from January 2011 to May 2011 (Period II).

This section shows the wave conditions of both Period I and II provide a fairly valid representation of the wave climate found at Hanstholm typically in these months.

Mean wave power in Period I, i.e. 9 kW/m, is 25% higher than the mean annual wave power, i.e. 7.1 kW/m, whereas the mean wave power in Period II, i.e. 5.5 kW/m, is 24% smaller than the average. This is due to the strong seasonal variability of the wave conditions at Hanstholm. This fact is analysed by Ramboll (1999b) and is reviewed in depth in Chapter VII.

PERIOD I

Period I embraces from 26/10/2010 to 9/02/2011. Figure 15 shows the mean wave parameters throughout this period.
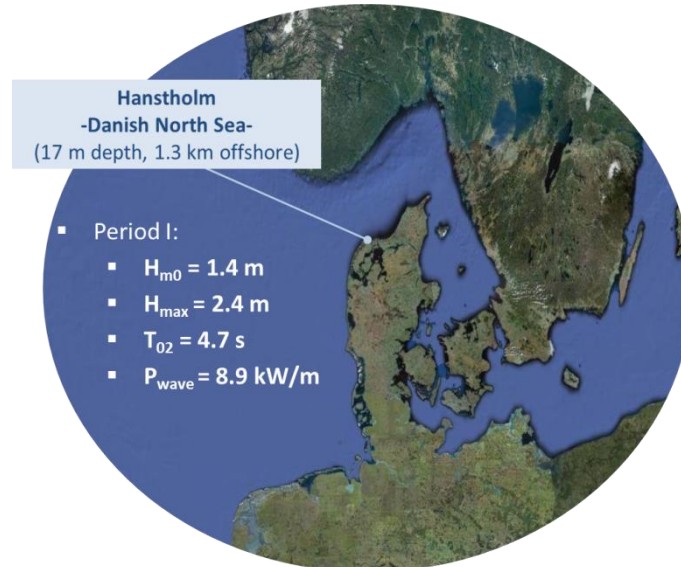
Figure 15. Hanstholm location and mean wave parameters in Period I, from 26/10/2010 to 9/02/2011.

Figure 16 depicts the wave conditions at Hanstholm from 26/10/2010 to 9/02/2011, in terms of H_{m0}, T_{02} and the contribution of each sea state, in percentage, to the mean wave power of the study period. Calculations are based on buoy-measurements of H_{m0} and T_{02} over 4 months. Figure 16 shows a dominant wind sea with a peak at $H_{m0}=2.2$ m and $T_{02}=5.3$ s and a secondary peak at $H_{m0}=4$ m and $T_{02}=6.5$ s.
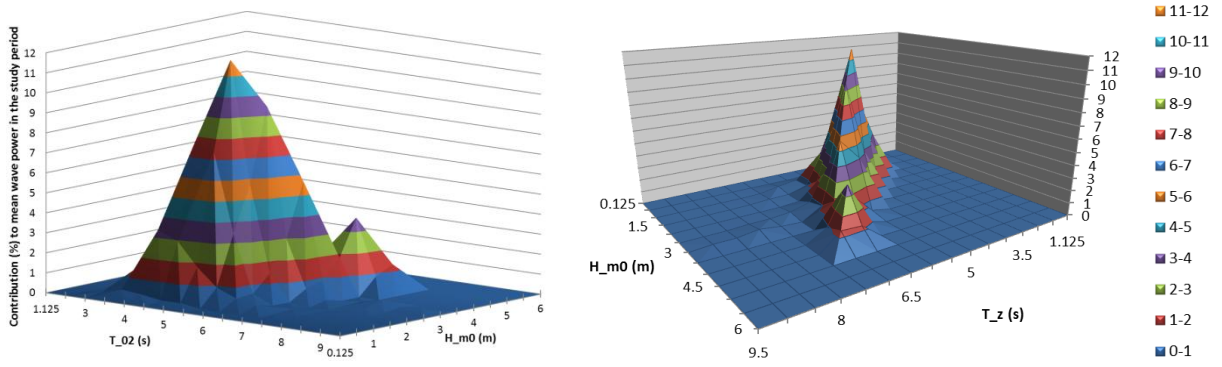
Figure 16. Wave conditions at Hanstholm from 26/10/2010 to 09/02/2011 in terms of H_{m0}, T_{02} and contribution of each sea state (in percentage) to the mean wave power of the study period.

Figure 17 shows the scatter diagram of Hanstholm in Period I, in terms of H_{m0} (m) and T_{02} (s). The dimension of the bins has been limited to 0.5 m for H_{m0} and 0.5 s for T_{02} in order to provide a reasonable resolution to the results. H_{m0} and T_{02} values indicate the mean values of the bins. The numbers in the matrix indicate the contribution of each sea state to the mean wave power, in absolute value. The colours give a graphical view of the results: green indicates no contribution and red maximum contribution.

$P_{wave}*Prob.$	T_{02}													
H_{mo}	2.5	3	3.5	4	4.5	5	5.5	6	6.5	7	7.5	8	8.5	9
0.125	0	0	0.00	0	0	0	0	0	0	0	0	0	0	0
0.5	0.00	0.01	0.03	0.02	0.01	0.01	0.00	0.00	0	0	0	0	0	0
1	0	0.00	0.10	0.24	0.21	0.13	0.07	0.04	0.02	0.00	0	0	0	0
1.5	0	0	0.01	0.29	0.55	0.53	0.25	0.04	0.01	0.01	0.00	0	0	0
2	0	0	0	0.01	0.32	0.85	0.41	0.10	0.01	0	0	0	0	0
2.5	0	0	0	0	0	0.28	0.68	0.22	0.04	0.01	0.01	0.01	0	0
3	0	0	0	0	0	0.01	0.30	0.41	0.06	0	0.01	0.02	0.01	0.01
3.5	0	0	0	0	0	0	0.02	0.13	0.13	0	0	0	0	0
4	0	0	0	0	0	0	0	0.03	0.26	0.06	0	0	0	0
4.5	0	0	0	0	0	0	0	0	0.09	0.09	0	0	0	0
5	0	0	0	0	0	0	0	0	0	0	0	0	0	0

Figure 17. Scatter diagram of Hanstholm in Period I.

TABLE II presents the mean and maximum value of the different wave parameters H_{m0}, H_{max}, T_{02}, P_{wave} and MWD_{wave} at Hanstholm from October 2010 to February 2011. It also presents the probability of occurrence of different states i.e. the less energetic and infrequent conditions as well as the most energetic and infrequent conditions, occurring less than 1% and less than 10% of the time. These results are based on buoy-measured data.

TABLE II
Occurrence of Wave Parameters H_{m0}, H_{max}, T_{02}, P_{wave} and MWD_{wave} at Hanstholm from 26/10/2010 to 09/02/2011.

	Mean	Max.	<1% time	<10% time	<10% time	<1% time	Days	N
H_{m0} (m)	1.4	4.7	≤ 0.4	≤ 0.7	≥ 2.3	≥ 3.7	87	4157
H_{max} (m)	2.4	8.5	≤ 0.7	≤ 1.1	≥ 3.8	≥ 6.0	87	4157
T_{02} (s)	4.7	8.8	≤ 3.1	≤ 3.8	≥ 5.7	≥ 6.7	87	4157
P_{wave} (kW/m)	8.9	98.6	≤ 0.4	≤ 1.3	≥ 19.6	≥ 58.4	87	4157
MWD_{wave} (°)	267	360	≤ 3	≤ 28	≥ 325	≥ 357	84	4015

* MWD_{wave} *has been calculated from DHI forecast data, since the Waverider buoy at Hanstholm is not directional.*

Since WECs are designed to harness the available wave energy, TABLE III shows the probability of occurrence of each parameter times the available wave power. Therefore, it indicates the wave conditions where most of the power is concentrated. Figure 18 also illustrates this.

TABLE III
Contribution to the Mean Energy Content of the Wave Parameters H_{m0} and T_{02} at Hanstholm in Period I.

	Mean	Max	<1% time	<10% time	<10% time	<1% time	Days	N
H_{m0} (m)	2.2	5.0	≤ 0.5	≤ 1.0	≥ 3.5	≥ 5.0	112	5392
T_{02} (s)	5.3	9.3	≤ 3.5	≤ 4.5	≥ 6.5	≥ 7.5	112	5392
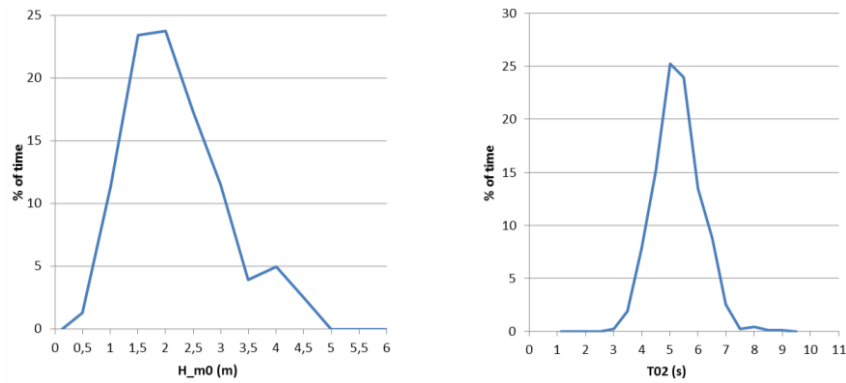
Figure 18 Contribution, in percentage, of H_{m0} (left) and T_{02} (right) to the mean energy content at Hanstholm in Period I.

PERIOD II

Period II embraces from 01/01/2011 to 31/05/2011. Figure 19 shows the mean wave parameters throughout this period.
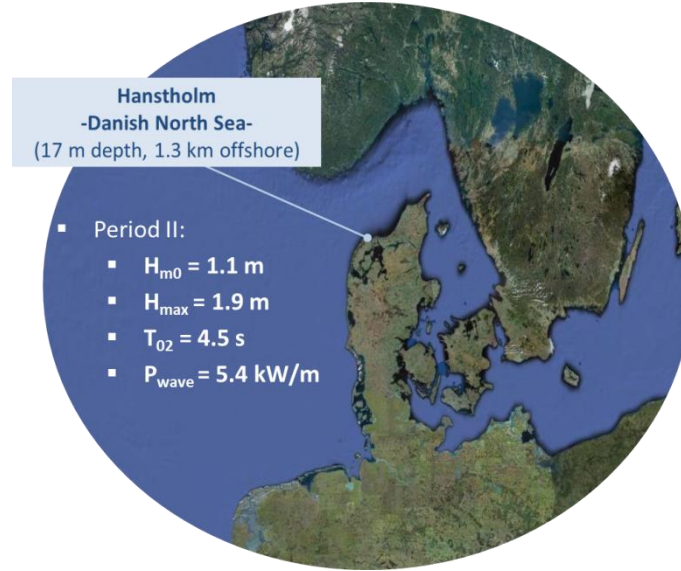
Figure 19. Hanstholm location and mean wave parameters in period II, from 01/01/2011 to 31/05/2011.

TABLE IV presents the mean and the maximum value of the different wave parameters H_{m0}, H_{max}, T_{02} and P_{wave} at Hanstholm in Period II. It also presents the probability of occurrence of different states i.e. the less energetic and infrequent conditions as well as the most energetic and infrequent conditions, occurring less than 1% and less than 10% of the time. These results are based on buoy-measured data.

TABLE IV
Occurrence of Wave Parameters H_{m0}, H_{max}, T_{02} and P_{wave} at Hanstholm from 01/01/2011 to 31/05/2011.

	Mean	Max	<1% time	<10% time	<10% time	<1% time	Days	N
H_{m0} (m)	1.1	4.3	≤ 0.3	≤ 0.5	≥ 2.0	≥ 3.1	130	6240
H_{max} (m)	1.9	7.6	≤ 0.5	≤ 0.8	≥ 3.4	≥ 5.3	130	6240
T_{02} (s)	4.5	8.5	≤ 2.7	≤ 3.3	≥ 5.7	≥ 6.7	130	6240
P_{wave} (kW/m)	5.4	91.8	≤ 0.2	≤ 0.5	≥ 12.8	≥ 41.1	130	6240

SWELL

The three following figures show the H_{m0} and T_{02} swell component of the waves. Figures are based on DHI forecast data, with a forecast horizon of 0 hours. It can be seen that swell is not constant but only present sometimes.

Figure 20 illustrates H_{m0} and T_{02} swell components from 18/12/2010 to 8/03/2011. The swell component of H_{m0} reaches 3.2 m, and T_{02} reaches 9 seconds. Figure 21 shows the evolution of H_{m0} from 28/12/2010 to 11/02/2011.

43
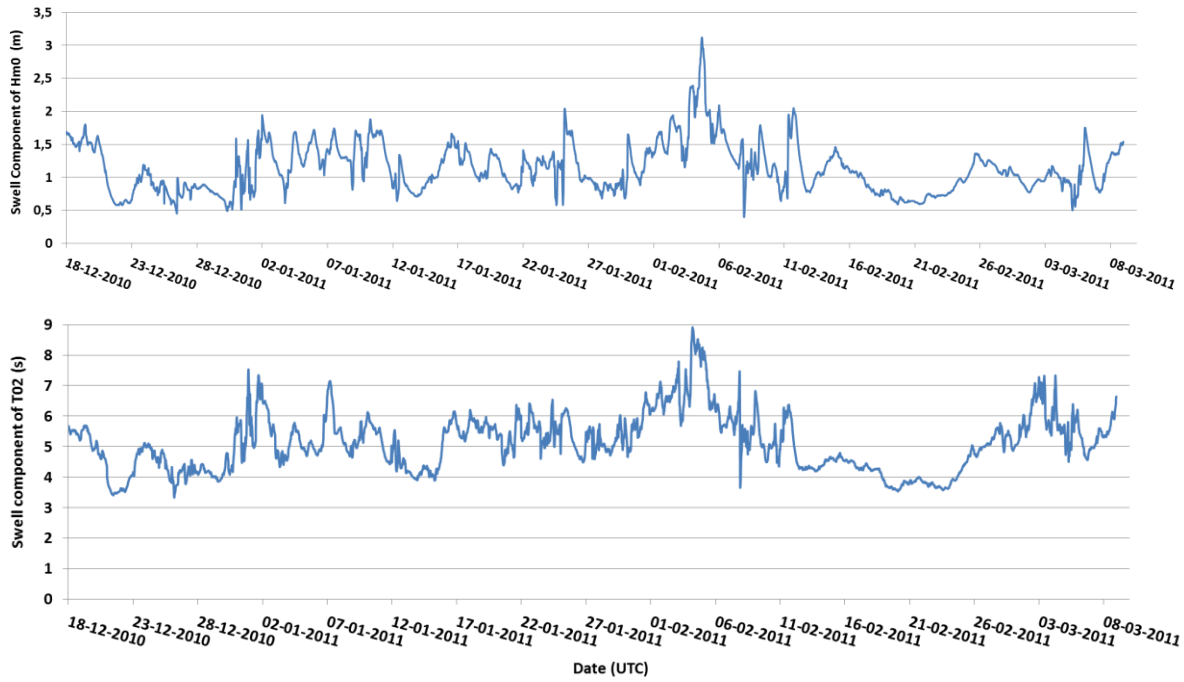
Figure 20. Evolution of H_{m0} (above) and T_{02} (below) swell components from 18/12/2010 to 8/03/2011.
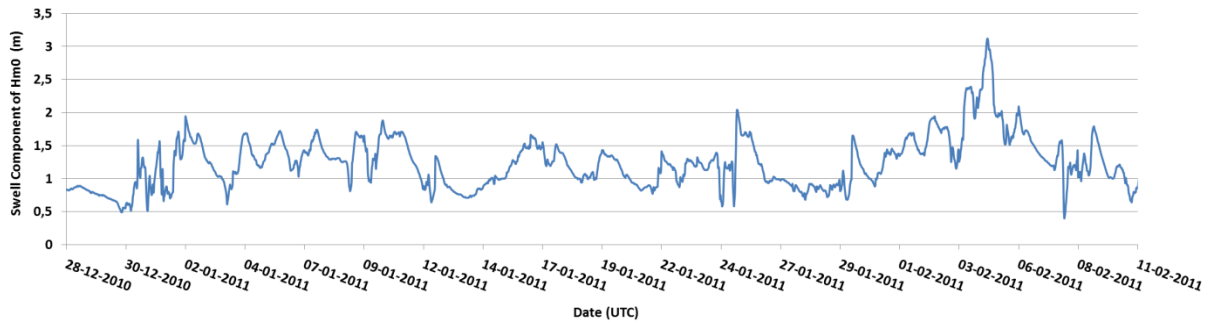
Figure 21. Evolution of H_{m0} swell component from 28/12/2010 to 11/02/2011.

III.5.2. WIND CONDITIONS AT HANSTHOLM

LONG-TERM WIND CLIMATE

Long-term prevailing wind directions are West, South-West and East, the strongest winds coming from North-West, West and South-West with wind speeds up to 10 m/s (Frydendahl, 1971). The maximum wind speed record is 30 m/s (Nielsen, et al., 2010) and there is strong seasonal variability (Cappelen, et al., 1999).

WIND CONDITIONS IN THE STUDY PERIOD

PERIOD I

TABLE V shows the mean and maximum value values of the wind speed (u_{wind}), MWD_{wind} and P_{wind} at Hanstholm from October 2010 to February 2011. It also presents the probability

of occurrence of different states i.e. the less energetic and infrequent conditions as well as the most energetic and infrequent conditions, occurring less than 1% and less than 10% of the time. These results are based on weather-station measured data.

u_{wind}, MWD_{wind} and P_{wind} characteristics at Hanstholm from 26/10/2010 to 09/02/201.

	Mean	Max	<1% time	<10% time	<10% time	<1% time	N	Days
u_{wind} (m/s)	7.7	21.5	≤ 1.5	≤ 3.6	≤ 12.5	≤ 17.0	6386	133
MWD_{wind} (°)	171	357	≤ 14	≤ 49	≤ 299	≤ 345	6386	133
P_{wind} (W/m^2)	472	6141	≤ 2	≤ 28	≤ 1196	≤ 3013	6386	133

PERIOD II

TABLE VI shows the mean and maximum value values of the wind speed, MWD_{wind} and P_{wind} at Hanstholm from January to May 2011. It also presents the probability of occurrence of different states i.e. the less energetic and infrequent conditions as well as the most energetic and infrequent conditions, occurring less than 1% and less than 10% of the time. These results are based on weather-station measured data.

TABLE VI
u_{wind}, MWD_{wind} and P_{wind} characteristics at Hanstholm from 01/01/2011 to 31/05/2011.

	Mean	Max	<1% time	<10% time	<10% time	<1% time	Days	N
u_{wind} (m/s)	7.1	21.5	≤ 0.2	≤ 2.9	≥ 11.7	≥ 15.8	151	7250
MWD_{wind} (°)	188	358	≤ 19	≤ 74	≥ 277	≥ 336	151	7250
P_{wind} (W/m^2)	387	6140	≤ 0	≤ 15	≥ 968	≥ 2418	151	7250

Prevailing mean wind direction in Period II is South-West, which coincides with the direction of the strongest winds, between 15 and 20 m/s, along with North-West and West directions. Most wind speeds vary in the range [5, 10) m/s and the average wind speed is close to 7 m/s (Figure 22, TABLE VI).
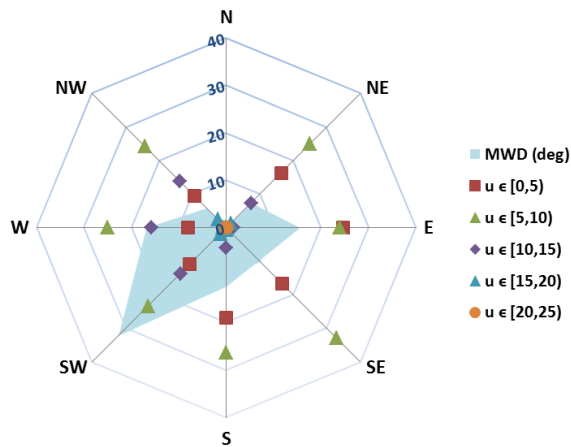
Figure 22. Wind Rose at Hanstholm throughout the study period. Numbers express percentage of time.

It is interesting to investigate whether the near-shore terrain at Hanstholm affects the wind pattern. Hanstholm faces the sea from South-west to North-east direction. TABLE VII provides the same results as TABLE VI but excluding the wind speeds arriving from direction contained in the interval [45,220].

TABLE VII

Mean and Maximum values of u_{wind}, MWD_{wind} and P_{wind} at Hanstholm from 01/01/2011 to 31/05/2011, excluding all MWD_{wind} in the interval [45,220].

	Mean	Max	N	days
u_{wind} (m/s)	7.8	21.5	3017	63
MWD_{wind} (°)	240	358	3017	63
P_{wind} (W/m^2)	465	6141	3017	63

The comparison between TABLE VI and TABLE VII shows slight differences between the wind speed average values for the period. Therefore, the influence of the land in the wind patterns will be disregarded throughout the study.

III.5.3. SUMMARY OF WAVE AND WIND CONDITIONS AT HANSTHOLM

TABLE VIII

Occurrence of Wave Parameters H_{m0}, H_{max}, T_{02} and P_{wave} and Wind Parameters u_{wind}, MWD_{wind} and P_{wind} at Hanstholm in Period I (from October 2010 to February 2011).

	Mean	Max	<1% time	<10% time	<10% time	<1% time	Days	N
H_{m0} (m)	1.4	4.7	≤ 0.4	≤ 0.7	≥ 2.3	≥ 3.7	87	4157
H_{max} (m)	2.4	8.5	≤ 0.7	≤ 1.1	≥ 3.8	≥ 6.0	87	4157
T_{02} (s)	4.7	8.8	≤ 3.1	≤ 3.8	≥ 5.7	≥ 6.7	87	4157
P_{wave} (kW/m)	8.9	99	≤ 0.4	≤ 1.3	≥ 20	≥ 59	87	4157
u_{wind} (m/s)	7.7	21.5	≤ 1.5	≤ 3.6	≤ 12.5	≤ 17.0	133	6386
MWD_{wind} (°)	171	357	≤ 14	≤ 49	≤ 299	≤ 345	133	6386
P_{wind} (W/m^2)	472	6141	≤ 2	≤ 28	≤ 1196	≤ 3013	133	6386

TABLE IX

Occurrence of Wave Parameters H_{m0}, H_{max}, T_{02} and P_{wave} and Wind Parameters u_{wind}, MWD_{wind} and P_{wind} at Hanstholm in Period II (from January to May 2011).

	Mean	Max	<1% time	<10% time	<10% time	<1% time	Days	N
H_{m0} (m)	1.1	4.4	≤ 0.3	≤ 0.5	≥ 2	≥ 3.1	130	6240
H_{max} (m)	1.9	8	≤ 0.5	≤ 0.8	≥ 3.4	≥ 5.4	130	6240
T_{02} (s)	4.5	8.8	≤ 2.7	≤ 3.3	≥ 5.7	≥ 6.7	130	6240
P_{wave} (kW/m)	5.4	92	≤ 0.2	≤ 0.5	≥ 13	≥ 41	130	6240
u_{wind} (m/s)	7.1	21.5	≤ 0.2	≤ 2.9	≥ 11.7	≥ 15.8	151	7250
MWD_{wind} (°)	188	358	≤ 19	≤ 74	≥ 277	≥ 336	151	7250
P_{wind} (W/m^2)	387	6140	≤ 0	≤ 15	≥ 968	≥ 2418	151	7250

III.6. TECHNOLOGIES DESCRIPTION

III.6.1. WECS: PELAMIS, WAVE DRAGON AND WAVESTAR

To take advantage of the variability of the wave energy resource along the coasts it is generally expected that several wave energy conversion solutions remain attractive for the market. Moreover, there are some features inherent to the WECs that will affect the pattern of their power output and thus, the predictability of their power output. Thus, this study covers different WECs responses to the wave climate. For example, Pelamis and Wavestar operation is more period dependent whereas Wave Dragon is more wave height dependent.

On top of that, is interesting to consider the differences in the operating conditions among the existing WECs, for example, the cut-off limit, i.e. interruption of power production in high sea-states, or the short-term storage in the conversion mechanism (i.e. Wave Dragon uses an open reservoir and Pelamis and Wavestar have high and low-pressure accumulators).

Three different technologies have been selected for the study. These are:

PELAMIS: (Figure 23), (Pelamis, 2011) It is an offshore floating heaving and pitching articulated WEC consisting of five hinges joined together by four modules hosting the Power Take-Off system (PTO). The wave is converted into mechanical movement as the wave passes along the device. The operation of Pelamis is very dependent on the period (i.e. on the wave length). Short-term energy storage is based on accumulators.

During storms with large, steep waves, Pelamis full submerges and emerges (hydrostatic-clipping). The hydraulic rams restraining the joints can generate sufficient moments to induce hydrostatic-clipping and therefore should never reach their end-stops (Yemm, et al.).

WAVE DRAGON: (Figure 23), (WaveDragon) It is a slack-moored floating WEC of the overtopping type. Incoming waves are focused towards the doubly curved ramp of the device by two wing reflectors, surging it without breaking and overtopping into a reservoir placed at a higher level than the mean water level. The PTO system consists of several variable-speed low-head hydro turbines directly coupled to permanent magnet generators. The power production takes place as the water stored in the reservoir is led back to the sea through the turbines.

Wave Dragon operation is more dependent on the wave height than on the period. Short-term energy storage is provided by the open reservoir.

When a storm approaches the deployed location Wave Dragon would decrease its floating level by pumping air out to the minimum crest level. At Hanstholm this would be around 0.5

meter waves. During the storm Wave Dragon continues producing at full power and the production would be dictated by the head of the turbines at that minimum crest height.

WAVESTAR: (Figure 23), (WaveStar) It is a multi-point absorber placed near-shore consisting of twenty floaters distributed in both sides of the platform. The wave is converted into a mechanical movement harnessed by a hydraulic PTO system.

Short-term energy storage is provided by high and low-pressure accumulators, which will be able to smooth the power from all the floats. These can give a smoothing in the power output of up to one minute.

Interruption of power production of Roshage prototype happens when the significant wave height exceeds 2.5 meters. At this time, the machine automatically enters the storm protection mode. This involves un-ballasting the floats and retracting the hydraulic cylinders, which pull the floats out of the water. Each single float is pulled out one at the time and all floats are out within approximately 30 minutes. Then, jacking up the structure into safety position takes about 1 hour (i.e. it takes 10 minutes to raise the structure half meter) (Kramer, et al., 2011).

| (a) | (b) | (c) |
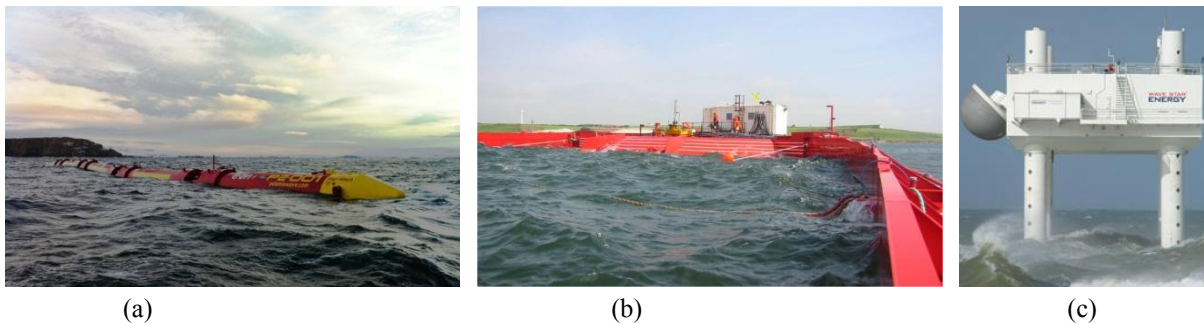
Figure 23. (a) Prototype of Pelamis P2 in Orkney Islands (Pelamis, 2011), (b) Prototype of Wave Dragon in Nissum Bredning, Denmark (WaveDragon), and (c) Prototype of Wavestar at Hanstholm, Denmark (WaveStar).

Whereas Pelamis is a Scottish invention, Wave Dragon and Wavestar are Danish developments. Both technologies have been largely tested at Danish waters (Nielsen, 2012).

III.6.2. WIND TURBINES

Three wind turbines have been selected for the study: the Tradewind offshore turbine, Horns Rev I turbine and the Nordic Folkecenter for Renewable Energy wind turbine.

TRADEWIND TURBINE: it represents the power production of a standard offshore wind turbine (McLean, 2008). The model has been developed within the Tradewind project.

HORNS REV I TURBINE: it represents the power curve of Horns Rev I wind energy farm. It has been developed by Soerensen et al. (2005). The curve represents the power production of a farm of offshore wind turbines at Horns Rev, on the West part of Jutland. It takes into

account the park effect such as wake and shadow effects. The curve is derived from measured power production at Horns Rev.

FOLKECENTER WIND TURBINE: it is a demonstration wind turbine rated at 525 kW. The turbine belongs to the Nordic Folkecenter for Renewable Energy (Nor). The turbine is located at Hanstholm, nearby Roshage pier where Wavestar prototype is located. The wind turbine was manufactured in 1992 and has an average production of 1.5 GWh/y (i.e. 3000 full-load hours). The tower is 40 m high and the blades are 17 m long.

III.7. MODELLED DATA

The project has requested the modelling of wave power and wind power time series, as well as of the electricity generation of each WEC and wind turbine. The four both modelling processes are described in this section.

III.7.1. WAVE POWER TIME SERIES

The data sets of forecast H_{m0} and T_{02}, and buoy-measured H_{m0} and T_{02} have been used to develop time series of forecast P_{wave} and buoy-measured P_{wave}, respectively, in terms of kW/m of incoming wave.
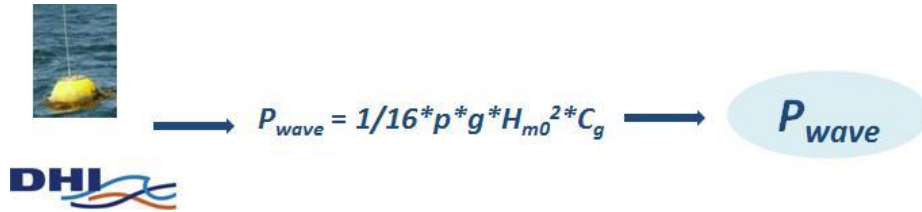
P_{wave} (power per unit of crest width) has been calculated according to the wave power density formula.

$$P_{wave}(W/m) = \frac{1}{16}\rho g H_{m0}^{2} \cdot C_g$$

where C_g is the group velocity, defined by:

$$C_g(m/s) = \frac{1}{2}\left[1 + \frac{2kd}{\sinh(2kd)}\right] \cdot \frac{gT_e}{2\pi} \cdot \tanh(kd)$$

- k (m^{-1}) = $2\pi/L$ is the wave number.
- L (m) = $g*T_e^2/(2\pi)* tanh(kd)$ is the wave length.

For Hanstholm the following values have been considered:
- $\rho_{salt\ water}$ =1027 kg/m^3 represents the water density considering an average water salinity concentration of 33 ppm and an average water temperature of 7 °C.

49

- $g = 9.82$ m/s^2 represents the gravity acceleration.
- $d = 17.5$ m represents the water depth.
- $T_e = 1.2T_{02}$, which is true assuming a Pierson-Moskowitz spectral shape (Nielsen, et al., 2010). T_e represents the energy period.

III.7.2. WIND POWER TIME SERIES

The data sets of forecast u_{wind} and weather station-measured u_{wind} have been used to develop time series of forecast P_{wind} and weather station-measured P_{wind}, respectively in terms of W/m^2 of area.

The wind resource is represented by the wind speed u_{wind}, mean wind direction MWD_{wind} and wind power P_{wind}.

$$P_{wind} = 0.5 \cdot \rho_{air} \cdot g \cdot u_{wind}^3 \quad \left[\frac{W}{m^2} \right]$$

where ρ_{air} (kg/m^3) represents the air density.

$\rho_{air} = 1.23$ kg/m^3, considering an average air temperature of 5 °C.

Note that the difference in units between P_{wave} and P_{wind}, i.e. kW/m and W/m^2 is due to the difference between $\rho_{salt\ water}$ and ρ_{air}. Salt water density is 800 times bigger than air density.

III.7.3. WECS POWER PRODUCTION MODELS

Each WEC of the study has different mean annual energy production related to its dimensions, rated power and technology characteristics. Moreover, the project also compares wind turbine and WECs power productions.

As a result, the study is based on non-dimensional power productions. This allows the comparison among the productions of the different technologies. Non-dimensional power productions are expressed as a percentage of maximum system power output.

Power productions of the three WECs have been modelled from H_{m0} and T_{02} forecast and buoy-measured time series. This process has required the application of a transfer function, i.e. a power matrix that represents the performance of the WEC at Hanstholm.

In this way, the records of forecast H_{m0} and T_{02}, and buoy-measured H_{m0} and T_{02} along with the power matrices have been used to model time series of forecast power production (P_{prod}) and buoy-measured P_{prod}, respectively.

Pelamis and Wave Dragon have been designed for the typical wave climates found at the Atlantic Ocean, characterized by longer period waves than in the North Sea. Therefore, to estimate the performance of the two WECs at Hanstholm, two new power matrices have been

calculated. On the other hand, Wavestar has provided a power matrix developed for this wave climate. Then, non-dimensional power matrices have been developed for each WEC.

POWER MATRICES CALCULATION FOR PELAMIS AND WAVE DRAGON

Pelamis and Wave Dragon publicly available power matrices correspond to full-scale units to be deployed in the Atlantic Ocean (mean wave power up to 36 kW/m). Pelamis power matrix has been obtained from (Pelamis, 2011) and Wave Dragon directly from the developer, although both power matrices are available at ECI (2005).

As a result, Pelamis and Wave Dragon power matrices have been down-scaled to match the predominant sea states at Hanstholm (TABLE VIII) and to optimize their power productions in the location during the study period.

The power matrix of Pelamis corresponds to the previous Pelamis design, P1. According to the developers it is the valid power matrix for the new design. The differences between the previous Pelamis, model P1, and the current version P2, are the dimensions. The rated power of the device remains the same.
- P1 main dimensions: 150 m long, 4 parts.
- P2 main dimensions: 180 m long, 4 m diameter, 5 parts.
- Power rating 750 kW. Expected annual power output: 2.7 GWh (Capacity factor f=41.07%).

DOWN-SCALE OF POWER MATRICES

Objective: select the most convenient scale for a Pelamis and a Wave Dragon to operate at Hanstholm throughout the study period, compared to an Atlantic Ocean full-scale model.

Comment: the down-scaling process carried out in this study is purely theoretical since it does not include the parameters 'Cost/installed MW' or 'Cost/Generated kWh'. These two parameters are essential in the techno-economic optimization of power performances.

Note: in comparison to other devices, the rated power of Wave Dragon depends on the number of turbines on-board of the device but not on the dimensions. Thus, a small device in size may have the same number of turbines than a big device. Once the dimensions of the WEC (i.e. the width and the length) are selected according to the predominant sea states in the selected location, the number of turbines on-board i.e. the device rated power, is decided. This will depend on the seasonal and inter-annual sea states variability. The more variable the more number of turbines to be installed, to cover the peaks in available wave energy. Ultimately, the number of turbines will depend on the ratio "turbine cost/added KWh of production".

Calculations and Methodology: Table X presents the main dimensions and characteristics for a Pelamis and a Wave Dragon suitable for the Atlantic Ocean. The power matrices for those conditions can be found in (Appendix B).

Table X
Dimensions and Characteristics of an Atlantic Ocean full-scale Pelamis and Wave Dragon

	Scale Ratio λ	Length (m)	Width (m)	P_{rated} (kW)
Pelamis	1:1	180	4	750
Wave Dragon	1:1	170	300	7000

The calculation of the optimal scale of Pelamis and Wave Dragon is based on their capture width: the length for Pelamis and the width for Wave Dragon. Several criteria have been investigated to maximize WECs power production. These criteria are presented below. Each criterion has been evaluated throughout Period I at Hanstholm for both Pelamis and Wave Dragon. In the calculations, "*f*" represents the capacity factor and "λ" the scale factor.

Appendix B presents a summary table with different scale ratios and dimensions, rated power, capacity factors, operating hours, etc. of the several models of Pelamis and Wave Dragon evaluated in this discussion.

MAXIMIZING WEC'S POWER PERFORMANCES IN TERMS OF:

The performance of a wave converter at a particular location can be optimized by maximizing the following parameters:

ANNUAL POWER PRODUCTION:

This parameter does not provide the optimal solution. A very big device, i.e. a full-scale model, would yield to large annual energy productions (E_{annual}) by working few hours per year but being stopped for very long periods (very low *f*). For example:

   a. Pelamis: λ=1:1, *length*= 180 m; P_{rated}= 750 kW => E_{annual}=*0.4* GWh/y ,, *f*= 8%.
   b. Wave Dragon: λ=1:1, *length*= 300 m; P_{rated}=1.5 MW => E_{annual}=*2.75* GWh/y ,, *f*= 5% .

OPERATING TIME

This parameter does not provide the optimal solution. Power productions have to be maximized according to (Prob*P_{wave}) but not to the probability of occurrence of the wave parameters. For example:

   a. Pelamis: λ=1:2, *length*= 90 m; P_{rated}= 66 kW => E_{annual}=*0.15* GWh/y ,, *Operating time*= 98%.
   b. Wave Dragon: λ=1:2, *length*= 150 m; P_{rated}= 619 kW => E_{annual}=*1.45* GWh/y ,, *Operating time*= 98%.

CAPACITY FACTOR OR FULL LOAD HOURS

This parameter does not provide the optimal solution. The maximization of the capacity factor provides low rated power and small devices that, although operative most of the time, even in very low sea states, may not be technically feasible. The length of both devices is too small for the design conditions at Hanstholm. For example:

a. Pelamis: λ= 1:3.3, *length*= 54 m; P_{rated}= 11 kW $\rightarrow$$E_{annual}$= *0.03* GWh/y ,, *f*= 26%.

b. Wave Dragon: λ= 1:3.3, *length*= 90 m; P_{rated}= 104 kW $\rightarrow$ E_{annual}= *0.41* GWh/y ,, *f*= 46%.

SAME CAPACITY FACTOR AS STATED BY THE DEVICE DEVELOPERS

This parameter does not provide the optimal solution. By choosing a scale that provides the same performance of the devices in terms of capacity factor as expected by the device developers, the devices are not technically feasible. The length of Pelamis and the length of Wave Dragon are very small compared to the predominant wave length at Hanstholm.

a. Pelamis: it is expected to have *f*=25-40%.

$\rightarrow$ Iterative process: *f*=30%; λ= 1:2.9; *length*= 63 m; P_{rated}= 19 kW,, E_{annual}=*0.05* GWh/y.

b. Wave Dragon: a 1.5 MW device is expected to produce 4 GWh/y or *f*=30.42%.

$\rightarrow$ Iterative process: *f*=30%; λ=1:2.1; *width*=140 m; P_{rated}= 485 kW,, E_{annual}=*1.29* GWh/y.

MAXIMIZING WEC'S POWER PRODUCTION IN TERMS (PROB*P$_{WAVE}$)

Since there is more energy accumulated at higher waves, it is of interest to optimize the devices to harness the high energy states, although the energy in the less energetic ones is lost. Hence, here WEcs are designed according to the most powerful and most common sea state, i.e. when (*Prob*$*P_{wave}$) is maximum. Note Pelamis operation is more dependent on the period and Wave Dragon operation on the wave height.

Figure 24 presents a comparison between the contribution of T_{02} to the mean wave power (in percentage) and Pelamis power production's dependency on T_{02} for different scaling ratios. Figure 25 presents a comparison between the contribution of H_{m0} to the mean wave power (in percentage) and Wave Dragon power production's dependency on H_{m0} for different scaling ratios.
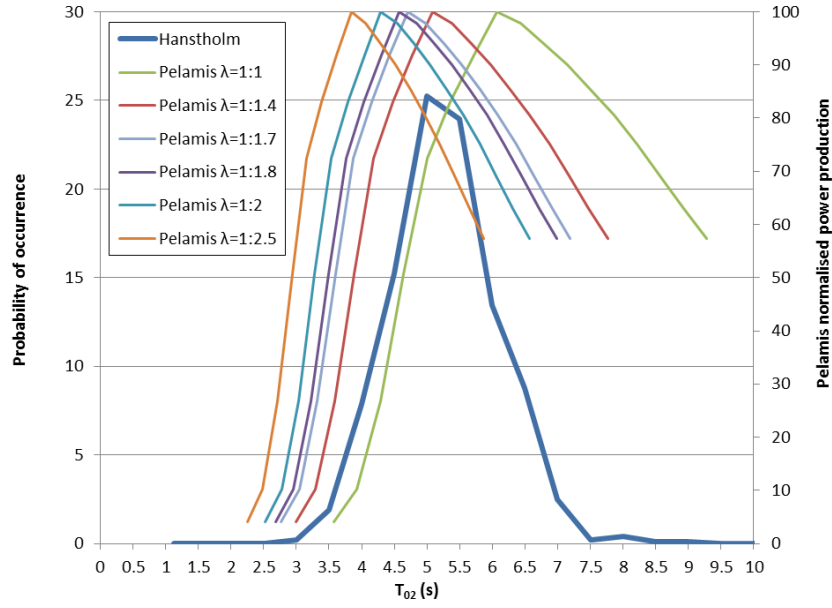
Figure 24. Contribution of T_{02} to the mean wave power at Hanstholm throughout Period I (as a percentage) and normalised power productions of Pelamis in terms of T_{02} and different λ in the study period. Note the curves for small λ should continue for increasing values of T_{02} up to 10 seconds.
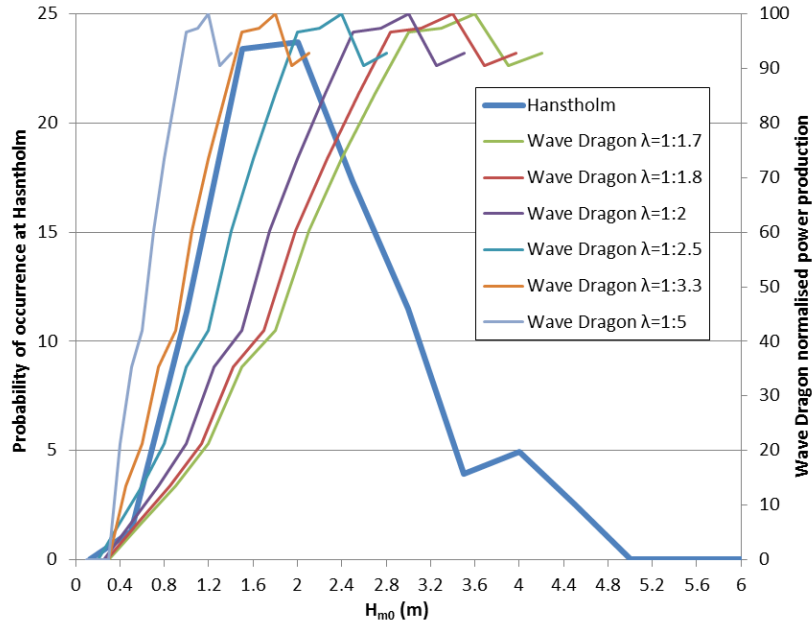
Figure 25. Contribution of H_{m0} to the mean wave power at Hanstholm throughout the Period I (as a percentage) and normalised power productions of Wave Dragon in terms of H_{m0} and different λ in the study period. Note the curves for small λ should continue for increasing values of H_{m0} up to 4.5 meters.

Figure 24 and Figure 25 show the best correlation between scale and maximum $Prob*P_{wave}$ is for a Pelamis of scale $\lambda=1:1.4$ and for a Wave Dragon with a scale of $\lambda=1:3.3$. Nevertheless, whereas Pelamis dimensions for a 1:1.4 model are too big for the wave climate at Hanstholm, the dimensions of a 1:3.3 Wave Dragon model are very small. Therefore, none of these devices are technically feasible.

54

COMPROMISE AMONG SEVERAL OPTIONS

Taking into account the results of options presented above, along with the design requirements for the devices, i.e. minimum length of Pelamis according to the typical wave length (L) or minimum concrete dimensions for Wave Dragon, the optimal WECs scales are:

- a. For Pelamis:
  - If λ=1:1.76 => 102 m long Pelamis divided in 5 sections => 20.4 m/section. Mean wave length value in Period I at Hanstholm is L=50 m.

    L/2 = 25 m

    Each section is about 20 m => OK.
  - If λ=1:1.76 → Ø= 2.3 m --> Results in a convenient diameter so a person can work inside the device.
- b. Wave Dragon:
  - 170 m width is the minimum feasible concrete structure for Hanstholm conditions

FINAL SCALING RATIOS

The selected scale ratios for Pelamis and Wave Dragon, their main dimensions, characteristics, design states and operating conditions are presented in TABLE XI:

For operational and design purposes it is imperative that the devices are designed in correspondence to the mean wave conditions and are able to operate in the range of H_{m0}=1-3.5 m and T_{02}=4.5–6.5 s (Figure 16, TABLE I). The design sea state i.e. H_{m0} and T_{02} when Hanstholm-scale Pelamis and Wave Dragon WECs reach full production is indicated in TABLE XI.

TABLE XI
Scale ration, Dimensions, Rated Power, Design and Operating Sea States for Pelamis and Wave Dragon at Hanstholm in Period I.

	Scale Ratio λ^1	Main dimensions (m)		P_{rated} (kW)	Design H_{m0} (m)	Design T_{02} (s)	H_{m0} min (m)	H_{m0} max (m)	T_{02} min (s)	T_{02} max (s)
Pelamis	1:1.76 or 1:180/102	l=102	Ø=2.3	103	3.1	4.6	0.4	4.6	2.5	7.1
Wave Dragon	1:1.76 or 1:300/170	l=96	w=170	960	3	5	0.4	4.1	2.6	9.3

[1] Scale ratios relative to the Atlantic Ocean.

POWER MATRICES FOR PELAMIS, WAVE DRAGON AND WAVESTAR

The power matrices for Pelamis and Wave Dragon have been calculated with the scaling ratios of previuous section. Some modifications have also been done to Wavestar power matrix.

The following calculation steps have been done to finally calculate the three power matrices:

- Down-scale the power matrices of the full-rated units of Pelamis and Wave Dragon. according to the scale factor and assuming Froude law (TABLE XII). According to the table, H_{m0} scales linearly, T_p scales by the square-root of the scale and P_{prod} by the scale to the power of 3.5.

TABLE XII - Scaling ratios

Unit	Scaling
Length	λ_L
Time	$\lambda_L^{0.5}$
Force	λ_L^3
Power	$\lambda_L^{3.5}$

- Defining Pelamis and Wave Dragon power matrices in terms of T_{02} (s) assuming the validity of the expression $T_{02}= T_p/1.4$ in the North Sea (Ramboll, 1999a).
- Homogenizing the dimension of the bins of the three power matrices. Thus, increasing the resolution of Wave Dragon and Wavestar's power matrices to have the same resolution in the bins as Pelamis, i.e. 0.2-03 m for H_{m0} and 0.2-0.3 s for T_{02}.
    - Wave Dragon: power matrix originally defined in steps of 1 second for T_p. Steps of 0.5 s in T_p introduced.
    - Wavestar: power matrix originally defined in steps of 1 second for T_{02} and 0.5 meters for H_{m0}. Steps of 0.5 s in T_{02} and 0.25 m in H_{m0} introduced.

The three power matrices for the Hanstholm-scale devices can be found in Appendix B. Based on these power matrices the power performances of the devices at Hanstholm throughout the study period have been calculated.

MODELLED POWER PRODUCTIONS OF PELAMIS, WAVE DRAGON AND WAVESTAR

A power matrix provides the expected power production (in kW or in non-dimensional units: kW/kW) of a WEC in terms of H_{m0} and T_{02}. The wave climate of Hanstholm during the study period is defined by a time-series of sea states, in terms of half-hourly values of H_{m0} and T_{02}.

Power production of each WEC has been obtained with the power matrix, for the bin (H_{m0}, T_{02}) corresponding to the half-hourly wave condition measured at the site.

Whenever the occurring sea state does not coincide with the intervals the power matrix is defined, the power productions are interpolated (i.e. a weighted average calculation) between the closest upper bin values, for both H_{m0} and T_{02} and the closest lower bin values, also for H_{m0} and T_{02}.

The sum of all power productions for a given period results in the expected power production of that period.

SUMMARY

TABLE XIII presents the scaling ratios, main dimensions, rated powers, annual energy productions, capacity factors and operating times for Pelamis, Wave Dragon and Wavestar at Hanstholm in Period I according to the selected scaling rations. TABLE XIV presents the design sea states i.e. H_{m0} and T_{02} where WECs reach full production and the operation limits of each device (minimum and maximum H_{m0} and T_{02}).

TABLE XIII

Scaling ratio, Dimensions, Rated Power, Energy production, Capacity Factor and Operating Time for Pelamis, Wave Dragon and Wavestar at Hanstholm in Period I.

	Scale Ratio λ*	Main dimensions (m)		P_{rated} (kW)	$\sum MWh$ (102 days)	E_{annual} (MWh/y)	Capacity factor f (%)	Oper. time (%)
Pelamis	1:1.76 or 1:180/102	l=102	Ø=2.3	103	72	203	23	98
Wave Dragon	1:1.76 or 1:300/170	l=96	w=170	960	637	1784	21	98
Wavestar	1:2 or 1:10/5	---	Ø=5	600	571	1600	30	93

* Pelamis and Wave Dragon scaling ratios are relative to the Atlantic Ocean and Wavestar's to the North Sea.

TABLE XIV

Design and Operating Sea States for Pelamis, Wave Dragon and Wavestar at Hanstholm

	Design H_{m0} (m)	Design T_{02} (s)	H_{m0} min (m)	H_{m0} max (m)	T_{02} min (s)	T_{02} max (s)
Pelamis	3.1	4.6	0.4	4.6	2.5	7.1
Wave Dragon	3	5	0.4	4.1	2.6	9.3
Wavestar	2.7	4.5	0.5	3	2	8.6

TABLE XIV shows Wavestar cuts-off production in lower sea states than Pelamis or Wave Dragon.

Figure 26 presents a comparison between the probability of occurrence of different sea conditions (defined by the contribution in percentage of H_{m0} and T_{02} to the mean wave power P_{wave}) and the dependency of the power productions of the three devices to these conditions. Pelamis and Wavestar are more dependent on the period whereas Wave Dragon is more dependent on the wave height.

Figure 26 shows Wavestar has the best correlation between maximum P_{prod} and probability of occurrence of the wave parameter T_{02}.

Due to the aim of the study of comparing the three devices and since the rated power of each device is different, non-dimensional or normalized power matrices have been developed (Appendix B) (Figure 27). These power matrices are used throughout the study. Hence, all power productions presented throughout the study are in terms of percentage of rated power, i.e. normalized P_{prod}.
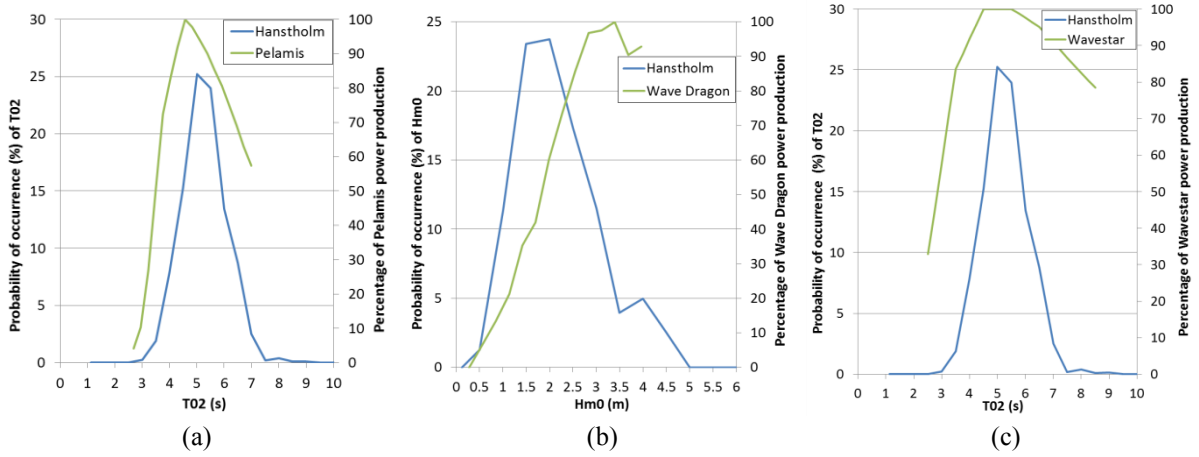
Figure 26. Contribution (in percentage) of T_{02} (a) and (c), and H_{m0} (b) to the mean wave power at Hanstholm throughout Period I and normalised power productions of Pelamis (a), Wave Dragon (b) and Wavestar (c) in terms of T_{02} (a) and (c), and H_{m0} (b) in the same period. Wave Dragon performance is more dependent on the variations of the wave height whereas Pelamis and Wavestar performances are more dependent on the period.
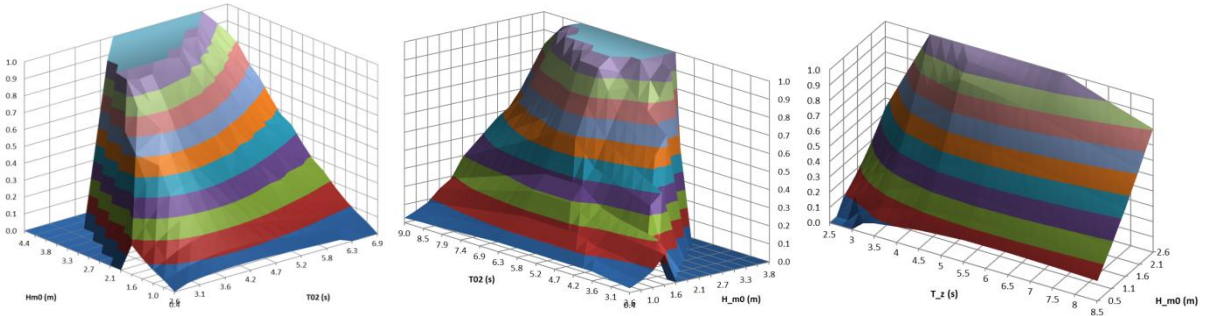
Figure 27. Non-dimensional power matrices of Pelamis, Wave Dragon and Wavestar for Hanstholm wave climate throughout Period I.

Looking into Figure 27 it can be seen that Wave Dragon is designed for high sea states, where it performs better. Pelamis is also designed for higher sea states than those usually found at Hanstholm, but in a smaller degree than Wave Dragon. On the contrary, Wavestar design conditions correlate very well with Hanstholm wave climate.

To conclude, this section has shown that to choose the scale of a device that fits better to a particular location different factors have to be taken into account and a compromise among them has to be found. Not only the scale is selected to achieve the maximum power production but also the dimensional requirements of the device have to be fulfilled. Moreover, the parameter *cost ratio* (defined as the cost of the device per energy unit produced, i.e. cost kW/price kWh produced) plays a major role in selecting the scale.

III.7.4. WIND TURBINES POWER PRODUCTION MODELS

The two following models of wind turbines are used to calculate theoretical power productions of wind turbines.

TRADEWIND MODEL

Tradewind power curve (McLean, 2008) represents the overall power production of an offshore wind turbine as a function of wind speed, in terms of percentage of rated power (Figure 28). Nominal or rated wind speed is 14 m/s.
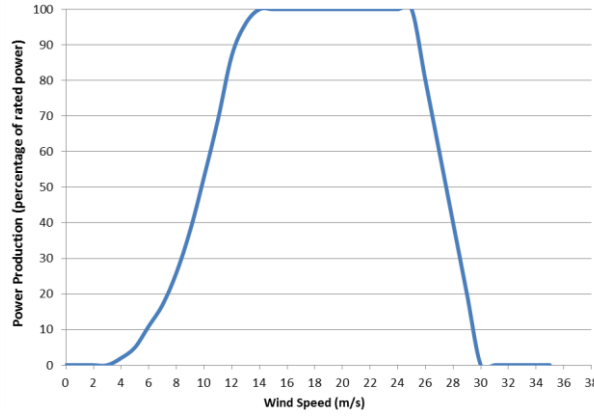
Figure 28. Tradewind power curve (McLean, 2008).

HORNS REV I MODEL

Horns Rev wind energy farm power curve represents the power production of a farm of offshore wind turbines at Horns Rev I (Figure 29). The wind speed (u_{wind}) represents the average 10-minute wind speed measured in the height of 22 meter. The curve is derived from measured power production at Horns Rev.

The equations defining the power curve are:

$P_{prod}(u_{wind}) = 0$ (MW) [if $u_{wind} < 3.5$ m/s ,, 25 m/s $< u_{wind}$]

$P_{prod}(u_{wind}) = 1.6775*u_{wind}^2 - 9.5402*u_{wind} + 14.825$ (MW) [if 3.5 m/s $< u_{wind} < 10.6$ m/s]

$P_{prod}(u_{wind}) = -2.9286*u_{wind}^2 + 87.971*u_{wind} - 501.22$ (MW) [if 10.6 m/s $< u_{wind} < 15$ m/s]

$P_{prod}(u_{wind}) = 158$ (MW) [if 15 m/s $< u_{wind} < 25$ m/s]

(*Note: in the original file the third equation starts with a positive term; here this is changed).
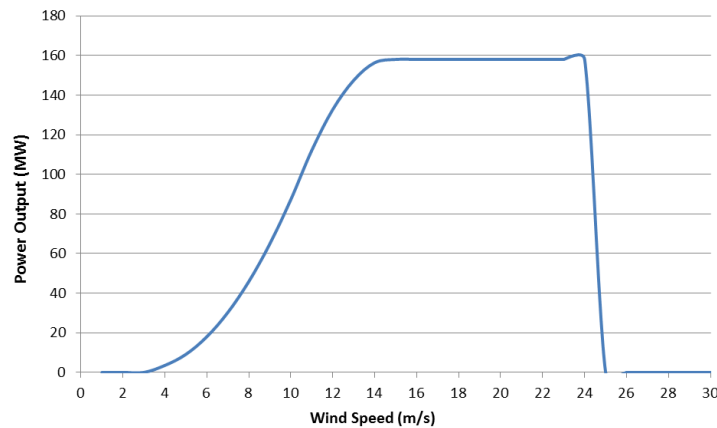
Figure 29. Horns Rev wind energy farm power curve (Soerensen, et al., 2005).

III.8. REAL DATA

Real data on power productions are provided by the Wavestar machine at Hanstholm (rated at 110 kW) and the 525 kW Folkecenter wind turbine (Figure 30).

Figure 30. Wavestar (on storm protection mode) and Folkecenter wind turbine, Hanstholm.

III.8.1. WAVESTAR POWER PRODUCTION

Time-series of Wavestar's production are available since May 2010. The study is based on production data from January to May 2011 expressed as 30-minute average values. Data correspond to hydraulic power measured at the output of the two cylinders connected to the floats. (From October 2011 and onwards power production data refers to electricity delivered to the grid).

Different control strategies have been tested since the installation of the device in September 2009 (Hansen, et al., 2011) and experience on Wavestar's performance and control has been gained. In fact, power production has improved during 2012 (Vidal, et al., 2012). For that reason, the operation data presented here should be read as initial prototype performance results.

III.8.2. FOLKECENTER WIND TURBINE POWER PRODUCTION

From 1996 there is available production data of the wind turbine as 15-minute average time-series of electrical power delivered to the grid.

Production data files available to the authors:
- From 01/06/2010 at 00:00 to 31/05/2011 at 23:45. As 15-minute records of power production (kWh).

A fast overview over the production data seems all data is correct and valid. 23% of the time the wind turbine is not producing and rarely at any time (0.25% of the total time) is having full-production.

In order to match Wavestar´s 30-minute average values with the turbine's production, wind turbine production data are recalculated as a weighted average of the 15-minute time-series, for Period II (from January to May 2011).

III.9. POWER MARKET DATA

Market data for West and East-DK have been retrieved from Energinet.dk (Energinet.dk). Data include hourly values of net consumption, system imbalances (deficit and surplus of power), regulating power (upward and downward regulation) and price for balancing power (upward and downward regulation prices).

To match power production data from WECs and wind turbines to electricity market data, the half-hour records of the former are expressed as hourly time series through a weighted average:
- Market Data is in Danish time and the hours indicate:
    o value t=01:00 indicates from 00:00 to 1:00
- Technologies Production:
    o a: value t=00:00 indicates from 23.45 to 00:15
    o b: value t=00:30 indicates from 00:15 to 00:45
    o c: value t=01:00 indicates from 00:45 to 01:15

To match Market data to Power Productions:
- Market Data:
    o value t=01:00 indicates from 00:00 to 1:00
- Technologies Production:
    o a: value t=00:00 indicates from 23.45 to 00:15
    o b: value t=00:30 indicates from 00:15 to 00:45
    o c: value t=01:00 indicates from 00:45 to 01:15

→ For t=01:00 (from 00:00 to 1:00) it is calculated $[(\frac{1}{2}a+b+\frac{1}{2}c)/2]$ and it is named thereafter t=00:00

III.10. FORECAST CHARACTERISTICS

III.10.1. FORECAST
A forecast predicts the local conditions in an area for a window up to few hours or several days.

A metocean[5] forecasting system comprises of a weather forecast, a tidal forecast and a wave and current forecast. For instance, the water forecast tool for Danish waters of DHI is a

---

[5] Metocean parameters is the abbreviation to both meteorological and oceanographic information.

regional full 3D hydrodynamic model covering the North Sea and the Baltic Sea. This model is *forced* by tidal predictions and by wind fields obtained from a global or regional meteorological model. Together with local models around the site of interest transform and detail the waves and current conditions to be expected in the forecast period. The local model of DHI is the MIKE21, which computes the local hydrodynamics (currents and water levels) and also the spectral wave model (wave field) in the area of interest (Kirkegaard, et al., 2010).

The difference between forecasts and hindcasts is the data used to compute the models. In hindcasts actual time-series of wind fields (measured wind fields) are used to compute time-series of wave conditions.

Weather forecasts were mainly used for demand management by grid operators and plant operators, to account for the varying energy demand on the different seasons and for daily weather variations.

Currently, weather forecasts are of the interest of many disciplines.

WIND FORECASTS

Meteorologists have a crucial role in the efficient planning of wind power production. *Grid management* needs the *24 hours forecasts*. For instance, if a low-pressure area produces peak wind values a few hours ahead of forecast, grid operators have to quickly ramp-down their own power plants to prevent excess power production. In contrast, *power plant operators* rely on *48 hours forecasts*. Central power plants can tailor their own power production to these forecasts in order to produce the exact amount of power needed.

Forecasts are to have greater detail and be exactly at the height of the hub. They answer the questions of: will the wind pick up to 24 or 26 m/s? will the wind farm then reach its peak capacity or have to switched off altogether if the 25m/s threshold is passed?

Grid operators have to react quickly if a storm causes a large number of wind farms to be shut off in a cascade and then brought back online again at full capacity when the strongest winds have died down. For 2008 meteorologists have been focusing on "day-ahead congestion forecasts" – short-term forecasts for grid interconnection points.

In wind calculation models a distinction is made between statistical and physical models. The former calculates future wind situations based on wind and air flow data from the past, while the latter include the surface properties of the areas affected down to the level of specific wind farms (i.e. the angles of slopes on a given landscape, and may also include a landscape evaporation behaviour, which can affect the dynamics of global weather trends). Nowadays these two approaches are mainly used simultaneously.

However, wind forecasts are not only of interest of meteorologists and wind producers but also for the grid management, power plants operators, distribution grid operators (i.e. to investigate when it can perform maintenance on its substations, to avoid repairs when stations are exposed to maximum wind power), stock traders (i.e. interested in wind forecasts for intraday trading of power volumes: utilities (E.on, RWE, Vattenfall, etc) buy and sell power up to 75 min. before it has to be provided: when they see they can get the power they need at a lower price on the spot market because of greater wind power production, they ramp down flexible generation such as small gas turbines).

Prices for meteorological forecasting services are at around 10,000 EUR/y for a wind energy farm. The following are models for wind power forecasting:
-   DWD (DE), "Deutsche Wetterdienst": Uses statistical models based on historical weather data.
-   ECMWF (UK).
-   Meteo-France (FR).
-   KNMI (NE).
-   NCAR (US): it is based on physical data.

III.10.2. TIME SCALES OF WEATHER FORECAST

Depending on the field of study the time scales of the forecasts vary. For example, in the context of smart grids and intra-day operations and scheduling, short-term forecasting may refer to a time horizon of 5 minutes. This project accepts the notations that are commonly used in the wind power forecasting community and by weather, wave and current forecasts (Madsen, 2004). The time spans of the different time-scales may overlap, therefore it is important to specify the time scales used in this study:

- Short-term forecasts: refers to the first hours forecasts up to 12 hours. Note it may also be used to denote 0 to 24 hours ahead or 0 to 48 hours ahead.
  o Useful for:
    ▪ Electric system operation, i.e. the Elbas market and the regulating market. Of interest for TSOs, to decide which generation enters the system.
    ▪ WECs' control strategies.
    ▪ WEC´s operation.
- Day-ahead forecasts: refers to the 12 hours to 36 hours forecasts.
  o Useful for day-ahead forecasting for the bids in day-ahead markets, i.e. Elspot market.
- Long-term forecasts: refers to the 48 hours forecasts up to 96 hours ahead, or to 2 to 4 days ahead. Note it may also be used to denote the first hour forecasts up to the 72 hours forecasts.
  o Useful for planning according to weather windows, i.e. of operation and maintenance (O&M) activities.

The following time-scales are also found in literature:
- Now-casts: a short-term weather forecast, generally for the next few hours.
  - The U.S. National Weather Service specifies 0 to 3 hours, although up to six hours may be also used.
  - In DHI it denotes the 0 hours forecast.
- Short-term forecasts: refers to the first hours forecasts up to some hours or several days ahead. These can be 6-hour ahead, i.e. 0-6 hours horizon forecast, although it may also be used to denote the 0 to 24 hours and the 0 to 48 hours ahead forecasts.
- Medium-term or Mid-term forecasts: refers to 0-48/72 hours forecasts.
- Long-term forecasts: refers to the first hours forecasts up to 48 or 72 hours ahead, i.e. 0-48 hours horizon forecast (Note that some fields long-term forecast can indicate the 12-36 hours forecasts or the 72 hours forecasts).

III.10.3. FORECAST HORIZON

This study uses the parameter *forecast horizon*. The forecast horizon, represented by "t", indicates the lead hour of the forecast. It denotes the forecast hour or the time horizon before real time, expressed in hours. In other words, it is the time-span between the forecast is calculated and the real measurement is done.

The forecast horizon throughout the study is calculated as follows:
- Forecast time: when the forecast is actually carried out.
  - Forecast time = Received time – delay

where
- "Received time" indicates the time when the file is received.
- "Delay" has a constant value of 19 h (for DHI forecast).

Then,
- Forecast horizon = Actual time - Forecast time [h]

Note it is assumed forecasts can be obtained with zero hours delay.

The study looks at forecast horizons of 0 to 120 hours (5 days), and particularly to day-ahead forecasts, covering from 12 hours (half a day) to 36 hours (one and a half day).

Other expressions can be found in literature that expresses the same as a forecast horizon:
- 1 hour forecast = the first look-ahead time = the 1st lead time = one-hour ahead predictions.
- 24th lead time = 24-hour ahead forecasts = 24-hour ahead prediction.
- Time horizon: look-ahead time: horizon of predictions (1,2, 3, …48, … hours ahead).

III.10.4. QUALITY INDECES FOR FORECAST ACCURACY EVALUATION

A number of quality indices can be calculated to obtain and objective and quantitative measure of the accuracy of model data compare to observed data. Verification of forecast data against measured data can be quantified by the following indices: the Bias, the Mean Absolute Error (MAE), the Root Mean Square of Difference (RMSE), the unbiased Scatter Index ($SI_{unbiased}$) and the Correlation Coefficient (CC).

Bias and MAE are non-statistical parameters that provide an absolute measurement of the error, whereas RMSE, $SI_{unbiased}$ and CC evaluate statistically the errors. Both *MAE/Mean* and the *SI* give a non-dimensional measurement of the error.

Research on wind forecasting generally evaluate the accuracies of the forecasts with MAE and RMSE. The former parameter is mostly utilised by TSOs and grid regulations, whereas the latter is mostly used by academia. The reason is that MAE can be directly related to a cost, whereas RMSE cannot. Since the final goal of this research is making an economic estimate (i.e. provide a value for balancing costs) final results on forecast errors are expressed in terms of MAEs.

The definition of each parameter is provided below, where *MOD* corresponds to modelled, calculated or forecast data and *OBS* to observed or measured data.

The *Mean* value of observations is defined as:

$$Mean = \frac{1}{N}\sum_{i=1}^{N} OBS_i$$

where *N* corresponds to the number of valid observations.

The mean of difference or *Bias* represents a measurement of the error that remains primarily constant in magnitude for all observations. It is somehow a systematic error. It is defined as:

$$Bias = \frac{1}{N}\sum_{i=1}^{N}(MOD-OBS)_i$$

The mean of absolute difference or *MAE,* also known as the mean absolute error, is defined as:

$$MAE = \frac{1}{N}\sum_{i=1}^{N}(|MOD-OBS|)_i$$

The root mean square of difference or *RMSE* is calculated assuming a normal distribution and represents the standard deviation of the mean (confidence level of 68.27%). It measured the 'spread' of the distribution and is defined as:

$$RMSE = \sqrt{\frac{1}{N}\sum_{i=1}^{N}(MOD-OBS)_i^2}$$

RMSE, being the standard deviation of the mean, represents the extent to which the measured power outputs are likely to be different from its mean or expected average power outputs, the standard deviation is used in finances to measure the risk.

The unbiased scatter index or $SI_{unbiased}$ is also calculated assuming a normal distribution. It provides a non-dimensional measure of the error and is defined as:

$$SI_{unbiased} = \frac{\sqrt{\frac{1}{N}\sum_{i=1}^{N}(MOD-OBS-Bias)_i^2}}{Mean}$$

The correlation coefficient or CC indicates the degree to which the variation in one parameter is reflected in the variation of the other parameter; the correlation is related to covariances. It is a non-dimensional variable ranging from 0 to 1, the former indicating no correlation between the two data sets and the latter perfect correlation. It is defined as:

$$CC = \frac{\sum_{i=1}^{N}(MOD_i - \overline{MOD})(OBS_i - Mean)}{\sqrt{\sum_{i=1}^{N}(MOD_i - \overline{MOD})^2 \sum_{i=1}^{N}(OBS_i - Mean)^2}}$$

CC measured the extent to which two things are related to each other. [-1, 1] = [Perfect negative relatedness, perfect positive relatedness]. CC or its statistical counterpart, the covariance, correlates the buoy-measured value with the forecast one.

It is important not to confuse CC with the "determination coefficient" (R^2), also widely used. While the correlation coefficient varies in the interval $-1 < CC < 1$, the determination coefficient has a varying range of $0 < R^2 < 1$.

When wave heights and wind speeds forecasts are evaluated the indexes MAE and MAE/Mean are provided, and for power productions the parameter NMAE is given, where N indicates *normalised,* and thus NMAE is the normalised value of MAE, in terms of maximum power production.

$$NMAE = \frac{1}{P_{rated} \cdot N} \sum_{i=1}^{N}(|P_{MOD} - P_{OBS}|)_i$$

III.11. ASSUMPTIONS

The following assumptions have been made in the study:

1. Errors in the wave buoy and in the weather station acquisition systems have been disregarded.

2. Validity of wind measurements by the weather station at Hanstholm is not certainly known. It has been highly confirmed that there have been no unstable periods in the study period.

3. The current delay in the forecasts has been disregarded. At present, due to the research purpose of the forecast, the model delivers the data with 19-hour delay. In real implementation of the forecasts this delay can be reduced to approx. 1 hour. The study assumes a zero hour delay.

The reason why DHI forecast model delivers the data with 19-hour delay is the following (personal correspondence with DHI):
- At 00 UTC the global GFS met model starts (run by NCEP in the US).
  - (GFS met model stands for Global Forecast System).
- When finished DHI's North Atlantic wave model starts.
- Also at 00 UTC the global ECMWF met model starts (run by ECMWF in the UK).
  - (ECMWF met model stands for European Centre for Medium Range Weather Forecasts).
- When it finished the European WRF met model starts (run by StormGeo in Norway).
  - (WRF met model stands for Weather Research and Forecasting model) (WRF, 2013).
- When it finishes DHI's North European hydrodynamic model starts.
- When it finishes DHI's North European wave model starts (assuming that DHI's North Atlantic wave model has finished) and DHI's Hanstholm hydrodynamic model starts.
- When they both have finished DHI's Hanstholm wave model starts.
- When it finishes we can provide you the 6 day wave forecast.

Hence, DHI starts receiving the wind from the WRF model run in Norway about 8 hours after forecast time, which means that wave forecasts for Hanstholm for the first day are ready 9½ hours after forecast time. Since the Hanstholm models have not been time critical their execution do not have a high priority. In case it was important to deliver a 6 days forecast quickly we can do that 12 hours after forecast time instead of 19 hours as we do presently.

4. Day-ahead electricity markets require the forecasts of the next 12 to 36 hours. However, the study considers a day-ahead forecast covering from 12 to 48 hours. The reason is the following: DHI delivers the forecast every 12 hours, which requires the establishment of 12-hour time-slots to get a comprehensive picture of the accuracy of the forecasts. Hence, to correctly evaluate the accuracy of the 36th lead time, the information from the 36th to the 47.5th lead time is used.

5. WECs and wind turbines power productions dependency on waves and winds directionality have been neglected.

6. Array interaction between WECs has not been taken into account in the evaluation of combinations of WECs. It is expected that WEC arrays, separated in distance according to the predominant wave length, reduce the variability of the power output and the errors in the predictions. This can be study using Hanstholm data and Fjaltring data, for example (Figure 31).
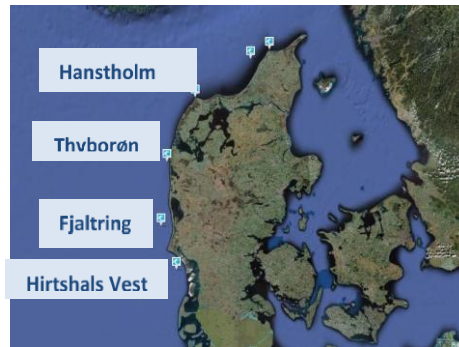
Figure 31. Hanstholm, Thyborøn, Fjaltring and Hirtshals Vest locations, Denmark (Kys).

7. Unless particularly specified, power productions of WECs and of wind turbines in the study are theoretical and derived from the WECs power matrices and from wind turbines power curves. Real power production data from Wavestar prototype at Hanstholm and the 525 kW Folkecenter wind turbine have only been used in Chapter VII.

8. The study assumes that the location of wind forecasts and wind measurements is the same. It also assumes that the location of wave and wind measurements is the same.

Buoy measurements and metocean DHI forecasts are from the same location, which is about 1.3 km North-west off the harbour, whereas weather data are obtained at the harbour (Figure 6).
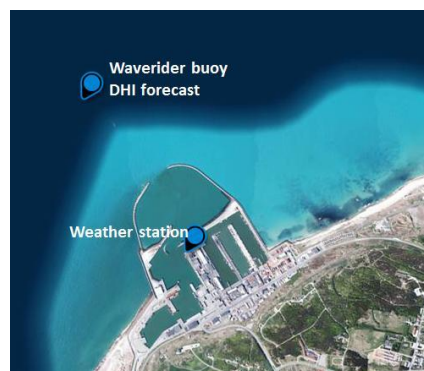
Figure 32. Location of the wave buoy, wind and wave forecasts (DHI forecasts) and the weather station (©COWI), (kra).

The assumption that weather data are recorded at the buoy location accepts two facts:
1) That the wind from offshore reaches the weather-station undisturbed.

68

2) That the buoy and the weather station record measurements at the same time, i.e. that the 1.3 km distance between them is negligible.

1) The mainland and the harbour structure can influence the weather-station measurements. However, since:

> i) wind usually blows from Western direction (no mainland influence), and
> ii) wind measurements are taken at 20 m heights

mainland and harbour influence can be neglected.

Nevertheless, when specified, only winds coming from the sea are considered, i.e. wind speeds with MWD_{wind} in the interval [45°, 220°] are disregarded.

2) Wave data and wind data are measured at the same time but at different locations (1.3 km apart). The time delay between the two set of measurements is investigated here:

The weather station is eastern and southern from the buoy. Wave buoy is at 6332100N, 474700E, and the weather station at 6331036 N, 475467 E. the distance between them is:

> East: 767 meter = 0.8 km
> North: 1064 meter = 1.06 km = 1 km
> Hypotenuse: 1311 meter = 1.3 km

The hypotenuse is the distance between the wave buoy and the weather station.

Mean wind speed in the study period is 7.5 m/s:

> s=v*t → t=s/v=1300/7.5=173 s = 2.9 minutes, i.e. 3 minutes delay in the records.

Provided wave measurements are in half-hour intervals, and wind measurements in 10-minute intervals, it can be considered that the 3-minute shift does not have a major impact on the results. As a result, we assume there is no relevant phase shift added by the difference in locations.

Therefore, due to the fact that i) mainland does not disturb wind measurements, ii) there is a small distance between the weather station and the forecast location, and iii) data are in half-hour resolution, the assumption that the location of wave and wind measurements is the same is considered valid.

9. The study between WECs and wind turbines power productions is based on the comparison between the pair of values H_{m0} [m] and u_{wind} [m/s]. The reasoning is discussed below:

Three pairs of parameters can represent the response of WECs and wind turbines to the resource:
   a) The available incoming power to the technology P_{wave} *[kW/m]* and P_{wind} *[W/m²]*.
   b) The parameters H_{m0} [m] and u_{wind} [m/s].
   c) The power productions of WECs and wind turbines.

69

The discussion then focuses on which of the three pairs of parameters represents more accurately the response to the resource of WECs and wind turbines:

Option *c* is disregarded first since the interest of this study relates to the analysis of raw data. Nevertheless, it is acknowledged that options *a* and *b* neither take into account cut-off limits nor the operational response of the technologies: i.e. options *a* and *b* disregard the fact that whilst metocean conditions vary, the output of the technologies remains constant between nominal and maximum values.

The discussion starts with the analysis of option *a*. In the comparison of the available incoming power to the technology P_{wave} *[kW/m]* and P_{wind} *[W/m²]* it is needed to unify the dimensions: P_{wave}*(WEC capture width) and P_{wind}*(Wind Turbine Capture Area). This results into *[kW]* units.

A positive reason to compare P_{wave} against P_{wind} is to take into account that wave power depends both on the wave height and on the wave period, and that wind power depends on the cube of the wind speed. Hence, P_{wave} depends on H_{m0}^2 and on T_{02}, or on $H_{m0}^{2.5}$ as shown in Ramboll (1999a):

$$P_{wave} = 2.05 \cdot H_{m0}^{2.5}$$

On the other hand, P_{wind} depends on u_{wind}^3.

Therefore, option *a* translates into the pair of values $H_{m0}^{2.5}$ and u_{wind}^3.

The question is then, which pair of parameter defines more linearly the evolution of power productions: is it $H_{m0}^{2.5}$ *or* H_{m0} for the wave power production, and is it u_{wind}^3 or u_{wind} for wind power production?

Comparisons show there linear relation between H_{m0} and the power production of a WEC is more correlated to H_{m0} (R^2=0.9) than to $H_{m0}^{2.5}$ (R^2=0.8), and the same happens for a wind turbine. The linear relation is more correlated to u_{wind} (R^2=0.9) than to u_{wind}^3 (R^2=0.8).

As a result, the study focuses on the comparison between the pair of values of option *b*, i.e. H_{m0} [m] and u_{wind} [m/s].

IV.1. INTRODUCTION

This chapter addresses the extent to which the wave and the wind conditions at Hanstholm, Denmark, can be predicted.

At the time WECs and wind turbines pour their electricity to the grid, electricity producers have to put their bids into the market. These bids are based on power production estimates of the technologies. These bids ultimately depend on the resource available at the WEC and at the wind turbine location, and on the accuracy in the predictions of those resources.

As a result, this section focuses on forecasting of wave and wind parameters. It estimates the accuracy in waves and in winds predictions. It investigates short-term, day-ahead and long-term forecasts, in both typical and storm-like conditions. The analysis embraces three complete and non-consecutive months, from end of October 2010 to middle of February 2011.

Therefore, this section covers:
- Predictability of wave parameters:
  - Day-ahead predictability of the significant wave height, zero crossing period, maximum wave height and wave power. The correlation between wave forecasts with buoy-measurements is examined.
  - Long-term and short-term predictability.
- Predictability of wind parameters:
  - Day-ahead predictability of the wind speed, mean wind direction and wind power, in normal conditions. The correlation between wind forecasts with weather-station measurements is examined.
  - Long-term and short-term predictability.
- Predictability of wave and wind parameters in stormy conditions.

There are two first indications on that waves are more predictable than winds:
 i) There is phase shift between winds and waves, which indicates that when a wind speed is known the corresponding wave can be estimated.
 ii) Waves are less variable and have more inertia than winds, so a wave can be estimated from the information of the precedent wave.

Ultimately, the phase shift and the predictability depends on the wave origin; swell waves are very predictable (in Danish coasts of the North Sea swells come from hundreds of kilometres away, such as from Scotland, 600 km fetch length, Iceland, 1700 km, or Greenland, 2800 km) and wind waves can be accurately predicted up to only a certain lead time.

The analysis of chapter VII on phase shifts between waves and winds (i.e. SBM diagram) proves there is a time delay between waves and winds, and serves to complement the discussion topic of this section about predictability of waves and winds.

IV.2. PREDICTABILITY OF WAVE PARAMETERS

This section evaluates the accuracy to which wave parameters can be predicted. Errors in the forecasts are obtained from the comparison of forecast H_{m0}, H_{max}, T_{02} and P_{wave} and buoy-measured H_{m0}, H_{max}, T_{02} and P_{wave}, respectively.

Forecast predictability is estimated for 6 different forecast horizons through the quality indices described before.

For all wave parameters it can be observed the relationship between forecast accuracy and forecast horizon. Generally, forecast accuracies worsen as the lead time increases. This is illustrated by the 84 to 96 hours forecast accuracies.

IV.2.1. SIGNIFICANT WAVE HEIGHT PREDICTABILITY

TABLE XV shows the error statistics obtained from the comparison of forecast H_{m0} and buoy-measured H_{m0} for different forecast horizons throughout the study period. Forecast accuracy is evaluated for a forecast horizon of 0 to 1 hour, 1 to 12 hours, 12 to 24 hours, 24 to 36 hours, 36 to 48 hours and 84 to 96 hours.

TABLE XV

H_{m0} - Comparison of different forecasts to buoy-measurements of H_{m0} from 26/10/2010 to 09/02/2011.

Forecast horizon (h)		Mean (m)	Bias (m)	MAE (m)	MAE/Mean	RMSE (m)	SI$_{unbiased}$	CC	N
≥ 0	< 1	1.5	0.2	0.3	18%	0.3	18%	0.94	501
≥ 1	< 12	1.5	0.2	0.2	17%	0.3	18%	0.93	3514
≥ 12	< 24	1.5	0.2	0.3	19%	0.3	20%	0.91	3991
≥ 24	< 36	1.5	0.2	0.3	20%	0.4	22%	0.89	3967
≥ 36	< 48	1.5	0.2	0.3	21%	0.4	25%	0.86	3943
≥ 84	< 96	1.5	0.2	0.4	28%	0.5	35%	0.72	3847

The positive *Bias* indicates a prevalent trend where the forecast overestimates the buoy-measured values. Then, an MAE larger in magnitude than the Bias denotes that also the opposite trend is found, i.e. the forecast also underestimates the buoy-measured values, particularly as the forecast horizon increases. This can be seen both in the table as well as in the figures below.

RMSE points out that 68% of the forecasts are within ±0.3 to 0.5 meters of the *Mean* measured value of H_{m0}, i.e. 1.5 m. The *SI$_{unbiased}$* illustrates an acceptable dispersion of the

distribution. Then, a *CC* about 0.9 suggests a high correlation between the two sets of compared values.

The following figures present a visual comparison between forecast H_{m0} and buoy-measured H_{m0} for different forecast horizons during a very energetic wave period (11/12/2010 to 13/01/2011). Figure 33 illustrates the 12th lead time forecast, Figure 34 the 24th, Figure 35 the 36th and Figure 36 the 108th. In Figure 37 the differences among the 12, 24 and 36 hours forecast horizons are represented and compared to the buoy-measured data.

The figures show the big waves passing Hanstholm on New Year's Eve.
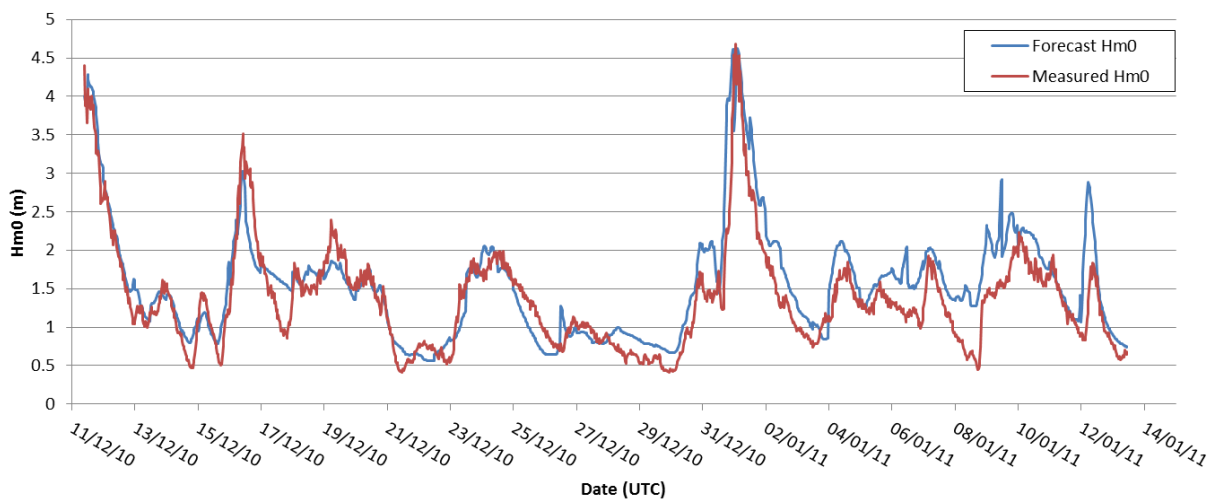
Figure 33. H_{m0} comparison of measured (in red) and 12-hour forecast (in blue).
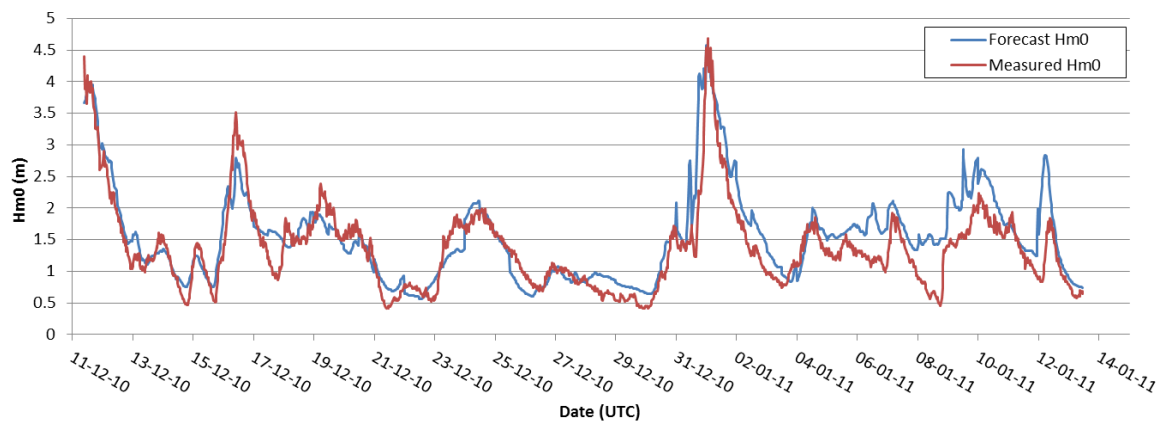
Figure 34. H_{m0} comparison of measured (in red) and 24-hour forecast (in blue).
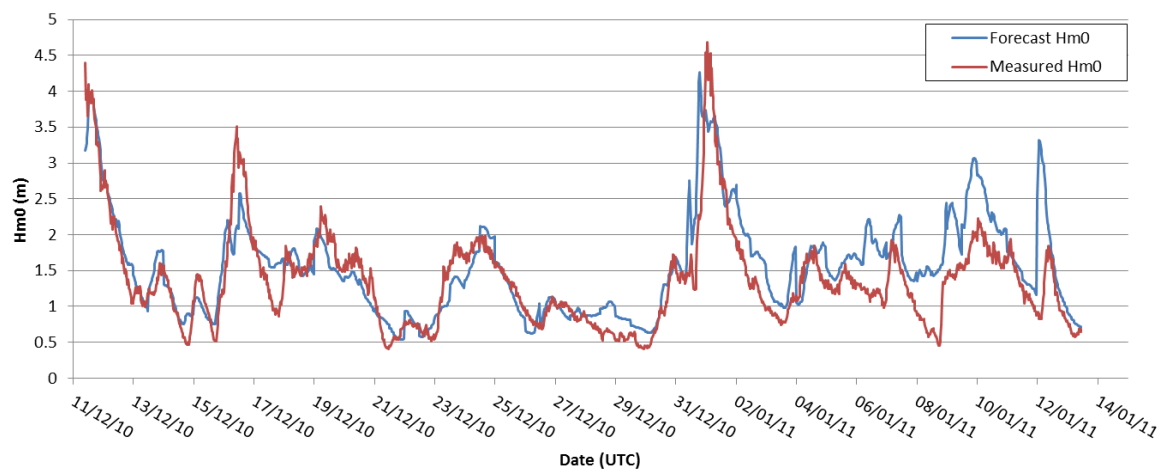
Figure 35. H_{m0} comparison of measured (in red) and 36-hour forecast (in blue).
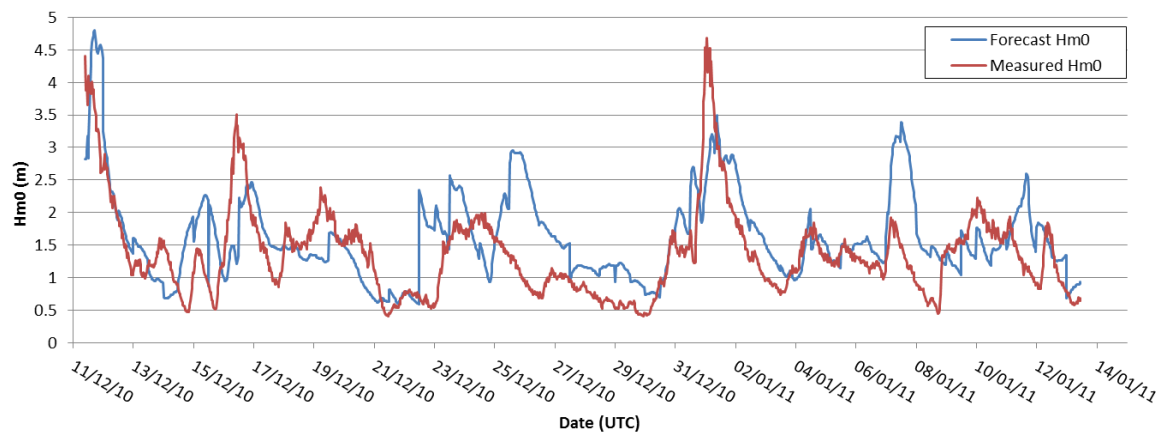
Figure 36. H_{m0} comparison of measured (in red) and 108-hour forecast (in blue).
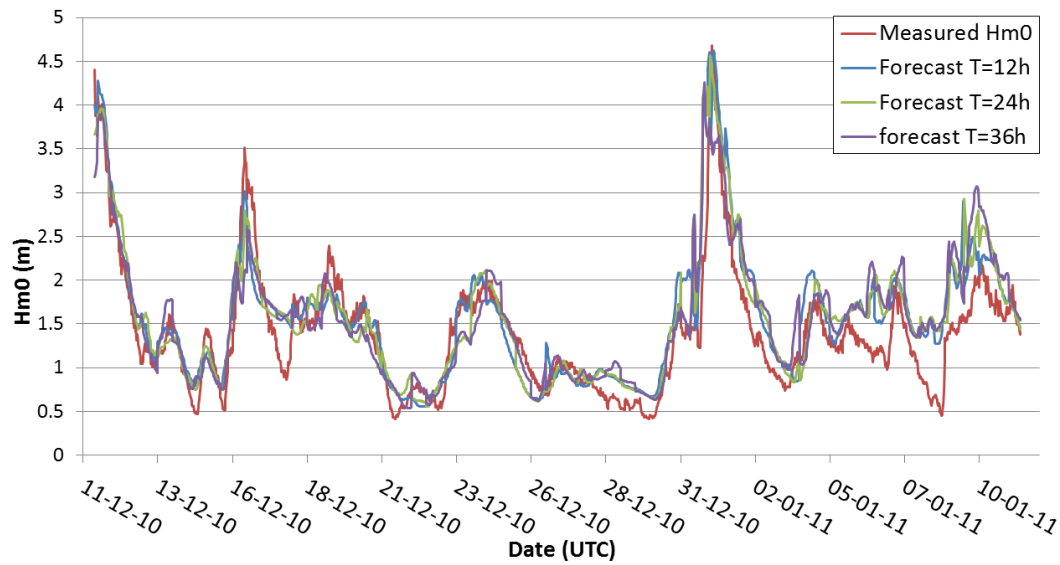
Figure 37. H_{m0} comparison of measured (in red) and 12 hours (In Blue), 24 hours (in green) and 36 hours forecast (in purple).

In summary, the agreement between H_{m0} forecasts and H_{m0} buoy-measured data is good for short-term forecasts and worsens as the lead time increases. Forecasts generally overestimate the measured data (positive bias).

IV.2.2. MAXIMUM WAVE HEIGHT PREDICTABILITY

TABLE XVI shows the error statistics obtained from the comparison of forecast H_{max} and buoy-measured H_{max} for different forecast horizons throughout the study period. Forecast accuracy is evaluated for a forecast horizon of 0 to 1 hour, 1 to 12 hours, 12 to 24 hours, 24 to 36 hours, 36 to 48 hours and 84 to 96 hours.

TABLE XVI

H_{max} - Comparison of different forecasts to buoy-measurements of H_{max} from 26/10/2010 to 09/02/2011.

Forecast horizon (h)		Mean (m)	Bias (m)	MAE (m)	MAE/Mean	RMSE (m)	SI$_{unbiased}$	CC	N
≥ 0	< 1	2.4	0.9	0.9	37%	1.0	23%	0.93	501
≥ 1	< 12	2.4	0.8	0.8	36%	1.0	23%	0.91	3514
≥ 12	< 24	2.4	0.8	0.9	36%	1.0	25%	0.90	3991
≥ 24	< 36	2.4	0.8	0.9	36%	1.0	28%	0.87	3967
≥ 36	< 48	2.4	0.8	0.9	37%	1.1	30%	0.85	3943
≥ 84	< 96	2.4	0.8	1.0	42%	1.2	40%	0.69	3847

In general, errors for H_{max} forecasting are always higher than for H_{m0}, although the quality indices follow the same trend. These errors can derive from the buoy-measured data. A known disadvantage of the spherical buoys (e.g. Datawell Waverider buoy) is that due to the single line mooring it circles around the crests of steep waves and thus, it does not reach the maxima in the surface elevation (Holthuijsen, 2007).

IV.2.3. ZERO CROSSING PERIOD PREDICTABILITY

TABLE XVII shows the error statistics obtained from the comparison of forecast T_{02} and buoy-measured T_{02} for different forecast horizons throughout the study period. Forecast accuracy is evaluated for a forecast horizon of 0 to 1 hour, 1 to 12 hours, 12 to 24 hours, 24 to 36 hours, 36 to 48 hours and 84 to 96 hours.

The negative *Bias* indicates a prevalent trend where the forecast underestimates the buoy-measured value. A *MAE* twice the *Bias* denotes that the forecast overestimates the measured values as well. However, both the *Bias* and *MAE* are small in magnitude compared to the *Mean* (MAE/Mean of 8-9%). *RMSE* indicates that 68% of the forecasts are within ±0.5 seconds of the *Mean* measured value of T_{02} i.e. about 4.7 seconds.

TABLE XVII

T_{02} - Comparison of different forecasts to buoy-measurements of T_{02} from 26/10/2010 to 09/02/2011.

Forecast horizon (h)		Mean (s)	Bias (s)	MAE (s)	MAE/Mean	RMSE (s)	$SI_{unbiased}$	CC	N
≥ 0	< 1	4.7	-0.2	0.4	8%	0.5	10%	0.81	501
≥ 1	< 12	4.7	-0.2	0.4	8%	0.5	10%	0.82	3514
≥ 12	< 24	4.7	-0.2	0.4	8%	0.5	10%	0.80	3991
≥ 24	< 36	4.7	-0.2	0.4	9%	0.5	11%	0.77	3967
≥ 36	< 48	4.7	-0.2	0.4	9%	0.6	11%	0.75	3943
≥ 84	< 96	4.7	-0.2	0.5	11%	0.7	14%	0.62	3847

Figure 38 presents a visual comparison of the 12-hour forecast of T_{02} and the buoy-measured values during the same winter month period shown for H_{m0} (11/12/2010 to 14/01/2011).
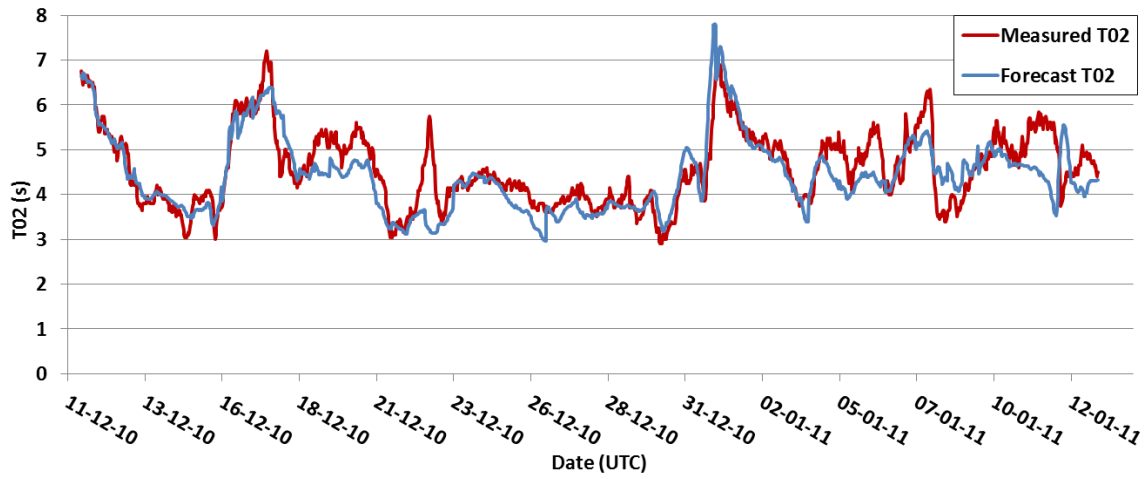
Figure 38. T_{02} comparison of measured (in red) and 12-hour forecast (in blue).

The graphical comparison illustrates the small and very acceptable dispersion of the distribution, which lies within small bounds ($SI_{unbiased}$ of 10-11%). The correlation between forecast and buoy-measured values (CC= 0.7-0.8) is lower than for H_{m0}. This can be clearly seen in the figures, where the pattern tendencies of the buoy-measured values are not strictly followed by the forecasts.

In summary, the comparisons show that T_{02} forecasts and T_{02} buoy-measurements are in very good agreement for the different forecast horizons. It can be seen that forecasts generally underestimate the measured data (negative bias).

IV.2.4. WAVE POWER PREDICTABILITY

TABLE XVIII shows the error statistics obtained from the comparison of forecast P_{wave} and buoy-measured P_{wave} for different forecast horizons throughout the study period. Forecast accuracy is evaluated for a forecast horizon of 0 to 1 hour, 1 to 12 hours, 12 to 24 hours, 24 to 36 hours, 36 to 48 hours and 84 to 96 hours.

In this case, it is important to note the relationship of P_{wave} with H_{m0} and T_{02}. Forecast errors in H_{m0} get raised to the power of two, and forecast errors in T_{02} to the power of one.

TABLE XVIII

Pwave - Comparison of different forecasts to buoy-measurements of Pwave from 26/10/2010 to 09/02/2011.

Forecast horizon (h)		Mean (kW/m)	Bias (kW/m)	MAE (kW/m)	MAE/Mean	RMSE (kW/m)	SI$_{unbiased}$	CC	N
≥ 0	< 1	9.1	2.3	3.5	39%	7.9	83%	0.89	501
≥ 1	< 12	8.8	1.9	3.1	35%	6.2	67%	0.92	3514
≥ 12	< 24	8.8	1.9	3.3	38%	6.3	68%	0.90	3991
≥ 24	< 36	8.9	1.6	3.6	40%	6.7	73%	0.86	3967
≥ 36	< 48	8.9	1.6	3.9	44%	7.3	80%	0.82	3943
≥ 84	< 96	8.9	1.2	5.1	57%	9.7	108%	0.64	3847

The positive *Bias* reveals the strongest influence of H_{m0}. It indicates that the forecast overestimates the derived buoy-measured value. As happens also in the case of H_{m0} and T_{02}, *MAE* is larger than the *Bias*, so the forecast also overestimates the buoy-measured values. Both *Bias* and *MAE* are quite large in magnitude compared to the *Mean*.

RMSE indicates that 68% of the forecasts are within ±6 and 9 kW/m of the *Mean* measured value of P_{wave}, i.e. 9 kW/m. This value suggests a quite inaccurate forecast; however, it is due to the peaks in P_{wave}, which reaches about 100 kW/m at certain periods of time (Figure 39). Similarly, *SI$_{unbiased}$* shows high dispersion of the distribution.

On the contrary, the correlation (*CC*= 0.8 to 0.9) between forecast and buoy-measured values is high, induced by the high value of *CC* for H_{m0}.

Figure 39 illustrates the peaks in P_{wave} in comparison to the *Mean* value of 8.9kW/m. This difference explains the high value of *RMSE* and *SI$_{unbiased}$*.
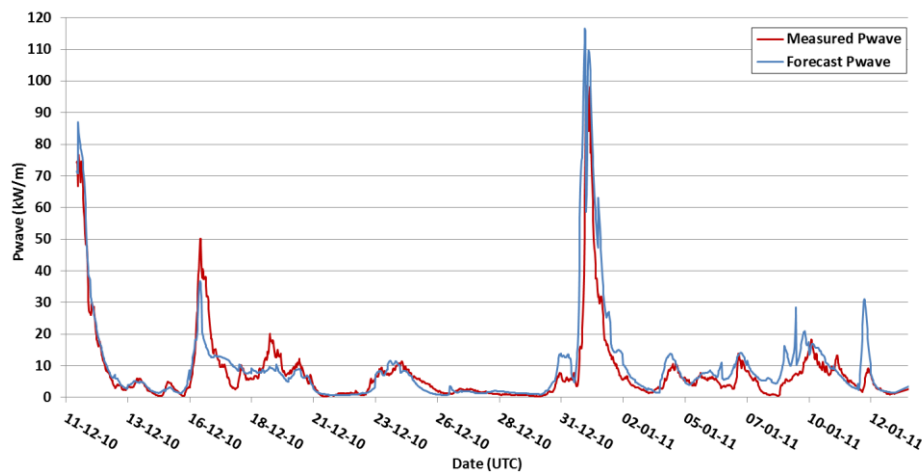
Figure 39. P_{wave} comparison of measured (in red) and 12-hour forecast (in blue).

Results show that P_{wave} forecasts and P_{wave} buoy-measurements derived values are in good agreement for small P_{wave} values and become inaccurate for the larger ones. Generally, forecasts overestimate the measured data (positive bias).

IV.2.5. DAY-AHEAD FORECASTS – SUMMARY

TABLE XIX summarises the results on predictability of wave parameters for the 12 to 48 hours forecast horizon, i.e. the day-ahead forecast. It shows the error statistics obtained from the comparison of forecast H_{m0}, H_{max}, T_{02} and P_{wave} and buoy-measured H_{m0}, H_{max}, T_{02} and P_{wave} throughout the study period.

TABLE XIX

H_{m0}, H_{max}, T_{02} and P_{wave} comparison of the 12 to 36 hours Forecast to buoy-measurements from 26/10/2010 to 09/02/2011.

	Mean	Bias	MAE	MAE/Mean	RMSE	$SI_{unbiased}$	CC	N
H_{m0} (m)	1.5	0.2	0.3	20%	0.4	22%	0.89	11901
H_{max} (m)	2.4	0.8	0.9	37%	1.0	28%	0.87	11901
T_{02} (s)	4.7	-0.2	0.4	9%	0.5	11%	0.77	11901
P_{wave} (kW/m)	8.9	1.7	3.6	41%	6.8	74%	0.86	11901

Results indicate that for day-ahead forecasts of wave parameters are accurate for H_{m0} and T_{02}, acceptable for H_{max} as well as for values of P_{wave} close to the mean, and not very accurate for larger P_{wave} values.

IV.2.6. SHORT-TERM AND LONG-TERM FORECASTS

This section compares the accuracy of short-term, day-ahead and long-term forecasts. Short-term refers to the first hour forecasts up to 12 hours, day-ahead to the 12 to 48 hours ahead forecast, and long-term to the 48 to 96 hours, or to 2 to 4 days ahead forecast. TABLE XX presents the accuracy of the forecasts of H_{m0}, H_{max}, T_{02} and P_{wave} in terms of MAE and MAE/Mean for three forecast horizons.

TABLE XX

H_{m0}, H_{max}, T_{02} and P_{wave} comparison of Forecast Accuracy for the 0-12 hours, 12-48 hours and 48 to 96 hours forecast horizon from 26/10/2010 to 09/02/2011.

	Mean	MAE $t=0-12h$	MAE/Mean $t=0-12h$	MAE $t=12-48h$	MAE/Mean $t=12-48h$	MAE $t=48-96h$	MAE/Mean $t=48-96h$
H_{m0} (m)	1.5	0.25	17%	0.29	20%	0.37	25%
H_{max} (m)	2.4	0.85	36%	0.87	37%	0.97	41%
T_{02} (s)	4.7	0.36	8%	0.41	9%	0.48	10%
P_{wave} (kW/m)	8.9	3.2	36%	3.6	41%	4.8	54%

Results show that as the lead time increases the errors also increase, most noticeable for P_{wave}. However, for T_{02} the errors for the 0-12 hours forecast are very similar to the 12-48 hours

forecast. For H_{m0}, short-term forecasts are 3 percentage points more predictable than day-ahead forecasts, and these are 5 percentage points more predictable than long-term forecasts. The biggest error happens in the 2-4 days forecast, although the accuracy remains very acceptable for T_{02} and acceptable for H_{m0}.

IV.2.7. 3-DAY PERIOD (23/12 TO 25/12/2010) - (BEST CASE SCENARIO)

Next chapter assesses the accuracy in the predictions of WEC´s power productions. To compare these to the forecast accuracy of wave parameters a 3-day winter period has been chosen, from 23/12 to 25/12/2010. These particular days provide a good representation of the typical operating conditions at the research site as well as fairly good forecast accuracy. It might be expected that future wave forecasts provide forecasts with the same accuracy as the ones presented here.

Figure 40 and Figure 41 show the evolution of the 12 hours forecast H_{m0}, T_{02} and P_{wave} and buoy-measured H_{m0}, T_{02} and P_{wave} over 23/12 to 25/12/2010. The three wave parameters oscillate around their mean values (TABLE XIX), giving a quite real representation of the typical sea states at Hanstholm during a winter month.
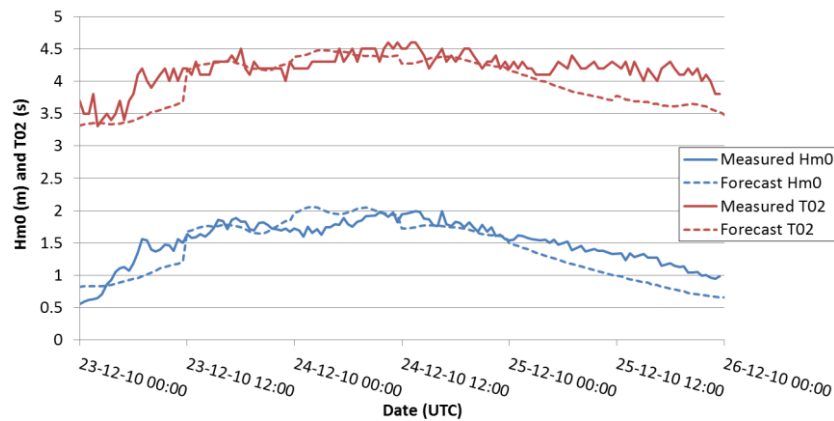
Figure 40. Evolution of buoy-measured (solid line) and 12 hours forecast (dashed line) of H_{m0} (in blue) and T_{02} (in red) over 23/12 to 25/12/2010.
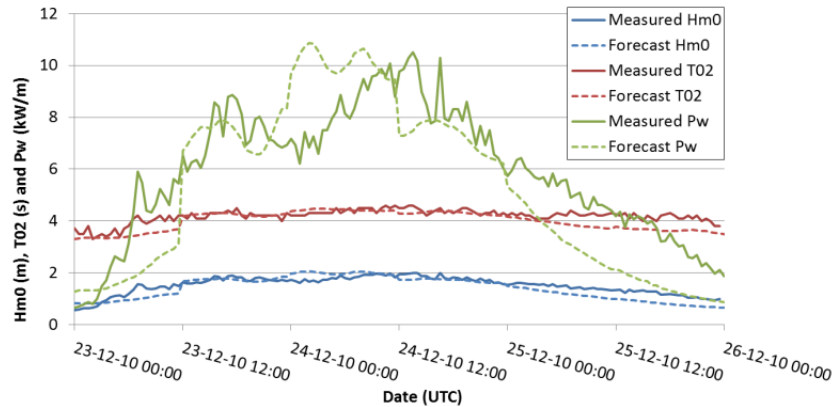
Figure 41. Evolution of buoy-measured (solid line) and 12 hours forecast (dashed line) of Hm0 (in blue), T_{02} (in red) and P_{wave} (in green) over 23/12 to 25/12/2010.

80

IV.3. PREDICTABILITY OF WIND PARAMETERS

This section evaluates the accuracy to which wave parameters can be predicted. Errors in the forecasts are obtained from the comparison of forecast u_{wind}, P_{wind} and MWD_{wind} and weather station measurements of u_{wind}, P_{wind} and MWD_{wind}, respectively.

Forecast predictability is estimated for 6 different forecast horizons through the quality indices described before.

For all wind parameters it can be observed the relationship between forecast accuracy and forecast horizon. Generally, forecast accuracies worsen as the lead time increases. This is illustrated by the 84 to 96 hours forecast accuracies.

It should however be noted that the wind energy sector has, along with meteorologists, focused on the wind forecasting for many years. This has allowed gaining knowledge and making a very fast improvement on weather forecasting. Here the accuracy of wind forecasting is evaluated in the same terms as the accuracy of wave forecasting; mostly as indicative results to allow comparison among the two sets of compared values. Hence, the results presented here should not be read as the current accuracy level on weather forecasting.

IV.3.1. WIND SPEED PREDICTABILITY

TABLE XXI shows the error statistics obtained from the comparison of forecast u_{wind} and weather-station measured u_{wind} for different forecast horizons throughout the study period. Forecast accuracy is evaluated for a forecast horizon of 0 to 1 hour, 1 to 12 hours, 12 to 24 hours, 24 to 36 hours, 36 to 48 hours and 84 to 96 hours.

TABLE XXI

u_{wind} - Comparison of different forecasts to weather-station measurements of u_{wind} from 26/10/2010 to 09/02/2011.

Forecast horizon (h)		Mean (m/s)	Bias (m/s)	MAE (m/s)	MAE/Mean	RMSE (m/s)	$SI_{unbiased}$	CC	N
≥ 0	< 1	7.9	0.8	1.8	23%	2.2	27%	0.83	642
≥ 1	< 12	7.8	0.6	1.7	22%	2.1	26%	0.83	4492
≥ 12	< 24	7.8	0.7	1.8	24%	2.3	28%	0.80	5110
≥ 24	< 36	7.8	0.7	2.0	25%	2.5	31%	0.77	5086
≥ 36	< 48	7.8	0.7	2.2	28%	2.7	34%	0.73	5062
≥ 84	< 96	7.8	0.7	2.8	36%	3.6	45%	0.52	4966

The following figure present a visual comparison between forecast u_{wind} and weather-station measured u_{wind} for the 12th lead time forecast.

81
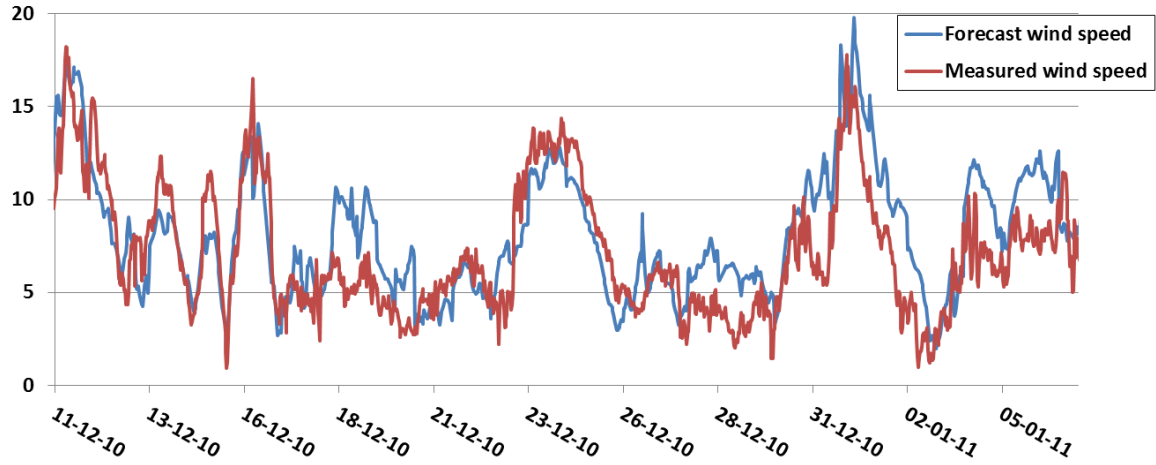
Figure 42. u_{wind} comparison of measured (in red) and 12-hour forecast (in blue).

IV.3.2. WIND POWER PREDICTABILITY

TABLE XXII shows the error statistics obtained from the comparison of derived data sets of forecast P_{wind} and real-time P_{wind} for different forecast horizons throughout the study period. Forecast accuracy is evaluated for a forecast horizon of 0 to 1 hour, 1 to 12 hours, 12 to 24 hours, 24 to 36 hours, 36 to 48 hours and 84 to 96 hours.

Note that for the wind power, the error in wind speed forecasts gets raised to the power of three.

TABLE XXII

P_{wind} - Comparison of different forecasts to weather-station measurements of P_{wind} from 26/10/2010 to 09/02/2011.

Forecast horizon (h)		Mean (W/m²)	Bias (W/m²)	MAE (W/m²)	MAE/Mean	RMSE (W/m²)	SI$_{unbiased}$	CC	N
≥ 0	< 1	508	108	301	59%	510	98%	0.77	642
≥ 1	< 12	496	56	255	51%	403	80%	0.80	4492
≥ 12	< 24	499	61	287	57%	454	90%	0.75	5110
≥ 24	< 36	501	66	303	61%	487	96%	0.71	5086
≥ 36	< 48	499	75	335	67%	531	105%	0.65	5062
≥ 84	< 96	497	77	428	86%	664	133%	0.46	4966

IV.3.3. MEAN WIND DIRECTION PREDICTABILITY

TABLE XXIII shows the error statistics obtained from the comparison of forecast MWD_{wind} and weather-station measured MWD_{wind} for different forecast horizons throughout the study period. Forecast accuracy is evaluated for a forecast horizon of 0 to 1 hour, 1 to 12 hours, 12 to 24 hours, 24 to 36 hours, 36 to 48 hours and 84 to 96 hours.

82

TABLE XXIII

MWD_wind - Comparison of different forecasts to weather-station measurements of *MWD_wind* from 26/10/2010 to 09/02/2011.

Forecast horizon (h)		Mean (°)	Bias (°)	MAE (°)	MAE/Mean	RMSE (°)	SI_unbiased	CC	N
≥ 0	< 1	176	3	27	16%	60	34%	0.81	642
≥ 1	< 12	172	17	29	17%	63	35%	0.81	4492
≥ 12	< 24	172	20	31	18%	64	35%	0.80	5110
≥ 24	< 36	172	20	33	19%	67	37%	0.78	5086
≥ 36	< 48	172	18	36	21%	71	40%	0.75	5062
≥ 84	< 96	171	15	46	27%	79	45%	0.68	4966

IV.3.4. DAY-AHEAD FORECASTS – SUMMARY

TABLE XXIV summarises the results on predictability of wind parameters for the 12 to 48 hours forecast horizon, i.e. the day-ahead forecast. It shows the error statistics obtained from the comparison of forecast u_{wind}, P_{wind} and MWD_{wind} and weather-station measured u_{wind}, P_{wind} and MWD_{wind} throughout the study period.

TABLE XXIV

u_{wind}, P_{wind} and MWD_{wind} Forecast Accuracy for the 12 to 48 hours forecast horizon from 26/10/2010 to 09/02/2011.

	Mean	Bias	MAE	MAE/Mean	RMSE	SI_unbiased	CC	N
u_{wind} (m/s)	7.8	0.7	2.0	26%	2.5	31%	0.76	15258
P_{wind} (W/m²)	500	67	308	62%	491	97%	0.70	15258
MWD_{wind} (°)	172	19	33	19%	67	37%	0.78	15258

Results of wind parameters predictability indicate that in the 12-48 hours horizon MWD_{wind} can be accurately predicted, u_{wind} presents errors up to 26%, in terms of *MAE/Mean*, and P_{wind} larger errors, 62%. Hence, u_{wind} predictability is more inaccurate than for H_{m0} and T_{02}. Generally the forecasts overestimate the real measured-values.

One main conclusion can be drawn from the comparison of day-ahead forecasting of wave parameters (TABLE XIX) and wind parameters (TABLE XXIV); day-ahead forecasting of waves is 23% more accurate than of winds.

IV.3.5. SHORT-TERM AND LONG-TERM FORECASTS

TABLE XXV presents the accuracy of the forecasts of u_{wind}, P_{wind} and MWD_{wind} in terms of MAE and MAE/Mean for the short-term (t=0-12 hours), the day-ahead and the long-term forecasts (t=2-4 days) forecast horizons.

It can be seen that forecasts improve as the lead hour decreases. The difference in accuracies between the long-term and the day-ahead forecasts is larger than between day-ahead and short-term forecasts.

TABLE XXV

u_{wind}, P_{wind} and MWD_{wind} comparison of Forecast Accuracy for the 0-12 hours, 12-48 hours and 48 to 96 hours forecast horizon from 26/10/2010 to 09/02/2011.

	Mean	MAE $t=0-12h$	MAE/Mean $t=0-12h$	MAE $t=12-48h$	MAE/Mean $t=12-48h$	MAE $t=48-96h$	MAE/Mean $t=48-96h$
u_{wind} (m/s)	7.8	1.7	22%	2.0	26%	2.60	33%
P_{wind} (W/m²)	500	260	52%	308	62%	399	80%
MWD_{wind} (°)	172	29	17%	33	19%	42	24%

IV.4. STORM CONDITIONS - WAVES PREDICTABILITY

Three periods with strong wave activity have been identified during the study period, one of them officially registered by the Danish Meteorological Institute on 8/02/2011 (DMI, 2012).

Table XXVI shows the characteristics of the three stormy periods: date, duration, date of maximum significant wave height and wave conditions, and date and values of maximum wind speeds. The duration of each period has been calculated from the time H_{m0} equals the average value over the study period (i.e. *Mean H_{m0}* of 1.45 m) and starts increasing, until the time H_{m0} drops and reaches the mean value again.

Table XXVI
Storms-like at Hanstholm in the study period.

	Date (UTC)	Duration (h)	Date max. u_{wind} (UTC)	max. u_{wind} (m/s)	Date max. H_{m0} (UTC)	max. H_{m0} (m)	H_{max} (m)	T_{02} (s)	Delay (max. u_{wind} - max H_{m0})
Period 1	11/12/2011 to 12/12/2012 at 18:00	33	11/12/2010 at 7:00	18.7	11/12/2010 at 9:30	4.4	7.1	7	2.5 h
Period 2	30/12/2010 at 19:30 to 02/01/2011 at 8.30	61	31/12/2010 at 22:00	18	01/01/2011 at 1:00	4.7	6.6	6.7	3 h
Period 3	07/02/2011 at 15:00 to 09/02/2011 at 9:30	43	07/02/2011 at 23:30	22.2	08/02/2011 at 2:00	4.3	7.4	6.8	2.5 h

The stormy period 3 was remarked by DMI (Danish Meteorological Institute) as "Storm, coastal areas" with a classification index "w1" (*w* indicates wind from west, *1* indicates stormy >21 m/s, and regional 10-30%).

For comparison, the wave and wind conditions of these three periods can be compared with the 10 year return period design wave parameters at Hanstholm: *Hs=6.6m* and *Tz=10s* (Nielsen et al., 2010), and a maximum wind speed of 30 m/s.

Figure 43 illustrates the evolution of P_{wave} before, during and after the 3-day stormy period on New Year's Eve on 2010 (i.e. Period 2). It can be seen P_{wave} increases from 4.3 kW/m to 95 kW/m in 11 hours.
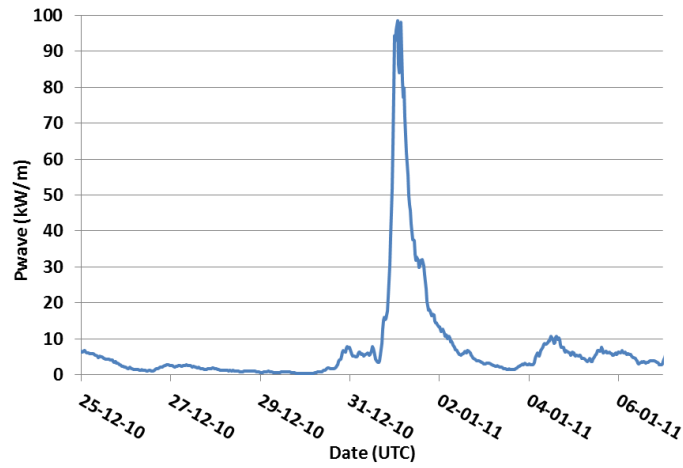
Figure 43. Evolution of P$_{wave}$ over the stormy period on 30/12/2010 to 02/01/2011.

Figure 43 also shows one of most important challenges of wave energy converters. In a matter of hours, the WEC has to withstand loads ten times higher than average loads. Hence, the WEC has to be designed to survive to extreme events but to operate in normal conditions. This issue particularly affects the capital cost of WECs. The infrequent extreme conditions at the deployment location dictate the structural design of the WEC, which is directly related to the capital costs of the WEC. However, the return of investment is given by the frequent low and medium wave states. This applies to both early stage small scale sea prototypes as well as full-scale commercial WECs.

Figure 44 illustrates the evolution of H_{m0} and T_{02} over the 2-day storm on February 2011. Both real-time and forecast data are represented.
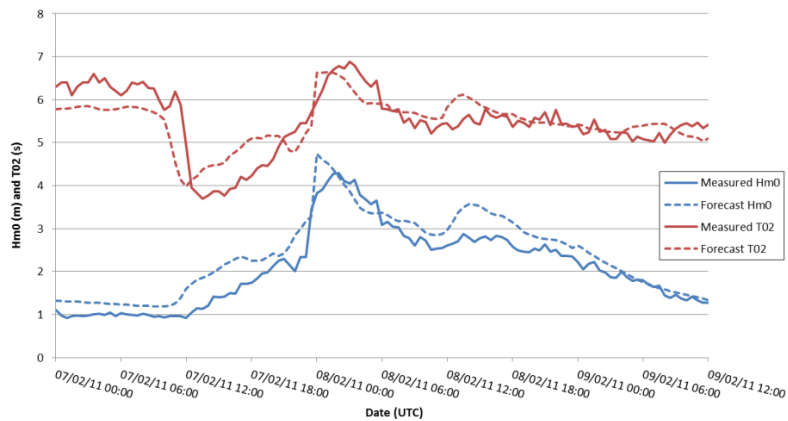
Figure 44. Evolution of real-time (solid line) and day-ahead forecasts (dashed lines) of H_{m0} (in blue) and T_{02} (in red) over the storm on 07/02 to 09/02/2011.

TABLE XXVII shows forecasts accuracy of wave parameters in the three storm-like conditions combined. It shows the error statistics obtained from the comparison of forecast

85

H_{m0}, H_{max} and T_{02} and buoy-measured H_{m0}, H_{max} and T_{02} for a forecast horizon of 12 to 48 hours during the three periods listed in Table XXVI.

H_{m0}, H_{max} and T_{02} - Comparison of day-ahead Forecasts to measurements throughout the three storms.

	Mean	Bias	MAE	MAE/Mean	RMSE	SI$_{unbiased}$	N
H_{m0} (m)	2.5	0.3	0.4	16%	0.5	19%	828
H_{max} (m)	4.0	1.3	1.3	33%	1.5	20%	828
T_{02} (s)	5.4	0.1	0.3	6%	0.5	8%	828

Note the number of points of this table is significantly lower than the number of points in all previous tables that showed forecasting errors of wave and wind parameters. Hence, results might be biased.

The following table shows the mean wave direction during the three storms. The Waverider buoy at Hanstholm is not directional; therefore, this data has its origin in DHI short-term forecasts. As a result, some errors in the data can be expected. The Table indicates mostly all waves come from South-West-West or North-West-West direction.

TABLE III
Characteristics of the Mean Wave Direction throughout the three storms.

	Mean	Max	Min	<1% time	<10%	<10%	<1%	N
MWD_{wave}	306	335	259	< 259	< 290	> 323	> 335	276

Next figure shows the swell component of the waves as calculated by DHI (2009). It can be seen that the swell component of H_{m0} remain normally within the same intervals. Since swells are more predictable than wind seas, it may be the case that predictability of the three stormy-periods is better than that of normal conditions, because of stronger present of swells during the storms. However, the swell component during the stormy periods (on 30/12/2010 and on 07/02/2011) is not particularly higher than in other periods. Therefore, this is not the reason of the apparent better predictability of the stormy conditions.
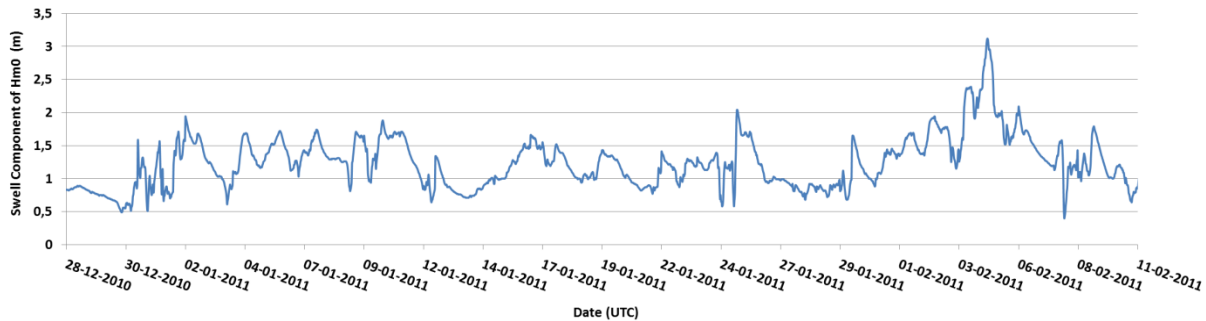
Figure 45. Evolution of H_{m0} swell component from 28/12/2010 to 11/02/2011.

In this particular study it proves more accurate (20% to 33%) to forecast wave parameters for storm-like conditions than for typical wave conditions (comparison between TABLE XIX and

TABLE XXVII). This does not represent the expected predictability of stormy periods, where weather conditions change very fast and are very difficult to predict. The reason for the accuracy can then be explained by the limited amount of data analysed, which corresponds to only one winter where weather patterns may get repeated. To draw final conclusions on storms predictability further data on stormy periods should be analysed.

IV.5. SUMMARY FORECASTS OF WAVES AND WINDS

Table XXVIII

Accuracy of day-ahead Forecasts of H_{m0}, H_{max}, T_{02}, P_{wave} and u_{wind}, P_{wind}, MWD_{wind} throughout Period I.

	Mean	MAE/Mean
H_{m0} (m)	1.5	20%
H_{max} (m)	2.4	37%
T_{02} (s)	4.7	9%
P_{wave} (kW/m)	8.9	41%
u_{wind} (m/s)	7.8	26%
P_{wind} (W/m^2)	500	62%
MWD_{wind} (°)	172	19%

Figure 46 illustrates waves and winds forecasts' accuracy for different forecast horizons, for the significant wave height, the zero-crossing wave period and the wind speed.
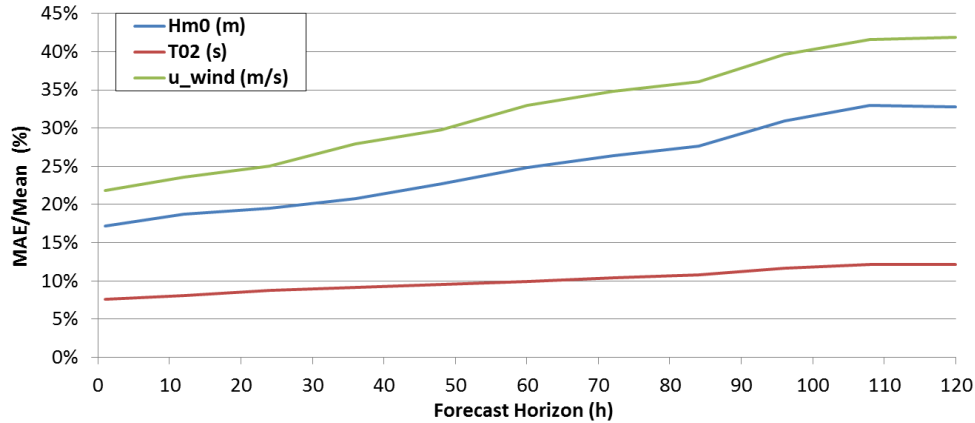
Figure 46. Five-day forecast errors, in terms of *MAE/Mean*, of H_{m0} (in blue), T_{02} (in red) and u_{wind} (in green) at Hanstholm during the study period.

Overall:

- Day-ahead forecasts of wave parameters are accurate for H_{m0} and T_{02}, acceptable for H_{max} as well as for values of P_{wave} close to the mean, and not very accurate for larger P_{wave} values.
  - The errors of day-ahead forecast of H_{m0}, H_{max}, T_{02} and P_{wave} is 20%, 37%, 9% and 41% (in terms of *MAE/Mean*), respectively.

- Short-term forecasts (*t=0-12 hours*) have better accuracy particularly for H_{m0} and P_{wave}, i.e. errors of 17%, 36%, 8% and 36% (in terms of *MAE/Mean*) for H_{m0}, H_{max}, T_{02} and P_{wave}, respectively.

- Day-ahead forecast of wind parameters are accurate for MWD_{wind}, acceptable for u_{wind} and a bit inaccurate for P_{wind}.
  - The errors of day-ahead forecast of u_{wind}, MWD_{wind} and P_{wind} is 26%, 19% and 62% (in terms of *MAE/Mean*), respectively.
  - Short-term forecasts (*t=0-12 hours*) have better accuracy particularly for u_{wind} and P_{wind}, i.e. errors of 22%, 17% and 52% (in terms of *MAE/Mean*) for u_{wind}, MWD_{wind} and P_{wind}, respectively.
  - Long-term forecasts present large errors: 33%, 24% and 80% (in terms of *MAE/Mean*) for u_{wind}, MWD_{wind} and P_{wind}, respectively.

- Hence, u_{wind} predictability is more inaccurate than for H_{m0} and T_{02}. Particularly, day-ahead forecasting of waves (i.e. H_{m0}) is 23% more accurate than of winds (i.e. u_{wind}), in terms of *MAE/Mean*. Day-ahead forecasting of P_{wave} is 50% more accurate than of P_{wind}, in terms of *MAE/Mean*.

- Generally forecasts overestimate the real measured-values, i.e. positive *Bias*.

- In this study it proves more accurate (20% to 33%) to forecast wave parameters for storm-like conditions than for typical wave conditions. This does not represent the expected predictability of stormy periods, where weather conditions change very fast and are more difficult to predict. Results can then be explained by the limited amount of data analysed, which corresponds to only one winter where weather patterns may get repeated. To draw final conclusions on storms predictability further data on stormy periods should be analysed.

- The three stormy periods in the analysis indicate a delay between 2.5 and 3 hours between max. u_{wind} and max. H_{m0}.

CHAPTER V – FORECASTS OF WECS AND WIND TURBINES POWER PRODUCTIONS

V.1. INTRODUCTION

This chapter addresses the accuracy in the forecasts of the power productions of WECs and of wind turbines. This is studied in normal and in stormy conditions. Ultimately, the outcome of this chapter is used to address the trading of WECs power productions into day-ahead electricity markets (Chapter VI).

Different scenarios are investigated:
- WECs operating alone.
- WECs operating two by two.
- WECs combined all together (100% wave energy).
- Wind turbines working alone (100% wind energy).
- WECs combined with wind turbines (50% wind + 50% wave energy).

The simultaneous and co-located forecasts and wave and wind measurement, along with the power matrices of the three WECs and the power curves of the wind turbines, are the basis of the study.

Therefore, this section covers:
- Predictability of WECs power production working alone:
  - Day-ahead predictability of the power production of Pelamis, Wave Dragon and Wavestar, based on theoretical power productions.
  - Day-ahead predictability of the power production of Wavestar, based on real power productions.
  - Predictability in stormy conditions.
- Predictability of WECs power production working combined.
  - Working together two by two.
  - Working the three combined.
- Predictability of wind turbines power production working alone:
  - Day-ahead predictability of the power production of Tradewind and Horns Rev I, based on theoretical power productions.
  - Day-ahead predictability of the power production of Folkecenter 525 kW wind turbine, based on real power productions.
- Predictability of WECs and wind turbines power production working combined.

This chapter focuses on the following question: Provided that winds are less predictable than waves, is the power output of wind turbines more or less predictable than the power output of WECs?

V.2. PREDICTABILITY OF WECS POWER PRODUCTION

This section evaluates the accuracy to which WECs power productions can be predicted. Errors in the forecasts are obtained from the comparison of theoretical power production forecast and theoretical *real-time* power productions. Results are presented in tables and figures. Forecast predictability is estimated for 6 different forecast horizons through the quality indices described before.

Real-time power outputs are modelled time-series; these have been derived from the power matrices of the three WECs. Only when specified, real power production data have been used.

This section shows that the general pattern is a positive *Bias* in the forecast, i.e. the forecast overestimates the measured production. As in the previuous chapter, forecast accuracies worsen as the lead time increases.

V.2.1. PELAMIS POWER PRODUCTION

Table XXIX shows the error statistics obtained from the comparison of P_{prod} based on forecast data and P_{prod} based on buoy-measurements for Pelamis throughout the study period. Forecast accuracy is evaluated for a forecast horizon of 0 to 1 hour, 1 to 12 hours, 12 to 24 hours, 24 to 36 hours and 36 to 48 hours. The last row in the table shows the accuracy of the 0th to the 48th lead time.

Table XXIX

Pelamis - Forecast accuracy of the Normalised Theoretical Power Production of Pelamis from 26/10/2010 to 09/02/2011.

Forecast horizon (h)		Mean (-)	NBias (-)	NMAE (-)	NRMSE (-)	$SI_{unbiased}$	CC	N
≥ 0	< 1	0.33	0.08	0.11	0.14	0.36	0.82	501
≥ 1	< 12	0.33	0.08	0.10	0.12	0.29	0.88	3514
≥ 12	< 24	0.33	0.08	0.11	0.14	0.35	0.82	3991
≥ 24	< 36	0.33	0.07	0.11	0.14	0.38	0.80	3967
≥ 36	< 48	0.33	0.08	0.11	0.15	0.38	0.80	3943
≥ 84	< 96	0.33	0.08	0.11	0.14	0.36	0.82	16079

Table XXIX shows that forecast accuracy (i.e. the spread of the distribution, $SI_{unbiased}$) is dependent on the forecast horizon; thus, forecasts become more inaccurate (i.e. higher values of $SI_{unbiased}$) as the forecast horizon increases.

It might be expected that the accuracy of P_{prod} predictions is also dependent on the amount of power produced. Figure 47 shows the influence of the amount of power produced, in terms of percentage of rated power, to the accuracy of the forecasts. The latter is evaluated by the normalised statistical parameter *NMAE*.
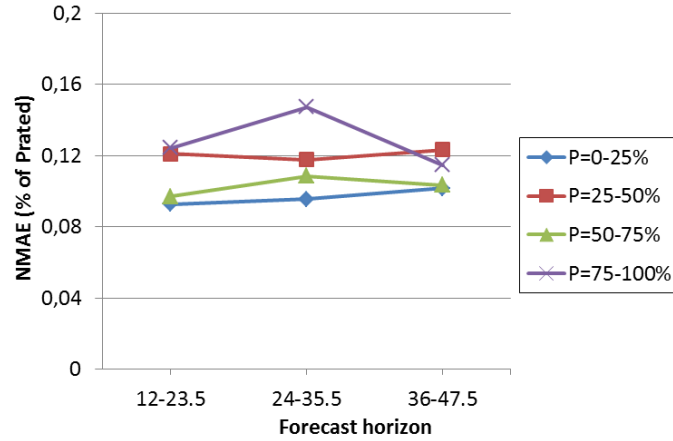
Figure 47. Influence of the *Forecast Horizon* (i.e. 12 hours forecast, 24 hours forecast and 36 hours forecast) and of the P_{prod} (in Percentage of Rated Power: 0 to 25% in Blue, 25 to 50% in Red, 50 to 75% in Green and 75 to 100% in Purple) on *Pelamis P_{prod} NMAE*.

Figure 47 shows that *NMAE* is more dependent on the amount of power produced than on the horizon forecast, particularly for power productions above 75% of rated power. The figure also shows that power generation levels up to 75% of rated power are more predictable than generation levels above 75%.

It is also interesting to look into the relationship of NMAE to the wave parameters H_{m0} and T_{02} for all forecast horizons. The following figures aims at answering the following questions:

- Is forecast accuracy related to H_{m0}, to T_{02} or to both parameters?
- Is this relation independent on the working principles of each device? For example, it is expected that NMAE of Pelamis and Wavestar is more dependent on the error in the prediction of T_{02} and Wave Dragon´s NMAE more dependent on the accuracy in the predictions of H_{m0}. Is this right?
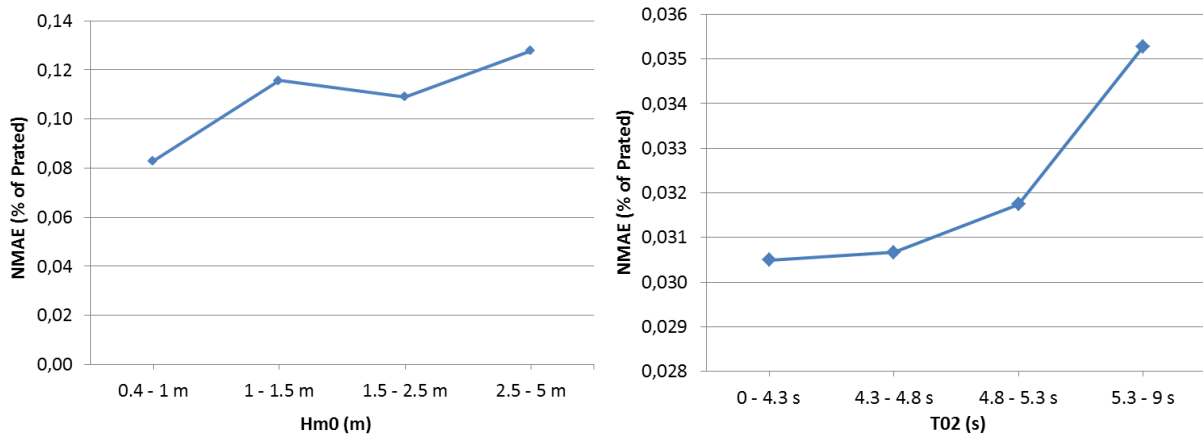
Figure 48. Relationship of Pelamis Power Production's *NMAE* to different values of H_{m0} (left figure) and T_{02} (right figure).

Figure 48 shows the errors in the forecasts have a stronger relationship with H_{m0} than with T_{02}. (*note this is the opposite relationship than for the working principle*). Errors induced by T_{02} are around 3%, whereas the errors induced by H_{m0} are about 8 to 13%. The largest errors are brought by the highest values of H_{m0}, which coincides with the maximum power production of the device.

V.2.2. WAVE DRAGON POWER PRODUCTION

Table XXX shows the error statistics obtained from the comparison of P_{prod} based on forecast data and P_{prod} based on buoy-measurements for Wave Dragon throughout the study period. Forecast accuracy is evaluated for a forecast horizon of 0 to 1 hour, 1 to 12 hours, 12 to 24 hours, 24 to 36 hours and 36 to 48 hours. The last row in the table shows the accuracy of the 0th to the 48th lead time.

Table XXX
Wave Dragon - Forecast accuracy of the Normalised Theoretical Power Production of Wave Dragon from 26/10/2010 to 09/02/2011.

Forecast horizon (h)		Mean (-)	NBias (-)	NMAE (-)	NRMSE (-)	SI$_{unbiased}$	CC
≥ 0	< 1	0.33	0.04	8%	0.13	0.37	501
≥ 1	< 12	0.33	0.03	7%	0.10	0.30	3514
≥ 12	< 24	0.33	0.03	8%	0.12	0.35	3991
≥ 24	< 36	0.33	0.03	9%	0.13	0.39	3967
≥ 36	< 48	0.33	0.04	10%	0.15	0.44	3943
≥ 84	< 96	0.33	0.04	9%	0.13	0.38	16079
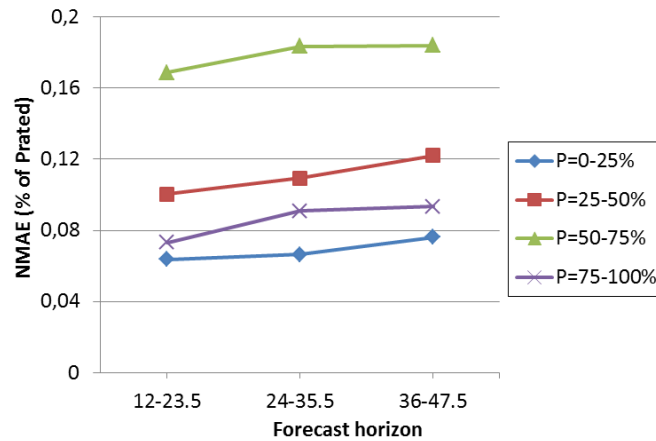
Figure 49. Influence on the Errors of the Power Production Forecasts of Wave Dragon of the forecast horizon (i.e. 12 hours forecast, 24 hours forecast and 36 hours forecast) and of the Pprod (in Percentage of Rated Power: 0 to 25% in Blue, 25 to 50% in Red, 50 to 75% in Green and 75 to 100% in Purple).

Figure 49 shows that, in the case of Wave Dragon, *NMAE* is very dependent on both the forecast horizons and on the percentage of rated power produced. As the time-horizon increases, the forecasts worsen. Regarding power productions, the most inaccurate forecast happens for power productions between 50 and 75% of rated power.
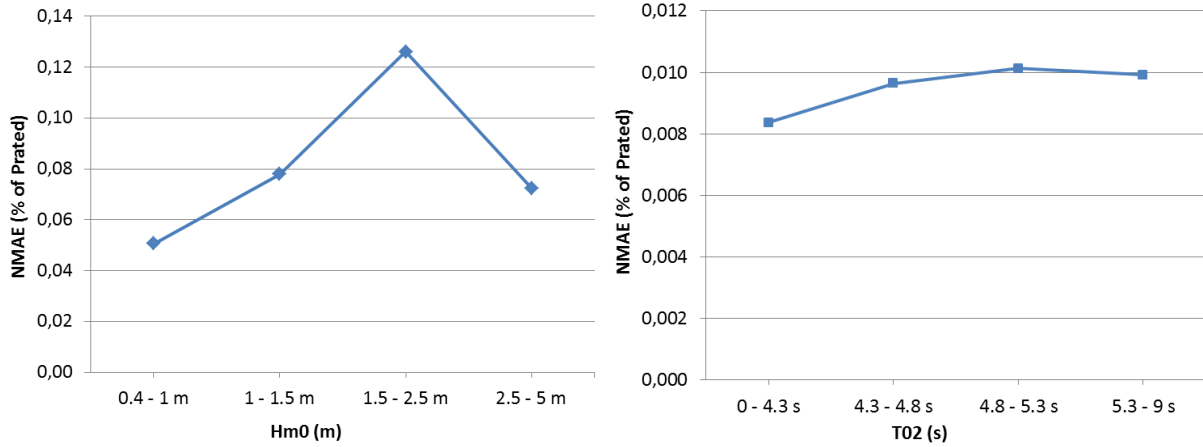
Figure 50. Relationship of Wave Dragon Power Production's NMAE to different values of H_{m0} (left) and T_{02} (right).

Figure 50 shows H_{m0} has larger influences on *NMAE* than T_{02}. *NMAE* for Wave Dragon is of the same order of magnitude than for Pelamis, but for H_{m0} ranging from 0.4 to 1 m, where the error in Wave Dragon is smaller. *NMAE* shows a peak for H_{m0} in between 1.5 and 2.5 meters. *NMAE* increases as T_{02} increases.

V.2.3. WAVESTAR POWER PRODUCTION

This section analyses the predictability of the power production of Wavestar for two different cases. The first one is based on modelled power production data of Wavestar, and the second one is based on real power production data of Wavestar's prototype operating at Hanstholm.

In order to investigate the accuracy of modelled Wavestar power production with respect to the real power production, the cross-correlation factor between Wavestar real production and modelled data from Wavestar power curve has been calculated. The cross-correlation factor between real power production and power production derived from the power matrix is of CC=0.91, which indicates the power matrix represents very accurately real power productions.

This section helps to validate the accuracy of the theoretical power productions compared to the real power productions. This might show whether the desk-study data are in accordance with real production data.

MODELLED POWER PRODUCTION

Table XXXI shows the error statistics obtained from the comparison of P_{prod} based on forecast data and P_{prod} based on buoy-measurements for Wavestar throughout the study period. Forecast accuracy is evaluated for a forecast horizon of 0 to 1 hour, 1 to 12 hours, 12 to 24 hours, 24 to 36 hours and 36 to 48 hours. The last row in the table shows the accuracy of the 0th to the 48th lead time.

Table XXXI
Wavestar - Forecast accuracy of the Normalised Theoretical Power Production of Wavestar from 26/10/2010 to 09/02/2011.

| Forecast horizon (h)		Mean (-)	NBias (-)	NMAE (-)	NRMSE (-)	$SI_{unbiased}$	CC	N
≥ 0	< 1	0.44	0.04	0.15	0.25	0.57	0.58	501
≥ 1	< 12	0.44	0.04	0.13	0.22	0.49	0.68	3514
≥ 12	< 24	0.44	0.04	0.14	0.23	0.52	0.65	3991
≥ 24	< 36	0.44	0.04	0.16	0.25	0.56	0.59	3967
≥ 36	< 48	0.44	0.04	0.15	0.25	0.54	0.62	3943
≥ 84	< 96	0.44	0.04	0.15	0.24	0.53	0.63	16079
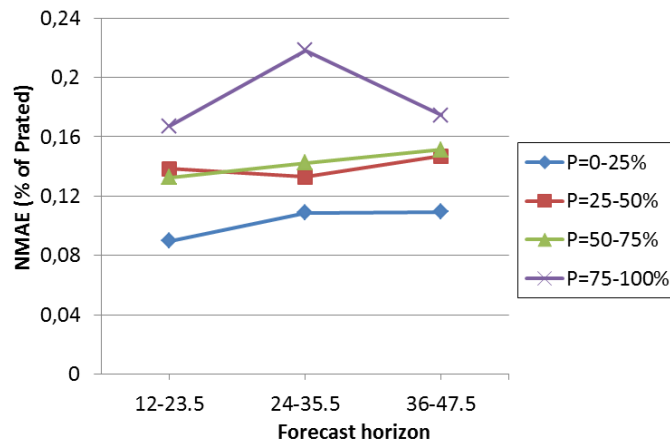
Figure 51. Influence on Wavestar NMAE of the forecast Horizon (i.e. 12 hours forecast, 24 hours forecast and 36 hours forecast) and of the Pprod (in Percentage of Rated Power: 0 to 25% in Blue, 25 to 50% in Red, 50 to 75% in Green and 75 to 100% in Purple).

Figure 51 presents the relationship between Wavestar´s P_{prod} and NMAE. Similarly as Pelamis, the most inaccurate forecasts happen for power productions between 75 and 100% of rated power. This is to say, power production between 0 and 75% of rated power are better predicted than those above 75% to 100% of rated power. This can be explained by the fact that WECs' maximum power production occur at maximum operating conditions (i.e. H_{m0} max. of 3 m) of the WEC. Thus, close values of H_{m0} and T_{02} can imply 100% power production or null production. Thus, small error in the higher values of H_{m0} and T_{02} predictions can induce noticeable errors. This fact is illustrated in the following figures (Figure 6).
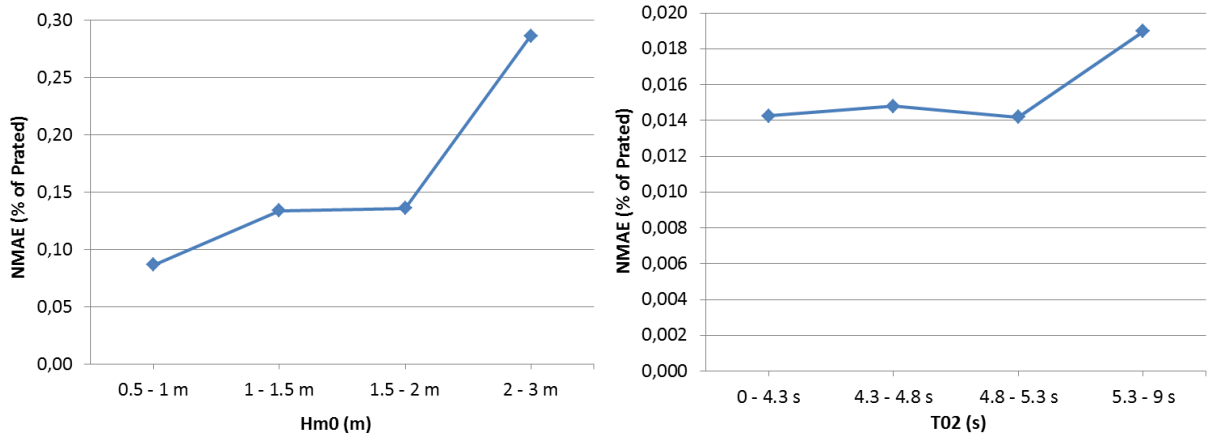
Figure 52. Relationship of Wavestar Power Production's NMAE to different values of H_{m0} (left) and T_{02} (right).

Figure 52 presents the variations of NMAE with H_{m0} and with T_{02}. As happens with the other WECs analysed, the influence of H_{m0} is higher than that of T_{02}.

To complement the three figures (Figure 47, Figure 49 and Figure 51) it is interesting looking into the percentage of time each device is producing 25% of rated power or 100% of rated power. Table XXXII shows the amount of power (in terms of percentage of rated power) each device is producing throughout the study period. This table along with the previous graphs allow understanding better the figures and draw out some conclusions.

Table XXXII

Percentage of Time the Power Productions of Pelamis, Wave Dragon and Wavestar are between the Indicated Percentages of Rated Power throughout Period I.

	Percentage of time x falls in the indicated intervals of production							
	x=0	0<x<20	20<x<40	40<x<60	60<x<80	80<x<100	x=100	N
Pelamis	1	28	31	28	10	2	0	4157
Wave Dragon	1	39	35	11	5	5	4	4157
Wavestar	5	16	27	24	14	9	4	4157

It can be seen that when the power production varies between 80 and 100% of rated power there are few data points for Pelamis and Wave Dragon, thus, results may be biased by the few data sets. The most accurate results are related to where the most data points exist, i.e. for power productions between 20 and 40% of rated power, and then for 0 to 20% and for 40 to 60% of rated power. These power productions will also have the most influence on the overall $SI_{unbiased}$ values. Therefore, the blue, the red and the green line are the most representative and the most trustable measurement.

An interesting finding from the three figures (Figure 47, Figure 49 and Figure 51) is that the errors in the production forecasts are different for each WEC, i.e. each WEC has a different relationship between *NMAE* and the forecast horizon and the power production. This

characteristic suggests that the forecast errors of the combined power production of the three WECs may be better than single power productions forecasting.

REAL POWER PRODUCTION

Table XXXIII shows the error statistics obtained from the comparison of P_{prod} based on forecast data and real power productions of Wavestar throughout the study period. Forecast accuracy is evaluated for a forecast horizon of 0 to 1 hour, 1 to 12 hours, 12 to 24 hours, 24 to 36 hours and 36 to 48 hours. The last row in the table shows the accuracy of the 0th to the 48th lead time.

Real-time production data correspond to Wavestar´s power production at Hanstholm. Forecast data have been derived from an adapted form of Wavestar's power matrix that considers that Wavestar´s cuts-off production at H_{m0} of 2.5 meters. This is done to have consistency between real power production and forecast derived power production. Also, all data points of null power production have been eliminated.

Table XXXIII

Wavestar - Forecast accuracy of the Normalised Real Power Production of Wavestar from 26/10/2010 to 09/02/2011.

Forecast horizon (h)		NMean (-)	NBias (-)	NMAE (-)	NRMSE (-)	$SI_{unbiased}$	CC	N
≥ 0	< 1	0.28	0.26	0.28	0.33	0.67	0.55	164
≥ 1	< 12	0.31	0.24	0.27	0.31	0.68	0.49	1158
≥ 12	< 24	0.30	0.25	0.28	0.32	0.66	0.53	1322
≥ 24	< 36	0.30	0.22	0.27	0.32	0.74	0.43	1322
≥ 36	< 48	0.30	0.23	0.29	0.34	0.81	0.34	1322

Table XXXIII shows a high NBias, a close value of NMAE to the NBias, and low NMean production.

The comparison between Table XXXIII and Table XXXI (note the difference in number of data points) shows better accuracy in the predictability of modelled data, particularly in terms of NBias, of the SI and of the CC, and higher Mean production. NMAE has a close value in the two tables.

V.2.4. DAY-AHEAD FORECASTS OF WECS ALONE – SUMMARY

TABLE XXXIV summarises the statistical parameters showing the errors in the forecast accuracy of the comparison of day-ahead forecasts and real-time normalized power productions of the three WECs:

TABLE XXXIV
Pelamis, Wave Dragon and Wavestar – Day-ahead Forecast accuracy of the Normalised Theoretical Real Power
Production of the three WECs from 26/10/2010 to 09/02/2011.

	NMean	NBias	NMAE	NMAE/ NMean	NRMSE	$SI_{unbiased}$	CC	N
Pelamis	0.33	0.08	11%	33%	0.14	0.37	0.80	11901
Wave Dragon	0.33	0.04	9%	27%	0.13	0.39	0.89	11901
Wavestar (modelled)	0.44	0.04	15%	34%	0.24	0.54	0.62	11901
Wavestar (real)	0.30	0.24	28%	93%	0.33	0.74	0.34	3966

V.2.5. STORM CONDITIONS

On February 8th a coastal storm with winds from West passed North Jutland. H_{m0} reached 4 m
and T_{02} 6.8 seconds (Figure 53). This section investigates the predictability of the power
production of the three WECs of the study during this storm.

Figure 44 presents the evolution of the day-ahead forecast and real-time wave parameters.
Figure 54, Figure 55 and Figure 56 show the evolution of the day-ahead forecast and real-time
modelled power productions of Pelamis, Wave Dragon and Wavestar for the 12th, 24th and
36th lead times, respectively.

Most of the forecasting errors happen for Wavestar, since a small error in the estimation of
H_{m0} affects gratefully the operating conditions of the device, either 100% of 0% production.
Then, Wave Dragon shows higher forecasting accuracy than Pelamis.

It should however be noted that, in real operation, WECs may enter into storm protection
mode as a storm approaches the deployment site. For instance, for Wavestar the storm
protection strategy involves un-ballasting the floats, raising them up from the water, and
jacking-up all the structure, which takes about an hour. Therefore, it is not expected that
WECs start and interrupt production from hour to hour (or from minute to minute) during a
storm, as it can be inferred from Figure 54.
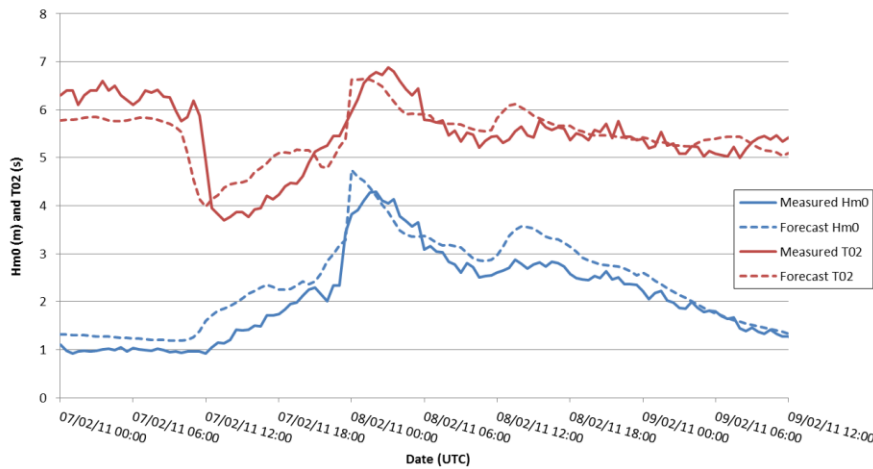
Figure 53. Evolution of Real-time (solid line) and of the Day-ahead Forecast (dashed lines) of H_{m0} (in blue) and
T_{02} (in red) over the storm on 07/02 to 09/02/2011.
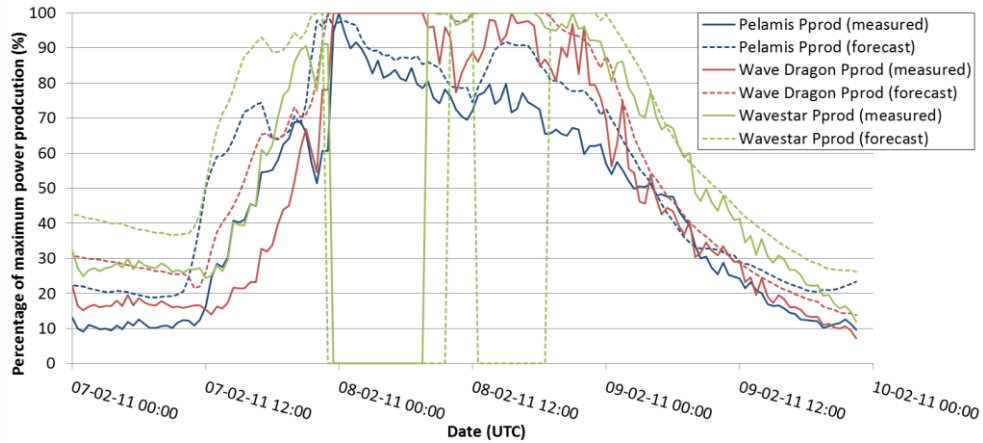
Figure 54. Evolution of Real-time (solid lines) and Forecast (dashed lines) Power Productions, in terms of percentage of rated power, of Pelamis (in blue), Wave Dragon (in red) and Wavestar (in green) for the 12th Lead hour, over a 3-day stormy period (07/02 to 10/02/2011).
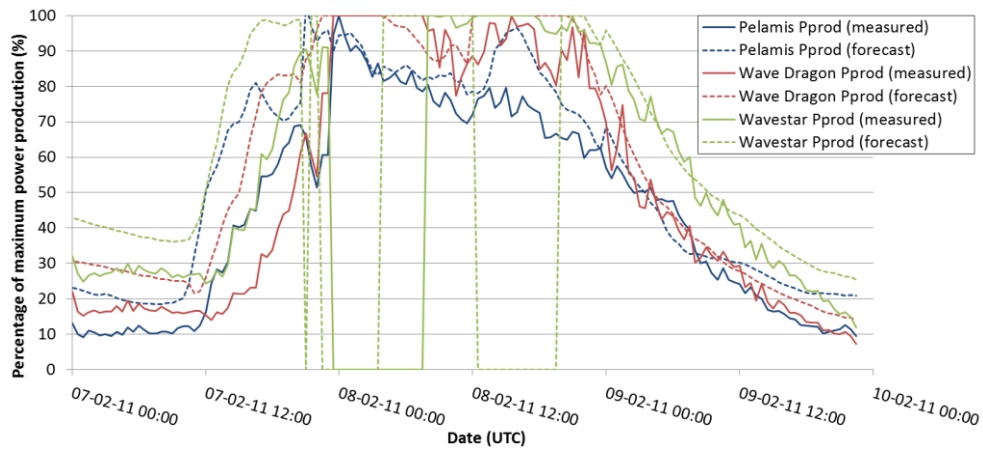
Figure 55. Evolution of Real-time (solid lines) and Forecast (dashed lines) Power Productions, in terms of percentage of rated power, of Pelamis (in blue), Wave Dragon (in red) and Wavestar (in green) for the 24th Lead hour, over a 3-day stormy period (07/02 to 10/02/2011).
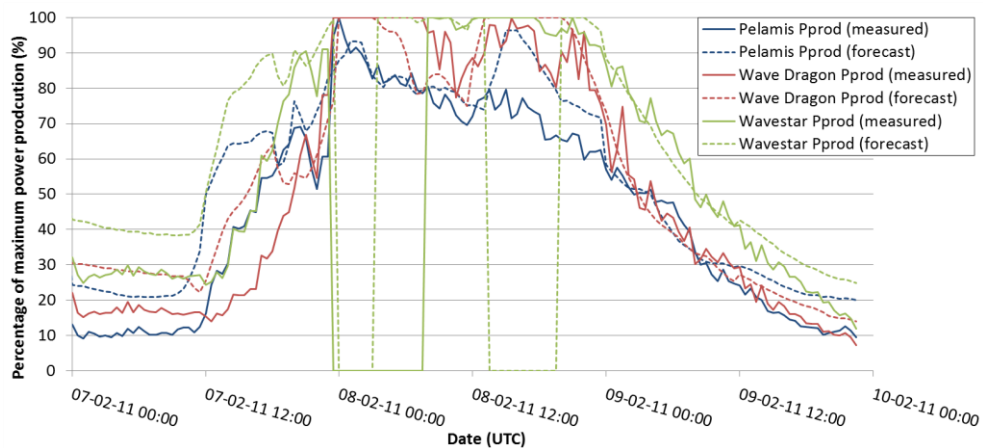
Figure 56. Evolution of Real-time (solid lines) and Forecast (dashed lines) Power Productions, in terms of percentage of rated power, of Pelamis (in blue), Wave Dragon (in red) and Wavestar (in green) for the 36th Lead hour, over a 3-day stormy period (07/02 to 10/02/2011).

V.3. PREDICTABILITY OF COMBINED PRODUCTIONS OF WECS

Two cases are evaluated in this section. WECs working combined two by two and all three WECs working together.

Errors in the forecasts are obtained from the comparison of theoretical power production forecast and theoretical *real-time* power productions. Results are presented in tables and figures. Forecast predictability is estimated for 5 forecast horizons covering the day-ahead forecasts. *Real-time* power outputs are modelled time-series; these have been derived from the power matrices of the three WECs.

V.3.1. WECS COMBINED TWO BY TWO

The cross-correlation factor between each pair of WECs is provided below. It indicates the degree in which the variation in the power production of one WEC is also happening in the other WEC.

Regarding predictabilities and variability of the power production, it is interesting that the WECs are not very much correlated. The more correlated the lowest probability to cancel out the errors in the forecast of power productions, and to cancel out the peaks in the production.

TABLE XXXVI shows Pelamis and Wave Dragon have the most correlated power productions (0.86), and Wave Dragon and Wavestar the lowest (0.73).

Table XXXV
Cross-correlation factors between Pelamis (P), Wave Dragon (WD) and Wavestar (WS) theoretical power productions when combined two by two.

	$CC_{between\ WECs}$
P+WD	0.86
WD+WS	0.70
P+WS	0.73

PELAMIS AND WAVE DRAGON POWER PRODUCTION PREDICTABILITY

TABLE XXXVI
Pelamis and Wave Dragon - Forecast accuracy of the Normalised Theoretical Power Production of the two WECs from 26/10/2010 to 09/02/2011.

Forecast horizon (h)		Mean (-)	NBias (-)	NMAE (-)	NRMSE (-)	$SI_{unbiased}$	N
≥ 0	< 1	0.34	0.06	9%	0.13	0.33	501
≥ 1	< 12	0.34	0.06	8%	0.11	0.26	3514
≥ 12	< 24	0.34	0.06	9%	0.12	0.31	3991
≥ 24	< 36	0.34	0.06	10%	0.13	0.34	3967
≥ 36	< 48	0.34	0.06	10%	0.14	0.37	3943

PELAMIS AND WAVESTAR POWER PRODUCTION PREDICTABILITY

TABLE XXXVII

Pelamis and Wavestar - Forecast accuracy of the Normalised Theoretical Power Production of the two WECs from 26/10/2010 to 09/02/2011.

Forecast horizon (h)		Mean (-)	NBias (-)	NMAE (-)	NRMSE (-)	$SI_{unbiased}$	CC	N
≥ 0	< 1	0.39	0.07	12%	0.16	0.37	0.77	501
≥ 1	< 12	0.40	0.06	11%	0.14	0.33	0.82	3514
≥ 12	< 24	0.40	0.06	12%	0.16	0.38	0.77	3991
≥ 24	< 36	0.40	0.06	13%	0.17	0.40	0.74	3967
≥ 36	< 48	0.40	0.07	13%	0.17	0.40	0.75	3943

WAVE DRAGON AND WAVESTAR PRODUCTION PREDICTABILITY

TABLE XXXVIII

Wave Dragon and Wavestar - Forecast accuracy of the Normalised Theoretical Power Production of the two WECs from 26/10/2010 to 09/02/2011.

Forecast horizon (h)		Mean (-)	NBias (-)	NMAE (-)	NRMSE (-)	$SI_{unbiased}$	N
≥ 0	< 1	0.38	0.04	11%	0.15	0.39	501
≥ 1	< 12	0.38	0.04	10%	0.14	0.35	3514
≥ 12	< 24	0.38	0.04	11%	0.15	0.39	3991
≥ 24	< 36	0.39	0.04	12%	0.16	0.42	3967
≥ 36	< 48	0.39	0.04	12%	0.17	0.42	3943

V.3.2. ALL WECS COMBINED

TABLE XXXIX shows the error statistics obtained from the comparison of P_{prod} based on forecast data and P_{prod} based on buoy-measurements for a combination of the three WECs. Different horizon forecasts have been considered. All results presented are non-dimensional and thus, can be read as percentage of rated power.

The 'All WECs Combined' scenario reflects the contribution of one normalised unit of each WEC.

TABLE XXXIX
Combined - Forecast accuracy of the Normalised Theoretical Power Production of the three WECs from 26/10/2010 to 09/02/2011.

Forecast horizon (h)		Mean (-)	NBias (-)	NMAE (-)	NRMSE (-)	$SI_{unbiased}$	CC	N
≥ 0	< 1	0.37	0.06	10%	0.13	0.33	0.83	501
≥ 1	< 12	0.37	0.05	9%	0.12	0.28	0.88	3514
≥ 12	< 24	0.37	0.05	10%	0.14	0.33	0.83	3991
≥ 24	< 36	0.37	0.05	11%	0.14	0.36	0.81	3967
≥ 36	< 48	0.37	0.06	11%	0.15	0.37	0.80	3943

Comparing power productions forecast accuracy of the combined production with the individual productions it can be seen that the best forecast occurs for the combined production of the WECs. The Bias, NMAE, NRMSE and $SI_{unbiased}$ improve compared to those of each single device. Moreover, not only the statistical parameters show a more accurate forecast but also maintain a high combined Mean P_{prod}.
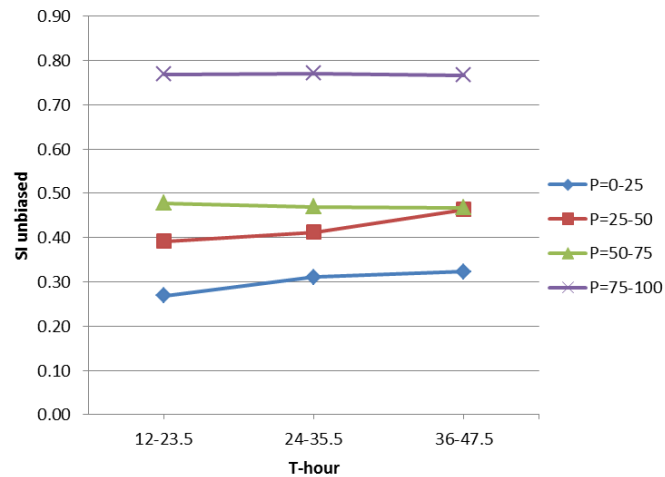
Figure 57. Influence of the Forecast Horizon (i.e. 12 hours forecast, 24 hours forecast and 36 hours forecast) and of the P_{prod} (in Percentage of Rated Power: 0 to 25% in Blue, 25 to 50% in Red, 50 to 75% in Green and 75 to 100% in Purple) on the Combined P_{prod} Scatter Index.

Table XL
Percentage of Time that the Combined Power Production is between the Indicated Percentages of Rated Power Throughout 26/10/2010 to 07/02/2011.

	Percentage of time x falls in the indicated intervals of production						
	x=0	0<x<20	20<x<40	40<x<60	60<x<80	80<x<100	x=100
All WECs Combined	1	27	33	23	11	6	0

Table XL show the combined production of the three WECs present the most levelised production and the lower percentage of time with zero production.

Figure 58 shows stronger variations of $SI_{unbiased}$ with H_{mo} than with T_{02}. Maximum $SI_{unbiased}$ coincides with maximum power production. $SI_{unbiased}$ is highly improved compared to the WECs working alone.
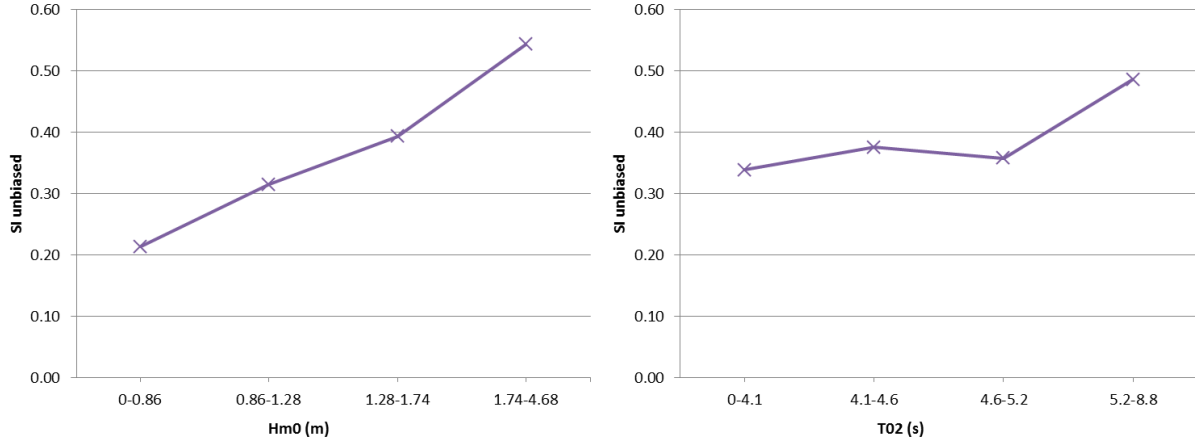
Figure 58. Relation of the Combined Power Production's $SI_{unbiased}$ to different values of H_{m0} (left) and T_{02} (right)

FORECAST ACCURACIES FROM 23/12 TO 26/12/2010

This section illustrates the errors in the forecasts of the power productions of the three WECs working alone and combined during a 3-day winter period, from 23rd to 26th December 2010. This time period has been selected since it represents normal operating conditions of Hanstholm.

Figure 59 shows the evolution of the real-time (solid lines) and of the forecasts (dashed lines) of H_{m0} and T_{02} during this period, as well as the 12-hour forecast horizons.
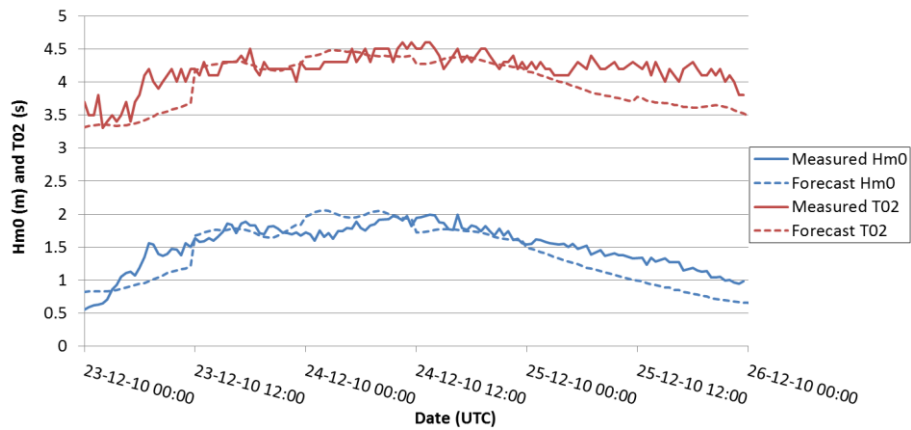
Figure 59. Evolution of buoy-measured (solid line) and 12 hours forecast (dashed line) of H_{m0} (in blue) and T_{02} (in red) over 23/12 to 25/12/2010.

Figure 60 depicts the 12 hours forecast, Figure 61 the 24 hours forecast and Figure 62 the 36 hours forecast for the power production of the three WECs. Both figures present real-time P_{prod} based on buoy-measurements (solid lines) and forecast P_{prod} based on forecast data

103

(dashed lines), in terms of percentage of rated power, of Pelamis (in blue), Wave Dragon (in red) and Wavestar (in green).

Figure 60. P_{prod} based on buoy-measurements (solid lines) and P_{prod} based on forecast data (dashed lines), in terms of percentage of rated power of Pelamis (in blue), Wave Dragon (in red) and Wavestar (in green) for the 12th lead hour over a 3-day period (23/12 to 25/12/2010).

Power productions reach up to 80% of rated power for Wavestar, 65% for Pelamis and 45% for Wave Dragon. These differences are the result of the selected location, since only Wavestar has been dimensioned for Hanstholm wave climate.

Along the curves, different prediction patterns can be found. Firstly, an underestimating forecast, then, and overestimating forecast 8-hour long, where Wavestar production is up to 80% overestimated, Pelamis 23% and Wave Dragon 60%. Then, a slightly underestimating forecast happens and lastly, a more inaccurate underestimating forecast.

Figure 61. P_{prod} based on buoy-measurements (solid lines) and P_{prod} based on forecast data (dashed lines), in terms of percentage of rated power of Pelamis (in blue), Wave Dragon (in red) and Wavestar (in green) for the 24th lead hour over a 3-day period (23/12 to 25/12/2010).

104
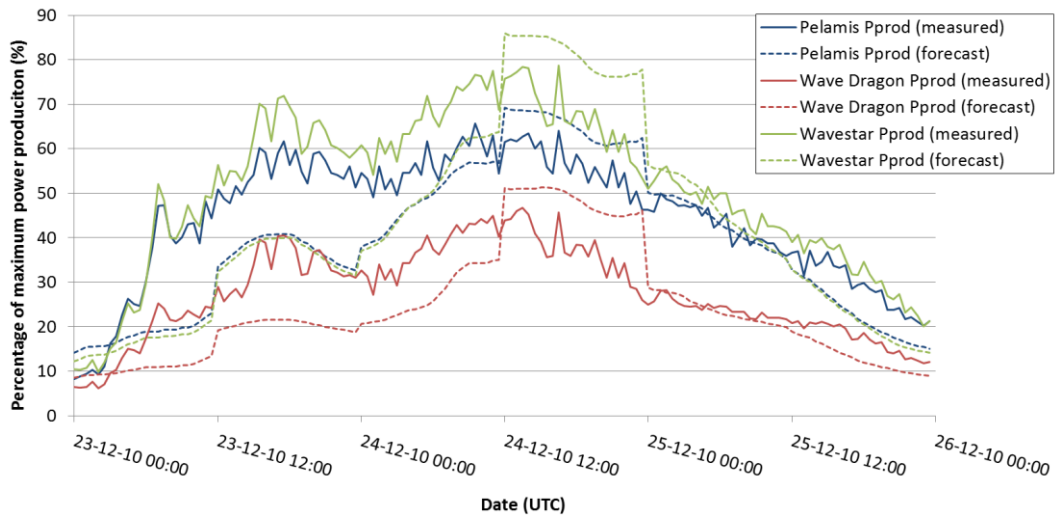
Figure 62. P_{prod} based on buoy-measurements (solid lines) and P_{prod} based on forecast data (dashed lines), in terms of percentage of rated power of Pelamis (in blue), Wave Dragon (in red) and Wavestar (in green) for the 36th lead hours over a 3-day period (23/12 to 25/12/2010).

The comparison of the figures above shows that the best forecast occurs for the 12-hour horizon forecast. Here there are some periods where the predictions coincide with the theoretical production. Although the errors for the 36 hours forecast are higher, in any case they exceed 30% of inaccuracy.

Wave Dragon shows the lowest errors among the three WECs and Wavestar the largest. This can be explained due to the more limited working conditions of Wavestar compared to Pelamis and Wave Dragon.

For a graphical overview, Figure 63 depicts the 12, 24 and 36 hours forecast P_{prod} and real-time P_{prod} for the combination of the three devices. For most samples the 12 hour forecast is the most accurate.
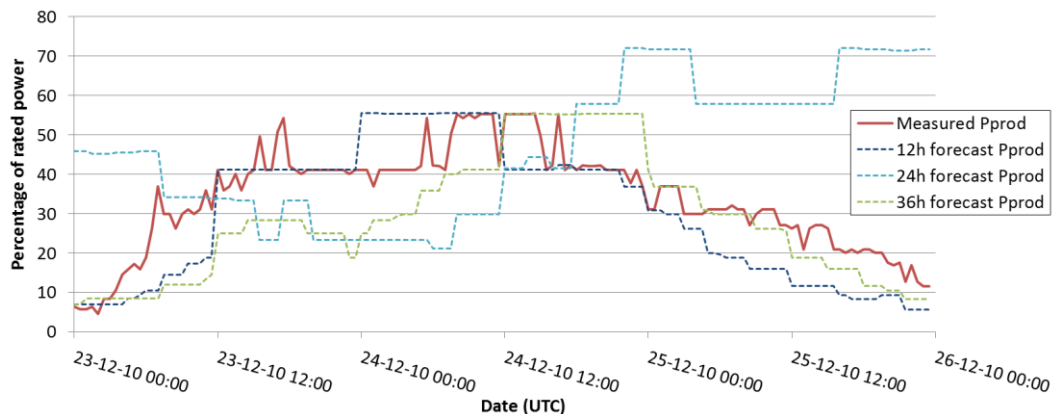
Figure 63. P_{prod} based on buoy-measurements (solid line) and P_{prod} based on forecast data (dashed lines), in terms of percentage of rated power of the combination of the three WECs, for a forecast horizon of 12 hours (dark blue), 24 hours (light blue) and 36 hours (green) over a 3-day period (23/12 to 25/12/2010).

The following figures (Figure 64 and Figure 65) complement the graphical comparisons. They illustrate the differences, in percentage, of forecast and real-time P_{prod} of Pelamis, Wave Dragon and Wavestar. The graphs cover the same 3-day period (23/12 to 25/12/2010). Figure 64 depicts the 12 hours forecast and Figure 65 the 36 hours forecast.

The bars above the 'x' axis indicate the forecast overestimates the real-time values. On the other hand, the bars below the 'x' axis read as that the forecast underestimates the real-time values. The samples where no bars are shown indicate that the forecast matches perfectly real-time P_{prod}.
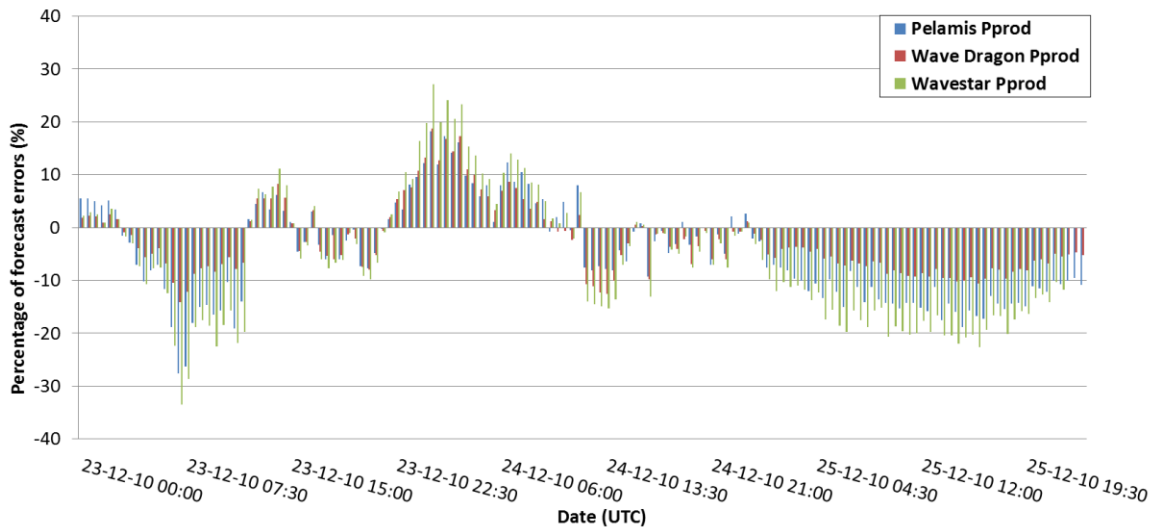
Figure 64. Difference, in percentage, of normalised forecast P_{prod} and normalised theoretical P_{prod} of Pelamis (in blue), Wave Dragon (in red) and Wavestar (in green) for forecast horizon of 12 hours, over a 3-day period (23/12 to 25/12/2010).
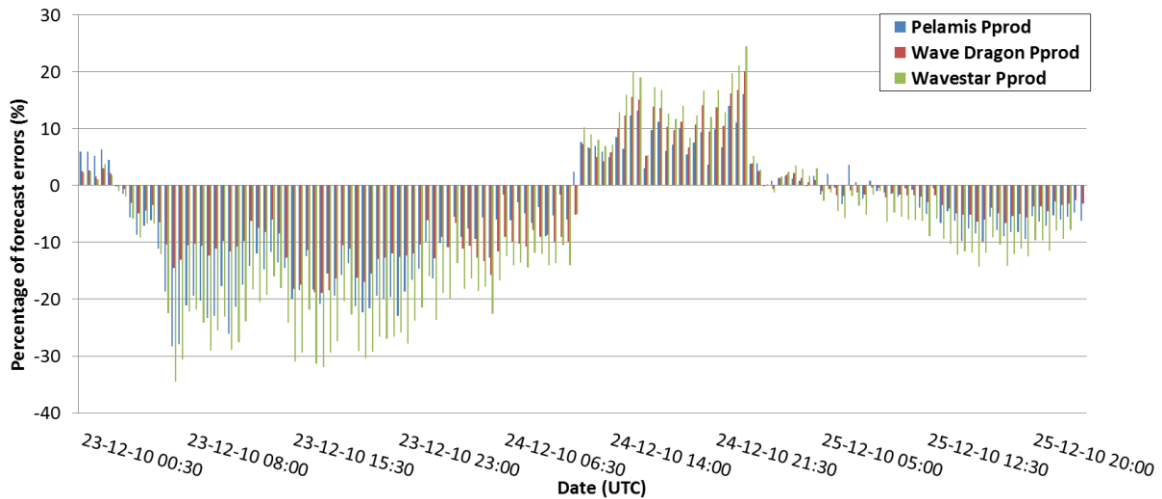
Figure 65. Difference, in percentage, of normalised forecast P_{prod} and normalised theoretical P_{prod} of Pelamis (in blue), Wave Dragon (in red) and Wavestar (in green) for a forecast horizon of 36 hours, over a 3-day period (23/12 to 25/12/2010).

Figure 64 shows that the error in the 12 hours forecast is generally around 10% of rated power and for the 36 hours forecast the error is around 15% of rated power, rising up to 30% in some samples (Figure 65).

FORECAST ACCURACIES FROM 09/11 TO 12/11/2010

This section illustrates the errors in the forecasts of the power productions of the three WECs working alone and combined during a 3-day autumn period, from 9th to 12th November 2010. This time period also represents normal operating conditions of Hanstholm. Figure 66 shows the evolution of buoy-measurements H_{m0} and T_{02} during these days.
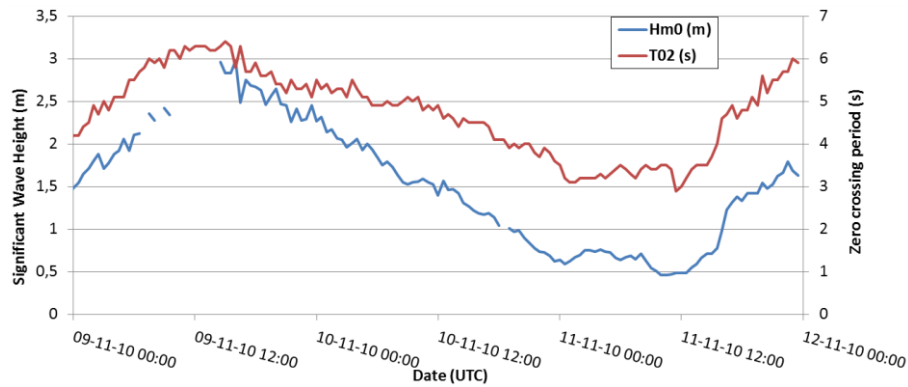
Figure 66. Evolution of H_{m0} (in blue) and T_{02} (in red) over 09/11 to 12/11.

For the same forecast horizon, Figure 67 presents a different forecast pattern for the WECs compared to Figure 112. It shows very accurate forecast for Wave Dragon, quite accurate for Pelamis and very inaccurate for Wavestar. The most remarkable effect here is that whereas Wave Dragon forecast is 100% correct, Wavestar power production is 100% underestimated (due to its survivability strategy) and Pelamis production is 60% overestimated. Therefore, each WEC presents different predictability patters.
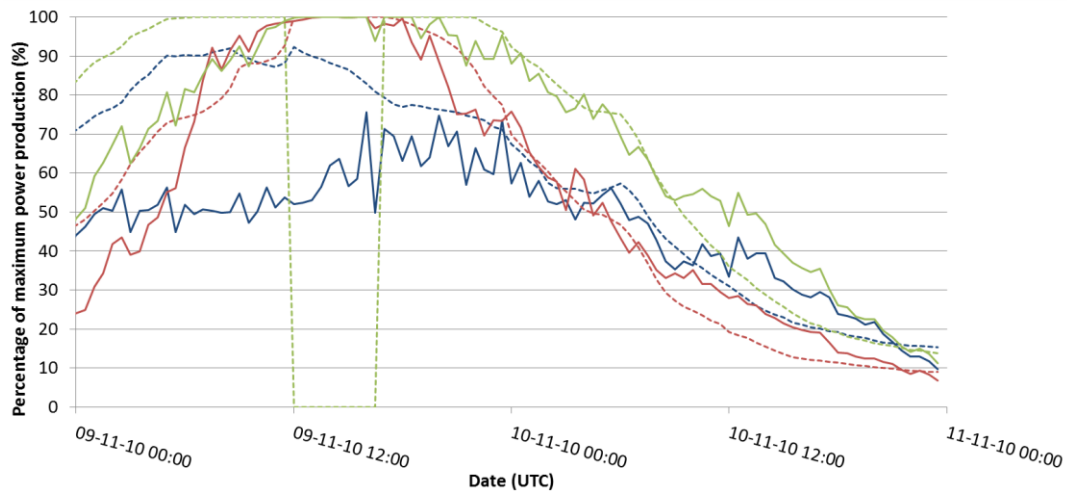
Figure 67. Real-time Pprod based on buoy-measurements (solid lines) and Forecast Pprod based on forecast data (dashed lines), in terms of percentage of rated power of Pel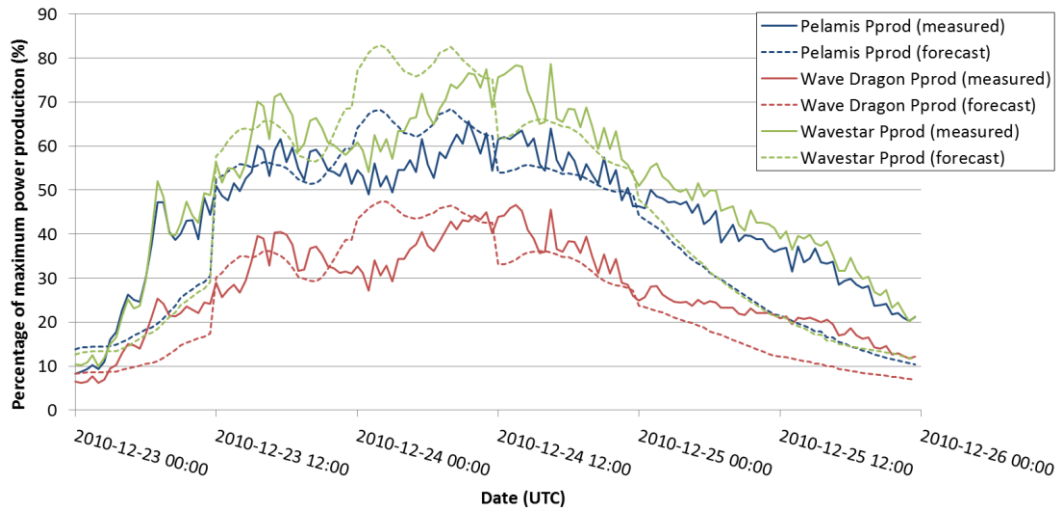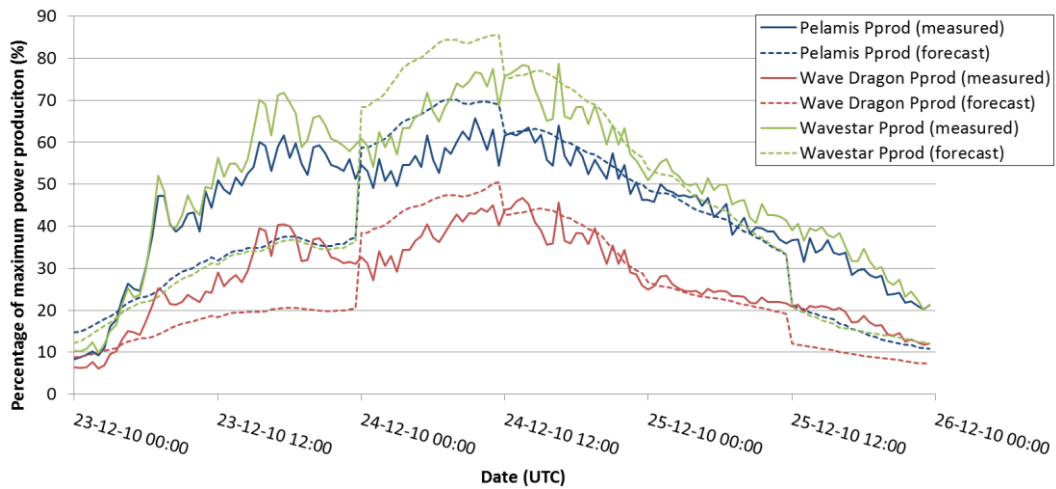amis (in blue), Wave Dragon (in red) and Wavestar (in green) for a 12th lead hour over a 2-day period (9/11 to 11/11/2010).

V.3.3. DAY-AHEAD FORECASTS OF WECS COMBINED – SUMMARY

TABLE XLI summarises the statistical parameters showing the errors in the forecast accuracy of the comparison of day-ahead forecasts and real-time normalized power productions of the three WECs working alone, the three WECs working combined in pairs, and the three WECs working all combined.

TABLE XLI

Pelamis, Wave Dragon and Wavestar - Forecast accuracy of the Normalised Power Production of the WECs, working alone and combined, from 26/10/2010 to 09/02/2011.

	NMean	NBias	NMAE	NMAE/ NMean	NRMSE	SI$_{unbiased}$	CC	N
Pelamis	0.33	0.08	11%	33%	0.14	0.37	0.80	11901
Wave Dragon	0.33	0.04	9%	27%	0.13	0.39	0.89	11901
Wavestar (modelled)	0.44	0.04	15%	34%	0.24	0.54	0.62	11901
Wavestar (real)	0.30	0.24	28%	93%	0.33	0.74	0.34	3966
P+WD	0.34	0.06	10%	29%	0.13	0.34	0.88	11901
WD+WS	0.39	0.04	12%	31%	0.16	0.41	0.79	11901
P+WS	0.40	0.06	13%	32%	0.17	0.39	0.77	11901
All WECs Combined	0.37	0.05	11%	30%	0.14	0.36	0.83	11901

The comparison among NMAE values and NMAE/NMean concludes that the combined power production (*All WECs combined*) results in high forecast accuracy and power production.

V.4. PREDICTABILITY OF WIND TURBINES POWER PRODUCTION

This section evaluates the accuracy to which the power productions of wind turbines can be predicted. Errors in the forecasts are obtained from the comparison of theoretical power production forecast and theoretical *real-time* power productions. Results are presented in tables and figures. Forecast predictability is estimated for 6 different forecast horizons through quality indices.

Real-time power outputs are either modelled or real time-series. Modelled time-series have been derived from the power curves of the Tradewind model or Horns Rev I model. Real time-series are real power production data from the Folkecenter wind turbine.

V.4.1. MODELLED POWER PRODUCTION

TRADEWIND POWER CURVE MODEL

Tradewind power curve has been developed by the Tradewind project to represent a typical power curve of an offshore wind turbine. Nominal power is reached at wind speeds of 14 m/s.

By contrast, mean wind speeds at Hanstholm in the study period are in the range of 7 to 8 m/s (TABLE VIII and TABLE IX). The power curve cuts-off production at wind speeds of 30 m/s. The cut-off points are not reached in this case study, since maximum wind speeds recorded at Hanstholm in the study period are of 21 m/s.

Table XLII shows the error statistics obtained from the comparison of forecast power productions and real-time power productions calculated with the Tradewind offshore wind turbine model throughout the study period. Forecast accuracy is evaluated for a forecast horizon of 0 to 1 hour, 1 to 12 hours, 12 to 24 hours, 24 to 36 hours and 36 to 48 hours.

Table XLII
Tradewind - Forecast accuracy of the Normalised Theoretical Power Production of Tradewind wind model from 26/10/2010 to 09/02/2011.

Forecast horizon (h)		Mean (-)	NBias (-)	NMAE (-)	NRMSE (-)	$SI_{unbiased}$	CC	N
≥ 0	< 1	0.34	0.08	0.15	0.23	0.63	0.80	642
≥ 1	< 12	0.34	0.06	0.14	0.21	0.59	0.82	4492
≥ 12	< 24	0.34	0.07	0.16	0.23	0.66	0.78	5110
≥ 24	< 36	0.34	0.07	0.17	0.25	0.71	0.74	5086
≥ 36	< 48	0.34	0.08	0.19	0.27	0.75	0.71	5062

HORNS REV I POWER CURVE MODEL

Horns Rev power curve (Soerensen, et al., 2005) represents the behaviour of Horns Rev I offshore wind energy farm. Nominal power is reached at wind speeds of 15 m/s. Mean wind speeds at Hanstholm in the study period are in the range of 7 to 8 m/s; therefore, the power curve developed by the Tradewind project represents better the wind conditions at the study location. The power curve cuts-off production at wind speeds of 25 m/s.

Table XLIII shows the error statistics obtained from the comparison of forecast power productions and real-time power productions calculated with the Horns Rev I offshore wind farm model throughout the study period. Forecast accuracy is evaluated for a forecast horizon of 0 to 1 hour, 1 to 12 hours, 12 to 24 hours, 24 to 36 hours and 36 to 48 hours.

Table XLIII
Horns Rev I - Forecast accuracy of the Normalised Theoretical Power Production of Horns Rev I wind model from 26/10/2010 to 09/02/2011.

Forecast horizon (h)		Mean (-)	NBias (-)	NMAE (-)	NRMSE (-)	$SI_{unbiased}$	CC	N
≥ 0	< 1	0.35	0.08	0.15	0.22	0.59	0.81	642
≥ 1	< 12	0.34	0.06	0.14	0.20	0.56	0.82	4492
≥ 12	< 24	0.35	0.07	0.16	0.23	0.62	0.78	5110
≥ 24	< 36	0.35	0.07	0.17	0.24	0.66	0.75	5086
≥ 36	< 48	0.34	0.08	0.19	0.26	0.71	0.72	5062

The comparison between Tradewind (one offshore wind turbine) and HornsRev (an offshore wind farm) indicates that Horns Rev has slightly higher Mean production, and better NMAE, SI and CC than Tradewind.

Note: there is available data, which has been provided by Energinet.dk, on the predictability values for Horn Rev 1. In the period Jan-Feb 2011, the accuracy of day-ahead forecasts has been *NMAE=11%*. Here, average value for the period Oct-Feb 2010-2011 is *NMAE=17%*.

V.4.2. REAL POWER PRODUCTION

In order to investigate the accuracies of the modelled wind power production with respect to the real power production, the cross-correlation factor between real productions (i.e. Folkecenter wind turbine) and modelled productions (i.e. Tradewind and Horns Rev power curves) have been calculated. Results are depicted in Table XLIV.

Table XLIV
Cross-correlation factors between the power productions of Folkecenter wind turbine and the models.

	$CC_{\text{between Wind turbines}}$
Folkecenter + HR	0.82
Folkecenter + TW	0.81

Table XLIV indicates both models represent well the real power production.

Similarly than with Wavestar, this section helps to validate the accuracy of the theoretical power productions compared to the real power productions. This might show whether the desk-study data are in accordance with real production data.

FOLKECENTER 525 KW WIND TURBINE

Table XLV and Table XLVI show the error statistics obtained from the comparison of forecast power productions and real-time power productions throughout the study period. In Table XLV forecast productions are calculated with the Tradewind (TW) model. In Table XLVI forecast productions are calculated with Horns Rev I (HR) model. In both tables, real-time power productions are those of the Folkecenter 525 kW wind turbine. Only the errors in the day-ahead forecasts are shown.

Table XLV
Folkecenter and Tradewind - Forecast accuracy of the Normalised Real Power Production of Folkecenter turbine.

	NMean	NBias	NMAE	NRMSE	SI_{unbiased}	CC	N
Folkecenter & TW	0.37	0.06	0.18	0.26	0.67	0.71	13950

Table XLVI
Folkecenter and HornsRevI- Forecast accuracy of the Normalised Real Power Production of Folkecenter turbine

	NMean	NBias	NMAE	NRMSE	SI_{unbiased}	N
Folkecenter & HR	0.36	0.06	0.18	0.25	0.68	14538

V.4.3. DAY-AHEAD FORECASTS OF WIND TURBINES ALONE – SUMMARY

Table XLVII summarises the statistical parameters showing the errors in the forecast accuracy of the comparison of day-ahead forecasts and real-time normalized power productions of Tradewind offshore wind turbine, Horns Rev offshore wind farm and Folkecenter 525 kW wind turbine.

Table XLVII

Day-ahead Power Production Statistical Parameters of different wind turbines in the Period 26/10/2010 to 09/02/2011

	NMean	NBias	NMAE	NMAE/ NMean	NRMSE	SI$_{unbiased}$	CC	N
Tradewind (TW)	0.34	0.07	0.17	0.50	0.25	0.71	0.74	15258
Horns Rev (HR)	0.35	0.07	0.17	0.49	0.24	0.67	0.75	15258
Folkecenter & TW	0.37	0.06	0.18	0.49	0.26	0.67	0.71	13950
Folkecenter & HR	0.36	0.06	0.18	0.50	0.25	0.68		14538

The comparison between NMAE or NMAE/NMean values shows very similar results for the four cases analysed. This indicates that the two models (Tradewind and Horns Rev) represent quite accurately the reality, which in this case is represented by the real power productions of Folkecenter wind turbine. By contrast, TABLE XXXIV has shown the comparison between modelled and real power productions for Wavestar, and high discrepancy between both sets of results can be found.

The next section analyses the predictability of the combined power output of WECs and wind turbines. To model the power output of wind turbines, Horns Rev power curve will be used. The reason is that is presents slightly better forecast accuracy than Tradewind power curve.

V.5. PREDICTABILITY OF COMBINED PRODUCTION OF WECS AND WIND TURBINES
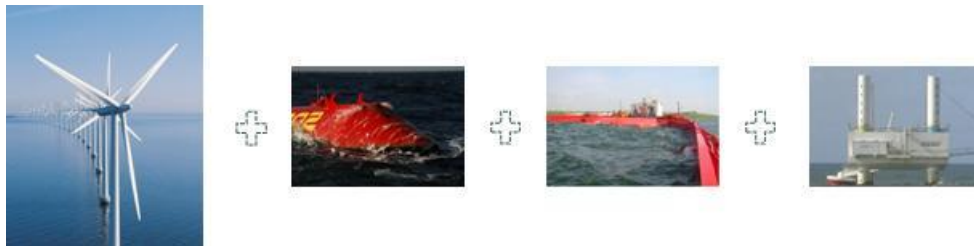
This section presents the accuracy in the prediction of the combined power output of WECs and of wind turbines. The WECs considered are Pelamis, Wave Dragon and Wavestar. For Pelamis and Wave Dragon, all power productions are modelled. For Wavestar, both real power productions and power matrix derived productions are included. The power production

of the wind turbine is represented by Horns Rev power curve. Normally, only the results of day-ahead forecasts are shown.

In the first place, the forecast accuracy of the combined production of Wavestar and a wind turbine is shown (Table XLVIII). Power productions are based on Wavestar power matrix and Horns Rev power curve. Table XLVIII shows the errors in the forecasts for different forecast horizons.

Table XLVIII

Wavestar and Horns Rev - Forecast accuracy of the Normalised Theoretical Power Productions of Wavestar and Horns Rev from 26/10/2010 to 09/02/2011.

Forecast horizon (h)		NMean	NBias	NMAE	NRMSE	SI$_{unbiased}$	CC	N
≥ 0	< 1	0.38	0.06	0.12	0.17	0.42	0.80	501
≥ 1	< 12	0.38	0.05	0.11	0.16	0.39	0.83	3510
≥ 12	< 24	0.38	0.05	0.13	0.18	0.44	0.78	3987
≥ 24	< 36	0.38	0.05	0.13	0.19	0.47	0.75	3963
≥ 36	< 48	0.38	0.06	0.14	0.20	0.49	0.74	3939

It should be noted that Wavestar cuts-off its power production at significant wave heights of 3 m. Therefore, the power output of Wavestar can present a similar pattern than that of wind turbines, i.e. reaching maximum production and dropping to zero in a small time interval. These fast changes from 100% to 0% production of Wavestar do not represent the behaviour of all WECs. Nonetheless, results indicate that Wavestar power output predictions are better than the wind energy farm power output prediction.

In the second place, the forecast accuracy of the combined production of Wavestar and the Folkecenter 525 kW wind turbine is shown (Table XLIX). Real-time power productions are based on Wavestar and on the Folkecenter 525 kW wind turbine productions. Forecast productions are based on Wavestar power matrix and on Horns Rev power curve. Table XLIX shows the errors in the forecasts for different forecast horizons.

Table XLIX

Wavestar and Folkecenter - Forecast accuracy of the Normalised Real Power Productions of Wavestar and Folkecenter from 26/10/2010 to 09/02/2011.

Forecast horizon (h)		NMean	NBias	NMAE	NRMSE	SI$_{unbiased}$	CC	N
≥ 0	< 1	0.29	0.15	0.17	0.21	0.49	0.77	164
≥ 1	< 12	0.31	0.13	0.16	0.20	0.48	0.75	1158
≥ 12	< 24	0.31	0.14	0.17	0.22	0.54	0.71	1322
≥ 24	< 36	0.31	0.12	0.16	0.21	0.57	0.66	1322
≥ 36	< 48	0.31	0.14	0.18	0.23	0.61	0.62	1322

It should be noted that the power productions behind Table XLIX derive from experimental technologies, and hence are power productions are lower and more variable than expected, and therefore more difficult to forecast.

In the third and last place, forecast accuracy of the combined production of the WECs and Horns Rev wind production is presented (Table L). Different cases are considered: all WECs and Horns Rev combined, the WECs combined two by two with Horns Rev, and Wave Dragon with Horns Rev. Power productions are based on the power matrices of the indicated WECs and on the power curve of Horns Rev. Table L shows the errors in the day-ahead forecasts.

Table L
WECs and Horns Rev - Day-ahead Forecast accuracy of the Normalised Theoretical Power Productions of WECs and Horns Rev from 26/10/2010 to 09/02/2011.

	NMean	NBias	NMAE	NMAE/NMean	NRMSE	SI$_{unbiased}$	N
WD+HR	33%	0.05	11%	0.33	0.16	0.45	11889
P+WD+HR	33%	0.06	11%	0.33	0.14	0.39	11889
WD+WS+HR	36%	0.05	11%	0.30	0.15	0.40	11889
P+WS+HR	37%	0.06	12%	0.32	0.16	0.40	11889
P+WD+WS+HR	36%	0.06	11%	0.30	0.14	0.36	11889

Results shows that the accuracy of day-ahead forecasts is very similar for the five cases analysed. The inclusion of WECs power productions improves the forecasts of the wind turbine. The most accurate forecast happens for two combinations: "Wave Dragon, Wavestar and Horns Rev" and for "Pelamis, Wave Dragon, Wavestar and Horns Rev". Moreover, the tables compare the power matrix of a single WEC with the power curve of a wind energy farm, i.e. Horns Rev. This favours the role of wave energy.

V.6. SHORT-TERM FORECASTS

A comparison summary between short-term (*t=0-12 hours*) and day-ahead forecasts is provided in Table LI. It shows that short-term forecasts are more accurate than day-ahead forecasts. The higher improvement happens for the wind turbine (*HR*), which improves in 9 percentage points. For WECs, accuracy improves in 3 to 6 percentage points.

Table LI
WECs and Wind Turbines – Short-term and Day-ahead Forecast accuracy of the Normalised Theoretical Power Productions of WECs and wind turbines working at Hanstholm from 26/10/2010 to 09/02/2011.

	NMean	NMAE *t=0-12h*	NMAE/NMean *t=0-12h*	NMAE *t=12-36h*	NMAE/NMean *t=12-36h*
Pelamis (P)	0.33	0.10	0.30	0.11	0.33
Wave Dragon (WD)	0.33	0.07	0.21	0.09	0.27
Wavestar (WS)	0.44	0.13	0.29	0.15	0.34
All Combined (P+WD+WS)	0.37	0.09	0.24	0.11	0.30
Horns Rev (HR)	0.35	0.14	0.40	0.17	0.49
WS + HR	0.38	0.11	0.29	0.14	0.39
WD + HR	0.33	0.09	0.27	0.11	0.33
P+WD+WS + HR	0.36	0.09	0.25	0.11	0.30

V.7. SUMMARY

Table LII summarises the accuracy of day-ahead forecast for WECs and wind turbines working alone and combined. Several conclusions can be reached from the results:

- Predictability of the combined power production of WECs (*NMAE=11%*) is better than the predictability of the individual units (*NMAE=9-15%*).
- Predictability of power production of WECs is better than for wind turbines (*NMAE=17-18%*).
- The predictability of the combined production of WECs and wind turbines (*NMAE=11%*). is the same as the predictability of the combined production of WECs. Thus, WECs have a positive influence on wind turbines power production predictabilities.
- There is good agreement between the real and theoretical results of the wind turbines.
- There is not good agreement between the real and theoretical results of Wavestar. A reason is the experimental stage of the prototype at Hanstholm.
- Short-term forecasts of power productions are more accurate than day-ahead forecasts, particularly for the wind turbine, which forecasts improve in 9 percentage points. For WECs, accuracy improves in 3 to 6 percentage points.

Figure 68 illustrates the results depicted above. It shows the evolution of day-ahead forecasts errors, in terms of NMAE, of WECs and wind turbines power productions in four different scenarios. These are: wind turbine working alone (*only wind*), WECs working alone (*only wave*), all WECs combined (*wave combined*) and WECs and wind turbines combined (*wave and wind combined*).

The reason why *only wave* has better accuracy than *wave combined* is that *only wave* shows the results of the most accurate WEC, i.e. Wave Dragon. If only wave considered a weighted average of the three WECs, the curve would change.
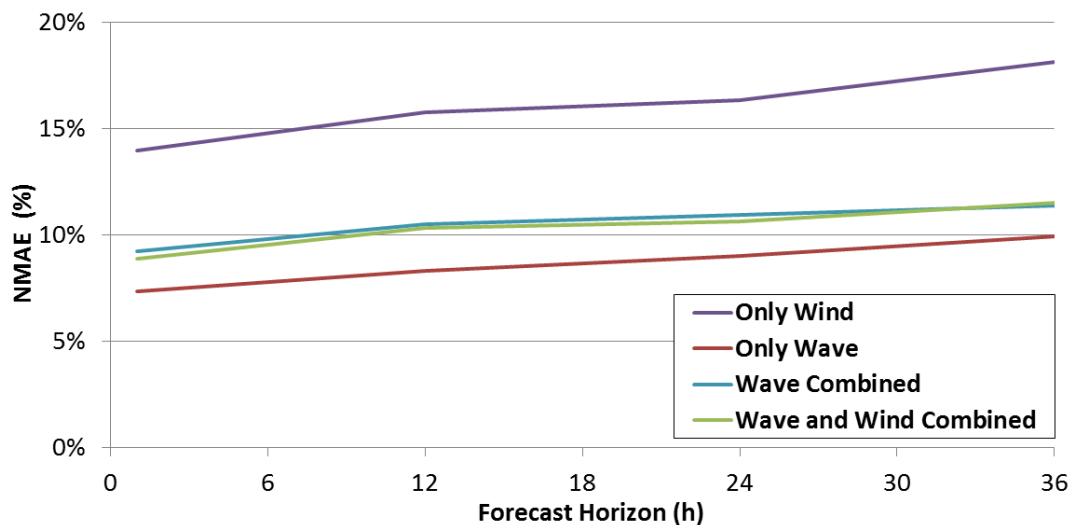
Figure 68. Day-ahead forecast errors (in terms of NMAE) of the power production of: wind turbines (in purple), WECs (in red), WECs working combined (blue) and WECs and wind turbines combined (in green) at Hanstholm.

Figure 68 also shows the errors in the wind turbine increase faster than the errors in the WEC alone as the forecast horizon increases. It can also be seen a big difference between the errors in the 36th lead hour compared to the 1st lead hour. The latter fact serves to introduce the next chapter, which deals with the current functioning of electricity markets and their impact on balancing costs of WECs and of wind turbines.

Table LII

WECs and Wind Turbines – Day-ahead Forecast accuracy of the Normalised (Theoretical and Real) Power Productions of WECs and wind turbines working at Hanstholm from 26/10/2010 to 09/02/2011.

	NMean	NBias	NMAE	NMAE/ NMean	N
Pelamis (P)	0.33	0.08	11%	0.33	11901
Wave Dragon (WD)	0.33	0.04	9%	0.27	11901
Wavestar (WS modelled)	0.44	0.04	15%	0.34	11901
Wavestar (WS real)	0.30	0.24	28%	0.93	3966
P+WD	0.34	0.06	10%	0.29	11901
WD+WS	0.39	0.04	12%	0.31	11901
P+WS	0.40	0.06	13%	0.32	11901
All WECs Combined	0.37	0.05	11%	0.30	11901
Tradewind (TW)	0.34	0.07	17%	0.50	15258
Horns Rev (HR)	0.35	0.07	17%	0.49	15258
Folkecenter & TW	0.37	0.06	18%	0.49	13950
Folkecenter & HR	0.36	0.06	18%	0.50	14538
WS (real) & Folkecenter	0.31	0.13	17%	0.55	3966
WS (modelled) & HR	0.38	0.05	14%	0.39	11889
WD & Horns Rev	0.33	0.05	11%	0.33	11889
P+WD+HR	0.33	0.06	11%	0.33	11889
WD+WS+ HR	0.36	0.05	11%	0.30	11889
P+WS+ HR	0.37	0.06	12%	0.32	11889
All WECs & HR	0.36	0.06	11%	0.30	11889

In Denmark, Energinet.dk has annual expenditures up to 36 MEUR (270 MDKK) for balancing wind energy [6]. This chapter estimates how much money would be needed to balance wave energy. Or, in other words, this chapter discusses the value of wave energy predictability.

To address this, the chapter covers:
- Background study on electricity markets: glossary of terms.
- Wind predictability and balancing power.
- Impact of wave power production forecasts in electricity markets and in balancing costs.
- Future electricity markets.

VI.1. GLOSSARY OF ELECTRICITY MARKETS

This glossary is a compendium of different sources: Gross et al. (2007), Nord Pool Spot (2009) and Nord Pool Spot (Nor1). Some of the text has been copied from these references.

*Balancing mechanism***:** Set of arrangements in place after *gate closure* in which the TSO can take bids and offers to balance the system. The prices of bids and offers are determined by market participants and, once accepted, are firm contracts, paid at the bid price. These bilateral contracts are between market participants and the TSO.

*Balancing services***:** Services purchased from balancing service providers by the TSO; includes balancing mechanism bids and offers, other energy trades, *response*, *reserve*, and other system services.

Balancing energy: electricity that the retailer trades with the *TSO* to balance between the retailer's total trading and the retailer's customers' consumption. Also the electricity a producer settles with the TSO if he fails to produce according to his plan. Balancing energy is related to *reserve services*. In some countries peak load reserves can be bid as balance regulation but the bids will be first offered to the day-ahead spot market.

Bidding area: due to grid bottlenecks, one power exchange system might be divided in various bidding areas.

*Capacity credit***:** measure of the amount of load that can be served on an electricity system by intermittent plant with no increase in the loss-of-load probability (LOLP); often expressed in terms of conventional thermal capacity that an intermittent generator can replace without

---

[6] Balancing premium for wind energy: 3 EUR/MWh
Total wind power installed by end 2011: 3900 MW
Total annual wind production in 2011: 3900 MW *0.35* 8760 h/y = 11,957 TWh/y
Annual Costs of balancing premiums = 3 EUR/MWh* 11,957 TWh/y = 36 MEUR/y

compromising system reliability. A value of 100% denotes one-for-one substitution with no loss of system reliability and 0% indicates that the intermittent source can displace no conventional capacity.

Capacity factor: energy produced by a generator as a percentage of that which would be achieved if the generator were to operate at maximum output 100% of the time. Capacity factor is sometimes combined with a related term, *load factor*, this differing from the former in that it is a measure of actual utilisation (h/y) rather than maximum output (%).

Dispatchable capacity: capacity that can be turn on and off when needed.

Dispatchable units: units which output can be controlled by the operator of the unit or by the TSO, i.e. units that allow total control of the power output. It has usually been used to describe conventional power generation, biomass and hydropower. For example, wind is regarded as non-dispatchable renewable capacity; although modern wind turbines are controllable (to a degree) they are generally not considered dispatchable.

Electricity markets: a market composed by commercial and non-commercial players. The commercial players trade with electricity and are not responsible for the security of supply; they only deliver the prices – they only deliver financial services. The non-commercial players are those responsible of security of supply, i.e. the TSOs.

- *Financial or bilateral electricity market*: financial domain of electricity markets, which appeared when electricity markets were liberalised. It is run by financial or commercial players. Trading takes place bilaterally (over the counter) outside the power exchange, and prices and amounts are not made public. In the financial market, the parties of a financial contract do not trade energy (not kWh), only money; the financial market is used for price hedging and risk management. It is the market for long-term contracts, i.e. future and forward contracts. It is also used to trade electricity among players in different bidding areas.

- *Day-ahead market (spot market)*: a physical market in which prices and amounts are based on supply and demand. The spot market is a day-ahead market that trades with deliveries from midnight to 36 hours ahead.
  - *Elspot:* Nord Pool Spot's day-ahead double auction market, where electrical energy is traded. It represents a double auction as both the buyers and the sellers submit their bids. Those who want to buy electricity from Elspot must send their purchase bids at the latest at noon the day before the energy is delivered to the grid. Correspondingly, those who want to sell energy must send their sale offers at the latest at noon the day before the energy is delivered to the grid. Each order specifies the volume (MWh/h) and the specific price levels (EUR/MWh) for each individual hour in the following day.

Elspot calculates the day-ahead prices i.e. an hourly price which balances the bids and offers from producers and consumers, and reports participants how much they have bought or sold for each hour of the following day. Hence, Nord Pool Spot publishes a spot price for each hour of the coming day. The Elspot price represents both:

i) the cost of producing one kWh of power from the most expensive source needed to be employed in order to balance the system (either from a domestic installation or from external imports), and

ii) the price that the consumer group is willing to pay for the final kWh required to satisfy demand.

This type of price formation is called *Marginal Price Setting*. It is characterised by the inelasticity of the market to store electricity.

- *Intra-day market*: markets in between the day-ahead market and the regulating power market. It is used to adjust and to minimize the deviations from production and consumption determined in the day-ahead market. Normally, only those participating in the corresponding day-ahead market are allowed to participate in it.
  - BETTA: intra-day UK market.
  - Elbas: intra-day Nord Pool market.
  - In Spain there are 6 intra-day markets.
  - In France there are 24 intra-day markets.

- *Balancing market:* its main function is to provide power regulation to counteract imbalances related to day-ahead planned operation. In the balance market there are two types of participants: active participants (mainly producers but also consumers who can regulate their generation or consumption on request from the TSO – bidding regulation) and passive participants (all companies connected to the central grid). The market closes one hour before the hour of operation.

- *Regulating power market:* a real-time market covering operation within the hour. The main function is to provide power regulation to keep the frequency of the system at 50 Hz.
  - Regulating bids have to be activated to the stated amount within 15 minutes.

Electricity prices: the price of electricity to households and day-ahead electricity prices are different. In Spain, for example, households pay about 150 EUR/MWh, whereas day-ahead electricity price is about 50 EUR/MWh. There are following reasons: the change in voltage level, transport and distribution costs, substations costs, reactive power consumption costs, etc. As a rule, the highest voltage level, the cheapest electricity price.

Gate closure: point in time at which the energy volumes in bilateral contracts between electricity market participants must be notified to the central settlement system. Between gate

closure and real time, the TSO is the sole counterparty for contracts to balance demand and supply. There are different gate closures for each market, i.e.:

- Gate closure of Day-ahead markets is usually at noon, i.e. Elspot market in the Nordic region closes at noon.
- Gate closure of intra-day markets, i.e. BETTA in UK or Elbas in the Nordic region, is one hour before the *hour of operation*.

Hour of operation: hour during which the energy is delivered and consumed.

Marginal cost: operational cost to produce one more *kWh* of electricity. In electricity markets the competition of a plant depends on the marginal cost.

- *High marginal cost units or Marginal costs units* are the units that enter the bids on peak demands. They are used for peak load generation and flexible generation. They are named as high marginal costs because they normally have high operational costs. It usually corresponds to coal, gas and CCGTs (combined cycle gas turbines) power plants.
- Gas-fired generation has predominantly been the marginal plant type on the Great Britain system, and there has correspondingly been a correlation between the cost of gas-fired generation (including carbon) and Great Britain power price.
- Flexible plants to operate: expensive: coal and natural gas.
- Inflexible plants to operate: cheap: nuclear.

Market price: day-ahead exchange price for a settled hour. For instance, Elspot day-ahead price is the underlying reference for the financial contracts. It is the reference price for futures, forwards and options traded in the financial market.

Market splitting and market coupling: related to the allocation of available cross-border capacities to deal with day-ahead congestion management. This can be done through explicit or implicit capacity auctions. Implicit capacity auctions ensure that the electricity flows from the surplus area (low price areas) toward the deficit areas (high price areas), thus also leading to price convergence.

- *Market splitting*: happens when the limited transmission capacity leads to a split between two market areas. Hence, there are different prices in different bidding areas. Market splitting involves only one electricity exchange, i.e. domestic bottlenecks in Norway or inter-state links of countries.
- *Market coupling:* is the used of implicit auctioning between two or more power exchanges, i.e. coupling of the Nordic and the German day-ahead markets.

Nordel: body for co-operation between the *TSOs* in Denmark, Finland, Iceland, Norway and Sweden towards a Nordic electricity market. It was also a forum for contacts between the TSOs and representatives of the market participants in the same countries. On July 2009, all operational tasks from Nordel were transferred to the *European Network of Transmission System Operators for Electricity* (*ENTSO-E*).

Nord Pool Spot: Nordic electricity market that offers both the day-ahead and the intra-day electricity markets to its participants. It covers Norway, Sweden, Finland and Denmark. In 2010 it had a turnover of 307 TWh, representing 18 billion EUR and 74% of the total electricity consumption in the Nordic countries (i.e. the rest, 26%, were electricity imports, bilateral contracts, etc).

Operating margin: the difference between available generation and actual demand.

Regulating energy: energy the TSO trades in order to keep the frequency at 50 Hz. It is related to the *response services*.
- *Upward-regulation:* when the consumption exceeds the production, the frequency of the alternating current falls to a value below 50 Hz. To counteract it, it is needed to increase generation in the system. In this case, the TSO must buy electricity from the producers.
- *Downward-regulation:* when the production exceeds the consumption, the frequency of the alternating current rises to a value above 50 Hz. To counteract it, it is needed to decrease generation in the system. In this case, the TSO must sell electricity to the producers, thereby causing producers to reduce their production.

*Response services***:** services purchased by the TSO in order to ensure there is sufficient capability in the short-term to undertake frequency control. It may be utilised in seconds through automatic controls on generators or loads. Steam generators may be held below maximum output to facilitate this.
- There are primary, automatic and manual reserves

Reserve services: services purchased by the TSO in order to ensure there is sufficient capability in the short-term to undertake system balancing actions. It is a capability to change output to meet TSO requests within a few minutes. Utilisation of this capability may be subject to payment in the balancing mechanism or through other balancing service agreements. There are various categories of reserve depending on speed of delivery and the nature of its provision. Fast reserve can be provided by demand reduction, pump storage or part-loaded steam plant connected to the system. The term 'spinning reserve' has in the past been used to describe a generator that is spinning and ready at very short notice to contribute power to the system.
- *Standing reserve* is ready for action within 20 min. As well as demand reductions it might consist of fast starting gas turbines or backup diesel generation.
- *Residual reserve* is the capability provided in the balancing mechanism (i.e. reserves that can be dispatched in response to market prices rather than contracted by the TSO).
- *Contingency reserve* is the capacity that should be established in the 24 h ahead period by the market. It is not usually purchased by the TSO but is monitored to ensure adequate short-term reserves will be available.

*System margin***:** difference between installed capacity, including imports and exports, and peak demand. Historically, the concept has been referred to as *capacity margin*, *system reserves* and *plant margin*.

    System balancing reserves maybe thought of as an operational issue – what is needed to manage the system at each and every hour of the day, throughout the year. By contrast, system margin may be thought of as a planning issue – an overall 'margin of error' that was historically designed into centrally planned electricity networks. The distinction between the system margin required for longer-term reliability and reserves required for short-term balancing is illuminated by the comparative size of the two quantities. In the UK, balancing reserves are purchased by the TSO and comprise about 4% of peak demand (in 2006). System margin is much larger than dedicated reserve and it is not contracted for: in 2006 the indicative level of adequate system margin was around 20% above current expected peak demand, including exports.

System operators: bodies responsible for their area to be electrically stable, i.e. frequency to be kept at 50 Hz. They are also responsible for the security of supply in their area. They have to be a non-commercial organization, neutral and independent with regard to market participants. In several countries, the system operators are also responsible for the high-voltage grid, hence the name *Transmission System Operators*.

Transmission System Operators (TSOs): bodies responsible for the security of supply in their countries. They also own and operate the high voltage grid. Consequently, the TSOs own, rule and operate the electricity system in their countries. National Grid undertakes this role in Great Britain, Energinet.dk in Denmark, Statnett in Norway, Svenska Kraftnät in Sweden, Fingrid in Finland and Red Eléctrica de España in Spain.

VI.2. WIND PREDICTABILITY AND BALANCING POWER

TSOs have the task of coordinating the prioritised access with general system operation, during which production and consumption are constantly adapted to market compensation. As part of the 2009 EU Renewable Energy Directive (DirRen, 2009) EU countries shall give priority to generating installations using renewable energy sources so far as the secure operation of the electricity system permits. In practice, this means that renewable power has access to grid capacity before all other electricity produced, in case of no grid limitations.

Correspondingly, each renewable energy electricity producer sends the predicted electricity productions over the next two days to the corresponding TSO, who plans the rest of generating capacity accordingly. To do this, wind or wave forecast is converted into predicted electricity (as seen in Chapter V).

Therefore, in a market-based system, large, varying and, to a certain extent, unpredictable quantities of electricity must be accommodated; and things like in Figure 69 may happen

(DEA, 2007). It shows the short-term (orange and red line) and day-ahead forecasts (green and blue lines, up to 32 hours) for a severe storm on western Denmark on January 8th, 2005.

According to the forecasts carried out 20 to 26 hours ahead, production capacity of approximately 2000 MW wind power was expected in the period between noon and 6 pm. The actual production around 4 pm reached no more a tenth of this estimate, since most of the wind turbines reached the end-stop (i.e. wind speed above 15 m/s).

Therefore, the system operator had to provide the remainder from up-regulated power (Figure 70).
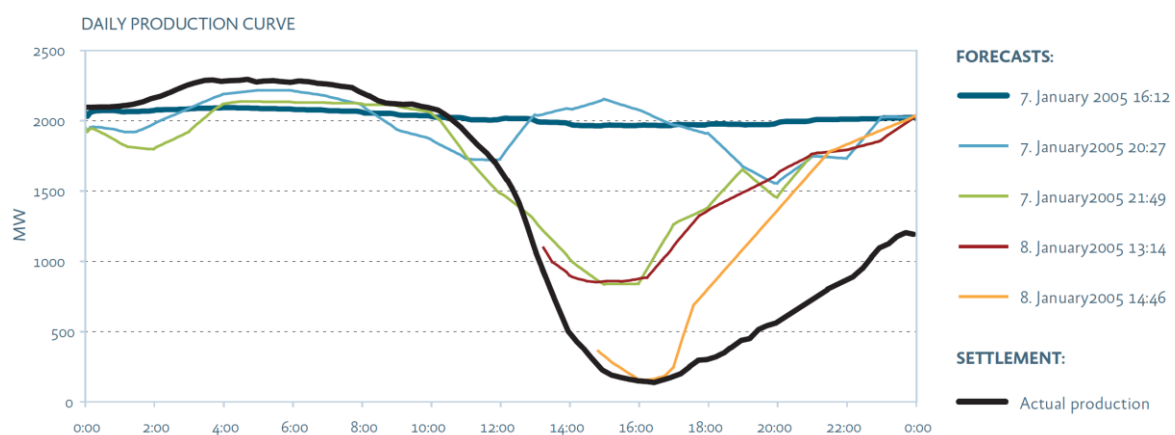
Figure 69. Wind power forecasts and real-time production on January 8th, 2005, Denmark (DEA, 2007).

Figure 70 shows the amount of power that was needed to regulate the errors in the day-ahead wind power predictions. Regulated power is shown in red, actual wind power production in green and day-ahead wind predictions in blue.
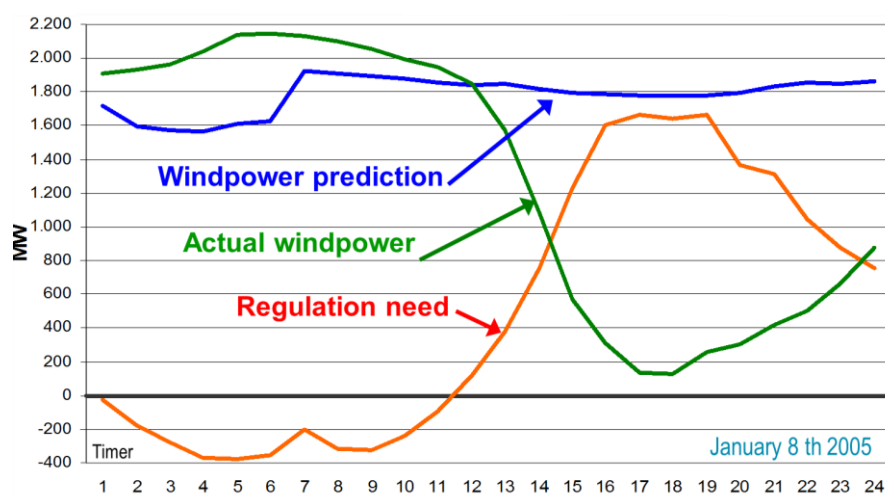
Figure 70. Wind power forecast, real-time production and regulated power on January 8th, 2005, Denmark (Helstrup-Jensen, 2011).

122

The regulated power was paid by the TSO with the up-regulation price. And its origin was brought by the partial unpredictability of wind energy. As the percentage of unpredictable renewable energy generation in overall production gradually increases, this unpredictability may become a growing problem for the electricity system, both operationally and economically (DEA, 2007). The extent of the problem depends on the accuracy of the forecasts and the possibilities for adapting electricity consumption and production from other plants on short notice. Inaccurate forecasts are a major reason for the need for upwards and downwards regulation capacity in the system and there is therefore a need for systems and instruments that can provide accurate forecasts for production from these generators.

According to current Danish rules (onshore) wind turbines receive a premium on top of the feed-in tariff to balance their power. The premium equals 3 EUR/MWh.

VI.3. WAVE POWER AND DAY-AHEAD ELECTRICITY MARKETS

Balancing costs of wave power can be calculated by taking as a reference value the balancing costs of wind power. Reference value is chosen at 3 €/MWh, which coincides with the current balancing premium for wind turbines and is accepted as the average balancing costs for wind power in Denmark.

Chapter V has calculated the errors in day-ahead power productions' forecasts of WECs and of wind turbines. This section assumes that electricity has been traded in the Danish day-ahead electricity market. Thus, forecasts horizons of interest are 12 to 36 hours.

The following lines calculate the balancing costs associated to the errors in those day-ahead forecasts. Balancing costs are dictated by a two-price model, where two factors interact: the direction of the imbalances of the traded power production, and the direction of the imbalances of the general power system. Day-ahead forecasts can under-predict or over-predict the real amount of power that is produced. Accordingly, a producer buys or sells the difference between predicted and real power. Then, system imbalances can cause the electric system to be in excess or in deficit of power – in other words, request downwards regulation or upwards regulation, – which influences the amount that is charged or paid to the producer, i.e. upward, downward or electricity market price.

Consequently, there are four possible cases (Figure 71):
a) A forecast overestimating the production and a system in deficit of power. The producer buys power at up-regulation price.
b) A forecast overestimating the production and a system in excess of power. The producer buys power at market price.
c) A forecast underestimating the production and a system in deficit of power. The producer sells power at market price.

d) A forecast underestimating the production and a system in excess of power. The producer sells power at down-regulation price.
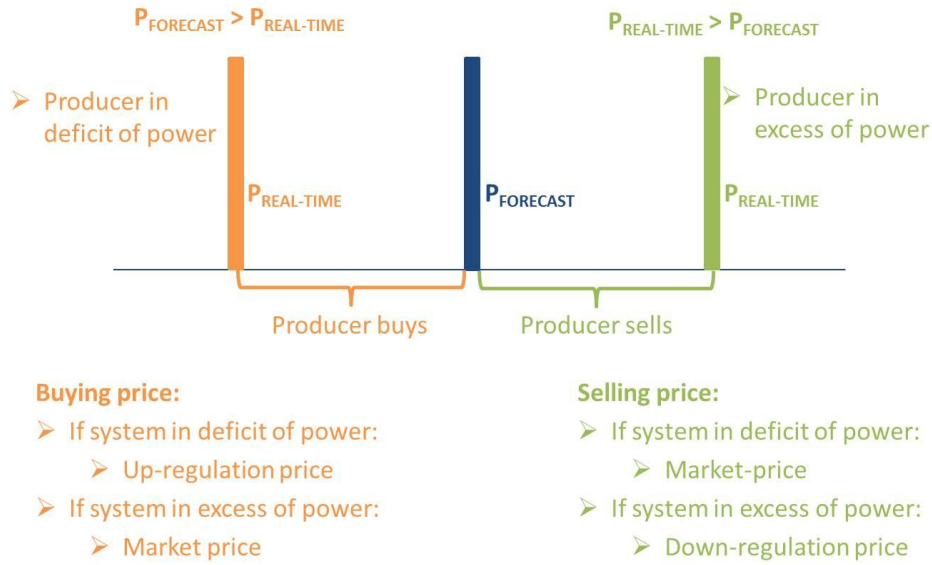
Figure 71. Illustration of the two-price model applicable in Denmark to calculate balancing costs. $P_{forecast}$ represents day-ahead production forecasts and $P_{real\text{-}time}$ the actual production in the generation hour.

These translate into the following formulas:

$if\ (P_{MOD} - P_{OBS})>0=>$ Producer buys deficit of power:

If the system is in deficit of power: $|Buying\ Cost|=|Up.RegPrice|*|P_{MOD} - P_{OBS}|$

If the system is in excess of power: $|Buying\ Cost|=|Market\ Price|*|P_{MOD} - P_{OBS}|$

$if\ (P_{MOD} - P_{OBS})<0=>$ Producer sells excess of power

If the system is in deficit of power: $|Selling\ Price|=|Market\ Price|*|P_{MOD} - P_{OBS}|$

If the system is in excess of power: $|Selling\ Price|=|Down.Reg.Price|*|P_{MOD} - P_{OBS}|$

For every hour of the study period the upward and downward regulation price and the electricity market price are known (Energinet.dk). Generally, downward regulation price is lower than market price, and upward regulation price is higher.

Hence, hourly balancing costs per unit of energy generated are calculated for the entire study period as the sum of the costs for buying deficit of power and the loss of income when selling excess of power generally at a lower price than the market price.

$$Balancing\ Costs$$
$$= \sum \frac{|Up.Reg\ Price| * |P_{MOD} - P_{OBS}|}{P_{OBS}}$$
$$+ \sum \frac{|Market\ Price| * |P_{MOD} - P_{OBS}|}{P_{OBS}} + \sum \frac{|Market\ Price - Down.Reg\ Price| * |P_{MOD} - P_{OBS}|}{P_{OBS}}$$
$$+ \sum \frac{|Up.Reg\ Price - Market\ Price| * |P_{MOD} - P_{OBS}|}{P_{OBS}}$$

The corresponding units are:

$|Up - Down - Market\ Price|$ in [DKK/MWh]

$|P_{MOD} - P_{OBS}|$ in [MWh/h * P_{rated}]

P_{OBS} in [MWh/h * P_{rated}]

$|Buying\ Cost - Selling\ Price|$ in [DKK/h * P_{rated}]

$Balancing\ costs$ in [DKK/MWh]

An exchange rate of 1 € = 7.5 DKK is assumed throughout the study.

Balancing costs have been calculated for the four following scenarios:

- A wind-only scenario, where the offshore turbines work individually;
- A wave-only scenario, where the WECs work alone;
- A combined wave scenario, with all WECs working combined;
- Two combined wave and wind scenario, with all WECs and the wind turbine working combined in different percentages:
  - 75%-25% wave-wind scenario.
  - 50%-50% wave-wind scenario.

Table LVIII presents the average balancing costs for the WECs and the wind turbines investigated in the previuous chapter. Balancing costs are given as a percentage of the balancing costs of the wind-only scenario and as an absolute value, calculated from the reference value for wind turbines.

Table LIII

Balancing costs of different systems working at Hanstholm in the period 26/10/2010 to 09/02/2011

	Balancing costs	
	(%) [1]	(€/MWh) [2]
Pelamis *(P)*	72%	2.2
Wave Dragon *(WD)*	55%	1.6
Wavestar *(WS)*	71%	2.1
Horns Rev *(HR)*	100%	3.0
P+WD+WS	63%	1.9
P+WD+WS+HR	64%	1.9
WS+HR	74%	2.2
WD+HR	69%	2.1

[1] Balancing costs as a percentage of the wind-only scenario.
[2] Balancing costs assuming a reference cost for wind of 3€/MWh.

Results on balancing costs go in line with the findings on forecasts accuracies (Chapter IV and V). When wave energy is integrated in a wind-only system, power productions' forecast accuracies improve. Similarly, any scenario with contribution of wave energy presents smaller balancing costs than the wind-only scenario. The reduction of overall balancing cost compared to the wind-only scenario reaches 45% when WECs work individually, 40% when WECs work combined and 35% in the combined wave and wind scenario.

VI.3.1. FUTURE ELECTRICITY MARKETS?

There are several ways to reduce balancing costs of non-fully predictable renewable energy sources:
- o Improve forecast tools.
- o Increase gate closure time of day-ahead marlets, i.e. shorten the bidding period of day-ahead markets. If gate closure occurs at 12 pm the day before, bids have to be made 12 to 36 hours in advance. Since forecasts improve as the forecast horizon decreases, a later gate closure implies more accurate forecasts.
- o Bid the power of several sites together, i.e. integrate in the same bid the generation from different sites of non-fully predictable sources. The aggregation of the power production of different sites reduces the total forecasting error.
- o Use intra-day electricity markets, where it is possible to adjust the schedules submitted for the day-ahead market.

VI.4. SUMMARY

Findings on forecasts accuracies have indicated that:
- o Power productions' forecasts of WECs are more accurate than of wind turbines.
- o Power productions' forecasts of WECs and wind turbines are more accurate than of only wind turbines.

Similarly, any scenario with contribution of wave energy presents smaller balancing costs than the wind-only scenario. The reduction of overall balancing cost compared to the wind-only scenario reaches:
- o 45% when WECs work individually.
- o 40% when WECs work combined.
- o 35% in the combined 75%-25% wave-wind scenario.
- o 30% in the combined 50%-50% wave-wind scenario.

Energinet.dk has annual expenditures up to 36 MEUR (270 MDKK) for balancing wind energy. If wave energy was added to Danish renewable generation, the combined production of wind and wave power could reduce balancing costs of wind power by 30% or 35%. This would imply annual savings to the Danish system of 13 MEUR (95 MDKK) in the 75%-25% wave-wind scenario, or 11 MEUR (81 MDKK) in the 50%-50% wave-wind scenario.

Moreover, if wave energy would be integrated in the Danish system, it would need lower balancing premiums than wind energy, about 40% lower: 1.8 EUR/MWh (wind energy receives a balancing premium of 3 EUR/MWh).

An important challenge ahead the integration of wave energy and wind energy into the grid is their variable power production. There are different variability time-frames. Wave energy, for example, can have intra-annual, seasonal, diurnal and hourly variations. Also fluctuations in the inter-minute (*i.e. minutes time-scale*) and intra-minute (*i.e. seconds time-scale*) time-frames can be found.

This chapter focuses on whereas WECs and wind turbines combined together provide smoother and more available power outputs than increasing the installed capacity of the same technology. Hence, this chapter investigates the variability of waves and winds and the hourly variability of WECs and wind turbines power productions, working alone and combined. Most of the data are based on half-hour values; therefore, due to lack of data it is not possible to investigate inter-minute and intra-minute variations. This short-term fluctuations of the power production are of outmost importance to grid operation.

Several studies address wave and wind power output variability, and assess the opportunities of co-locating farms of WECs and of wind turbines to smooth-out the combined power output (Chapter II). This chapter complements those studies.

This chapter addresses:
- Average delay between waves and winds at Hanstholm:
  - Theoretical, experimental and statistical study.
- Variability of waves and winds:
  - Seasonal and half-hour variability.
- Variability of the power productions of WECs and wind turbines:
  - Half-hourly variability of the power productions of Pelamis, Wave Dragon, Wavestar and Folkecenter wind turbine.
  - Correlation in the power output of WECs and of wind turbines.
- Variability of the combined productions of WECs and of wind turbines:
  - Introduction to diversified systems
  - Hanstholm real case study with combined production of Wavestar and Folkecenter wind turbine.
  - Horns Rev 2 theoretical case study with combined production of Wavestar and the wind farm.
    - Delay between WECs and wind turbines maximum power productions.
    - Which mix of wind and wave energy provides the less variable output? 50%/50% wind-wave, 100% wind or 100%wave?

- When wind stops, how long can the power output from wave energy continue?
   o Variability of power productions in storm conditions.

VII.2. PHASE SHIFT BETWEEN WAVES AND WINDS

This section investigates the average delay between waves and winds at Hanstholm based on three approaches:
1. A theoretical approach with SMB diagram
2. An experimental approach based on wave and wind measurements.
3. A statistical approach based on the cross-coreelation factor.

VII.2.1. SMB DIAGRAM – THEORETICAL DELAY OF WAVES AND WINDS

Wave generation depends on the wind speed, on the fetch and on the storm duration. Hence, for a given wind speed the time it takes a wave to grow varies. This time is known as the phase shift between waves and winds, and represents how waves build up due to the effect of winds.

As Holthuijsen (2007) explains, "the first systematic observations of the significant wave height and period under fetch-limited conditions (on lakes and reservoirs) were made by Sverdrup and Munk (1946, 1947) and, somewhat later, by Bretschneider (1952). Their results have been used widely and, in honour of their contribution the corresponding parameterisations (analytical functions approximating such data) are called SMB (Sverdrup–Munk–Bretschneider) growth curves".

SMB diagram quantitatively illustrates the relationship between wind speed, wind duration, fetch length and wave growth. Fetch length is charted on the x-axis and wind speed on the y-axis (Appendix B). Contour lines represent wind duration, wave height and wave period. The change in fetch length has its greatest effect on wave height for small fetches. When a given wind speed has persisted over a long distance, wave height changes due to increases in fetch length are fairly small. Wind duration is the length of time a wind in a given fetch affects wave growth. Given a high wind speed and long fetch length, the longer the wind blows, the larger the waves will grow.

Based on the information of the SMB diagram, the following curves (Figure 72, Figure 73, Figure 74) provide the time, in hours, that takes a particular wind to create a corresponding wave, for three different fetch lengths of 100 km, 200 km and 300 km, respectively. They indicate the phase shift between a constant wind speed and a corresponding generated significant wave height.
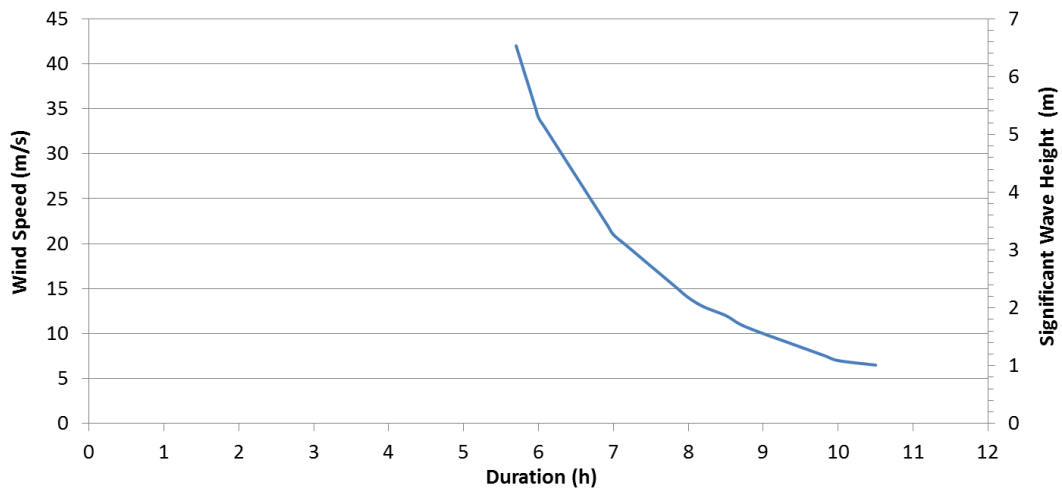
Figure 72. Time, in hours, to generate a significant wave height with constant wind speeds blowing in 100 km fetch.
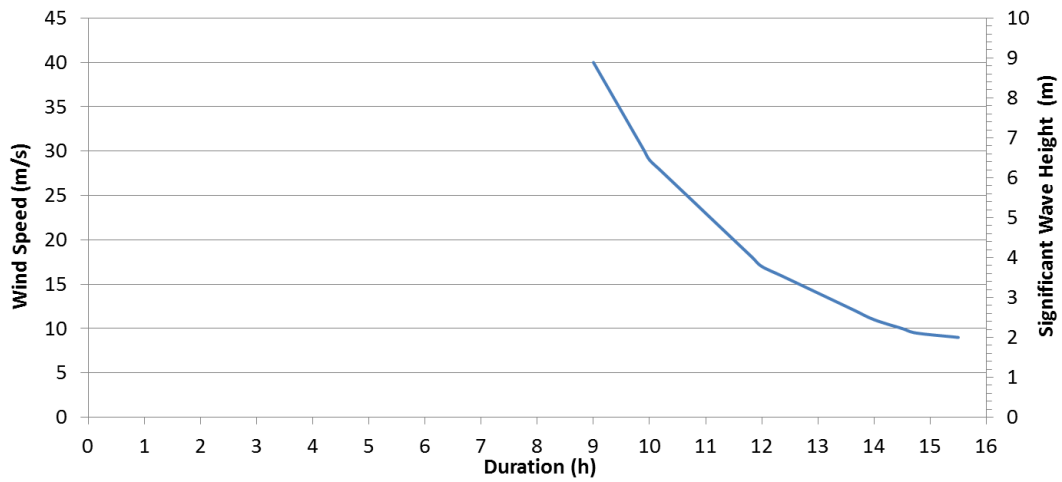
Figure 73. Time, in hours, to generate a significant wave height with constant wind speeds blowing in 200 km fetch.
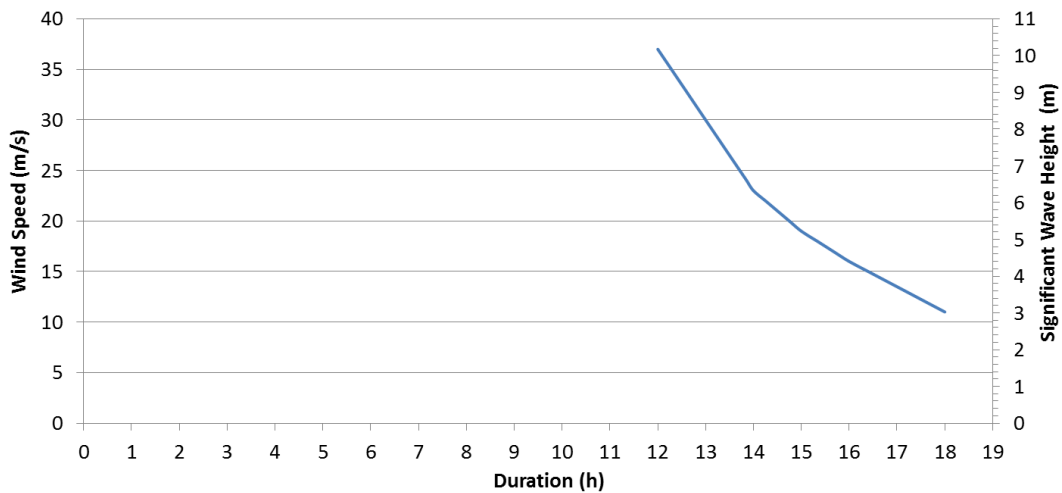
Figure 74. Time, in hours, to generate a significant wave height with constant wind speeds blowing in 300 km fetch.

130

The three figures show wind durations of 6 to 10 hours for 100 km fetch lengths, of 9 to 15.5 hours for 200 km, and 12 to 18 hours for 300 km. This discussion focuses on the average delay that can be found between waves and winds at Hanstholm.

Typical wind speeds of the study period are in the range of 5 to 25 m/s (which are also the operational wind speeds for wind turbines). The upper limit (u_{wind}=25 m/s) shows wind durations of 6.5 hours, 10.5 h and 13.5 h, to create significant wave heights of 4 m, 5.5 m and 8.7 m, respectively.

In Danish coasts of the North Sea waves are generally wind seas and have a secondary swell component. Swells may come from hundreds of kilometres away, such as from Scotland (600 km distance), Iceland (1700 km distance) or Greenland (2800 km distance) or from closer locations like Norway (100 km distance) or Sweden (200 km distance) (Figure 75).
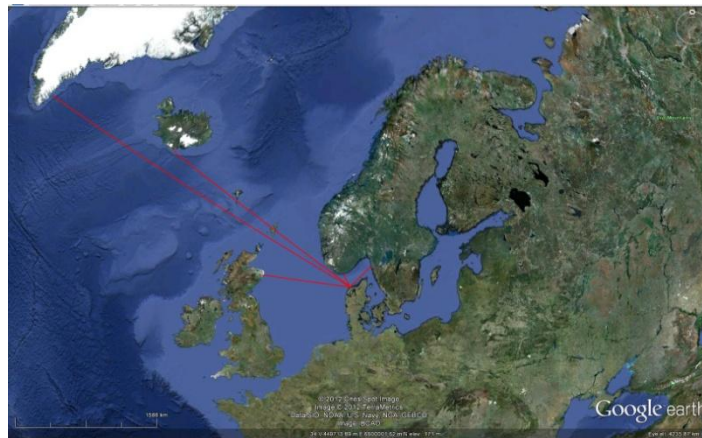
Figure 75. Fetch distances of waves arriving to Hanstholm.

Figure 75 shows that waves from many different directions and diverse originated can arrive at Hanstholm, which makes difficult to determine a constant fetch. And the information from SMB diagram assumes a wind speed blowing constantly over a fetch. However, considering that a 100 km fetch length can be common, that wind speeds in the study period are in the range 5 to 25 m/s, and wave conditions in the study period are in the range 1 m to max. 4 m waves, Figure 72 indicates that, theoretically, phase shifts up to 6 and 8 hours can be found at Hanstholm.

The next section reviews the delay between waves and winds at Hanstholm based on measured data.

VII.2.2. OBSERVED DELAY BETWEEN WAVES AND WINDS

To examine the phase shift between waves and winds based on observed data, Figure 76 shows the evolutions of the significant wave height and the wind speed during November 2010. The fetch and the storm duration are unknown variables, so the mean wind speed is presented in order to draw more conclusions on the relationship between the two curves.

Firstly, data presented show that for a given wind speed wave growth varies. On 3rd and 4th Nov., H_{m0} goes above 3 meter for wind speeds of 18 m/s, whereas on 9th-10th Nov., where higher wind speeds are present, the significant wave height is below 3 meters. To draw any conclusion wave spectra would be needed. However, by looking into the lower graph representing mean wind direction it is seen that on 3rd-4th Nov. winds come from West, whereas for the 9th-10th Nov. winds come from North-East, a more limited fetch area, which do not allow waves to grow as much as on 9th-10th Nov.

Looking at the phase shifts when wind and waves are at their maximum, it can be seen that phase shifts between peaks are of about 3 hours (first blue light circle), 7 hours (second blue light circle) and 0.5 hours (third blue light circle). Then, the yellow circle shows a delay of 6.5 hours, the black circle a delay of 6 hours (between the lowest peaks of u_{wind}=2.4m/s and of H_{m0}=1m) and the green circle a delay of 5.5 hours (between mean values).
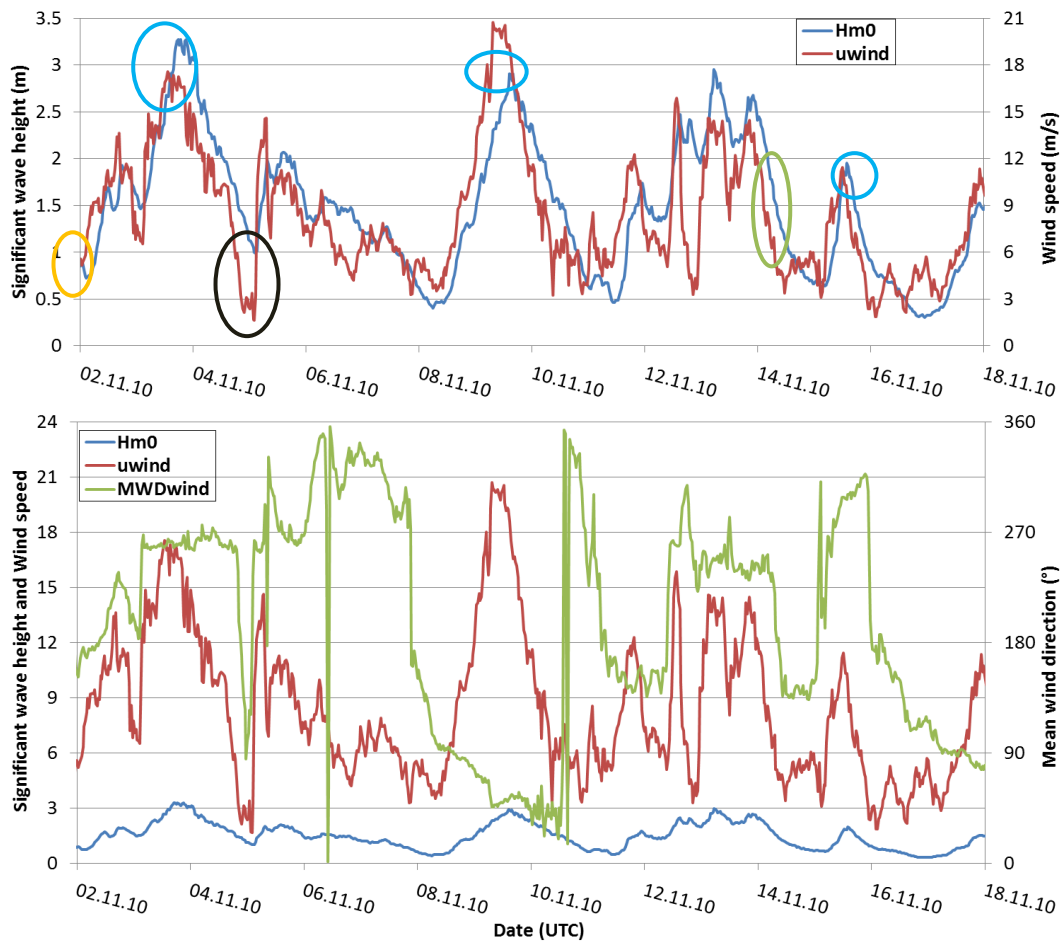
Figure 76. Evolution of u_{wind}, H_{m0} and MWD_{wind} from 02 to 18/11/2010.

Thus, observed data indicate a phase shift between waves and winds of about 0.5 to 2 hours that goes up to 6 to 7 hours.

132

It is interesting to compare these values with the phase shift given by the SMB diagram. It cane be assumed that the fetch length approximately corresponds to 100 km:

→3-4/11/2010: u_{wind}=18m/s and H_{m0}=3.2m → fetch: 125 km and duration of 8.5 hours.

→9-10/11/2010: u_{wind}=21m/s and H_{m0}=3m → fetch: 80 km and duration of 6 hours.

Thus, there is an agreement between the two sources of information, which indicate the two phase shifts of observed data are in line with the theoretical phase shifts given by the SMB graph.

Last but not least, it is also noticeable the smaller variability of waves compared to the variability of winds (both for u_{wind} and MWD_{wind}).

STORM CONDITIONS – COMPARISON OF WAVES AND WINDS

The following figure illustrates the evolution of H_{m0} and the wind speed u_{wind} before, over and after the 2-day storm on February 2011 (i.e. stormy period 3). It gives a good representation of the evolution of waves and winds over a 6-day period.
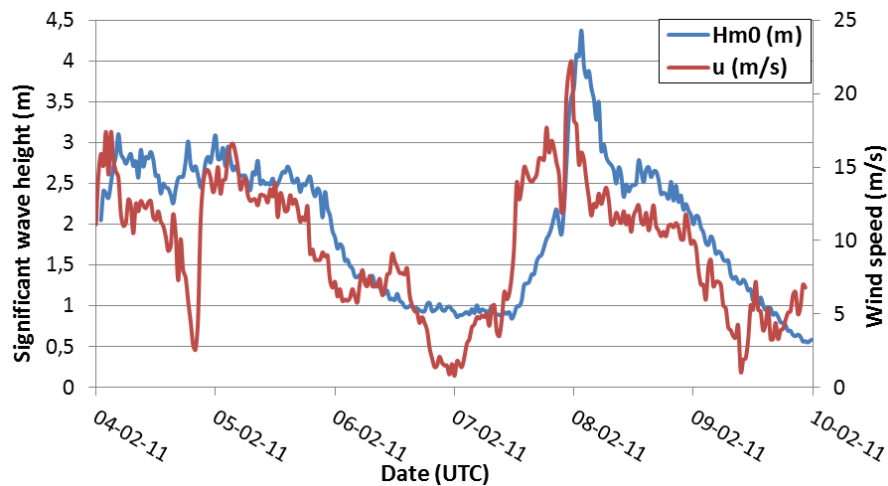
Figure 77. Evolution of H_{m0} (in blue) and u_{wind} (in red) over the storm on 07/02 to 09/02/2011.

Next figure depicts in more detail the evolution of waves and wins during the storm, and draws further conclusions on the relationship between waves and winds. Figure 78 illustrates the evolution of H_{m0} and the wind speed u_{wind} over the 2-day storm on February 2011 (i.e. stormy period 3).

133
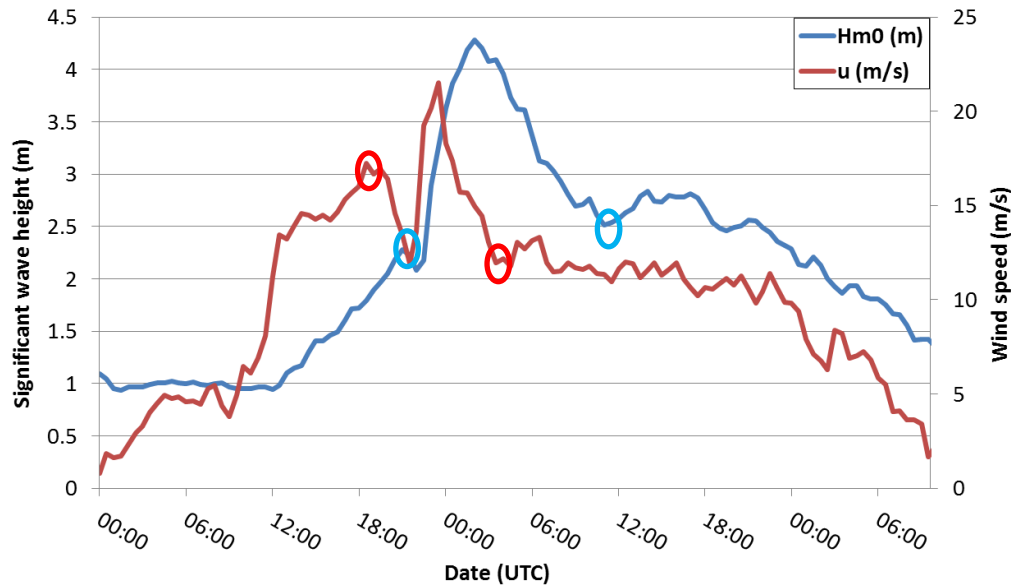
Figure 78. Evolution of H_{m0} (in blue) and u_{wind} (in red) over the storm on 07/02 to 09/02/2011.

The following findings derive from Figure 78:

- Wind decreases, increases and decreases faster than the corresponding waves. This demonstrates waves have higher inertia and lower fluctuation than winds. The time span measured from high peaks to low peaks for winds and waves are:
  - o Winds: from red to red circle: 9 hours (7/2 at 18:30 to 8/2 at 3:30).
  - o Waves: from blue to blue circle: 14 hours (7/2 at 21:00 to 8/2 at 11:00).
- The time delay between waves and winds increases as the storm moves forward. Note the delay on the first increasing part and the delay on the decaying part:
  - o Increasing part: delay=0.5 to 1hour.
  - o Decreasing part: delay= 5.5 to 6 hours.
- Waves take about twice the time wind takes to reduce from the peak to half the peak value:
  - o Winds:
    - ▪ 4h to reduce by a 45%, from 21.5 m/s to 12 m/s.
    - ▪ 12h to reduce by a 50%, from 21.5 m/s to 10.8 m/s.
    - ▪ 25h to reduce by a 63%, from the maximum record in the storm, 21.5 m/s, to the average value of the whole analysed period, 8 m/s.
  - o Waves:
    - ▪ 9h to reduce by a 42%, from 4.3 m to 2.5 m.
    - ▪ 22.5h to reduce by a 50%, from 4.3 m to 2.1 m.
    - ▪ 30.5h to reduce by a 65%, from the maximum record in the storm, 4.5 m, to the average value of the whole analysed period, 1.5 m.

As a result, the comparison of wind and wave patterns during the storm shows that waves (represented by the wave height) take about twice the time winds (represented by the wind speed) take to reduce from the peak value in the storm to its half. Thus, when the wind has

134

dropped back to the average value the corresponding wave remains at high values for a longer time (up to 12 hours more). This finding is very important for the operation and power production of WECs. It indicates that any combination of a WEC with a wind turbine will benefit towards a more continuous production of power compared to the operation of wind turbines alone.

VII.2.3. CROSS-CORRELATION AND DELAY OF WAVES AND WINDS

The relationship between waves and winds can also be studied with the following formula (Fusco et al., 2010):

$$CC(t) = \frac{1}{N} \sum_{k=1}^{N-t} \frac{[(x(k) - \mu_x)(y(k + t) - \mu_y)]}{\sigma_x \, \sigma_y}$$

The cross-correlation CC is a function of a time lag t, which reflects the temporal relationship between two variables, x and y, representing the wind speed and the significant wave height, respectively. k is a counter indicating time, N is the number of samples, μ the sample mean and σ the standard deviation.

CC indicates the degree to which the variation in one parameter, x, is reflected in the variation of the other parameter, y. CC ranges from 0, indicating no correlation, to 1, which denotes perfect correlation. The time lag at which the correlation reaches a maximum is defined as the average delay.

The relationship between waves and winds is evaluated by comparing the significant wave height and the wind speed in Period II, (from January to May 2011); results are shown in Figure 79 and Figure 80. In Figure 79 all wind speeds are considered, independently of their direction. Figure 80 only takes into account wind speeds coming from the sea; hence, all wind speeds with MWD_{wind} in the interval [45,220] are eliminated.
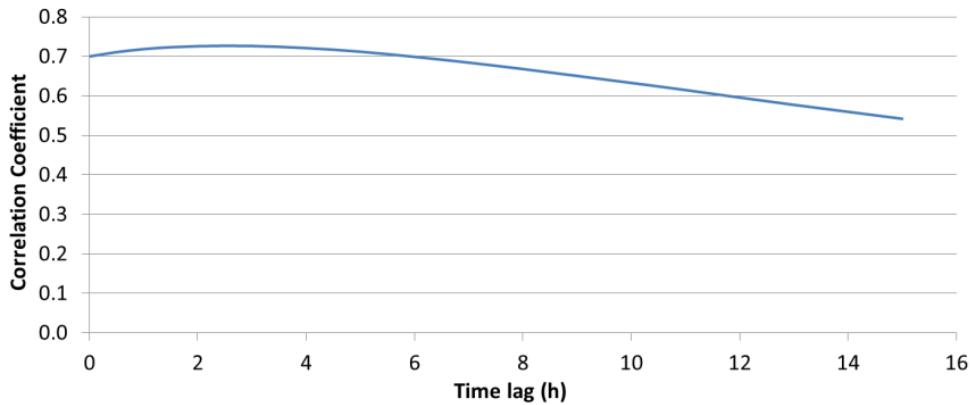
Figure 79. Cross-correlation (CC) coefficient between waves and winds for different time delays. All wind speeds are considered.
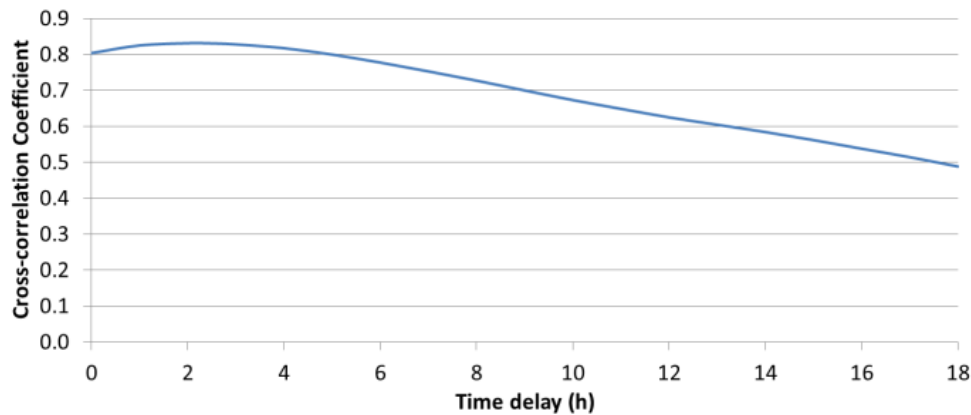
Figure 80. Cross-correlation (CC) coefficient between waves and winds for different time delays. Only wind speeds with MWD_{wind} in the intervals [0,45) and (220,360] are considered.

Both figures indicate there is high correlation between waves and winds, which is explained by the fact that Hanstholm is dominated by wind seas. Figure 79 shows cross-correlation of 0.7 and Figure 80 of 0.8, i.e. *CC(0)*.

The point in time when *CC(t)* is maximum indicates the *average* phase shift between winds and waves. This is in between 2 to 3 hours (Figure 79) and between 2 and 2.5 hours (Figure 80). Maximum CC reaches 0.73 and 0.83, respectively.

Figure 80 also shows for a delay up to 5 hours the correlation is high (*CC=0.8*) and up to 9 hours there is a correlation above 0.7, also high.

VII.2.4. SUMMARY
Three different analyses have been carried out to investigate the phase shift between waves and winds at Hanstholm: a theoretical analysis using SMB diagram, an experimental analysis with measured data, and a stastiscal analysis using the CC function.

These analyses indicate an average delay between waves and winds at Hanstholm of 2-3 hours. In storm conditions, a phase shift of 6-8 hours can be found.

Analyses also indicate there is high cross-correlation between waves and winds.

VII.3. VARIABILITY OF WAVES AND WINDS

VII.3.1. SEASONAL VARIABILITY OF WAVE ENERGY
This section analyses the seasonal changes of wave energy. As an example, the seasonal variability of wave energy in Hanstholm is compared to the seasonal variability in Canary Islands, which represents a milder wave climate. The two locations have been selected due to data availability.

136

The wave climate in the Danish part of the North Sea has been extensively analysed by Ramboll (1999b). This study investigates wave variability and waves characteristics in eight different locations. Hanstholm is not part of the study; however, the results for Fjaltring – very close to Hanstholm (Figure 81) and with quite similar wave climate – can be taken as a reference.
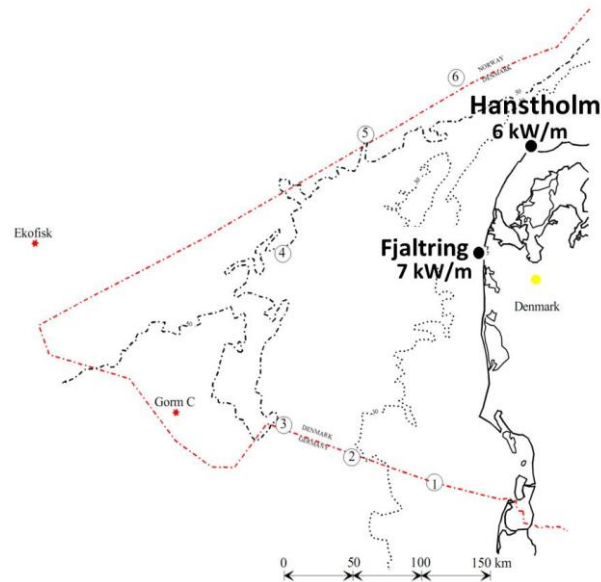
Figure 81. Map of the Danish North Sea. The red dashed line indicate the Danish Exclusive Economic Zone. The eight study locations of Ramboll (1999b) are indicated by numbers. Hanstholm and Fjaltring mean wave power and locations are also indicated.

Figure 82 and Figure 83 show the annual and the monthly variability of wave power (in W/m) at Fjaltring.

Figure 82 illustrates the variation in mean wave power throughout fourteen years, from 1979 to 1993. Mean wave power is 7 kW/m, the minimum value recorded in the period is 5 kW/m and the maximum value 10 kW/m. This shows an annual variability of up to 40% from the mean annual value.

Figure 83 presents monthly average values of wave power. Maximum wave power is reached in January, with mean value of 14 kW/m, and the minimum value is recorded in May, of 3 kW/m. November, December and January are the most energetic months, and from April to August the less energetic. With respect to mean wave power values, there is a seasonal variability of up to 100%. Thus, strong seasonal variability can be found at Fjaltring.
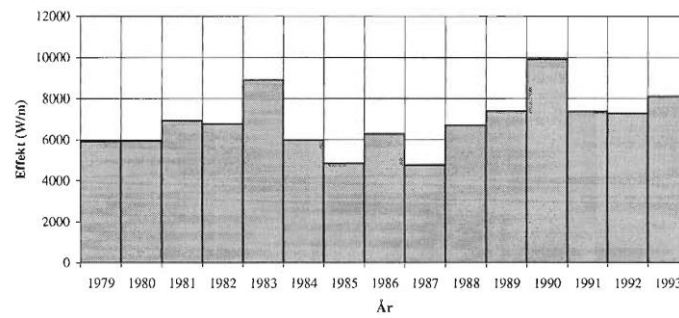
Figure 82. Variation in mean wave power (in W/m) in the period 1979-1993 at Fjaltring (Ramboll, 1999b).
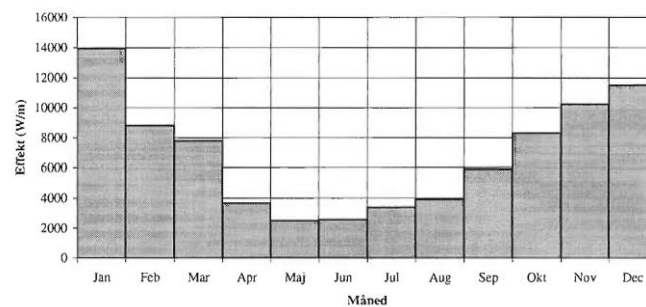
Figure 83. Monthly variation in wave power (in W/m) at Fjaltring (Ramboll, 1999b).

The three following figures also illustrate the seasonal and monthly variations in the wave conditions at Hanstholm. Note Figure 90 represents the significant wave height during the big storm.
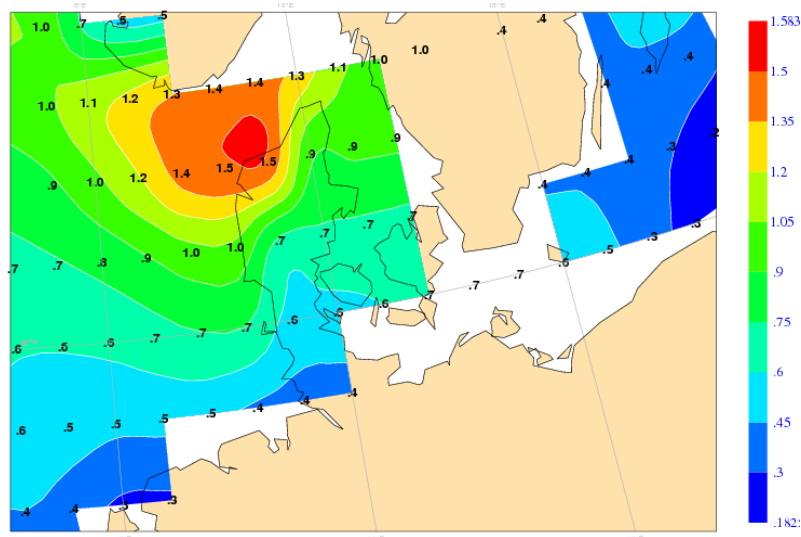
Figure 84. Historical data – hindcast – of the significant wave height of Wednesday 30th June 2010 at 12:00 (UTC). Retrieved from ECMWF database (Storm Geo, 2012).
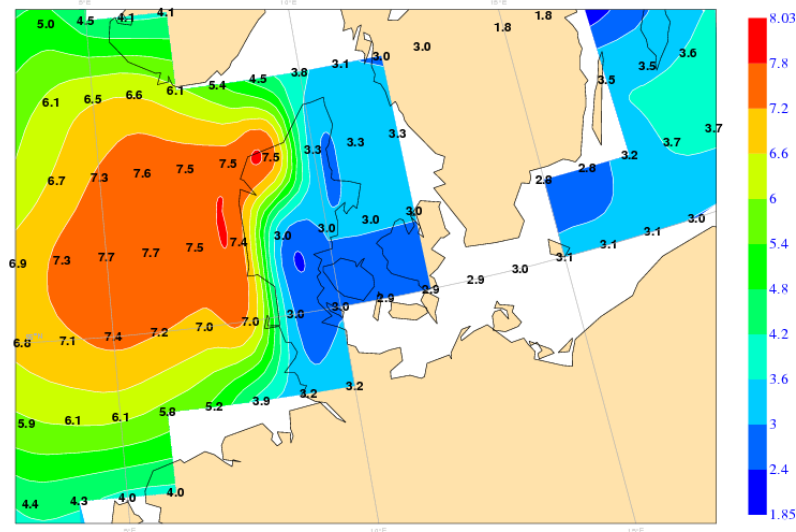
Figure 85. Historical data – hindcast – of the significant wave height of 8th January 2005 at 12:00 (UTC). Retrieved from ECMWF database (Storm Geo, 2012).
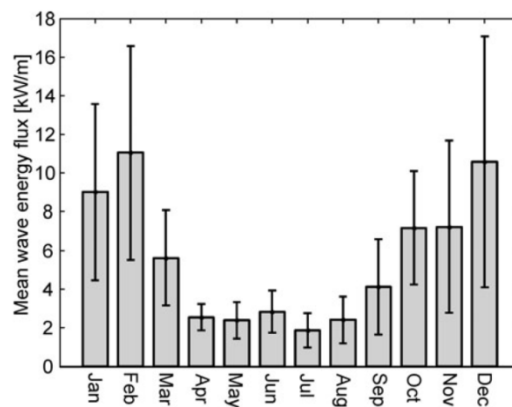
Figure 86. Variations in the average monthly wave energy flux off Lysekil , Sweden (Waters, 2008).

Next figures show the annual and the seasonal mean wave power levels in Canary Islands. Figures have been retrieved from (Enola). Figure 87 illustrates annual mean wave powers, Figure 88 shows spring mean wave powers, Figure 89 presents summer mean values, Figure 90 autumn mean values and Figure 91 shows winter mean values. The average wave powers in Canary Islands are:

- o Annual: 18 kW/m.
- o Spring: 20 kW/m.
- o Summer: 9 kW/m.
- o Autumn: 17 kW/m.
- o Winter: 30 kW/m.

The comparison among all the figures shows a seasonal variability of about 60%, with respect to the mean annual value.
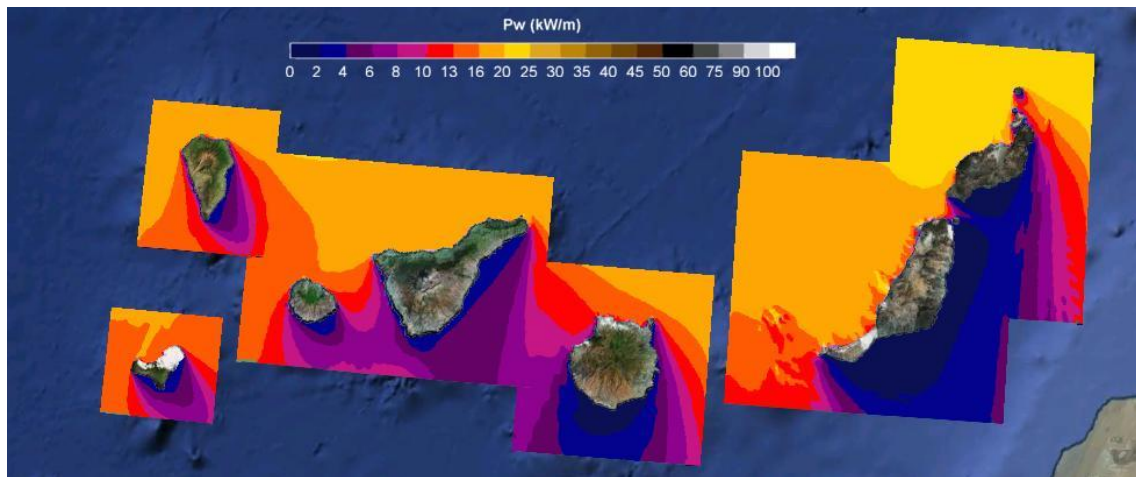
Figure 87. Annual mean wave power (in kW/m) in Canary Islands (Enola).
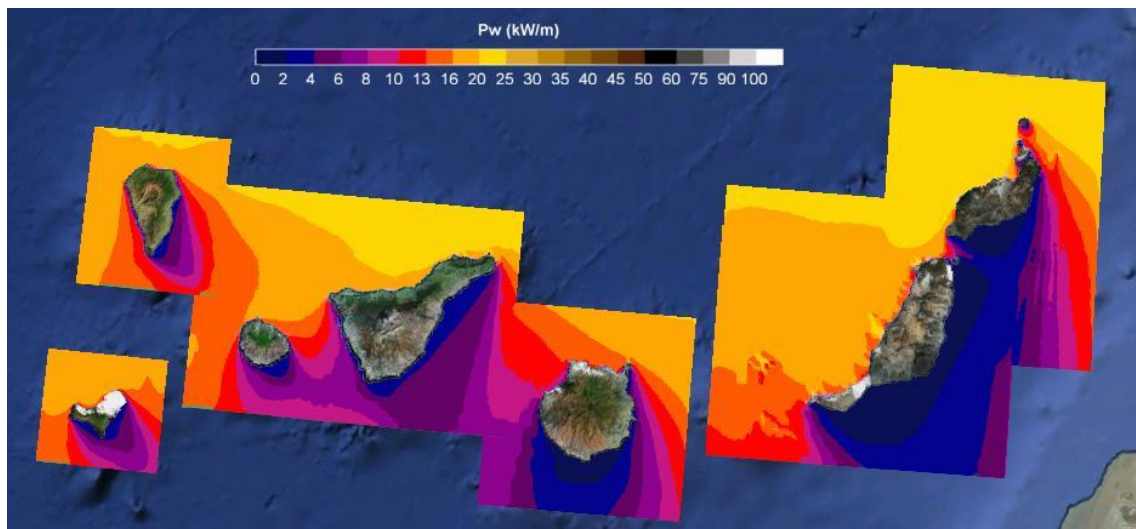
Figure 88. Spring mean wave power (in kW/m) in Canary Islands (Enola).
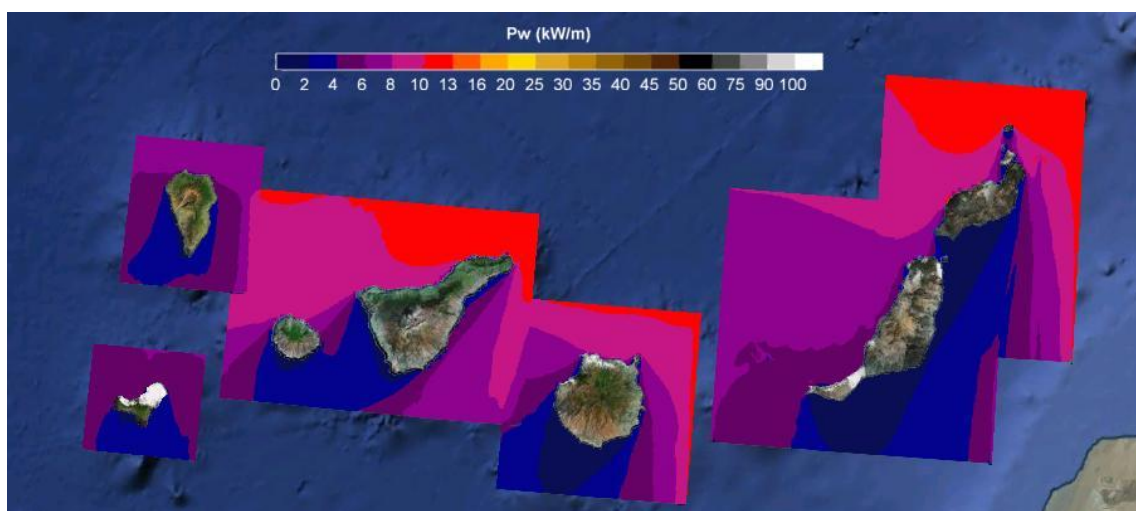
Figure 89. Summer mean wave power (in kW/m) in Canary Islands (Enola).
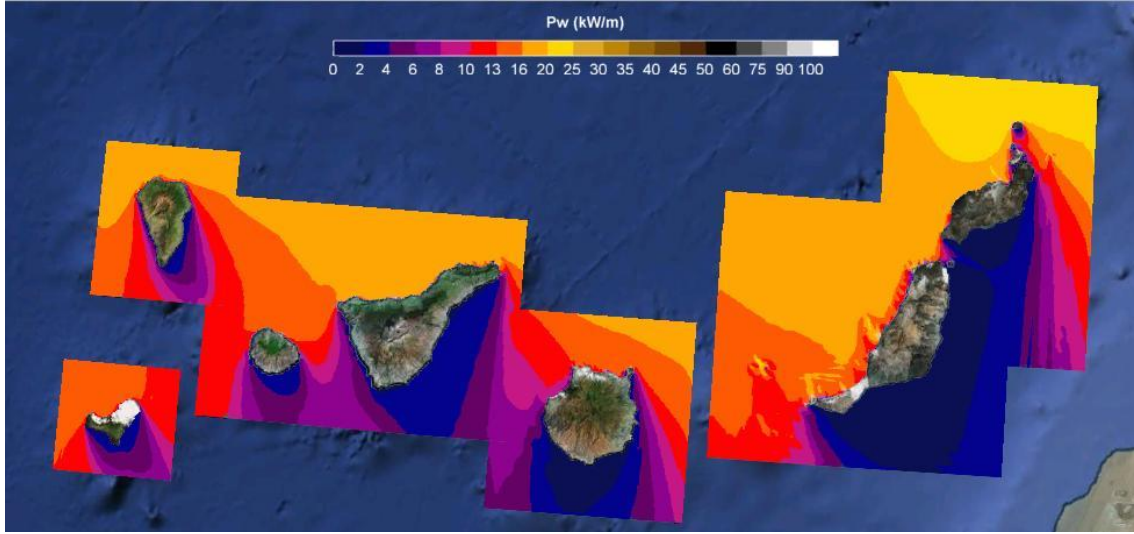
Figure 90. Autumn mean wave power (in kW/m) in Canary Islands (Enola).
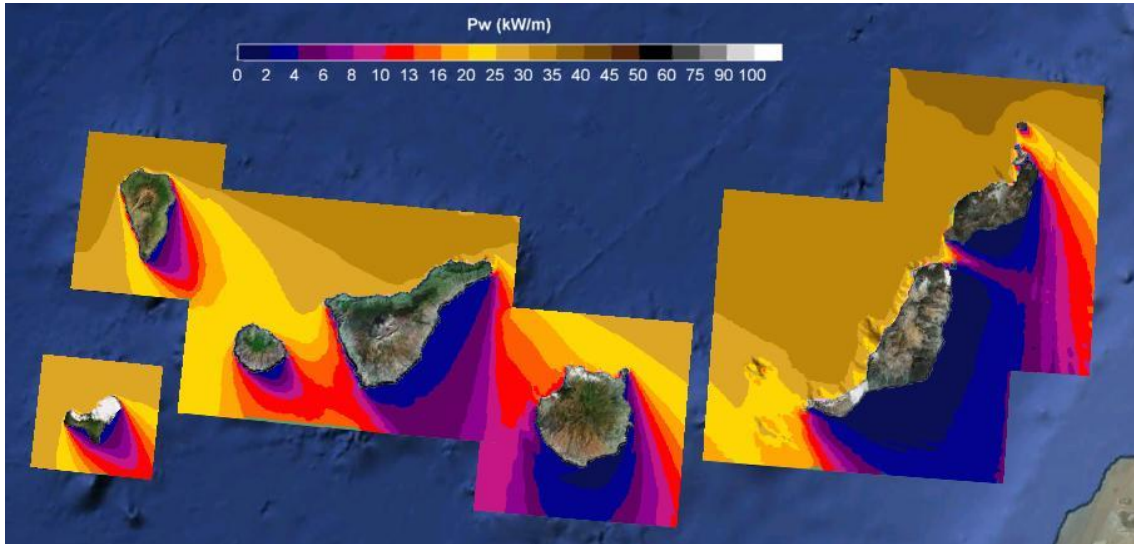
Figure 91. Winter mean wave power (in kW/m) in Canary Islands (Enola).

The comparison between Fjaltring and Canary Islands leads to the conclusion that seasonal variability of wave energy in mild climates is lower than in extreme climates. Moreover, note Fjaltring represents a particular location whereas Canary Islands is a much larger area.

VII.3.2. HALF-HOUR VARIABILITY OF WAVES AND WINDS

The following tables show the half-hour variability of waves and winds parameters in terms of $\sigma/Mean$. T_{02} does not vary much in time (12-16%), H_{m0} and u_{wind} vary 30-46%, and P_{wave} and P_{wind} a lot more. Generally, P_{wind} varies more than P_{wave} (up to 90% more) and u_{wind} than H_{m0} (up to 40% more). These results would differ if the intra-minute variability was considered instead.

TABLE LIV

Half-hour Variability of H_{m0}, H_{max}, T_{02}, P_{wave} and u_{wind}, MWD_{wind} and P_{wind}, at Hanstholm from 26/10/2010 to 09/02/2011.

	Mean	Max	σ	σ/Mean	N
H_{m0} (m)	1.4	4.7	0.7	46%	4157
H_{max} (m)	2.4	8.5	1.1	48%	4157
T_{02} (s)	4.7	8.8	0.8	16%	4157
P_{wave} (kW/m)	8.9	99	10.9	122%	4157
u_{wind} (m/s)	7.7	21.5	3.5	46%	6386
MWD_{wind}	171	357	91	53%	6386
P_{wind} (W/m²)	472	6141	641	136%	6386

TABLE LV

Half-hour Variability of H_{m0}, H_{max}, T_{02}, P_{wave} and u_{wind}, MWD_{wind} and P_{wind}, at Hanstholm during 1 month from 03/01/2011 to 31/01/2011.

	Mean	Max	σ	σ/Mean
H_{m0} (m)	1.2	2.7	0.4	32%
H_{max} (m)	4.8	6.8	0.5	12%
T_{02} (s)	2.1	5.7	0.7	33%
P_{wave} (kW/m)	5.1	28.5	3.7	72%
u_{wind} (m/s)	6.8	16.7	3.2	46%
MWD_{wind}	195	357	75	38%
P_{wind} (W/m²)	331	2864	453	137%

To finalise this section, a note on the daily variability of waves and winds is added. It is based on a study of the pattern of waves and winds along UK coast. According to Cradden et al. (2011): "the diurnal variability of wind and wave power are quite different, with wind power typically showing some evidence of morning and evening peaks at each site. Wave power tends to be quasi-independent of the time of day (except when the variation of the wave height is seemingly affected by the tidal regime), and thus adding wave generation to a site could provide more constant production."

VII.4. VARIABILITY OF WECS AND WIND TURBINES POWER PRODUCTIONS

VII.4.1. WECS POWER PRODUCTION VARIABILITY
This section examines the variations of the power production of WECs.

The following figures show the non-dimensional power productions of Pelamis, Wave Dragon and Wavestar, respectively, throughout a 10-day period (16/01 to 26/01/2011). For comparison, the evolution of H_{m0} is also shown.

Power productions derive from Pelamis, Wave Dragon and Wavestar power matrices, and from Wavestar real power production data.
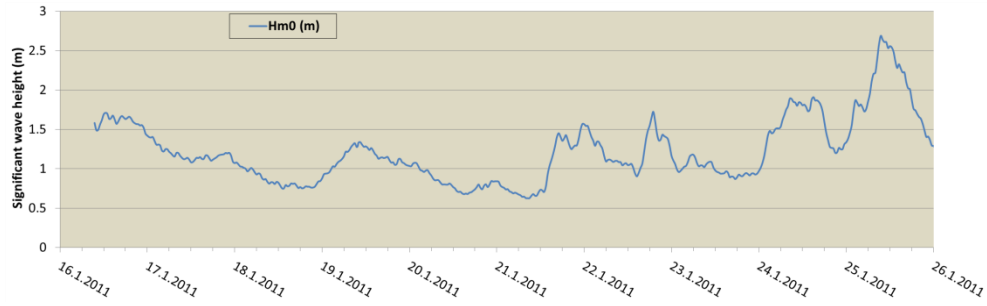
Figure 92. Evolution of H_{m0} from 16/01 to 26/01/2011.
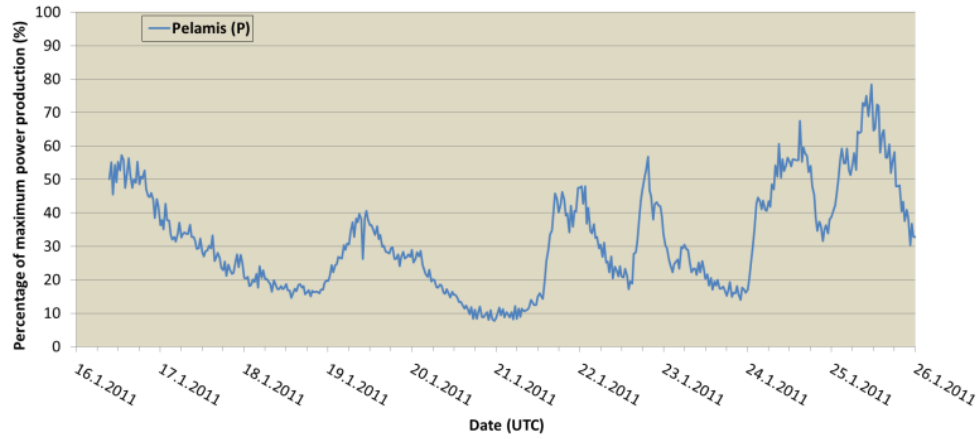
Figure 93. Pelamis non-dimensional theoretical power production from 16/01 to 26/01/2011.
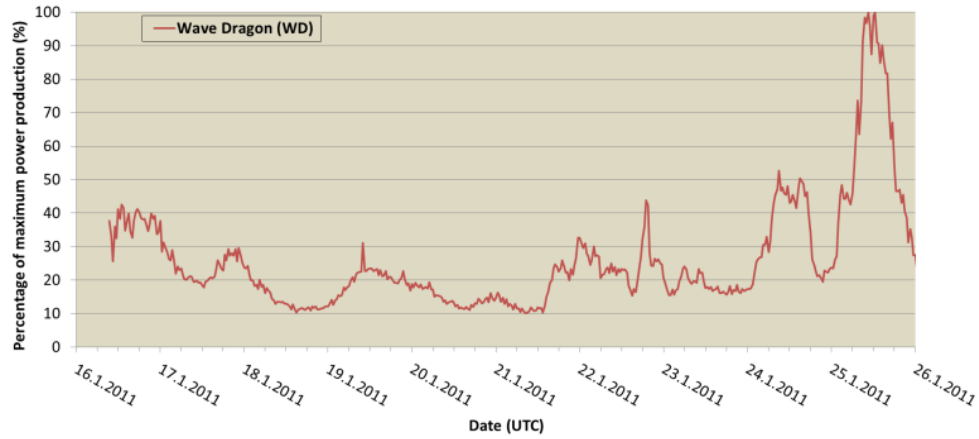
Figure 94. Wave Dragon non-dimensional theoretical power production from 16/01 to 26/01/2011.
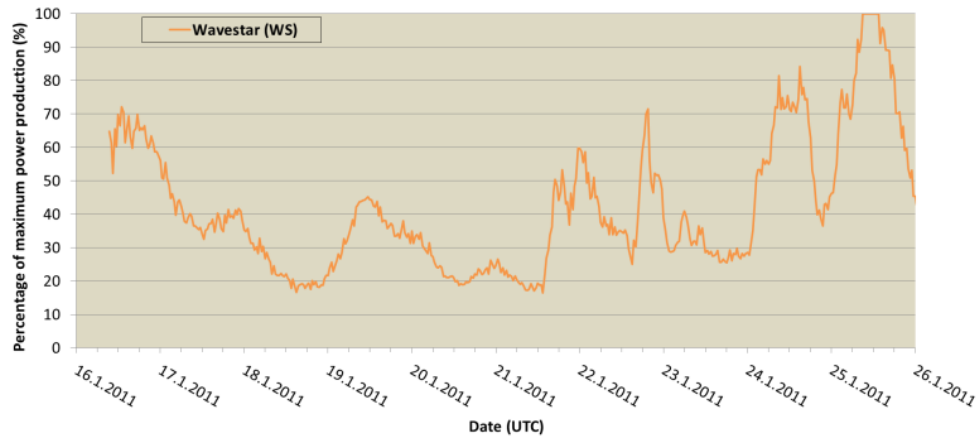
Figure 95. Wavestar non-dimensional theoretical power production from 16/01 to 26/01/2011.

143
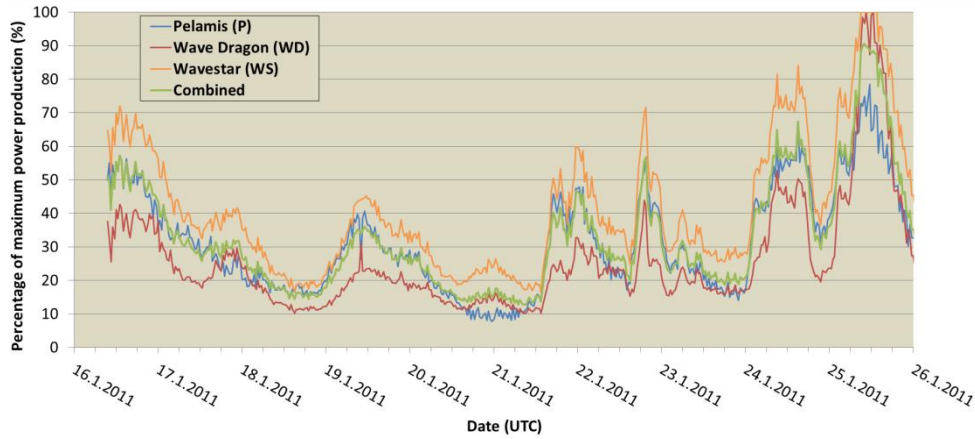
Figure 96. WECs individual and combined non-dimensional theoretical power productions from 16/01 to 26/01/2011.
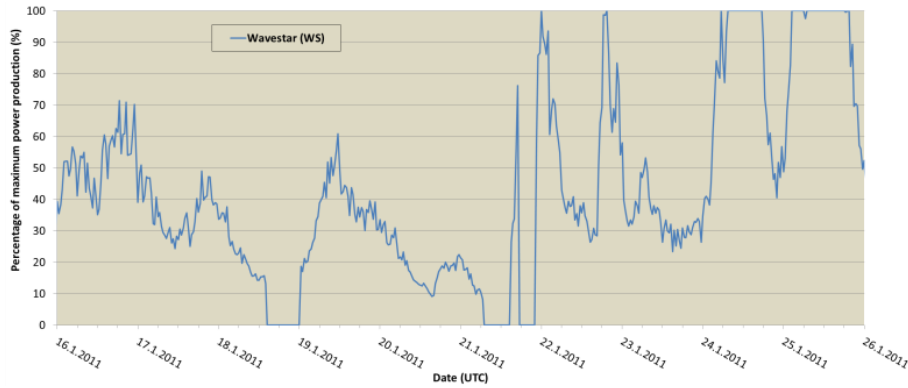
Figure 97. Wavestar non-dimensional real power production from 16/01 to 26/01/2011.

The evolution of H_{m0} shows H_{m0} oscillates around its mean value, it reaches a minimum of 0.7 m and a maximum of 2.7 m. Maximum power production of the three WECs coincide with this peak of H_{m0}. None of WECs' power production drops to zero.

Pelamis shows a power production mainly concentrated in between 10 and 60% full-production. It reaches a peak of 80% at maximum value of H_{m0}.

Wave Dragon has a power production mainly concentrated in between 10 and 40% full-production. It reaches 100% production at maximum value of H_{m0}. When this happens, Wave Dragon shows sharper peaks than Pelamis, since Wave Dragon reaches full-production at lower sea states than Pelamis. It is interesting to look at the variations from zero to full power: on 24/01 production rises from 20% to 100% power in 13 hours, and then decays to 20% power again in 13 hours.

Wavestar has a power production mainly concentrated in between 20 and 70% full-production. As Wave Dragon, it reaches 100% production at maximum value of H_{m0}, and it takes the same time as Wave Dragon to go from low production to full-production, i.e. 13 hours.

144

The three WECs show similar evolution in their power productions, but the amount of power produced differs. However, since the amount of power depends on the rated power of the device, and this is a parameter that can be adjusted, this cannot be regarded as a significant difference. This is further examined below, where the cross-correlation factor between the power productions of the three WECs is calculated.

When studying combinations of WECs it is usually desired that these reach maximum production at different sea states, to control and to reduce the variability of the power produced.

Then, numerical values on the half-hour variability of the power production of the three WECs and a combination of them are provided. The percentages of time the power productions fall within different ranges of maximum power production is also shown, i.e. null production, >0-20%, 20-40%, 40-60%, 60-80%, 80- <100% and full-production.

From Table LVI it can be inferred which WEC or combination of WECs provides the smallest percentage of time with zero production, the highest percentage of time with maximum production, the maximum average production and the lowest variability in production.

Table LVI
Half-hour variability and Percentage of Time the Productions of Pelamis, Wave Dragon, Wavestar and Combined are between the Indicated Percentages of Rated Power from 26/10/2010 to 09/02/2011.

	Mean	σ	σ/Mean	Percentage of time x falls in the indicated intervals of production						
				x=0	0<x<20	20<x<40	40<x<60	60<x<80	80<x<100	x=100
Pelamis	35%	31%	88%	1	28	31	28	10	2	0
Wave Dragon	32%	39%	122%	1	39	35	11	5	5	4
Wavestar	44%	42%	95%	5	16	27	24	14	9	4
P+WD	34%	34%	100%	1	32	36	17	7	6	0
P+WS	36%	35%	97%	1	29	35	19	10	6	0
WD+WS	38%	37%	97%	1	26	33	23	9	7	1
All WECs Combined	37%	34%	92%	1	27	33	23	11	6	0

The following conclusions derive from Table LVI, which are in line with the patterns of the power productions presented in the previous figures:
- Pelamis power production is mostly concentrated between 0 and 60% full-production. Only 1% of the time it has null production.
- Wave Dragon has most of its production concentrated in the lower percentages, up to 40%. It reaches 100% production 4% of the time. Only 1% of the time it has null production.

- Wavestar has the maximum percentage of time with null production (5% of the time). It also has the largest full-production (14% of the time production is above 80%).
- All WECs combined show only 1% of the time with null production, higher mean production than Pelamis and Wave Dragon, and lowest variability than Wavestar and Wave Dragon alone.

VII.4.3. CROSS-CORRELATION BETWEEN WECS

The cross-correlation factor between each pair of WECs is provided below. It indicates the degree in which the variation in the power production of one WEC is also happening in the other WEC.

Regarding predictabilities and variability of the power production, it is interesting that the WECs are not correlated. The more correlated the lowest probability to cancel out the errors in the forecast of power productions, and to cancel out the peaks in production.

Table LVII shows Pelamis and Wave Dragon have the most correlated power productions (0.86), and Wave Dragon and Wavestar the lowest (0.73).

Table LVII
Cross-correlation factors between Pelamis (P), Wave Dragon (WD) and Wavestar (WS) theoretical power productions when combined two by two.

	$CC_{between\ WECs}$
P+WD	0.86
WD+WS	0.70
P+WS	0.73

VII.4.2. WIND TURBINES POWER PRODUCTION VARIABILITY

This section examines the variations of the power production of wind turbines.

The following figures show the non-dimensional real power productions of the Folkecenter 525 kW wind turbine, throughout the same 10-day period (16/01 to 26/01/2011) of the previous section. For comparison, the evolution of u_{wind} is also shown.

Power productions derive from Folkecenter 525 kW wind turbine real power production data.

u_{wind} oscillates around its mean value, it reaches a minimum of 0 m/s and a maximum of 17 m/s. Maximum and minimum power production of Folkecenter wind turbine coincide with the two peaks. It can be seen null power production for u_{wind}<3 m/s and 100% production for u_{wind}>15 m/s.

Contrarily than the pattern of WECs, Folkecenter wind production drops to zero in several periods. It can also be seen faster changes in the production.
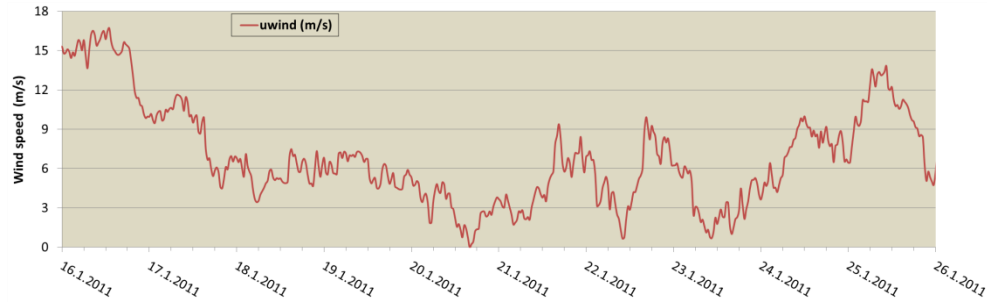
Figure 98. Evolution of u_{wind} from 16/01 to 26/01/2011.
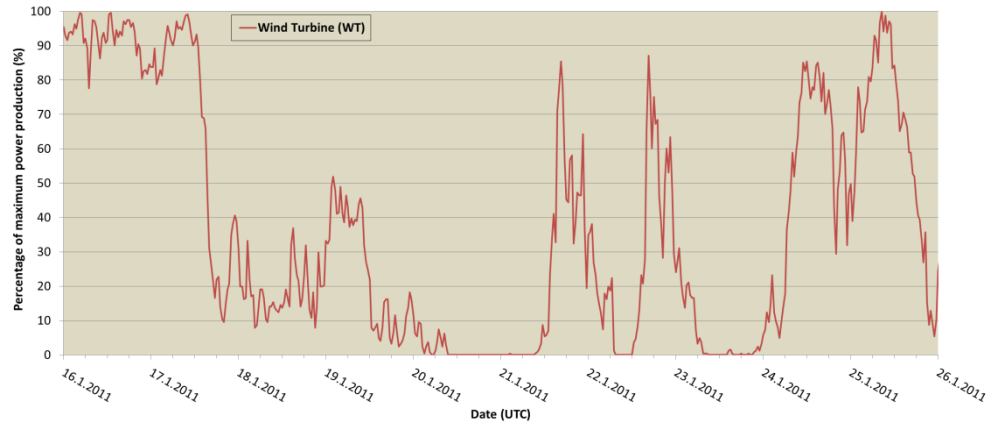
Figure 99. Folkecenter Wind Turbine real non-dimensional power production from 16/01 to 26/01/2011.

Table LVIII shows the cross-correlation factor between the power production of Folkecenter wind turbine, which represents real power productions, and the two theoretical power productions of the study. Cross-correlation factors are of the same order and are high.

Table LVIII
Cross-correlation factors between Folkecenter wind turbine real production and theoretical productions.

	$CC_{between \ Wind \ turbines}$
Folkecenter + HR	0.82
Folkecenter + TW	0.81

VII.5. VARIABILITY AND DIVERSIFIED WAVE AND OFFSHORE WIND ENERGY SYSTEMS

VII.5.1. INTRODUCTION

This section focuses on the opportunities of combining the power production of different technologies in the same site. Particularly, it looks into the combined power production of WECs and wind turbines.

The term diversified renewable systems refers to an energy system composed of various renewable resources, located in a range of areas within the same or in a different energy system. These systems usually embrace solar (thermal and photovoltaic), biomass, wind, wave and tidal generation, or any combination among them. The two key benefits of

diversification are that the variability of the produced power can be decreased, and power availability can be increased. These benefits can be achieved by combining different resources, the more un-correlated the better. Otherwise, when only one resource is available – wind energy for example – these benefits can only be realised by aggregating the power of geographically disperse sites.

As Diesendorf (2007) states: "Although a single wind turbine is indeed intermittent, this is not generally true of a system of several wind farms, separated by several hundred kilometers". Moreover, "for large amounts of wind power connected to the grid from several geographically dispersed wind farms, total wind power generally varies smoothly and therefore cannot be described accurately as 'intermittent'. Thus, the variability of large-scale dispersed wind power is unlike that of a single wind turbine".

In finance, this property also applies, i.e. "the part of the standard deviation of return of individual assets is diversified away when they are included in a portfolio with other assets". Portfolio risk is different as average individual security risk, and risk reduction through diversification is the reason (in finance, risk corresponds to the standard deviation of the rates of return).

This section focuses on diversified systems composed by WECs and wind turbines. The benefits of a combined wave and wind power output compared to the individual productions of the technologies are investigated.

Two case studies are analysed. The first one is based on real power productions of a prototype of Wavestar and a 525 kW wind turbine at Hanstholm. The second case study is based on modelled power productions of a commercial Wavestar working at Horns Rev 2 wind energy farm. These analyses sought to find the optimal mix of i) WECs and of ii) wind turbines and WECs, that resulted in the "best" pattern of electricity supply from the WEC system. For this study, the homogenised energy output, expressed as a percentage of maximum system output, has been chosen as the optimisation parameter.

VII.5.2. HANSTHOLM – A REAL CASE STUDY

This case study is based on simultaneous, real power production data from Wavestar and a Nordisk Folkecenter for Renewable Energy wind turbine (Nor) placed on the coast. To the author's best knowledge the study comprises the first research investigating and comparing real power productions of WECs and of wind turbines.

Figure 100. Wavestar (on storm protection mode) and Folkecenter wind turbine at Hanstholm, Denmark.

Wavestar and the wind turbine are located at Hanstholm, on the North-West coast of Jutland, in Denmark. Wavestar is in near-shore waters 300 m offshore and the wind turbine is lying on the coast, in a straight line 350 m from the WEC (Figure 100). The Wavestar prototype at Hanstholm corresponds to a section of the full-scale WEC, and it is rated at 110 kW. It was deployed in September 2009, and since September 2010 it has achieved relatively continuous power production (Vidal, et al., 2012). The wind turbine was manufactured in 1996 and has been in operation from that date. It is rated at 525 kW.

Simultaneous power production data from both technologies are available for a five-month period, ranging from January to May 2011. (In order to compare the performance of the two technologies, non-dimensional power productions – expressed as a percentage of maximum power output – have been used throughout the study). Also, wave and wind measurements on the same site have been recorded for that period. The two sets of measurements have been used to compare the resources and the power productions, since results on the combined power output strongly depend on the relationship between waves and winds.

Figure 101 illustrates the evolution of the wave and the wind resource (upper graph) and the power production of Wavestar, of the wind turbine, and of a combination of the two in equal parts, i.e. 50%:50% scenario (lower graph).

It should however be noted that there are certain limitations within the direct comparison of the sea states recorded by the Waverider buoy, and the wave conditions at Wavestar location. Whereas mean wave power at the Waverider is approx. 7 kW/m, mean wave potential at Wavestar is about 3 kW/m (Wave Star, 2012).

Figure 101 shows waves present lower variability and slower changes than winds. These two features affect the pattern of the individual and the combined power production of Wavestar and of the wind turbine. Overall, the combined power output is smoother and provides higher availability than the individual productions.

Figure 101. Significant wave height (blue), wind speed (red), and real power productions of Wavestar (blue), of the wind turbine (red) and a combination of both (green), expressed as a percentage of maximum power output, during 10 days of January 2011.

A smooth or less variable output refers to the fact that both the peaks and the fast changes found in the individual productions reduce when these are combined. This can also be seen in Table LIX. It shows the percentage of time with power productions above 80% drops to 3% of the time when the technologies are combined, compared to 11% and 9% of the time if the WEC and the wind turbine work alone, respectively. Figures on power output variability (σ/Mean of Table LIX) indicate that the combined scenario reduces 11% to 31% the variability of the power output.

Availability is improved thanks to a significant reduction of the time the combined power production drops to zero (6% of the time), compared to the periods where the individual productions are at null power (13% of the time for wind and 36% for wave) (Table LIX).

These results are complemented by Figure 103. It shows the cross-correlation between the real power productions for Wavestar and Folkecenter wind turbine for the period January to May 2011. (i.e. N=±3700). It shows there is low correlation between the two power outputs (*CC(0)=0.23*), what improves significantly the properties of the combined production. Moreover, maximum CC=0.30, is reached for a time delay of 5.5 hours; which indicates this is the average time delay between Wavestar and Folkecenter power productions.

Table LIX

Percentage of Time the Combined Power Production is between the Indicated Percentages of Rated Power (from 01/01/2011 to 31/05/2011)

	Mean	σ	σ/ Mean	x=0	0<x<20	20<x<40	40<x<60	60<x<80	80<x<100	x=100
				Percentage of time x falls in the indicated intervals of production						
				(where *x* represents percentage of maximum power production)						
100% Wavestar	30%	32%	106%	36	11	22	13	8	5	6
75% Wave - 25% Wind	31%	26%	84%	6	38	26	14	8	8	0
50% Wave - 50% Wind	32%	23%	73%	6	31	30	19	10	5	0
25% Wave - 75% Wind	34%	24%	73%	6	32	23	20	16	3	0
100% Wind turbine	35%	29%	82%	13	26	20	17	15	9	0
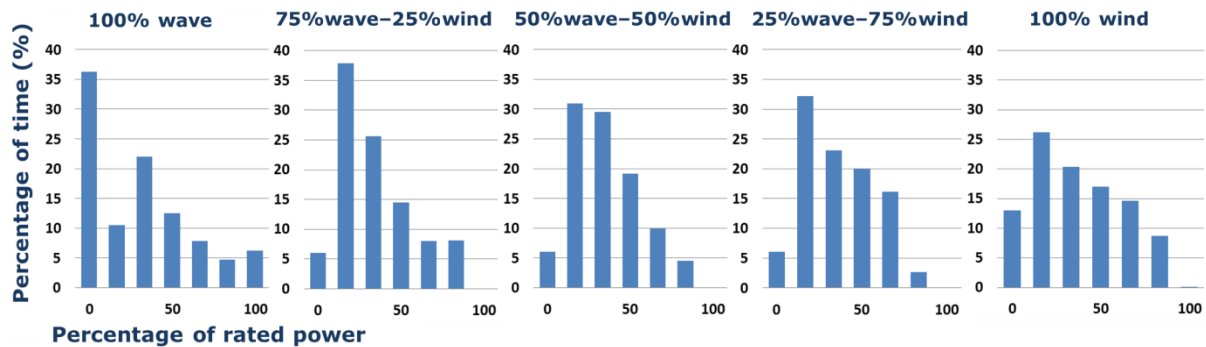
Figure 102. Percentage of time the combined power production is between the indicated percentages of rated power in five different scenarios: 100% wave, 75%wave – 25% wind, 50%wave – 50% wind, 25%wave – 75% wind, and 100% wind.
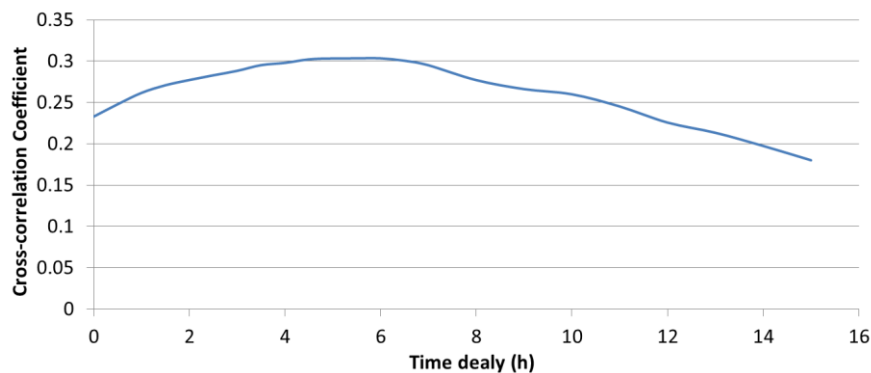
Figure 103. Cross-correlation (CC) coefficient between Wavestar and Folkecenter power productions for different time delays.

Results obtained in this study are site specific and highly dependent on the strong relationship (high cross-correlation) between waves and winds. In swell dominated locations, where resources are less correlated, the benefits of combined wave and wind scenarios are more evident. Moreover, the case study is based on two technologies with more than one decade of difference in gained operating experience. Whereas Wavestar was first deployed in Hanstholm in 2009, the wind turbine was commissioned 13 years before.

Moreover, despite the fact that the general advantages of combined developments have been identified, this case study has evaluated the case of one WEC and one ashore wind turbine. A change in power outputs' pattern is expected if several WECs and offshore wind energy turbines, and if more than one type of WEC are considered.

VII.5.3. HORNS REV 2 – A THEORETICAL CASE STUDY

Wavestar is planning the installation of a 600 kW Wavestar WEC, which is to be connected to a wind turbine at the wind power plant *Horns Rev 2,* placed off the western coast of Denmark.

The aim of this case study has been to assess the opportunities of combining wind and wave energy production on a commercial scale and to demonstrate the reduction of energy fluctuations with this combination. Results of this study have been presented by Marquis et al. (2012) and the main details and findings are summarised below. (Most of the text below is quoted from (Marquis, et al., 2012)).

Horns Rev 2 wind farm, in operation since 2009, has a total capacity of 209 MW. It consists of 91 wind turbines rated at 2.3 MW. The site is placed approximately 30 km from the Danish west coast near Esbjerg, on a reef at water depths between 9 and 17 m. Here, there is an average wind speed of 10 m/s and an average H_s of 1.5 m. The Wavestar 600 kW WEC is planned to be situated 300 m north-east of turbine number H7 of Horns Rev 2. The location has been chosen mainly based on an accessible connection point. H7 was already from the start equipped with an extra J-tube for the potential connection of a WEC.

The Wavestar 600 kW WEC is designed to deliver maximum 600 kW in electrical power to the grid at approximately H_s=2.3 m. The WEC is equipped with 20 floats, each float having a diameter of 6 m. The individual float is mounted on a 12 m long steel arm which is hinged on the main tube. 10 arms are placed on each side of the tube. If H_s<0.5 m, the WEC is stopped due to the calm waves, and if H_s>4.0 m, the WEC shuts down and enables storm protection.

Figure 104 illustrates the evolution of H_s and u_{wind} at Horns Rev 2 during a 13-day period (upper part). The lower figure shows the simulated power production of Wavestar, an offshore Siemens wind turbine and a 50%/50% combination of both technologies. The theoretical power productions are based on Wavestar C6 power matrix, and Siemens 2.3 MW power curve.

The following comments result from the curves presented in Figure 104:

-   The evolution of H_s and u_{wind} shows a certain correlation between the two resources, i.e. the blue and the red curves on the upper graph follow the same pattern. However, whenever the wind stops blowing, waves continue rolling for some time afterwards thereby causing a delay between waves and winds. Figure 104 shows a time delay of

up to 9 hours for H_s and u_{wind}. The same delay is found when comparing the pattern of the production from the WEC and the wind turbine.

- The combination of wave and wind power reduces the percentage of time that the combined production drops to zero. In Figure 104, the wind turbine has zero production in several time-intervals. However, the combined production does not drop to zero at any time.

- The comparison of wind and wave power production shows that abrupt changes in wind power (i.e. increasing from a minimum to a maximum value and vice versa) are faster than the same changes in wave power. The evolution of the three power curves from 01/11 to 01/12 illustrates that:
    o Wind turbine increases from 30% to maximum production in 8 hours.
    o Wavestar increases from 30% to maximum production in 11 hours.
    o The combined production increases from 30% to maximum production in 11 hours.

Hence, when wave power is included in the system, the fast changes of wind power reduce.

- It can also be seen that waves are more constant than winds; and hence, the power output from the WEC is smoother than the power output from the wind turbine. The combination of both outputs results in an overall less-fluctuating power, which indeed has a potential benefit for cable losses.
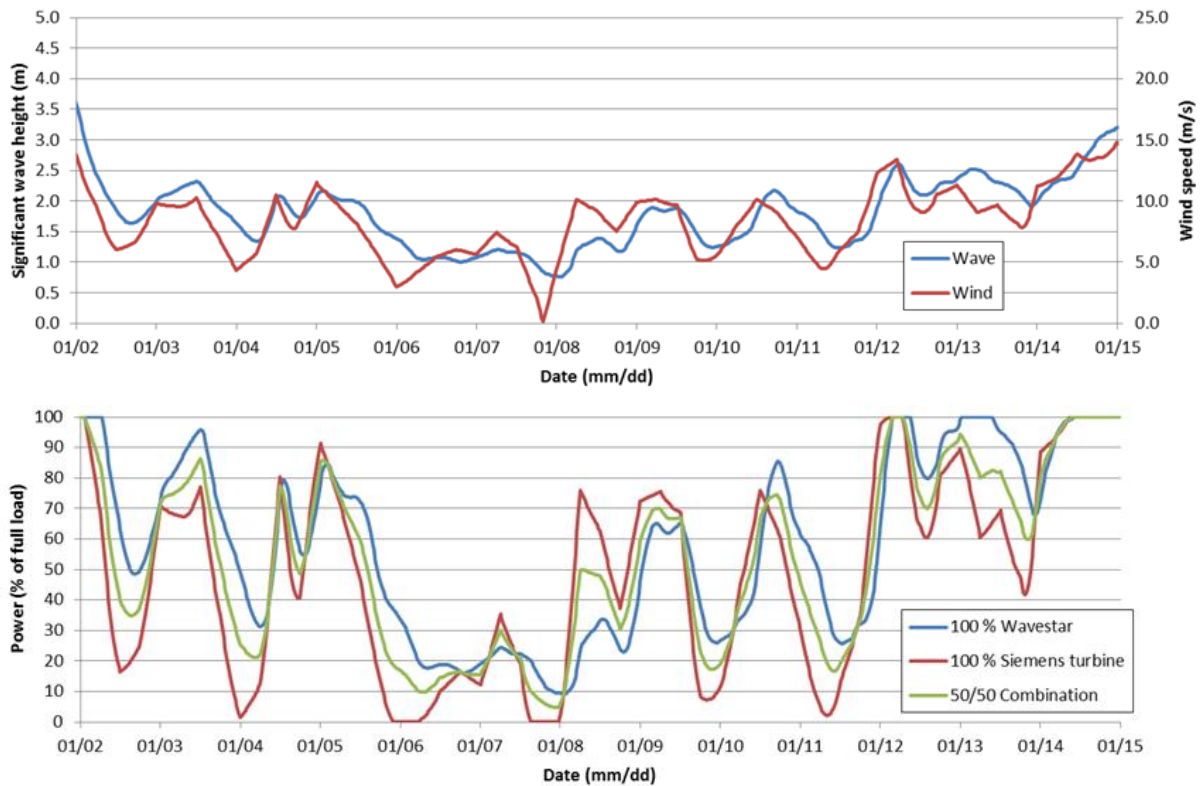
Figure 104. Time series of a 13-day period. Upper graph: Environmental conditions for waves (blue) and wind (red). Lower graph: Power production simulations of Wavestar (blue), wind turbine (red) and a combination of both (green).

VII.6. VARIABILITY IN STORMY CONDITIONS

On February 8th, 2011 a coastal storm with winds from West passed North Jutland. H_{m0} reached 4 m, T_{02} 6.8 seconds and the wind speed 22 m/s (Figure 105).

The evolution of the wind speed and the wave height during the storm (Figure 105) shows two facts. First, that the wave height takes about twice the time the wind speed takes to reduce from the peak value in the storm to its half. When the wind has dropped back to its average value the corresponding wave remains at high values for a longer time (up to 12 hours more). Then, the time delay between waves and winds increases as the storm moves forward. There is a 0.5 to 1 hour delay on the first increasing part on 8th February, and a 5.5 to 6 hours delay on the following decaying part.

VII.6.1. HANSTHOLM WAVESTAR AND FOLKECENTER CASE STUDY
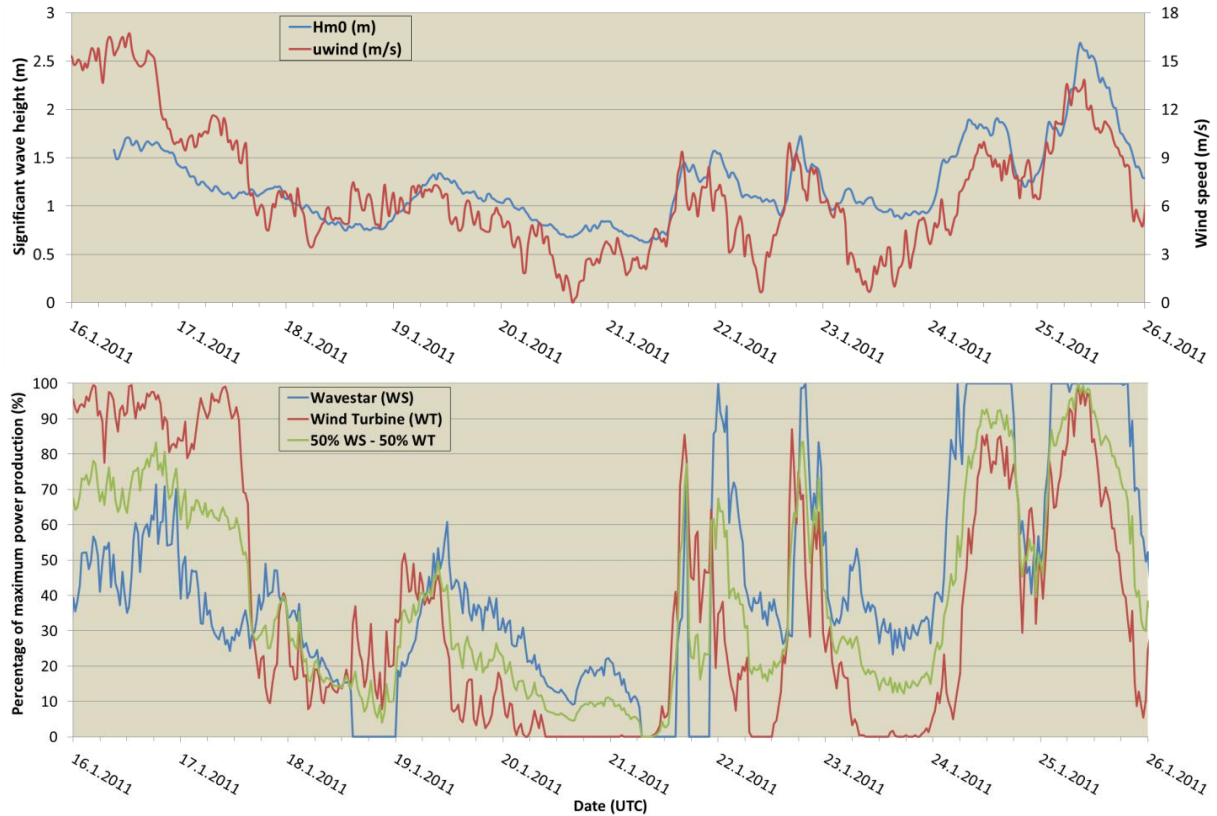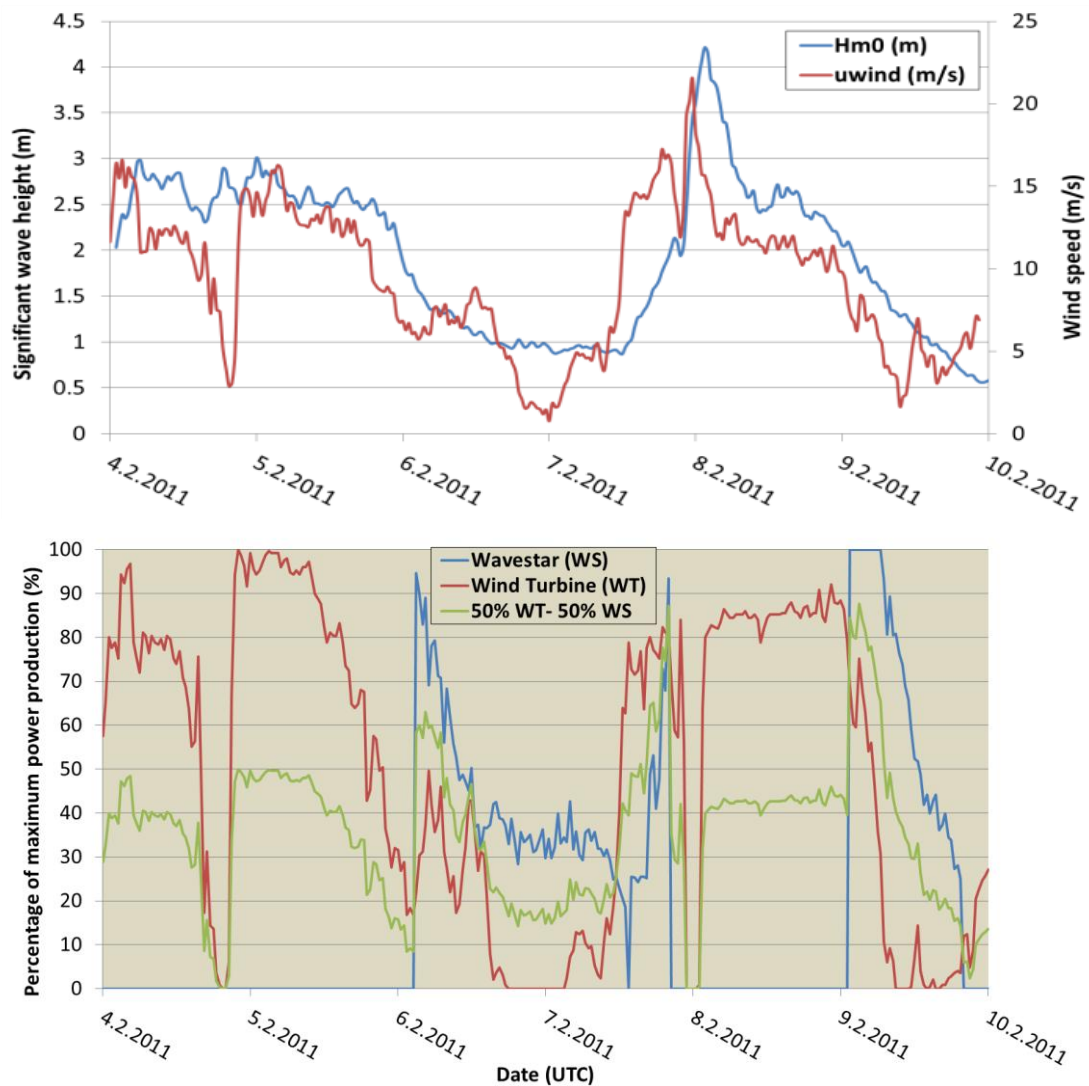

Figure 105. Significant wave height (blue), wind speed (red) and power productions of Wavestar (blue), the wind turbine (red) and a combination of both (green), expressed as a percentage of maximum power output, during a storm period in February.

It is particularly interesting to study the evolution in the power productions of the wind turbine and the WEC in this period, provided the fast changes in the production of wind turbines has been claimed as one of the major problems in their operation. After a storm the production of a turbine may decrease from full-production to its half or less, or vice versa.

Correspondingly, the power production of Wavestar follows that of the turbine with some delay. Figure 105 presents the productions of Wavestar, the wind turbine and a combination of both (50-50% scenario) before, during and after the 2-day storm.

Before the storm, the wave conditions are above the cut-out limit of Wavestar, which stays out of operation while the turbine is working. Then, there is a drop in the wind speed, followed by a drop in H_{m0}, and Wavestar starts producing while the turbine stops. As the storm conditions start, Wavestar enters into survival mode and the turbine produces. After the storm, Wavestar re-starts operation but again the wind turbine stops. Thus, the combined production only drops to zero at 2 particular points, which can be neglected compared to the times the production of WECs and wind turbines working alone drops to zero.

As a result, this figure shows that, during a storm, the combined power production has higher availability and is less variable than the individual productions. It is important noting that this evolution of the power output is very dependent on the technologies and the environmental conditions of the study.

VII.6.2. PELAMIS, WAVE DRAGON AND WAVESTAR

Section III.7. has shown the nominal and maximum operating conditions for the three WECs. Whereas Wavestar stops producing at H_{m0}=3m, Pelamis and Wave Dragon can continue working for H_{m0} above 4 meters. Therefore, different patterns in the power production of the three WECs can be expected during storm conditions.

Figure 107 illustrates the operation of the three WECs, Pelamis, Wave Dragon and Wavestar, in the storm of 7th February 2011 (Figure 105). When the storm starts, Wavestar enters into survivability mode and stops producing. This is however not the case for Pelamis and Wave Dragon, Wave Dragon reaches full-production and Pelamis produces above 70% maximum power during the storm period.

Above all, Wave Dragon and Pelamis power productions illustrate a more real situation.

The comparison between Figure 105 and Figure 107 shows a different pattern of Wavestar's power production. The reason is that Figure 105 is based on real power production of Wavestar´s prototype at Hanstholm, and the illustration of Figure 107 is based on theoretical data derived from Wavestar´s power matrix.

It should however be noted that, in real operation, WECs may enter into storm protection mode as a storm approaches the deployment site. For instance, for Wavestar the storm protection strategy involves un-ballasting the floats, raising them up from the water, and jacking-up all the structure, which takes about an hour. Therefore, it is not expected that WECs start and interrupt production from hour to hour during a storm.
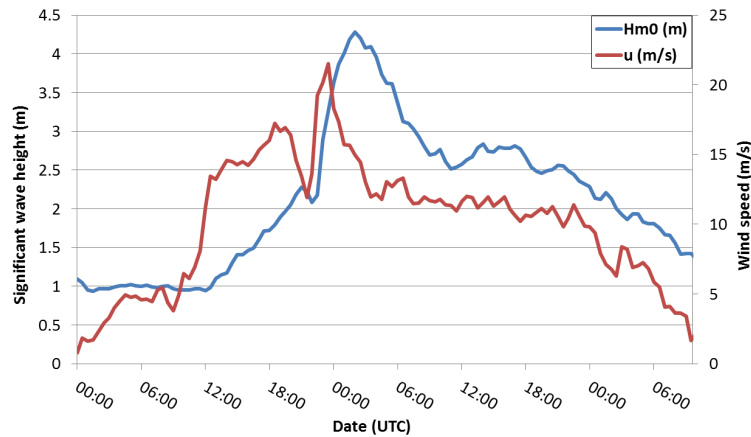
Figure 106. Evolution of H_{m0} (in blue) and u_{wind} (in red) over the storm on 07/02 to 09/02/2011.

Figure 107. Power productions of Wavestar (green), Wave Dragon (red) and Pelamis (blue), expressed as a percentage of maximum power output, during a storm period in February.

VII.6.3. WAVE DRAGON AND WIND TURBINE

Figure 108 presents the modelled power productions of Wave Dragon and a wind turbine before, during and after the 2-day storm of February 2011.

The response of Wave Dragon and the wind turbine to the storm conditions can be seen in Figure 108. Wind power production varies a lot, especially in the following times:
-    On 4th Feb at 19:30: it increases from 0% to 100% in 2 hours.

156

- On 5th Feb at 18:00: it decreases from 80% to 10% in 8 hours.
- On 6th - 7th Feb it has null production during 7.30 hours (from 18:30 to 2:00).
- On 7th Feb at 08:30: it increases from 3% to 69% in 4 hours.

Contrarily, the simulated wave power system, i.e. Wave Dragon modelled power production, during the same period of time, remains at high productions and has no time of null power output. The fastest change of wave power production happens on 7th Feb at 12:00, where production increases from 15% to 100% in 11 hours.

Figure 108. Power productions of Wave Dragon (red) and a wind turbines (blue), expressed as a percentage of maximum power output, during a storm period in February.

This confirms the more gradual change of power production from waves compared to winds.

The delay between wave and wind production can also be observed.

VII.6.4. HORNS REV 1 CASE STUDY

Sørensen et al. (2005) also studied the evolution of the power production of wind turbines and WECs during a storm period. Their findings coincide with the conclusions described above. The following text has been quoted from Sørensen et al. (2005).

"About 18:00 in the evening the wind speed slowed down and 20:30 the wind speed was only 6 m/s. Half an hour later there were full gale with wind speeds of about 16 m/s. The duration of this "wind hole" below 15 m/s were about 1:30 hour. At the same time interval the significant wave height maintained its value of about 2 meters. The response to the "wind hole" is shown in the figure below. The wind power production decreases within one hour from 100% to only 10% of the rated power. Half an hour later the system is at full production again. The simulated wave power system during the same period slightly increases its

157

production from 65% to 75% of rated power down to 60% as the wind farm is at full power again."
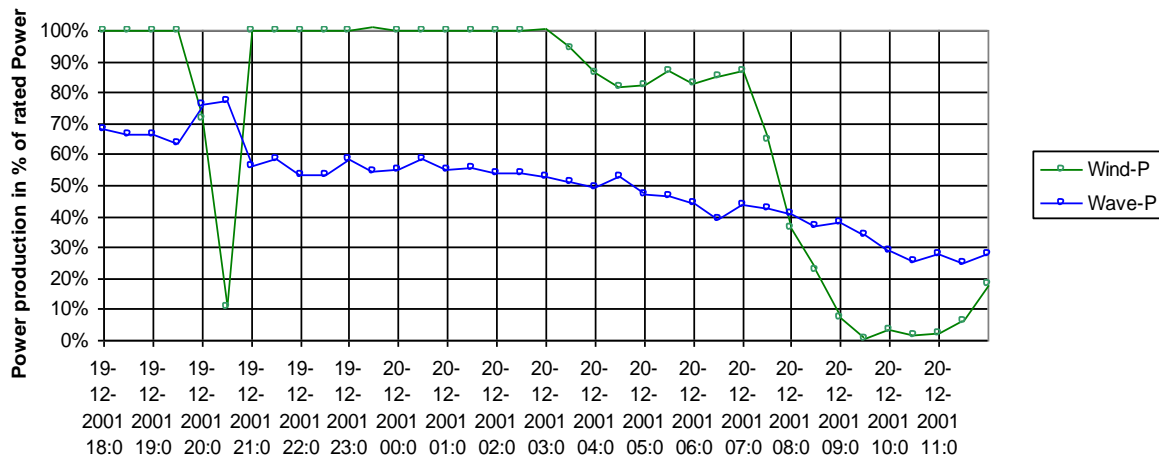
Figure 109. 18-hour of power production on December 19th-20th, 2001, of the simulated power productions of a WEC and Horns Rev 1 wind farm (Soerensen, et al., 2005).

VII.7. FURTHER CHARACTERISTICS OF DIVERSIFIED SYSTEMS

Combining in the same location wind turbines and WECs also provide the following advantages to the diversified system:

- Higher utilisation of a common cable.
- Lower peaks allows for a lower rated power of the cable.
- Overall, cable costs reduce.
- Increase the site utilisation factor, i.e. the energy production from the area.
- Reduce capital costs (CAPEX), and installation and maintenance costs (OPEX), and thus, the cost per unit of energy produced (COE). The costs of cable laying and of the O&M facilities can be shared. In hybrid solutions, the structure cost may be shared too.
- Reduce efforts and time with regards to marine policies, marine stakeholders, spatial constraints and environmental impact assessments.
- The wind and wave energy sector share synergies within offshore grids and the lack of strong grid connection points close to shore able to absorb the power generated offshore (Fernandez-Chozas et al., 2010).
- The lee behind WECs benefits the wave loads on wind farms: better access to the wind turbines for maintenance activities.
- Reduces the cost of reserve capacity.
- In offshore developments, there might be an opportunity to supply electricity to oil and gas fields.

Here, it might be worth discussing how much offshore wind and wave energy is competing for space as most WECs are preferably deployed at deeper waters than the ones wind energy

is currently utilizing. Even if going for the very same area, many WECs should be able to share the area with offshore wind. Only a potential conflict can be seen when comparing WECs located at shallow waters, i.e. mounted at bottom fixed at poles. On the other hand, a common use of towers may benefit both parties.

VII.8. SUMMARY

- The average delay between waves and winds at Hanstholm is of 2-3 hours. In storm conditions, a phase shift up to 6-8 hours can be found.
- There is high cross-correlation between waves and winds, CC=0.8.
- Mean wave power in Hanstholm has an annual variability up to 40% (with respect to mean annual value) and a seasonal variability up to 100% (with respect to mean monthly value).
- Variability of wave energy in mild climates (i.e. Canary Islands) is lower than in extreme climates (i.e. Hanstholm).
- P_{wind} can vary 90% more than P_{wave}, and u_{wind} 40% more than H_{m0}.
- Waves have lower variability and slower changes than winds (Figure 110).
- The combined power output of WECs and of wind turbines is smoother and provides higher availability than the individual productions (Figure 110):
  - ○ Null production is reduced to a minimum.
  - ○ Peaks are eliminated.
- Average delay of 5.5 hours between Wavestar and Folkecenter wind turbine power production.
- Storm conditions: faster changes in wind than in wave power production:
  - ○ At Hanstholm, based on real data:
    - ▪ Wind turbine increases from 30% to 100% production in 8 hours.
    - ▪ Wavestar increases from 30% to 100% production in 11 hours.
    - ▪ The combined production increases from 30% to 100% production in 11 hours.
  - ○ At Hanstholm, based on modelled data (Figure 111):
    - ▪ 4th Feb at 19:30: Wind turbine increases from 0% to 100% in 2 hours. Wave Dragon remains above 80% production.
    - ▪ 7th Feb at 08:30: Wind turbine increases from 3% to 69% in 4 hours. Wave Dragon increases from 15% to 100% in 11 hours.

Overall, this advocates a lower use of wind energy if the power variability is sought to be minimized.

Significant wave height and Wind speed

Waves take twice the time to increase
from average to peak value

6h   12h
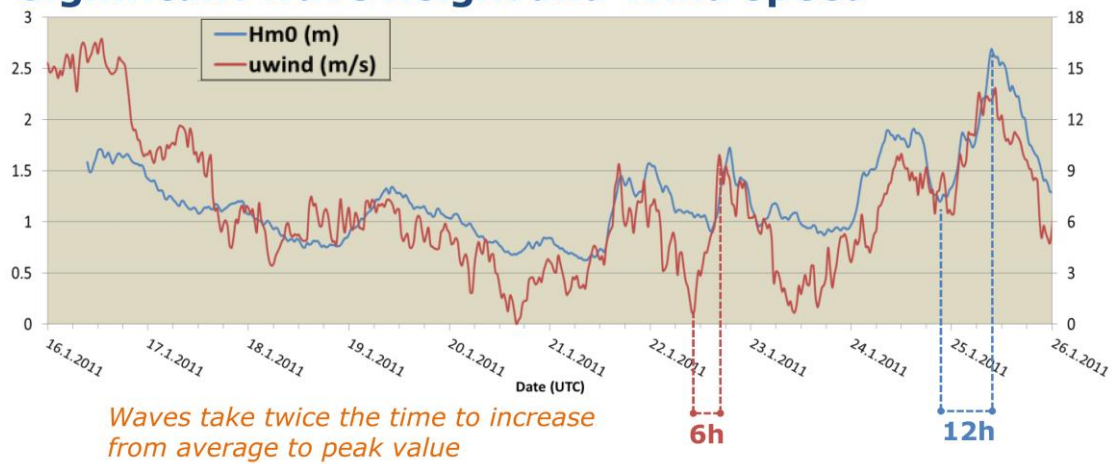
Percentage of maximum production (%)

No zero-values in 50:50 scenario

No peak-values in 50:50 scenario

6h

12h

50%-50% scenario: smoother
changes from zero to peak value
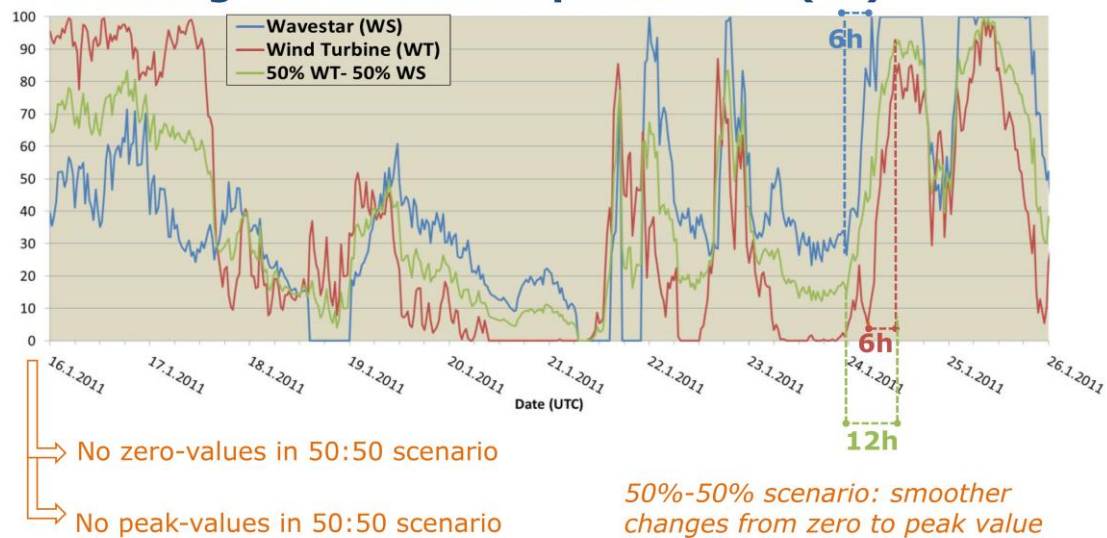
Figure 110. Same as Figure 101 with comments.

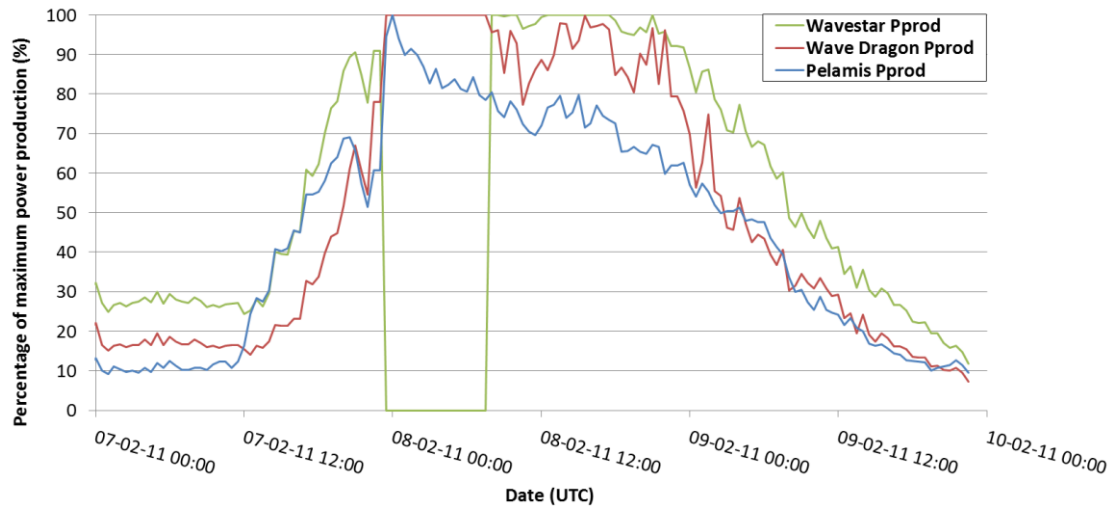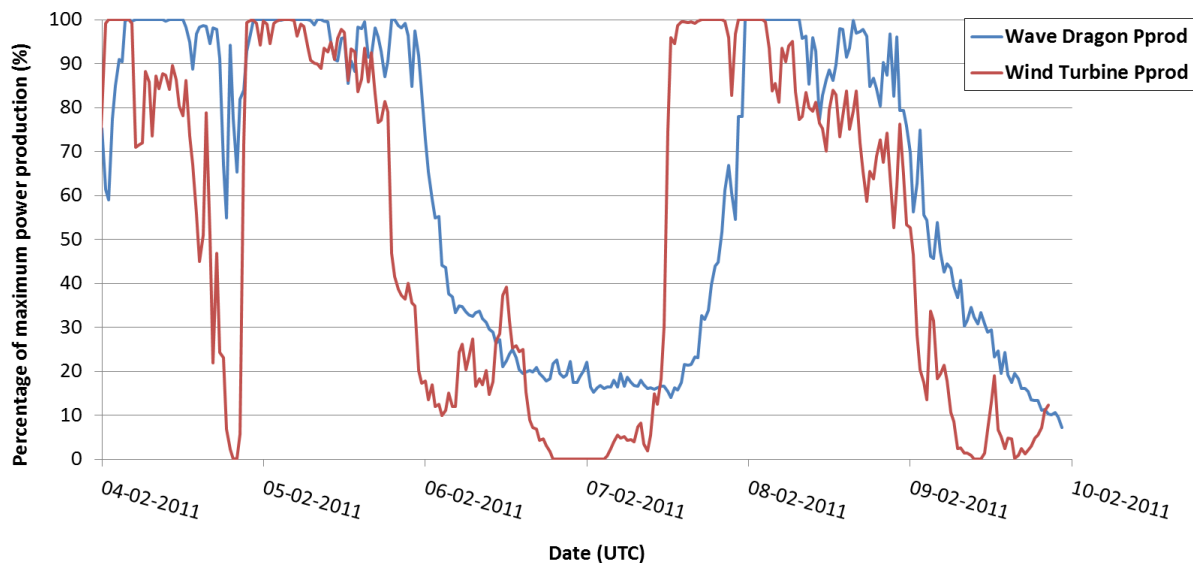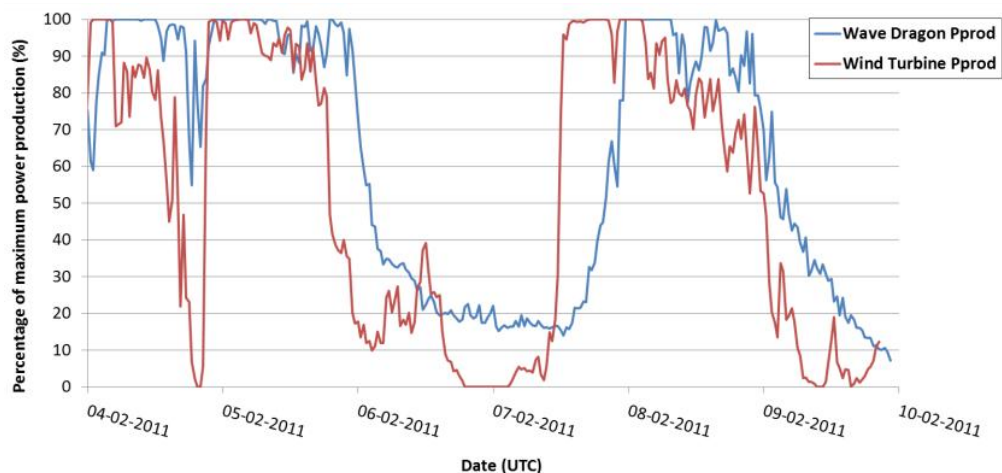Figure 111. Power productions of Wave Dragon (red) and a wind turbines (blue), expressed as a percentage of
maximum power output, during a storm period in February.

160

CHAPTER VIII – DISCUSSION

VIII.1. LIMITATIONS OF THE STUDY

There are several limitations to this study that should be taken into account when analysing the results.

1. The selected WECs have not been originally designed for the typical wave climate at Hanstholm. Pelamis has been modelled for the wave climate of the Atlantic Ocean, characterised by longer period swells in comparison to the shorter and more irregular waves found at Hanstholm. This is the same for Wave Dragon, it reaches maximum power production at sea states characterised by high waves and high periods, which rarely occur at Hanstholm.

Although the main dimensions of the devices have been changed to suit the predominant wave climate at Hanstholm, performances of the WECs may differ from those expected at more powerful sites, and thus, its predictability might be compromised. WECs might not operate optimally at Hanstholm wave climate.

Moreover, competitive comparisons between the performances of the WECs should be avoided and cannot be conclusively drawn from these results. Most of results are theoretical or derive from real – yet experimental – data.

2. The WECs of the study aim at representing three types of WECs; however, not all existing types of WECs have been represented in this study.

3. This study is not a resource assessment of Hanstholm site or the North Sea. The analysed data comprises of a limited time period.

4. In few years time, there would be better knowledge about WECs performances. This will decrease the uncertainty inherent to the power matrices and thus, it will lead to more accurate predictions of the power production. This project can be regarded as a first approach towards the study of predictability of WECs power production. Future studies with more accurate production data will probably show higher forecast accuracies.

5. The study is mostly based on theoretical power productions of only one particular site, which derive from three power matrices and one power curve. These represent only to a certain extent a real scenario. In reality, generation would be distributed over a wide area and would come from wave arrays and wind farms. Since power production forecast accuracy improves with diversification, more accurate prediction are expected in real scenarios.

6. All findings of the study are dependent on the metocean conditions of the Danish North Sea, and particularly of Hanstholm. In a wave climate characterised by swell waves, the accuracy in the predictions will improve significantly; since swells are more regular compared

to wind seas. In a wind sea, where the cross-correlation between waves and winds patterns is high, short-term forecast errors in winds are more reflected in waves predictions.

7. The study illustrates predictability of wind power production with theoretical power productions derived from a power curve. This has allowed the comparison of wind production forecasts to wave production forecast, but it does not coincide with the current accuracy level on wind forecasting. The wind energy sector has, along with meteorologists, focused on wind forecasting for many years, which has allowed gaining knowledge and making a very fast improvement on weather forecasting. Here the accuracy of wind forecasting is evaluated in the same terms as the accuracy of wave forecasting; mostly as indicative results to allow comparison among the two sets of compared values. Hence, the results presented here should not be read as the current accuracy level on weather forecasting.

8. Intra-day electricity markets are used to correct the errors in the estimates of future power production bid in the day-ahead market. These corrections have not been considered in the calculations.

9. Balancing costs for a generation technology depend on various factors: the type of other generating equipment ready to provide balancing power, the predictability of the variations in demand, penetration levels of the technologies, the extent of the balancing area, and the system interconnection. None of these factors have been included in this study. Moreover, the study is based on the Nord Pool Market, which has significantly lower up- and down-regulation prices in comparison to other European markets (i.e. Germany).

10. With regard to diversified systems, and the benefits of combining wind turbines and WECs, the findings are also very dependent on the metocean conditions of the study location. A wave climate dominated by swells will derive into less correlated waves and winds and into higher delays between both resources. This translates into less-correlated power outputs from the wind turbine and the WEC, and thus, the combined production would results much more attractive. It will be less variable and more available than as presented in this study.

11. The case study comparing WEC and wind turbine real power productions is based on two technologies with more than one decade of difference in gained operating experience. Whereas Wavestar was first deployed in Hanstholm in 2009, the wind turbine was commissioned 13 years before. Moreover, the study examines the power production of only one WEC, whereas the sector is expected to be comprised by different WECs based on various principles. Indeed, the prototype of Wavestar cuts-off production at lower sea-states than the commercial unit or than other WECs. On the other hand, wind turbines generally stop production at 25 m/s, at the same wind speed considered in the study.

12. The study evaluates the combined production of only one WEC and one ashore wind turbine. If the analyses covered various WECs and wind turbines, placed further offshore and

spread over a wider area, the combined power output would be more constant and less-fluctuating and with a higher average. These are the result of reduced variability through regional diversification, of the different response of technologies to metocean conditions and of the higher energy potentials available offshore.

13. Results on predictabilities for forecast horizons from 0 to 1 hour, as well as from 120 hours (5 days) to 132 hours (5½ days) are biased compared to results from the other forecast horizons (i.e. from 1 to 120 hours). The reason is there is much lower number of data points for those lead times.

VIII.2. LESSONS LEARNED

1. This project has requested extensive work on data management, including data gathering, processing and analysis. Data processing:
- o Data validity of buoy-measurements and weather data
- o Unify date format – everything put into UTC time.
- o Manage and process seven different data sources: Kyst-buoy, Kyst-weather station, AAU buoy, AAU weather station, DHI, Wavestar, Folkecenter turbine and Energinet.dk market data.
- o Time-series of each data source indicated to different average values, i.e. average of the last half-hour, average of the next half-hour, average of the half-hour.
- o Different time-intervals: as 10-minutem, as 30-minute or as 1-hour averages.
- o Identify what each value represents.

2. Bias and MAE firstly calculated as the difference between observed and forecasted data, i.e. (OBS-MOD). It has been later changed to (MOD-OBS). Also, MAE was firstly named "AME".

3. Available wave power at Hanstholm was first calculated by the deep-water formula. Hence, it was assumed the validity of deep-water theory at the Waverider buoy (17 m water depth). This was changed into the general formula of wave power in order to take into account the influence of intermediate water depths.

4. Combined power production was firstly calculated as the sum of productions, not taking into account different rated powers among the WECs and wind turbines, and hence, that each contribution was different. This was changed into the sum of percentages of maximum power productions.

5. Power productions of WECs were not calculated as weighted averages, but by taking the closest minimum value from the power matrices. These resulted into power productions

varying in steps (Figure 112). The first *EWTEC* paper, *EWTEC* oral presentation and *Modern Energy Review* article were published with the first values.
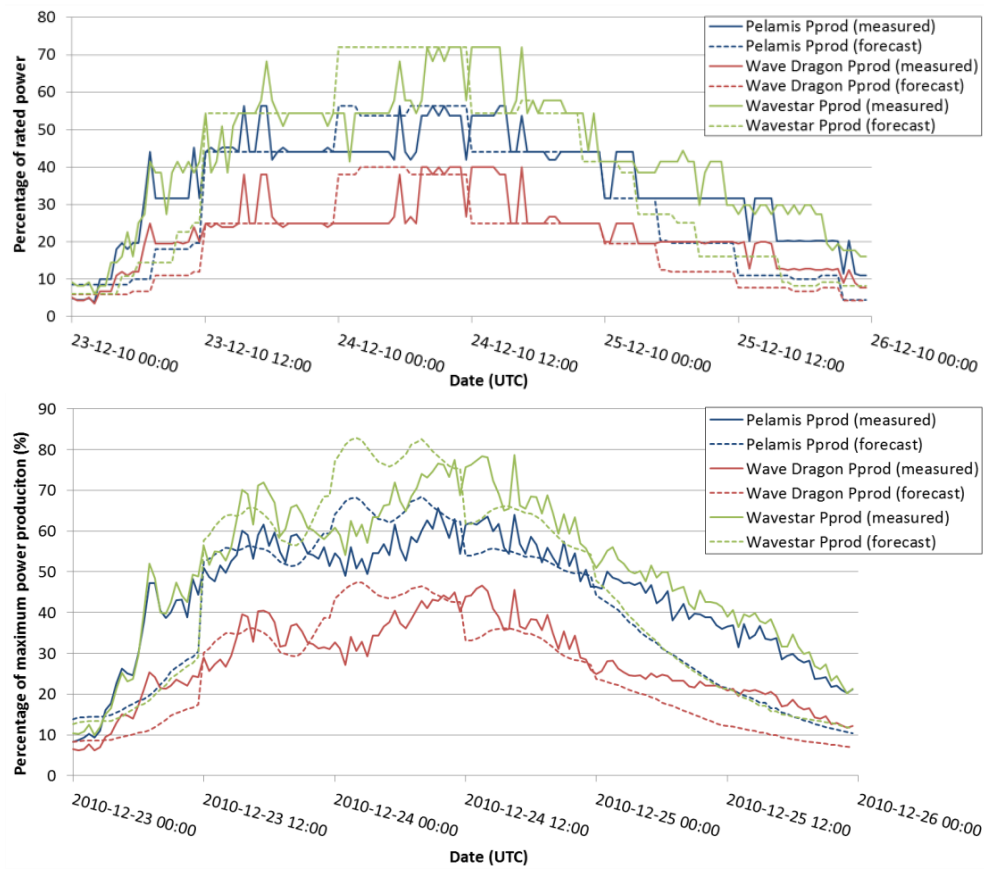
Figure 112. Comparison between old (upper figure)and new (lower figure) calculated values of WECs power productions.

6. The wind energy sector has done years of work on the subject of winds predictability. Enormous knowledge has been gained from their work, mostly on the methodology and on the study approach.

7. Lastly, the author of the project J. Fernández-Chozas would like to highlight the contribution of this project into her understanding of a research problem, and into her abilities to approach it and analyse it. It has also contributed to the analysis of case studies and fieldwork, as well as to gain abilities in oral and written communications skills. Moreover, she has expanded her knowledge on complementary fields like resource assessment; WECs' design, Froude scaling and power matrices calculations; wind turbines wind resource assessment (i.e. wind roses and influence of orography into measurements); economics; electricity markets design and functioning; and statistics. Most notably, this research project has contributed to link the knowledge of different areas, and hence, to gain a broad perspective for problem solving.

IX.1. GENERAL CONCLUSIONS

The main conclusions derived from the study are the following. First, conclusions on wave energy predictability and electricity markets are provided and secondly, results on variability of the power output of WECs in diversified systems.

Wave energy predictability and electricity markets:

- Day-ahead forecasts of wave parameters are accurate for H_{m0} and T_{02}, acceptable for H_{max} as well as for values of P_{wave} close to the mean, and not very accurate for larger P_{wave} values.
  - The errors of day-ahead forecast of H_{m0}, H_{max}, T_{02} and P_{wave} are 20%, 37%, 9% and 41% (in terms of *MAE/Mean*), respectively.
  - Short-term forecasts (*t=0-12 hours*) have better accuracy particularly for H_{m0} and P_{wave}, i.e. errors of 17%, 36%, 8% and 36% (in terms of *MAE/Mean*) for H_{m0}, H_{max}, T_{02} and P_{wave}, respectively.

- Day-ahead forecast of wind parameters are accurate for MWD_{wind}, acceptable for u_{wind} and a bit inaccurate for P_{wind}.
  - The errors of day-ahead forecast of u_{wind}, MWD_{wind} and P_{wind} are 26%, 19% and 62% (in terms of *MAE/Mean*), respectively.
  - Short-term forecasts (*t=0-12 hours*) have better accuracy particularly for u_{wind} and P_{wind}, i.e. errors of 22%, 17% and 52% (in terms of *MAE/Mean*) for u_{wind}, MWD_{wind} and P_{wind}, respectively.
  - Long-term forecasts present large errors: 33%, 24% and 80% (in terms of *MAE/Mean*) for u_{wind}, MWD_{wind} and P_{wind}, respectively.

➔ Hence, u_{wind} predictability is more inaccurate than for H_{m0} and T_{02}. Particularly, day-ahead forecasting of waves (i.e. H_{m0}) is 23% more accurate than of winds (i.e. u_{wind}) and day-ahead forecasting of P_{wave} is 50% more accurate than of P_{wind} (in terms of *MAE/Mean)*.

- Generally forecasts overestimate real-time values, i.e. positive *Bias*.

- In this study it proves more accurate (20% to 33%) to forecast wave parameters for storm-like conditions than for typical wave conditions. This does not represent the expected predictability of stormy periods, where weather conditions change very fast and are more difficult to predict. Results can then be explained by the limited amount of data analysed, which corresponds to only one winter where weather patterns may

get repeated. To draw final conclusions on storms predictability further data on stormy periods should be analysed.

- The three stormy periods in the analysis indicate a delay between 2.5 and 3 hours between max. u_{wind} and max. H_{m0}.

- Day-ahead predictability of the combined power production of WECs (*NMAE=11%*) is better than the predictability of the individual units (*NMAE=9-15%*).
  - Day-ahead forecast error (*NMAE*) of Pelamis is 11%, of Wave Dragon 9% and of Wavestar 15% with *NMean* of 33%, 33% and 44%, respectively.
  - Day-ahead forecast error (*NMAE*) of the combined production of the three WECs is 11%, with *NMean* of 37%.
  - Day-ahead forecast errors (*NMAE*) of WECs working two by two are: for Pelamis and Wave Dragon 10%, for Pelamis and Wavestar 12%, and for Wave Dragon and Wavestar 13%, with *NMean* of 34%, 39% and 40%, respectively.

- Predictability of power production of WECs is 32 to 46% better than for wind turbines
  - Day-ahead forecast errors (*NMAE*) of wind turbines working alone is 17%, with *NMean* of 35%.
  - Day-ahead predictability of the power production of WECs working alone is 32 to 46% more accurate than for wind turbines working alone (in terms of *NMAE/NMean*).
  - Day-ahead predictability of the power production of WECs combined is 36 to 42% more accurate than for wind turbines working alone (in terms of *NMAE/NMean*).

- Predictability of the combined production of WECs and wind turbines is the same as the predictability of the combined production of WECs (*NMAE=11%*). Thus, WECs have a positive influence on wind turbines power production predictabilities.
  - Day-ahead forecast error (*NMAE*) of the combined production of WECs is 11%, with *NMean* of 37%.
  - Day-ahead forecast error (*NMAE*) of the combined production of WECs and wind turbines is 11%, with NMean of 36%.

- There is good agreement between the real and theoretical results of the wind turbines, but there is not good agreement between the real and theoretical results of Wavestar. A reason is the experimental stage of the prototype at Hanstholm.

- Short-term forecasts of power productions are more accurate than day-ahead forecasts, particularly for the wind turbine, which forecasts improve in 9 percentage points. For WECs, accuracy improves in 3 to 6 percentage points.

- Short-term forecasting of wind production improves 6% when wave production is added.

➔ Hence, wave energy improves predictability of wind energy. Day-ahead forecasting of WECs power production is 32 to 46% more accurate than of wind turbines power production; and day-ahead forecasts of the combined production of WECs and of wind turbines improve by 60% compared to forecasting of only wind turbines.

- Improved predictability affects positively:
  - Planning of operational and maintenance activities.
  - Planning of storm periods.
  - Planning of testing of control strategies.
  - Improved accuracy in the bids to day-ahead electricity markets.

- Power production of WECs is more predictable than power production of wind turbines. Thus, wave energy needs lower balancing premium tariffs than wind energy, about 40% lower: 1.8 EUR/MWh (wind energy receives a balancing tariff of 3 EUR/MWh).

- Any scenario with contribution of wave energy presents smaller balancing costs than the wind-only scenario. The reduction of overall balancing cost compared to the wind-only scenario reaches:
  - 45% when WECs work individually.
  - 40% when WECs work combined.
  - 35% in the combined 75%-25% wave-wind scenario.
  - 30% in the combined 50%-50% wave-wind scenario.

➔ Energinet.dk (and Danish electricity consumers) has annual expenditures up to 36 MEUR to cover balancing costs of wind energy. If wave energy was added to Danish renewable generation, the combined production of wind and wave power could reduce balancing costs of wind power by 30% or 35%. This would imply annual savings to the Danish system of 13 MEUR in a 75%-25% wave-wind scenario, or 11 MEUR in a 50%-50% wave-wind scenario.

Variability of the power output of WECs in diversified systems:

- There is high cross-correlation between waves and winds at Hanstholm, CC=0.8.

- The average delay between waves and winds at Hanstholm is of 2-3 hours. In storm conditions, a phase shift up to 6-8 hours can be found.

- Waves have lower variability and slower changes than winds.
  - P_{wind} can vary 90% more than P_{wave}, and u_{wind} 40% more than H_{m0}.
  - Waves take up to 12 hours more than winds to reduce from peak values to their half.

- The combined power output of WECs and of wind turbines is smoother and provides higher availability than the individual productions of the technologies:
  - Null production is reduced to a minimum
    - Availability of the power production improves: percentage of time of zero production reduces to a minimum, i.e. 6% of the time.
  - Peaks are eliminated
    - Peaks smoothen out and variability reduces up to 31%.
  - Improved performances for base-load generation.
  - Average delay of 5.5 hours between Wavestar and Folkecenter wind turbine power production.

- Storm conditions: faster changes in wind than in wave power production. Overall, the combined power output is more continuous.
  - Wind turbine increases from 30% to 100% production in 8 hours, whereas the combined wind turbine and WEC production increases from 30% to 100% production in 11 hours.
  - Wind turbine increases from 3% to 69% in 4 hours. WEC increases from 15% to 100% in 11 hours.

➔ The combined power production of WECs and wind turbines reduces the fluctuations of wind turbines and reduces the percentage of time of no production.

IX.2. FURTHER RECOMMENDED WORK

There are following studies that can complement and continue this project. These are described below:

- Compare wave forecasts from two different sources, i.e. StormGeo and DHI.

- Investigate predictability of waves and of WECs power productions in swell dominated locations, i.e. Atlantic coast.
  - Forecast accuracies should be better.

- Estimate wave predictability at Horns Rev, and compare the results to those found at Hanstholm.
  - There is available wind power production data (DONG own the wind farm).
  - The wave climate is more dominated by swells.

o DONG might have forecast data for winds and waves.

- Develop a tool which, based on forecast data, it is able to predict WECs and wind turbines future power productions for different forecast horizons.

- Develop control strategies according to the prediction accuracy of wave and wind parameters.

- Study regional diversification of wave energy:
  o Within the Danish North Sea: by taking into account WECs working at Hanstholm, Thyboron, Fjaltring, Horns Rev, etc.
  o Within the North Sea: Combining WECs at e.g. Hanstholm and WECs at German North Sea, i.e. Alpha Ventus, located 80 km offshore (where there should be wave and wind measurements).
  o Including swell dominated sites, i.e. Atlantic coasts.

- Study combined production of wind turbines and WECs from multiple sites:
  o With Hanstholm and Horns Rev data.
  o With Alpha Ventus.
  o In swell dominated areas, where there is higher delay between waves and winds.

- Study the influence of wave directionality in diversified systems.

- Investigate correlation of power production with Danish consumers demand:
  o of WECs working alone.
  o of wind turbines working alone.
  o of combinations of WECs and wind turbines.

- Investigate the impact of WECs power output predictability and balancing costs in other electricity markets.
  o Denmark, the Nord Pool Market has low prices for up and down regulation.

- Study balancing costs of combined 25%-50% wave-wind energy system.

REFERENCES

AnemosPlus. (2013). [Online]: www.anemos-plus.eu [Accessed January 3rd, 2013].

Babarit A., Ben Ahmed H., Clément A. and Debusschere V. (2006). "Simulation of electricity supply of an Atlantic island by offshore wind turbines and wave energy converters associated with a medium scale local energy storage". Renewable Energy, Vol. 31, pp. 153-169.

Bedard R. (2008). "Feasibility of Using Wavewatch III for Days-Ahead Output Forecasting for Grid Connected Wave Energy Projects in Washington and Oregon". Electric Power Research Institute, (EPRI).

Beels C., Troch P., Kofoed J.P., Frigaard P., Kringelum J., Kromann P., Donovan M.H., De Rouck J. and De Backer G. (2011). "A methodology for production and cost assessment of a farm of wave energy converters". Renewable Energy, Vol. 36.

Cappelen J and Jørgensen B. (1999)."Observed Wind Speed and Direction in Denmark - with Climatological Standard Normals, 1961-90", Danish meteorological Institute of Transport. ISSN 1399-1388.

Cradden L., Mouslim H., Duperray O. and Ingram D. (2011). "Joint Exploitation of Wave and Offshore Wind Power", in Proceedings of the 9th European Wave and Tidal Energy Conference (EWTEC). Southampton.

Crestwing (2013). [Online]: www.waveenergyfyn.dk.

DanWEC. Danish Wave Energy Centre [Online]: www.danwec.com.

DEA. (2006). "Offshore Wind Farms and the Environment. Danish experiences from Horns Rev and Nysted". Copenhagen: Danish Energy Authority.

Denniss T. (2005). "Comparing the Variability of Wind Speed and Wave Height Data". Australia. Energetech.

DexaWave [Online]: www.dexawave.com.

DHI. Danish Hydraulic Institute. [Online]: www.dhi.dk.

DHI. (2009). "MIKE 21, Spectral Wave Module, Scientific Documentation". Danish Hydraulic Institute (DHI).

Diesendorf M. (2007). "The Base-Load Fallacy,". Institute of Environmental Studies.

DirRen. (2009). EU Renewable Energy Directive (2009/28/EC). [Online]: ec.europa.eu/energy/renewables/targets_en.htm [Accessed December 10th, 2012].

DMI. (2012). "Storms in Denmark since 1891". Danish Meteorological Institute (DMI).

ECI. (2005). "Variability of UK Marine Resources". Environmental Change Institute (ECI), University of Oxford, The Carbon Trust.

ECI. (2006). "Diversified renewable energy sources". Environmental Change Institute (ECI), The Carbon Trust.

EMEC European Marine Energy Centre [Online]: www.emec.org.uk.

Energinet.dk Download of Market data [Online]: www.energinet.dk/EN/El/Engrosmarked/Udtraek-af-markedsdata/Sider/default.aspx.

Enola [Online]: www.enola.ihcantabria.com.

EREC. (2011). "Mapping Renewable Energy Pathways towards 2020". European Renewable Energy Council (EREC).

Fernandez-Chozas J, Sørensen H. C. and Korpås M. (2010). "Integration of wave and offshore wind energy in a European offshore grid". International Society of Offshore and Polar Engineers (ISOPE). Beijing.

Figueras Alvarez A. (2010). "Estimation of Available Wave Power in the near-shore area around Hanstholm Harbor". Aalborg University. Aalborg.

Frydendahl K. (1971). "Danmarks klima i vind standardnormaler 1931-60". Charlottenlund.

Fusco F., Nolan G. and Ringwood J. (2010). "Variability reduction through optimal combination of wind/wave resources – An Irish case study". Energy, Vol. 35, pp. 314-325.

Gross, R; Heptonstall, P; Leach, M; Anderson, D; Green, T; Skea, J. (2007). "Renewables and the grid: understanding intermittency," Proceedings of the Institution of Civil Engineers. Energy, Vol. 160, pp. 31-41.

H2Ocean. (2013). [Online]: www.h2ocean-project.eu [Accessed January 3rd, 2013].

Hansen R.H. and Kramer M.M. (2011). "Modelling and Control of the Wavestar Prototype". 9th European Wave and Tidal Energy Conference, Southampton.

Helstrup-Jensen N.E. (2011). "Udvikling og indpasning af bølgekraft i elnettet". IDA, Bølgekraft Conference.

Holthuijsen L. H. (2007). "Waves in Oceanic and Coastal Waters". Cambridge.

Holttinen H. (2005). "Optimal electricity market for wind power". Energy Policy.

IEA. (2011). "Harnessing Variable Renewables – A Guide to the Balancing Challenge". International Energy Agency (IEA).

IEA (2008). "Innovative Electricity Markets to Incorporate Variable Production". International Energy Agency (IEA). Renewable Energy Technology Deployment.

IEA (2005). "Variability of wind power and other renewable-management options and strategies,". International Energy Agency (IEA).

Juhl J. (1994). "Danish experience and recent Research on Vertical Breakwaters". Wave Barriers '94. Yokosuka, Japan.

Kariniotakis G., Pinson P., Siebert N., Giebel G. and Barthelmie R. (2004a). "The state of the art in short-term prediction of wind power – from an offshore perspective". Sea Technology Week.

Kariniotakis G., I. Martí, D. Casas, P. Pinson, T. S. Nielsen, H. Madsen, G. Giebel, J. Usaola, I. Sanchez, A.M. Palomares, R. Brownsword, U. Focken, M. Lange, J. Tambke, P. Louka, G. Kallos, C. Lac, G. Descombes and G. Sideratos. (2004b). "What performance can be expected by short-term wind power prediction models depending on site characteristics?". European Wind Energy Conference and Exhibition. London.

Kirkegaard J. (1987). "Naturforhold og deres betydning for projeltering af offshore konstruktioner". DIA Introduktionkursus I. Olie/gas Teknologi. Danish Hydraulic Institute (DHI).

Kirkegaard J., Kofoed-Hansen H., Sloth P. and Tacher E. (2010). "Metocean forecasting for ports and terminals". Delft, The Netherlands: Port Infrastructure Seminar.

Kofoed J.P. (2009). "Ressourceopgørelse for bølgekraft i Danmark". Report No.59 for the Clima Commission.

krak [Online]: www.map.krak.dk.

Kramer M., Marquis L., and Frigaard P. (2011). "Performance Evaluation of the Wavestar Prototype", in Proceedings of the 9th European Wave and Tidal Energy Conference (EWTEC). Southampton.

Kystdirektoratet [Online]: www.kyst.dk.

Madsen (2004). "A Protocol for Standardizing the performance evaluation of short-term wind power prediction models". Deliverable 2.3 to the Anemos Project.

Margheritini L. and Nørgaard J. H. (2012). "Key Aspects of Wave Energy" in Proceedings of Sustainable Energy and Environmental Sciences (SEES 2012). Singapore.

Margheritini L. (2012). "Review on available information on waves in the DanWEC area" Dep. Civil Engineering, Aalborg University.

MarinaPlatform. (2013). [Online]: www.marina-platform.info [Accessed January 3rd, 2013].

Marquis L., Kramer M., Kringelum J., Fernández-Chozas J. and Helstrup Jensen N.E. (2012). "Introduction of Wavestar wave energy converters in the Danish offshore wind farm Horns Reef 2", in Proceedings of the 4th International Conference on Ocean Energy (ICOE). Dublin.

Martí I., G. Kariniotakis, P. Pinson, I. Sanchez, T. S. Nielsen, H. Madsen, G. Giebel, J. Usaola,A.M., Palomares, R. Brownsword, J. Tambke, U. Focken, M. Lange, G. Sideratos, G. Descombes. (2006). "Evaluation of Advanced Wind Power Forecasting Models – Results of

the Anemos Project" in Proceedings of the European Wind Energy Conference and Exhibition, Athens.

McLean J.R. (2008). "Equivalent Wind Power Curves". Deliverable 2.6 of the Tradewind Project, Garrad Hassan.

Mermaid. (2013). [Online]: www.mermaidproject.eu [Accessed January 3rd, 2013].

Morthorst P. (2007). "Detailed investigation of electricity market rules". Deliverable D4.1 to the TradeWind project.

Mørk G., Barstow S., Kabuth A. and Pontes T. (2010). "Assessing the Global Wave Energy Potential", in Proceedings of the 29th International Conference on Ocean, Offshore and Arctic Engineering (ASME). Shanghai.

Nielsen K. and Pontes T. (2010). "Generic and Site-related Wave Energy Data". Annex II. Task 1.1 International Energy Agency Ocean Energy Systems (IEA-OES).

Nielsen K. (2012). "Ocean Energy Technology Study". DanWEC; Technical Report No.1 for The Alliance for Offshore Renewables.

Nord Pool spot [Online]: www.nordpoolspot.dk.

Nord Pool Spot. (2009). "The Nordic electricity Exchange and the Nordic Model for a Liberalised Electricity Market". Denmark: Nord Pool Spot.

Nordic Folkecenter for Renewable Energy. (2013). [Online]: www.folkecenter.net [Accessed January 3rd, 2013].

Nørgaard J.H., Andersen T.L. and Kofoed J.P. (2011). "Wave Dragon Wave Energy Converters Used as Coastal Protection: a physical model test study" Coastal Structures 2011. Yokohama : The Coasts, Oceans, Ports, and Rivers Institute (COPRI) : The American Society of Civil Engineers.

Orecca. (2013). [Online]: www.orecca.eu [Accessed January 3rd, 2013].

Pecher A., Kofoed J.P and Larsen T. (2012). "Design Specifications for the Hanstholm WEPTOS Wave Energy Converter". Energies, Vol. 5 (4).

Pelamis. (2013). [Online]: www.pelamiswave.com [Accessed January 5th, 2013].

Pinson P., Reikard G. and Bidlot J. (2012). "Probabilistic forecasting of the wave energy flux". Applied Energy, Vol. 93.

Ramboll (1996). "Hanstholm Phase 2B, Offshore wave energy test 1994-96". Danish Wave Power Aps, Project report.

Ramboll (1999a). "Bølgekraft - forslag til forsøg og rapportering". Bølgekraftudvalgets sekretariat, Danish Energy Agency.

Ramboll (1999b). "Kortlægning af Bølgeenergiforhold i den Danske del af Nordsøen". Ramboll, Danish Hydraulic Institute, Danish Metereological Institute.

Resen Energy. (2013). [Online]: www.resen.dk [Accessed January 5th, 2013].

Rugbjerg M., Soerensen O. and Jacobsen V. (2006). "Wave forecasting for offshore wind farms", 9th International Workshop on Wave Hindcasting and Forecasting. Victoria.

Ruol, P.; Zanuttigh, B.; Martinelli, L.; Kofoed, J. P.; Frigaard, P., (2010). "Near-Shore Floating Wave Energy Converters : applications for coastal protection.". Coastal Engineering 2010 : Proceedings of the 32nd International Conference on Coastal Engineering.

Safewind. (2013). [Online]: www.safewind.eu [Accessed January 3rd, 2013].

Soerensen H.C., Nielsen K., Steenstrup P., Friis-Madsen E. and Wigant L. (2005). "Bølgekraftanlæg ved Horns Rev – Screening (Wave energy deployment at Horns Rev Wind Farm)". Copenhagen: PSO project 2004: 5705.

Soerensen H.C. and Fernández-Chozas J. (2010). "The Potential for Wave Energy in the North Sea", in Proceedings of the 3rd International Conference on Ocean Energy (ICOE). Bilbao.

Storm Geo. (2012). [Online]: www.stormgeo.com [Accessed December 28th, 2012].

Stoutenburg E., Jenkins N. and Jacobson M. (2010). "Power Output Variability of Co-located offshore wind turbines and wave energy converters in California". Renewable Energy.

Tropos. (2013). [Online]: www.troposplatform.eu [Accessed January 3rd, 2013].

Vicinanza D., Margheritini L., Kofoed J.P. and Buccin M. (2012). "The SSG Wave Energy Converter: Performance, Status and Recent Developments". Energies, Vol. 5 (2).

Vidal E., Hansen R. and Kramer M. (2012). "Early Performance Assessment of the Electrical Output of Wavestar's prototype", in Proceedings of the 4th International Conference on Ocean Energy (ICOE). Dublin.

Waters R. (2008). "Energy from ocean waves. Full scale experimental verification of a wave energy converter". Acta Universitatis Upsaliensis Uppsala.

Wave Star (2012). "Wavestar prototype at Roshage - Performance data for ForskVE project no 2009-1-10305. Phase 1 & 2", Project report. Wave Star.

WaveDragon [Online]: www.wavedragon.net.

Waveplam [Online]: www.waveplam.eu.

WaveStar [Online]: www.wavestarenergy.com.

WRF Model. (2013). [Online]: www.wrf-model.org [Accessed Februray 28th, 2013].

Yemm R.W., Henderson R.M. and Taylor C.A.E. (2011). "The OPD Pelamis WEC Current Status and Onward Programme," [Online]: http://www.inference.phy.cam.ac.uk/sustainable/refs/PelamisStatus.pdf

Zanuttigh B., Martinelli L., Castagnetti M., Ruol P., Kofoed J.P. and Frigaard P. (2010). "Integration of Wave Energy Converters into Coastal Protection Schemes", in Proceedings of the 3rd International Conference on Ocean Energy (ICOE), Bilbao, 2010.

APPENDIX A – PROJECT DISSEMINATION

DISSEMINATION

Part of the project outcomes have been published and made available to the general public through the following conferences, journals, meetings and oral and poster presentations[7]. By chronological order, these are:

- **Midterm Wavetrain2 Conference, Nantes**: J. Fernández-Chozas, "Wave energy power output predictability and variability, Integration into electricity markets".
  - First idea and brain-storming towards this project.
  - Oral presentation.

- **INORE Alcoutim, 2011**: J. Fernández Chozas, "Predictability and Variability of the Power Output of Selected Wave Energy Converters"
  - First idea and brain-storming towards this project.
  - Oral and Poster Presentation.

- **EWTEC Southampton, 2011**: J. Fernández-Chozas, N. E. Helstrup Jensen, H. C. Sørensen, J. P. Kofoed and A. Kabuth, "Predictability of the Power Output of Three Wave Energy Technologies in the Danish North Sea".
  - First project results.
  - Conference Paper and Oral Presentation.

- **Meeting DONG:** October 2011.
  - Project Presentation, discussion of collaborations and, synergies with MARINA project.

- **Final Wavetrain2 Conference, Canary Islands**: J. Fernández-Chozas, "Issues towards commercialization of wave technologies".
  - Oral presentation.

- **Meeting DONG:** March 2012.
  - PSO project up-date: project description and objectives. Introduction to balancing costs.

---

[7] Please contact the correspondance author (julia.fernandez.chozas@gmail.com) to have any of these material. Alternatively these can be found at <tinyurl.com/d4lqjxq>.

- **Journal Paper:** J. Fernández-Chozas, "Predictability of wave energy and electricity markets", Modern Energy Review, Vol. 4 (1), pp. 59-61, 2012.
  - Summary of EWTEC paper and new extra results.

- **INORE Thisted:** J. Fernández-Chozas, "Co-production of wind and wave power and its integration into Electricity Markets – Case study: Wavestar and 525 kW wind turbine". 6th INORE Symposium, Thisted, 2012.
  - Preliminary results of the coming ICOE paper.
  - Poster presentation.

- **Deliverable of Wavetrain2 project**: J. Fernández-Chozas, "Predictability of wave parameters at Hanstholm, Denmark. Wave resource and forecast", Deliverable 26 of Wavetrain2 Project, Case studies development of Work Package 7, 2012.

- **Meeting DONG:** September 2012.
  - Project Presentation, discussion of collaborations and, synergies with MARINA project.

- **ICOE Dublin, 2012:** L. Marquis, M. M. Kramer, J. V. Kringelum, J. Fernández-Chozas and N. E. Helstrup Jensen, "Introduction of Wavestar wave energy converters at the Danish offshore wind power plant Horns Rev 2".
  - Conference Paper and Oral Presentation.

- **ICOE Dublin, 2012**: J. Fernández-Chozas, N. E. Helstrup Jensen and H. C. Sørensen, "Economic Benefit of Combining Wave and Wind Power Productions in Day-Ahead Electricity Markets".
  - Conference Paper and Oral Presentation.

- **ICOE Dublin, 2012**: J. Fernández-Chozas, J. P. Kofoed, M. M. Kramer and H. C. Sørensen, "Combined Production of a full-scale Wave Converter and a full-scale Wind Turbine - a Real Case Study".
  - Conference Paper and Poster Presentation.

- **PSO Final report**: Fernández-Chozas J., Sørensen H.C. and Kofoed J.P. "Final project report: Analysis of Power Output Predictability of Wave and Wind", Energinet.dk, PSO project 10791, 2013.

- **PhD Thesis**: J. Fernández-Chozas, "Technical and Non-technical Issues Towards the Commercialisation of Wave Energy Converters", Aalborg: PhD Thesis (DCE Thesis no. 44), Aalborg University, 2013.
  - PhD Thesis
  - Public defence

APPENDIX B

POWER MATRICES OF PELAMIS AND WAVE DRAGON FOR THE FULL-SCALE ATLANTIC WECS

Pelamis Power Matrix for a full-scale device for the Atlantic Ocean: rated power 750 kW - Defined for Hs = 0.75 to 8.25 m and Tp = 4.75 to 13.25 s
Device length 180 meters, 4 meters diameter

Power (kW)	Tp (s)																
H_{m0} (m)	5.0	5.5	6.0	6.5	7.0	7.5	8.0	8.5	9.0	9.5	10.0	10.5	11.0	11.5	12.0	12.5	13.0
0.5	0	0	0	0	0	0	0	0	0	0	0	0	0	0	0	0	0
1	0	22	29	34	37	38	38	37	35	32	29	26	23	21	0	0	0
1.5	32	50	65	76	83	86	86	83	78	72	65	59	53	47	42	37	33
2	57	88	115	136	148	153	152	147	138	127	116	104	93	83	74	66	59
2.5	89	138	180	212	231	238	238	230	216	199	181	163	146	130	116	103	92
3	129	198	260	305	332	340	332	315	292	266	240	219	210	188	167	149	132
3.5	0	270	354	415	438	440	424	404	377	362	326	292	260	230	215	202	180
4	0	0	462	502	540	546	530	499	475	429	384	366	339	301	267	237	213
4.5	0	0	544	635	642	648	628	590	562	528	473	432	382	356	338	300	266
5	0	0	0	739	726	731	707	687	670	607	557	521	472	417	369	348	328
5.5	0	0	0	750	750	750	750	750	737	667	658	586	530	496	446	395	355
6	0	0	0	0	750	750	750	750	750	750	711	633	619	558	512	470	415
6.5	0	0	0	0	750	750	750	750	750	750	750	743	658	621	579	512	481
7	0	0	0	0	0	750	750	750	750	750	750	750	750	676	613	584	525
7.5	0	0	0	0	0	0	750	750	750	750	750	750	750	750	686	622	593
8	0	0	0	0	0	0	0	750	750	750	750	750	750	750	750	690	625

180

Wave Dragon Power Matrix for a full-scale device for the Atlantic Ocean - rated power 7 MW. Defined for Hs = 0.75 to 7.25 m and Tp = 4.75 to 17.3 s

Total width 170 meters and length 300 meters

Power (kW)	Tp (s)												
H_{m0} (m)	5	6	7	8	9	10	11	12	13	14	15	16	17
7.0						7000	7000	7000	7000	7000	7000	6650	5740
6.5						7000	7000	7000	7000	7000	7000	5950	4970
6.0					6720	7000	7000	7000	7000	7000	6860	5110	4200
5.5					5740	7000	7000	7000	7000	7000	6090	4320	3600
5.0				4610	5320	6020	7000	7000	6790	6090	5250	3950	3300
4.5				3920	4550	5180	6650	6720	5600	4970	4030	3450	2880
4.0			2840	3220	3710	4200	5320	5320	4430	3930	3440	2950	2460
3.5			2420	2660	2940	3220	4100	4100	3690	3280	2870	2460	2050
3.0		1450	1610	1750	2000	2620	2620	2620	2360	2100	1840	1570	1310
2.5	1170	1260	1330	1400	1580	2040	2040	2040	1830	1630	1430	1220	1020
2.0	640	700	840	900	1190	1190	1190	1190	1070	950	830	710	590
1.5	360	420	540	740	740	740	740	740	660	590	520	440	370
1.0	160	250	360	360	360	360	360	360	320	280	250	220	180

COMPARISON OF SCALE FACTORS AND POWER PRODUCTIONS FOR PELAMIS AND WAVE DRAGON

PELAMIS

	Scale Ratio λ		Length (m)	∑kWh (in 120 days)	MWh/y	Not operative (0.5h)	P$_{rated}$ (kW)	Capacity factor f (%)	Operating time (%)	Full load hours
(1)	1:1	1:180/180	180	200629	562	1149	750	9	78	749
(0.7)	1:1.4	1:180/126	126	114227	320	305	215	17	94	1486
(0.567)	1:1.8	1:180/102	102	72506	203	126	103	23	98	1977
(0.5)	1:2	1:180/90	90	52835	148	110	66	25	98	2232
(0.35)	1:2.9	1:180/63	63	17741	50	525	19	30	90	2604
(0.3)	1:3.3	1:180/54	54	9196	26	1247	11	26	76	2322
(0.25)	1:4	1:180/45	45	3743	10	2288	6	20	57	1789

WAVE DRAGON

	Scale Ratio λ		Length (m)	∑MWh (in 120 days)	GWh/y	Not operative (0.5h)	P$_{rated}$ (kW)	Capacity factor f (%)	Operating time (%)	Full load hours	Capture width ratio (%)
(1)	1:1	1:300/300	300	1345	3.77	918	7000	6	83	538	25
(0.7)	1:1.4	1:300/210	210	853	2.39	257	2009	14	95	1188	22
(0.567)	1:1.8	1:300/170	170	637	1.78	120	959	21	98	1859	21
(0.5)	1:2	1:300/150	150	518	1.45	104	619	27	98	2345	19
(0.466)	1:2.1	1:300/140	140	460	1.29	89	485	30	98	2651	18
(0.437)	1:2.3	1:300/131	131	407	1.14	109	385	34	98	2959	17
(0.36)	1:2.8	1:300/108	108	259	0.72	288	196	42	95	3696	13
(0.3)	1:3.3	1:300/90	90	148	0.41	596	104	46	89	4010	9
(0.2)	1:5	1:300/60	60	26	0.07	2295	25	33	56	2921	2

PELAMIS POWER MATRIX FOR HANSTHOLM

Pelamis Power Matrix for Hanstholm: rated power 103 kW - Defined for H_{m0} = 0.4 to 4.7 m and T_{02} = 2.6 to 7.1 s

Device lenght: 102 meters - Note: approx. Half scale of an Atlantic Pelamis

Power kW	T_{02} (s)																
H_{m0} (m)	2.7	3.0	3.2	3.5	3.8	4.0	4.3	4.6	4.8	5.1	5.4	5.6	5.9	6.2	6.5	6.7	7.0
0.6	0	3	4	5	5	5	5	5	5	4	4	4	3	3	0	0	0
0.9	4	7	9	10	11	12	12	11	11	10	9	8	7	6	6	5	5
1.1	8	12	16	19	20	21	21	20	19	17	16	14	13	11	10	9	8
1.4	12	19	25	29	32	33	33	32	30	27	25	22	20	18	16	14	13
1.7	18	27	36	42	45	47	45	43	40	36	33	30	29	26	23	20	18
2.0	0	37	48	57	60	60	58	55	52	50	45	40	36	32	29	28	25
2.3	0	0	63	69	74	75	73	68	65	59	53	50	46	41	37	32	29
2.6	0	0	75	87	88	89	86	81	77	72	65	59	52	49	46	41	36
2.8	0	0	0	101	99	100	97	94	92	83	76	71	65	57	51	48	45
3.1	0	0	0	103	103	103	103	103	101	91	90	80	73	68	61	54	49
3.4	0	0	0	0	103	103	103	103	103	103	97	87	85	76	70	64	57
3.7	0	0	0	0	103	103	103	103	103	103	103	102	90	85	79	70	66
4.0	0	0	0	0	0	103	103	103	103	103	103	103	103	93	84	80	72
4.3	0	0	0	0	0	0	103	103	103	103	103	103	103	103	94	85	81
4.5	0	0	0	0	0	0	0	103	103	103	103	103	103	103	103	95	86

WAVE DRAGON POWER MATRIX FOR HANSTHOLM

Wave Dragon Power Matrix for Hanstholm - Rated power: 959 kW. Defined for H_{m0} = 0.4 to 4.1 m and T_{02} = 2.6 to 9.3 s
Width 170 meters and length 96 meters

Power kW H_{m0} (m)	2.7	3.0	3.2	3.5	3.8	4.0	4.3	4.6	4.8	5.1	5.4	5.6	5.9	6.2	6.5	6.7	7.0	7.3	7.5	7.8	8.1	8.3	8.6	8.9	9.1
4.0	0	0	0	0	0	0	0	0	0	0	959	959	959	959	959	959	959	959	959	959	959	937	911	851	786
3.7	0	0	0	0	0	0	0	0	0	0	959	959	959	959	959	959	959	959	959	959	959	890	815	751	681
3.4	0	0	0	0	0	0	0	0	920	941	959	959	959	959	959	959	959	959	959	951	940	825	700	640	575
3.1	0	0	0	0	0	0	0	371	786	870	959	959	959	959	959	959	959	959	959	900	834	718	592	544	493
2.8	0	0	0	0	0	0	631	680	729	776	825	891	959	959	959	947	930	885	834	780	719	634	541	498	452
2.6	0	0	0	0	0	252	537	580	623	666	710	807	911	917	920	848	767	727	681	619	552	514	473	435	394
2.3	0	0	0	0	389	415	441	474	508	541	575	650	729	730	729	671	607	575	538	507	471	439	404	372	337
2.0	0	0	0	154	331	348	364	384	403	422	441	500	562	563	562	536	505	479	449	423	393	366	337	310	281
1.7	0	0	199	210	221	231	240	257	274	315	359	360	359	360	359	342	323	307	288	271	252	234	215	198	179
1.4	160	167	173	178	182	187	192	204	216	247	279	280	279	280	279	266	251	238	223	210	196	182	167	154	140
1.1	88	92	96	105	115	119	123	142	163	163	163	163	163	163	163	155	147	139	130	122	114	106	97	89	81
0.9	49	53	58	66	74	87	101	102	101	102	101	102	101	102	101	96	90	86	81	76	71	66	60	56	51
0.6	22	28	34	41	49	49	49	49	49	49	49	49	49	49	49	47	44	41	38	36	34	32	30	28	25
0.4	10	12	15	18	22	22	22	22	22	22	22	22	22	22	22	21	20	19	17	16	15	14	13	12	11

The header row includes **T_{02} (s)** spanning the data columns.

WAVESTAR POWER MATRIX FOR HANSTHOLM

Wavestar Power Matrix for Hantsholm. Rated power: 600 kW - Defined for Hs = 0.5 to 3 m and Tz = 2 to 8.6 s

Floats diameter: 5 meters

Power (kW) H_{m0} (m)	T_{02} (s)																								
	2.5	2.8	3	3.3	3.5	3.8	4	4.3	4.5	4.8	5	5.3	5.5	5.8	6	6.3	6.5	6.8	7	7.3	7.5	7.8	8	8.3	8.5
0.75	0	0	0	37	49	55	61	67	73	76	79	82	85	85	86	86	86	85	85	84	83	82	81	79	78
1	0	0	44	65	87	97	107	117	127	130	134	138	141	141	140	140	139	137	136	134	132	130	127	125	123
1.25	54	75	95	116	136	150	165	179	193	196	199	202	205	203	201	198	196	193	189	186	182	178	175	171	167
1.5	78	107	137	166	195	213	231	249	266	269	271	273	275	271	267	263	259	254	249	244	239	234	228	223	218
1.75	106	146	186	225	265	286	306	327	347	347	347	347	347	341	335	328	322	315	308	301	294	287	280	272	265
2	138	189	240	291	343	365	388	410	433	431	428	426	424	416	407	399	391	382	373	364	355	346	337	329	320
2.25	175	239	302	366	429	452	476	499	522	516	511	505	499	489	478	468	457	446	435	423	412	402	392	382	372
2.5	216	290	365	439	513	527	541	556	570	567	563	560	556	549	543	537	530	517	504	491	477	466	454	442	430
2.75	262	347	431	516	600	600	600	600	600	600	600	600	600	600	600	600	600	585	570	555	540	526	512	498	484

PELAMIS NON-DIMENSIONAL POWER MATRIX FOR HANSTHOLM

Non-Dimensional Pelamis Power Matrix for Hstandholm. Defined for Hm0 = 0.4 to 4.7 m and T02 = 2.6 to 7.1s

Device lenght: 102 meters

Power (pu)	T_{02} (s)																
H_{m0} (m)	2.7	3.0	3.2	3.5	3.8	4.0	4.3	4.6	4.8	5.1	5.4	5.6	5.9	6.2	6.5	6.7	7.0
0.6	0.00	0.03	0.04	0.05	0.05	0.05	0.05	0.05	0.05	0.04	0.04	0.03	0.03	0.03	0.00	0.00	0.00
0.9	0.04	0.07	0.09	0.10	0.11	0.11	0.11	0.11	0.10	0.10	0.09	0.08	0.07	0.06	0.06	0.05	0.04
1.1	0.08	0.12	0.15	0.18	0.20	0.20	0.20	0.20	0.18	0.17	0.15	0.14	0.12	0.11	0.10	0.09	0.08
1.4	0.12	0.18	0.24	0.28	0.31	0.32	0.32	0.31	0.29	0.27	0.24	0.22	0.19	0.17	0.15	0.14	0.12
1.7	0.17	0.26	0.35	0.41	0.44	0.45	0.44	0.42	0.39	0.35	0.32	0.29	0.28	0.25	0.22	0.20	0.18
2.0	0.00	0.36	0.47	0.55	0.58	0.59	0.57	0.54	0.50	0.48	0.43	0.39	0.35	0.31	0.29	0.27	0.24
2.3	0.00	0.00	0.62	0.67	0.72	0.73	0.71	0.67	0.63	0.57	0.51	0.49	0.45	0.40	0.36	0.32	0.28
2.6	0.00	0.00	0.73	0.85	0.86	0.86	0.84	0.79	0.75	0.70	0.63	0.58	0.51	0.47	0.45	0.40	0.35
2.8	0.00	0.00	0.00	0.99	0.97	0.97	0.94	0.92	0.89	0.81	0.74	0.69	0.63	0.56	0.49	0.46	0.44
3.1	0.00	0.00	0.00	1.00	1.00	1.00	1.00	1.00	0.98	0.89	0.88	0.78	0.71	0.66	0.59	0.53	0.47
3.4	0.00	0.00	0.00	0.00	1.00	1.00	1.00	1.00	1.00	1.00	0.95	0.84	0.83	0.74	0.68	0.63	0.55
3.7	0.00	0.00	0.00	0.00	1.00	1.00	1.00	1.00	1.00	1.00	1.00	0.99	0.88	0.83	0.77	0.68	0.64
4.0	0.00	0.00	0.00	0.00	0.00	1.00	1.00	1.00	1.00	1.00	1.00	1.00	1.00	0.90	0.82	0.78	0.70
4.3	0.00	0.00	0.00	0.00	0.00	0.00	1.00	1.00	1.00	1.00	1.00	1.00	1.00	1.00	0.91	0.83	0.79
4.5	0.00	0.00	0.00	0.00	0.00	0.00	0.00	1.00	1.00	1.00	1.00	1.00	1.00	1.00	1.00	0.92	0.83

Non-dimensional Wave Dragon Power Matrix for Hanstholm - Defined for H_{m0} = 0.4 to 4.1 m and T_{02} = 2.6 to 9.3s
Width 170 meters and length 96 meters

| Power (pu) H_{m0} (m)	2.7	3.0	3.2	3.5	3.8	4.0	4.3	4.6	4.8	5.1	5.4	5.6	5.9	6.2	6.5	6.7	7.0	7.3	7.5	7.8	8.1	8.3	8.6	8.9	9.1
4.0	0.0	0.0	0.0	0.0	0.0	0.0	0.0	0.0	0.0	0.0	1.0	1.0	1.0	1.0	1.0	1.0	1.0	1.0	1.0	1.0	1.0	1.0	1.0	0.9	0.8
3.7	0.0	0.0	0.0	0.0	0.0	0.0	0.0	0.0	0.0	0.0	1.0	1.0	1.0	1.0	1.0	1.0	1.0	1.0	1.0	1.0	1.0	0.9	0.9	0.8	0.7
3.4	0.0	0.0	0.0	0.0	0.0	0.0	0.0	0.0	1.0	1.0	1.0	1.0	1.0	1.0	1.0	1.0	1.0	1.0	1.0	1.0	1.0	0.9	0.7	0.7	0.6
3.1	0.0	0.0	0.0	0.0	0.0	0.0	0.0	0.4	0.8	0.9	1.0	1.0	1.0	1.0	1.0	1.0	1.0	1.0	1.0	0.9	0.9	0.7	0.6	0.6	0.5
2.8	0.0	0.0	0.0	0.0	0.0	0.0	0.7	0.7	0.8	0.8	0.9	0.9	1.0	1.0	1.0	1.0	1.0	0.9	0.9	0.8	0.8	0.7	0.6	0.5	0.5
2.6	0.0	0.0	0.0	0.0	0.0	0.3	0.6	0.6	0.7	0.7	0.7	0.8	1.0	1.0	1.0	0.9	0.8	0.8	0.7	0.6	0.6	0.5	0.5	0.5	0.4
2.3	0.0	0.0	0.0	0.0	0.4	0.4	0.5	0.5	0.5	0.6	0.6	0.7	0.8	0.8	0.8	0.7	0.6	0.6	0.6	0.5	0.5	0.5	0.4	0.4	0.4
2.0	0.0	0.0	0.0	0.2	0.3	0.4	0.4	0.4	0.4	0.4	0.5	0.5	0.6	0.6	0.6	0.6	0.5	0.5	0.5	0.4	0.4	0.4	0.4	0.3	0.3
1.7	0.0	0.0	0.2	0.2	0.2	0.2	0.3	0.3	0.3	0.3	0.4	0.4	0.4	0.4	0.4	0.4	0.3	0.3	0.3	0.3	0.3	0.2	0.2	0.2	0.2
1.4	0.2	0.2	0.2	0.2	0.2	0.2	0.2	0.2	0.2	0.3	0.3	0.3	0.3	0.3	0.3	0.3	0.3	0.2	0.2	0.2	0.2	0.2	0.2	0.2	0.1
1.1	0.1	0.1	0.1	0.1	0.1	0.1	0.1	0.1	0.2	0.2	0.2	0.2	0.2	0.2	0.2	0.2	0.2	0.1	0.1	0.1	0.1	0.1	0.1	0.1	0.1
0.9	0.1	0.1	0.1	0.1	0.1	0.1	0.1	0.1	0.1	0.1	0.1	0.1	0.1	0.1	0.1	0.1	0.1	0.1	0.1	0.1	0.1	0.1	0.1	0.1	0.1
0.6	0.0	0.0	0.0	0.0	0.1	0.1	0.1	0.1	0.1	0.1	0.1	0.1	0.1	0.1	0.1	0.0	0.0	0.0	0.0	0.0	0.0	0.0	0.0	0.0	0.0
0.4	0.0	0.0	0.0	0.0	0.0	0.0	0.0	0.0	0.0	0.0	0.0	0.0	0.0	0.0	0.0	0.0	0.0	0.0	0.0	0.0	0.0	0.0	0.0	0.0	0.0

WAVESTAR NON-DIMENSIONAL POWER MATRIX FOR HANSTHOLM

Non-dimensional Wavestar Power Matrix for Hanstholm - Defined for H_{m0} = 0.5 to 3 m and T_{02} = 2 to 8.6 s

Floats diameter: 5 meters

Power (pu)	T_{02} (s)																								
H_{m0} (m)	2.5	2.8	3	3.3	3.5	3.8	4	4.3	4.5	4.8	5	5.3	5.5	5.8	6	6.3	6.5	6.8	7	7.3	7.5	7.8	8	8.3	8.5
0.75	0.0	0.0	0.0	0.1	0.1	0.1	0.1	0.1	0.1	0.1	0.1	0.1	0.1	0.1	0.1	0.1	0.1	0.1	0.1	0.1	0.1	0.1	0.1	0.1	0.1
1	0.0	0.0	0.1	0.1	0.1	0.2	0.2	0.2	0.2	0.2	0.2	0.2	0.2	0.2	0.2	0.2	0.2	0.2	0.2	0.2	0.2	0.2	0.2	0.2	0.2
1.25	0.1	0.1	0.2	0.2	0.2	0.3	0.3	0.3	0.3	0.3	0.3	0.3	0.3	0.3	0.3	0.3	0.3	0.3	0.3	0.3	0.3	0.3	0.3	0.3	0.3
1.5	0.1	0.2	0.2	0.3	0.3	0.4	0.4	0.4	0.4	0.4	0.5	0.5	0.5	0.5	0.4	0.4	0.4	0.4	0.4	0.4	0.4	0.4	0.4	0.4	0.4
1.75	0.2	0.2	0.3	0.4	0.4	0.5	0.5	0.5	0.6	0.6	0.6	0.6	0.6	0.6	0.6	0.5	0.5	0.5	0.5	0.5	0.5	0.5	0.5	0.5	0.4
2	0.2	0.3	0.4	0.5	0.6	0.6	0.6	0.7	0.7	0.7	0.7	0.7	0.7	0.7	0.7	0.7	0.7	0.6	0.6	0.6	0.6	0.6	0.6	0.5	0.5
2.25	0.3	0.4	0.5	0.6	0.7	0.8	0.8	0.8	0.9	0.9	0.9	0.8	0.8	0.8	0.8	0.8	0.8	0.7	0.7	0.7	0.7	0.7	0.7	0.6	0.6
2.5	0.4	0.5	0.6	0.7	0.9	0.9	0.9	0.9	1.0	0.9	0.9	0.9	0.9	0.9	0.9	0.9	0.9	0.9	0.8	0.8	0.8	0.8	0.8	0.7	0.7
2.75	0.4	0.6	0.7	0.9	1.0	1.0	1.0	1.0	1.0	1.0	1.0	1.0	1.0	1.0	1.0	1.0	1.0	1.0	1.0	0.9	0.9	0.9	0.9	0.8	0.8
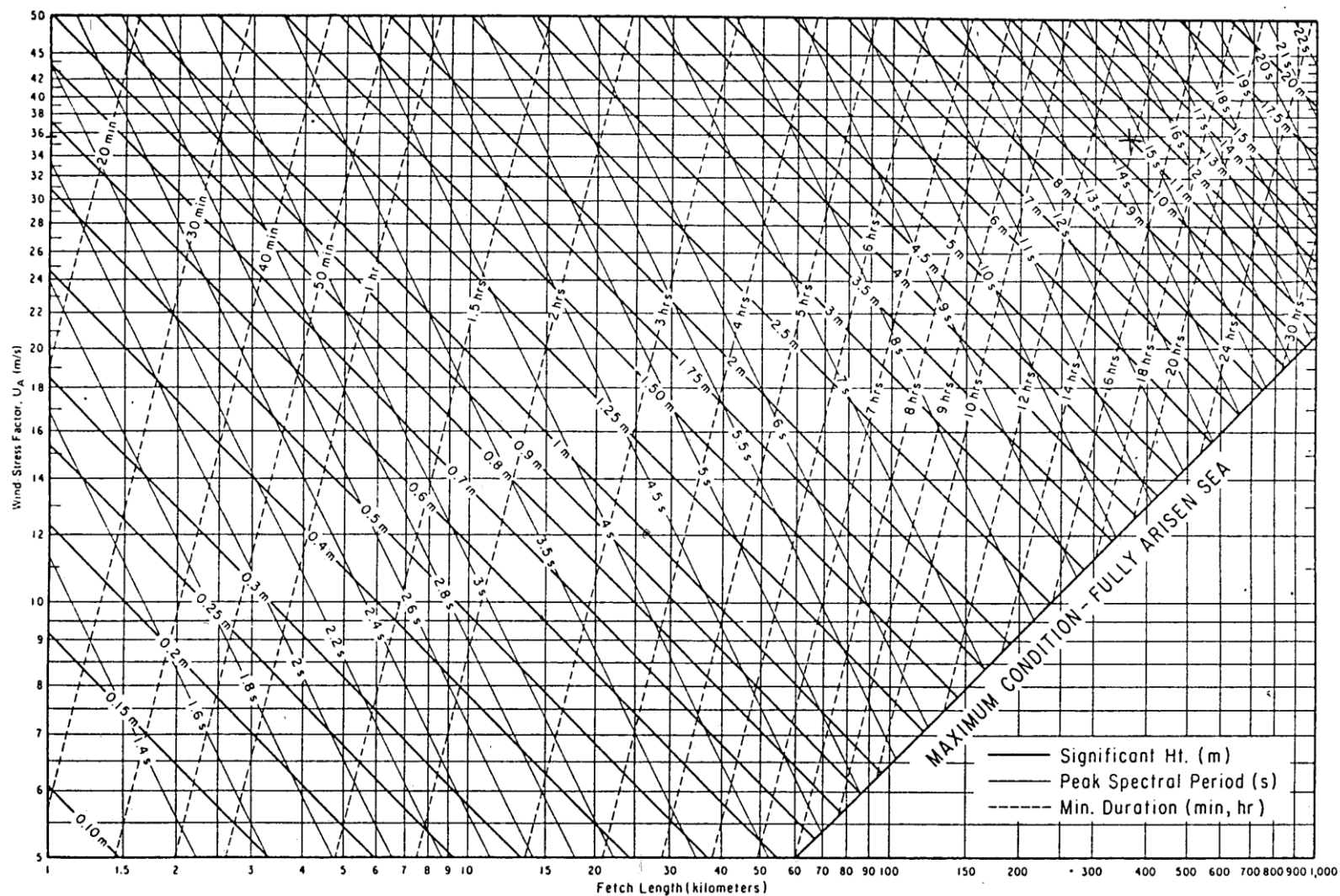
Figure 113: Nomograms of deep water significant wave prediction curves as functions of windspeed, fetch length and wind duration, SI units.